2012

# INVESTIGATIONS OF OXIDATIVE STRESS EFFECTS AND THEIR MECHANISMS IN RAT BRAIN AFTER SYSTEMIC ADMINISTRATION OF CERIA ENGINEERED NANOMATERIALS

Sarita S. Hardas
*University of Kentucky*, saritash135@gmail.com

STUDENT AGREEMENT:

I represent that my thesis or dissertation and abstract are my original work. Proper attribution has been given to all outside sources. I understand that I am solely responsible for obtaining any needed copyright permissions. I have obtained and attached hereto needed written permission statements(s) from the owner(s) of each third-party copyrighted matter to be included in my work, allowing electronic distribution (if such use is not permitted by the fair use doctrine).

I hereby grant to The University of Kentucky and its agents the non-exclusive license to archive and make accessible my work in whole or in part in all forms of media, now or hereafter known. I agree that the document mentioned above may be made available immediately for worldwide access unless a preapproved embargo applies.

I retain all other ownership rights to the copyright of my work. I also retain the right to use in future works (such as articles or books) all or part of my work. I understand that I am free to register the copyright to my work.

REVIEW, APPROVAL AND ACCEPTANCE

The document mentioned above has been reviewed and accepted by the student's advisor, on behalf of the advisory committee, and by the Director of Graduate Studies (DGS), on behalf of the program; we verify that this is the final, approved version of the student's dissertation including all changes required by the advisory committee. The undersigned agree to abide by the statements above.

Sarita S. Hardas, Student

Dr. D. Allan Butterfield, Major Professor

Dr. John Anthony, Director of Graduate Studies

# INVESTIGATIONS OF OXIDATIVE STRESS EFFECTS AND THEIR MECHANISMS IN RAT BRAIN AFTER SYSTEMIC ADMINISTRATION OF CERIA ENGINEERED NANOMATERIALS

---

ABSTRACT OF DISSERTATION

---

A dissertation submitted in partial fulfillment of the requirements for the degree of Doctor of Philosophy in the College of Arts and Sciences at the University of Kentucky

By

Sarita S. Hardas

Lexington, Kentucky

Director: Dr. D. Allan Butterfield, Professor of Chemistry

University of Kentucky

Lexington, KY

2012

ABSTRACT OF DISSERTATION

INVESTIGATIONS OF OXIDATIVE STRESS EFFECTS AND THEIR MECHANISMS IN RAT BRAIN AFTER SYSTEMIC ADMINISTRATION OF CERIA ENGINEERED NANOMATERIALS

Advancing applications of engineered nanomaterials (ENM) in various fields create the opportunity for intended (e.g. drug and gene delivery) or unintended (e.g. occupational and environmental) exposure to ENM. However, the knowledge of ENM-toxicity is lagging behind their application development. Understanding the ENM hazard can help us to avoid potential human health problems associated with ENM applications as well as to increase their public acceptance. Ceria (cerium [Ce] oxide) ENM have many current and potential commercial applications. Beyond the traditional use of ceria as an abrasive, the scope of ceria ENM applications now extends into fuel cell manufacturing, diesel fuel additives and for therapeutic intervention as a putative antioxidant. However, the biological effects of ceria ENM exposure have yet to be fully defined. Both pro-and anti-oxidative effects of ceria ENM exposure are repeatedly reported in literature. EPA, NIEHS and OECD organizations have nominated ceria for its toxicological evaluation. All these together gave us the impetus to examine the oxidative stress effects of ceria ENM after systemic administration.

Induction of oxidative stress is one of the primary mechanisms of ENM toxicity. Oxidative stress plays an important role in maintaining the redox homeostasis in the biological system. Increased oxidative stress, due to depletion of antioxidant enzymes or molecules and / or due to increased production of reactive oxygen (ROS) or nitrogen (RNS) species may lead to protein oxidation, lipid peroxidation and/or DNA damage. Increased protein oxidation or lipid peroxidation together with antioxidant protein levels and activity can serve as markers of oxidative stress.

To investigate the oxidative stress effects and the mechanisms of ceria-ENM toxicity, fully characterized ceria ENM of different sizes (~ 5nm, 15nm, 30nm, 55nm and nanorods) were systematically injected into rats intravenously in separate experiments. Three brain regions (hippocampus, cortex and cerebellum) were harvested from control and ceria treated rats after various exposure periods for oxidative stress assessment. The levels of oxidative stress markers viz. protein carbonyl (PC), 3-nitrotyrosine (3NT), and protein bound 4-hydroxy-2-trans-nonenal (HNE) were evaluated for each treatment in each control and treated rat organ. Further, the levels and activities of antioxidant

proteins, such as catalase, glutathione peroxidase (GPx), glutathione reductase (GR), super oxide dismutase (SOD), were measured together with levels of heat shock proteins heme oxygenase -1 and 70 (HO-1 and Hsp-70). In addition, the levels of pro-inflammatory cytokines IL-1β, TNF-α, pro-caspase-3, and autophagy marker LC-3A/B were measured by Western blot technique. In agreement with the literature-proposed model of oxidative stress hierarchy mechanism of ENM-toxicity, the statistical analysis of all the results revealed that the ceria ENM-induced oxidative stress mediated biological response strongly depends on the exposure period and to some extent on the size of ceria ENM. More specifically, a single intravenous injection of ceria ENM induced tier-1 (phase-II antioxidant) response after shorter exposure periods (1 h and 20 h) in rat brain. Upon failure of tier-1 response after longer exposure periods (1 d to 30 d), escalated oxidative stress consequently induced tier-2 and tier-3 oxidative stress responses. Based on our observations made at chronic exposure period (90 d) after the single i.v. injection of ceria ENM, we could extend the model of oxidative stress hierarchy mechanisms for ceria-ENM-induced toxicity. Considering the evaluation of all the oxidative stress indices measured in 3-brain regions, oxidative stress effects were more prominent in hippocampus and the least in cerebellum, but no specific pattern or any significant difference was deduced.

Keyword: Ceria, cerium oxide, nanomaterial, nanoparticles, nanotoxicity, oxidative stress, phase-II enzymes.

Sarita S. Hardas

May 2, 2012

INVESTIGATIONS OF OXIDATIVE STRESS EFFECTS AND THEIR MECHANISMS IN RAT BRAIN AFTER SYSTEMIC ADMINISTRATION OF CERIA ENGINEERED NANOMATERIALS

By

Sarita S. Hardas

Dr. D. Allan Butterfield, PhD

Director of Dissertation

Dr. John Anthony

Director of Graduate Studies

May 2, 2012

Date

To my parents and my teachers

तया सर्वात्मका ईश्वरा। स्वकर्मकुसुमांची वीरा।
पूजा केली होय अपारा। तोषालागी॥

-ज्ञानेश्वरी अ १८-९७

## ACKNOWLEDGMENTS

I would like to extend my deep regards to my PhD advisor, Dr. D. Allan Butterfield. His attention, support, mentorship, and guidance have been of great assistance to me in my PhD life here at UK and it will continue helping me in my future. I would like to extend deep thanks to all my present and past graduate committee members; Dr. Boyd Haley, Dr. Stephen Testa, Dr. Folami Ladipo, and Dr. M. Paul Murphy for providing direction in my graduate studies. I am very grateful to research faculty Dr. Rukhsana Sultana for her help with learning experimental techniques, trouble shooting and her constant support. I would also like to thank the past and present post-docs Dr, Hafiz Mohammad Abdul, Dr. Rena Sowell, and Dr. Giovanna Cenini for their hands on assistance with experiments and data analysis.

I would like to offer special thanks to Dr. M. Paul Murphy and his lab members Tina Brackett, Dr. Dana Niedowicz, Chris Holler, and Robin Webb for making all the resources of their lab available without any reservation, for their help in designing new experiments and learning new experimental techniques. I am also thankful to our collaborators and their lab members (Dr. Robert Yokel, Dr. Jason Unrine, Dr. Michael Tseng, Dr. Uschi Graham and Dr. Eric Grulke) for their valuable inputs in my research. I would like to thank Chemistry department and EPA for being resourceful and for providing finding for my research.

I will always cherish the friendships I formed at UK, in the Butterfield group and outside. My present and past lab members, Gururaj (Joshi), Opii, Miranda (Bader Lange), Josh (Owen), Chris (Aluise), Ada (Fironi), Govind (Warrior), Michael (Goodman), Michelle, Jerry (Keeney), and my friends outside my research lab who have become a scientific confidents and with whom I created a long lasting relationship over the years. I am grateful of my friendship to Abhay (Ladhe), Anjali (Chhabra), Jivan (Yewle) Nitin (Satarkar), Rashmi (Jadhav), Kunal (Joshi), Hari (Speciale et al.), Sweta (Modi), Archisman (Gosh), Paritosh (Wattamwar), Abhijit (Bhagavatulla), Nikhil (Patil), Lakshmi (Pillai), Vrushali (Angadi), Ranjana (Sing), and many more. It is simply impossible to include all the names, but you all are part of my extended family at UK.

You guys have been my life-line and made these past 7 years most memorable years of my life.

Although I am going to thank my parents and my family at the end, in reality they are the ones who laid foundation of all my achievements. I do not have enough words to express my feelings and immense gratitude towards my parents, my family and my local host family (Mr. Ron and Mrs. Barbara Halloway). Aai-Baba, and Kaka-Bai your unconditional support, encouragement, patience, and love have been constant source of strength and positive energy for me. Thank you for always being there for me.

TABLE OF CONTENTS

LIST OF TABLES

LIST OF FIGURES

# CHAPTER 1

# INTRODUCTION

The rapid growth of nanotechnology has given rise to vast array of engineered nanomaterials (ENM) that vary in size, shape, charge, chemistry, coating, and solubility. The present generation ENMs are designed to accomplish one type of task, but next generation ENM are envisioned to accomplish multiple tasks such as smart drug delivery devices, sensors, actuators. Due to the unique physical, chemical, electrical, optical, and magnetic properties, ENMs could accomplish variety of applications in various field including electronics, electrical, medicinal, chemical industry etc. The significantly different properties of ENM compared to constituent bulk material are attributed to the size- surface area, chemical composition, crystallinity, and surface functionalization of ENM. These very properties also dictate chemical and biological behavior of ENM and hence their toxicity (Nel et al. 2006; Buzea et al. 2007).

According to U.S. National Nanotechnology Initiative (NNI), an intentionally manufactured material with one or more dimensions in the range of 1 to 100 nm is referred to as engineered nanomaterial (ENM) (NSET). ENM are compatible in size to viruses, and due to their small sizes ENM can enter, and translocate within with circulatory system, penetrate biological barriers, and gain access to different biological compartments, as well as organelles. Therefore, although impressive from useful application point of view, the novel properties of ENM raise concern about detrimental effects on biological systems. There are about 40,000 publications discussing the usefulness of nanomaterials, however, only 500 discuss the potential toxic effects of the same (Buzea et al. 2007). As much as it is important to give attention to the health effects

related to ENM, at the same time it is important to remember that although by virtue of their unique physico-chemical properties all the ENM have potential to have toxic biological effects, not all the ENM are actually toxic to biological system (Oberdorster et al. 2009). Therefore, the major challenge before toxicologists is not to test every variation of new nanoparticles generated but to identify key factor andor tests that can be used to predict toxicity of ENM (Stone et al. 2006). Nel and co-worker and some other researchers are proposing that the biological hazards associated with ENM are best predicated by examining the oxidative stress effects within cells (Nel et al. 2006; Stone et al. 2006; Xia et al. 2006; Buzea et al. 2007; Meng et al. 2009).

One such metal oxide ENM is ceria (a.k.a. Cerium oxide, $CeO_2$, CAS# 1306-38-3), it has wide range of commercial applications including, abrasive for chemical-mechanical planarization, of advanced integrated circuits, as a diesel fuel catalyst ceria it is used to improve combustion, reduce fuel consumption, and decrease exhaust emission, solid oxide fuel cells solar cells (Murray et al. 1999; Esposito et al. 2008), (Corma et al. 2004) gas sensors (Izu et al. 2003), and UV screens (Gilliss et al. 2005). The popularity of ceria has drawn attention of NIEHS and OECD. Both these organization have nominated nano-scale ceria for toxicological consideration (NIEHS 2006; Oberdorster et al. 2009).

The primary anticipated routes of human exposure to ENMs intended for industrial or environmental applications include inhalation exposure, dermal uptake, and oral ingestion with possible subsequent absorption of ENMs into systemic circulation. Translocation from the lung to systemic organs, particularly the liver, has been observed before (Yokel et al. 2009). There is considerable interest in ENMs to enhance drug delivery to the brain (Koziara et al. 2006; Nazem et al. 2011). Although some data exist

on the absorption properties and associated toxicities of ENMs after exposure via the pulmonary, oral, and topical routes, little is known about their distribution into the brain once they reach systemic circulation.

We selected ceria for the present dissertation work because; ceria has been reported to have both anti- and pro-oxidant effects. Ceria ENMs have toxic effects associated with increased oxidative stress (Brunner et al. 2006; Thill et al. 2006) . However, numerous studies reported ceria ENM to be neuroprotective, suggesting that it has utility in medical disorders caused by reactive oxygen species (ROS) (Chen et al. 2006; Schubert et al. 2006; Das et al. 2007; Xia et al. 2008). Many of these results were attributed to antioxidant effects caused by defects (vacancies) in the ENM lattice structure and/or cerium (Ce) ion redox cycling. All these studies of the oxidative stress of ENMs were conducted in cell culture.

In addition to this, ceria is a very good candidate to characterize ENM biodistribution from blood and its effect on oxidative stress points because 1) It is an insoluble metal oxide that can be readily observed in situ by electron microscopy (EM), making it a useful in vivo tracer, 2) it is redox active (Zhang et al. 2004), 3) it can be functionalized [e.g. (Qi et al. 2008)], 4) it is available in sizes relevant to for up take across the blood brain barrier, one of the most limiting mammalian membranes, and it can be produced in a variety of different shapes by many different methods (Yokel et al. 2009).

The interest in ceria as a potential therapeutic agent with anti-oxidant properties is also increasing and there is possibility of future research for medical applications probability that it will be further studied for medical applications (Celardo et al. 2011). Therefore, understanding of its distribution from the central compartment (blood) and resultant

effects is important. The current study is the first report of the distribution and effects of ceria from the central compartment, after introduction into blood. As stated in a review of the risks of industrial nanomaterials, 'The effect of nanomaterials on organs ''inside'' the body (e.g., liver and brain) and the blood have been studied from the few publications on the permeation of nanomaterials through the lung, skin, or intestinal barrier . . . ' (Wolfgang 2004). 2004). However, the form of ceria employed in the present study would not be effective as a vehicle for drug delivery to the brain.

The objective of this work is;

1) To determine oxidative stress end-points in rat brain after its biodistribution from blood;
    a. Measure marker of cellular redox status GSH:GSSG ratio
    b. Measure levels and activities of phase II enzymes GPx, GR, catalase, SOD, GST etc.
    c. Measure levels of protein oxidation, protein nitration and lipid peroxidation markers, as well as heat shock proteins.
    d. Measure levels of cytokines, pro-apoptotic proteins, marker of autophagy.
2) Influence of size, shape and exposure period on the oxidative stress effects of ceria ENM
    a. Sizes: ~5nm, 15 nm, 30 nm, 55 nm
    b. Aspect ratio / Shapes: cubic (aspect ratio-1), nanorod (aspect ratio- 5-60)
    c. Exposure periods: 1 h, 20 h, 1 d, 7 d, 30 d, and 90 d
3) To understand the mechanism of oxidative stress effects induced by ceria ENM

Obtain different oxidative stress end-points from different exposure period after 30 nm ceria ENM administration.

.

# CHAPTER 2

# BACKGROUND

The various new technologies are continuously exploring new avenues for applications of different nanoscale products and materials in optoelectronics, electronics, magnetic, medicine imaging, drug delivery, catalysis, dental bonding, corrosion-resistance, coating applications, consumer goods, motor vehicles, personal care products, and cosmetics (O'Brien et al. 2008). These applications capitalize on the physico-chemical properties of engineered nanomaterials (ENMs) such as strength, stiffness, weight reduction, stability, anti-fogging, scratch resistance, as well as optical, electromagnetic, catalytic, and pharmacokinetic. ENMs such as carbon based single walled (SWCNTs) and multiwall (MWCNTs) nanotubes, metal and metal oxide based nanoparticles, and nanofilaments, and quantum dots are building block for various current technological application. There are ~2500 commercial nanomaterials have been identified by Nanowrek, which includes ~27% metal oxides, 24% CNTs, 18% elements, 7% quantum dots and 5% fullerenes (Yokel et al. 2011).

## 2.1. What are engineered nanomaterials (ENMs)?

According to U.S. National Nanotechnology Initiative (NNI), nanoscale materials that are intentionally manufactured with at least one dimension in the range of 1 to 100 nanometers (nm) and have properties that are often unique owing to their dimensions (Yokel et al. 2011) (Figure 2.1a) can be termed as engineered nanomaterials (ENMs).

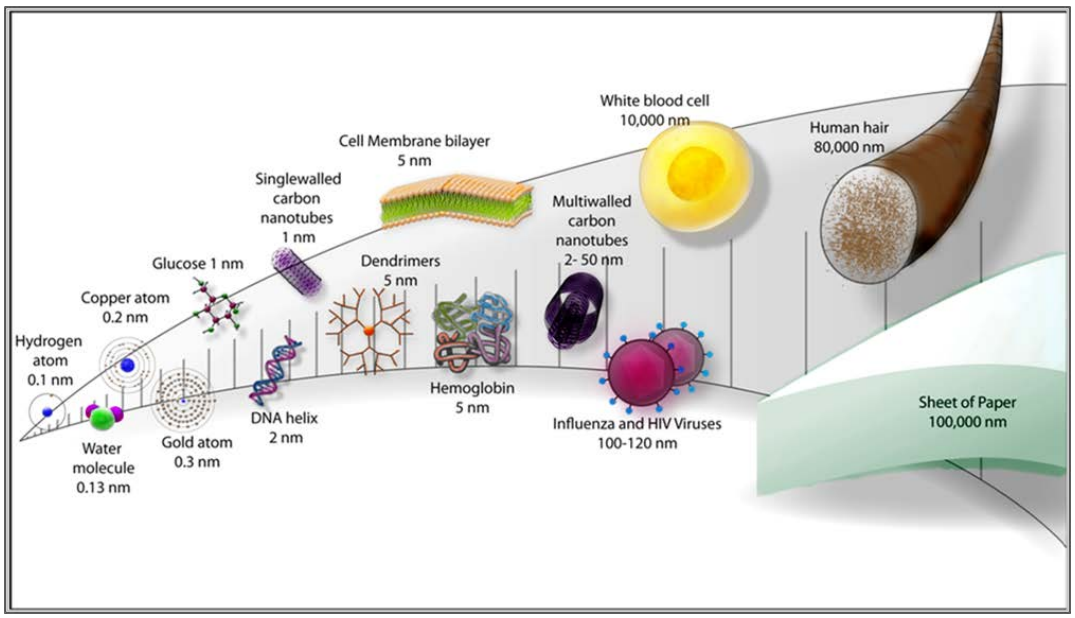


**Figure 2.1a:** The size of nanomaterials plays key role in determining their physico-chemical and biological behavior. Typical nanoparticles size can vary from 1-100 nm and could be as small as glucose molecules or DNA or as big as a virus and can get access to the cellular compartments. Due to the smaller size of a nanomaterial the quantum effects becomes dominant, so similar to atoms and molecules nanomaterials may behave according to lows of quantum mechanics instead of laws of classical mechanics. [Adapted from (Yokel et al. 2011) with the copyright permission from BioMed Central publishing groups]

ENMs exhibit properties which differ in fundamental and valuable ways from those of individual atoms, molecules and bulk matters. There are two main size-dependent factors that govern the properties of nanomaterials: surface effects (related to the fraction of atoms or molecules present on the surface), and quantum effects (related to the materials with delocalized electrons) (Roduner 2006). Compare to micromaterials or bulk materials, for a given mass or volume nanomaterials have very large surface areas and a

high particle number per unit mass.. The specific surface area (surface area/ mass) and fraction of atoms or molecules on the surface of nanomaterial are inversely proportional to the size of nanomaterials (Figure 2.1b). Due to availability of larger specific surface area, chemical reactivity of nanomaterials may enhance by multiple -folds (Buzea et al. 2007). Thus the surface effects are a key to define the chemical and biological properties of nanomaterials.

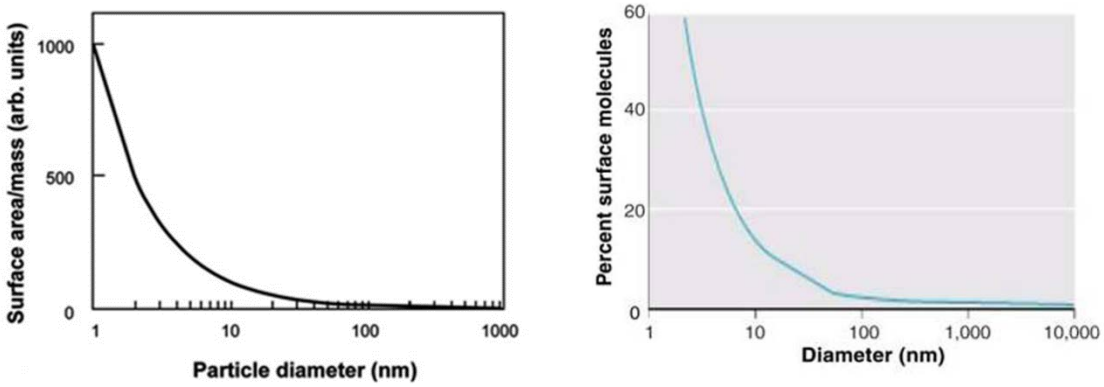


**Figure 2.1b:** Specific surface area (surface area/ mass) (left) and the percent molecules present on the surface of ENMs (Bhabra et al.) are inversely proportional to the size of ENM. At 100 nm of size ~2% of molecules are present on the surface, but when size decreases to 10 nm or 2 nm, number of surface molecules increases up to 20% and 60%. As molecules present on surface are involved in the chemical interaction with surroundings, % surface molecules determines the chemical and biological reactivity of nanomaterials. [Courtesy (Roduner 2006)and (Oberdörster et al. 2005)]

## 2.2. Physico-chemical properties of ENMs

The differential chemical as well as biological reactivity of ENMs than their bulk materials is by virtue of physico-chemical properties such as size, shape or aspect ratio, aggregation, composition, and surface functionalization etc.

**2.2.1. Size and surface area:** Due to their small size, ENMs can be translocated from their point of entry to circulatory or lymphatic systems and gain access to various remote cellular compartments like the cardiovascular system or even brain, which are usually inaccessible to larger particles. Studies have demonstrated that small ENMs (<100 nm) cause adverse respiratory health effects compare to larger ENM of same material (Oberdörster et al. 1994; Donaldson et al. 2003; Oberdörster et al. 2005; Buzea et al. 2007). As the size of ENMs decreases, their specific surface area and fraction of atoms or molecules present on the ENM-surface increases exponentially (Figure 2.1b). With decreasing size, surface effects and quantum effects also become dominant, which are primary factors that render the physico-chemical properties of ENM significantly different than bulk materials. Especially ENM with one or more dimensions in the range of ~15 nm to 30 nm, exhibits differential chemical behavior and potential for more profound biological effects than either smaller or larger ENM with similar composition (Jiang et al. 2008; Auffan et al. 2009; Yokel et al. 2011). Therefore, size and specific surface area, are important factors to determine the toxicity of ENMs.

**2.2.2. Aspect ratio:** The morphology of ENMs can be sub- categorized as high aspect ratio and low aspect ratio ENMs. The classification of aspect ratio (length to diameter) is a relative terminology, typically ENMs with length ≤ 1 μm is considered as low aspect ratio materials, length >1 μm is considered as high aspect ratio materials (Yokel et al.

2011). Low aspect ratio morphology includes spheres, ovals, cubes, prisms, helices, pillar, wires or rods (Buzea et al. 2007). High aspect ratio morphology includes nanotubes and nanowires, with various shapes like helices, zigzags,belts, with varing diameters and lengths (Buzea et al. 2007). Depending up on the aspect ratio (L-length / D-diameter) of nanofilament, the toxicity of ENM varies, generally higher the aspect ratio, the more toxic the particle is (Lippmann 1990). Due to low clearance of long length fibers or high aspect ratio ENM (> 20 μm) by alveolar microphages, their accumulated lead to various degrees of pulmonary toxicity ranging from asbestosis, mesothelioma to lung cancer (Lippmann 1990; Buzea et al. 2007). High aspect ratio material with length > 5μm and diameter ≥ 100 nm is considered highly toxic, regardless of its chemical composition (Buzea et al. 2007; Lewinski et al. 2008). However, studies with long SWCNT's and MWCNT's with diameter < 100 nm are reported to produce significant pulmonary toxicity compared to short length or spherical nanomaterials (Lam et al. 2004; Warheit et al. 2004; Muller et al. 2005; Bottini et al. 2006; Kostarelos 2008; Kim et al. 2010). Similarly, even low aspect ratio material (D < 100 nm, L < 1 μm) which can escape phagocyte clearance entering into vascular system, might end up in various organs including brain, liver, kidney etc., causing adverse health effects (Buzea et al. 2007; Oberdorster et al. 2009; Yokel et al. 2011).

**2.2.3. Agglomeration:** Depending upon chemical and electromagnetic properties on ENMs, they can exist as dispersed aerosols, suspension or colloidal solution or in the form of aggregates. ENMs composed of single constituent material like metal, metal oxide, or carbon have a tendency to agglomerate; similarly, ENMs with magnetic properties tend to form clusters. In an agglomerated state, ENM lose its high-surface area

property and may behave as large particle depending upon the size of agglomerate. To prevent agglomeration, ENM are either coated with suitable materials or mixed with some other nanoscale material. For example magnetic ENM are coated with nonmagnetic materials (Buzea et al. 2007), metal oxide ENMs are coated with citrates (Hardas et al. 2010), whereas mixing nanopowders of silica (SiO2) or titania (TiO2) with CNTs can reduce agglomeration of CNTs (Davé et al. 2006).

**2.2.4. Chemical composition:** As stated on physico-chemical properties of ENM and their toxicity relation, "….Therefore, the toxic potential (of ENM) may change by reducing the size of particles, but the threshold value depends upon the chemical nature of (nano) particles….." (Fubini et al. 2010). ENM can be composed of single constituent materials like metal, metal oxides, inorganic material or carbon or composites of several materials as a mixture or doping of one material with other. The chemical properties of constituent materials play important roles in chemical reactivity of ENM as well as in the interaction of ENM with biological matter. For example, transition or redox active metal/ metal-oxide based ENMs also exhibit high catalytic behavior and often facilitate biological reactions or generate free radicals (Nel et al. 2006). This point is exemplified by the finding that zero valent iron ENM induced ROS levels in human bronchial epithelial cells owing to the redox properties of iron (Keenan et al. 2009). On other hand, $TiO_2$ responding to UV radiation can generate electron-hole pairs which can further induce reactive oxygen species (ROS) levels in biological system (Xia et al. 2008), whereas zinc metal is important for mammalian cells and therefore exposure to ZnO ENM can interfere with various metabolic reactions; in addition, the zinc ions that leach out from the ENM can induce ROS levels in cells (Xia et al. 2008).

**2.2.5. Surface coating or functionalization:** The surface of ENM is a key in determining the toxicity of ENM, as the surface makes direct contact with biological matter. Surface modification employed in drug development research, usually prolong ENM circulation in the blood, enhance its uptake at target site, affect its translocation, and alter the excretion of ENM. Surface coating can dramatically change the magnetic, electric, optical properties and chemical reactivity ultimately manipulating the biological toxicity. Researchers have shown that the presence of oxygen, ozone (Risom et al. 2005), oxygen radicals (Lioy et al. 2002), and transition metals on surface of ENM (Fubini et al. 2003), lead to generation of ROS and induction of inflammation. Studies on hamsters showed that formation of blood clots was increased when the surface of polystyrene ENM was functionalized by amine groups (Nemmar et al. 2002). Nickel ferrite ENM showed differential cytotoxic effects with and without surface coating of oleic acid (Yin et al. 2005). The cytotoxicity of fullerenes was systematically correlated with the chemical functionalization on the surface of ENM, and with decreased cell viability in human (skin and liver) carcinoma cells caused by increased lipid peroxidation mediated by ROS production (Sayes et al. 2004). Gold ENMs with CTAB coating were rendered nontoxic when the coating was replaced by benign polyethylene glycol moieties (Goodman et al. 2004; Connor et al. 2005). Cytotoxicity of quantum dots of CdS was dramatically reduced after application of proper surface coating material (Derfus et al. 2003).

### 2.3. Interactions at nano-bio interface

Currently our understanding of bio-physicochemical interactions at the nano-bio interface is far from clear; however, some pockets of knowledge available can guide us to develop

an understanding of this matter. As explained in detailed in Section 2.2., chemical activity as well as biological reactivity of ENMs depend on factors like size, surface area, chemical composition, crystallinity and surface coating, etc. Due to the size, which is 1000 to 10,000 smaller than a white blood cell, ENMs can travel with blood flow, potentially pass through cell membranes and can gain access to the various cellular compartments. However, once suspended in biological medium, it is the surface of the ENMs that directly interacts with biological environment. For a given size or specific surface area, the surface properties of ENMs are shaped by the material's inherent properties like, chemical composition, surface functionalization, shape and angle of curvature, porosity, charge, crystallinity, heterogeneity, roughness, and hydrophobicity or hydrophilicity (Vertegel et al. 2004; Oberdörster et al. 2005; Nel et al. 2006). On the other hand, by virtue of characteristic like the ionic strength, pH, temperature, presence of large organic molecules of the surrounding media, ENMs may acquire some properties such as effective surface charge, particle aggregation, and state of dispersion, stability / biodegradability, dissolution characteristics, hydration and valence of the surface layer. With the combined contribution of the inherent and acquired properties, ENMs can interact with bio-medium through (i) promoting the adsorption of ions, biomolecules, and natural organic materials, (ii) double layer formation, (Owens Iii et al.) dissolution, or (Owens Iii et al.) minimizing free surface energy by surface reconstructuring.

In biological fluid, blood or plasma, by virtue of original or pre-existing surface properties (hydrophobicity, size, radius of curvature, charge, coating that exert steric or electrostatic effects, etc.) of ENMs, proteins interact and form a corona around the ENM constituting a primary nano-bio interface. The dynamic nature of protein corona comprise

of characteristic protein adsorption and desorption, competitive binding interactions, steric hindrance offered by pre-adsorbed polymer or presence of detergent (from ENM suspension), and the protein profile of the biological fluid. The nature of corona also changes as ENM moves from one biological compartment to another.

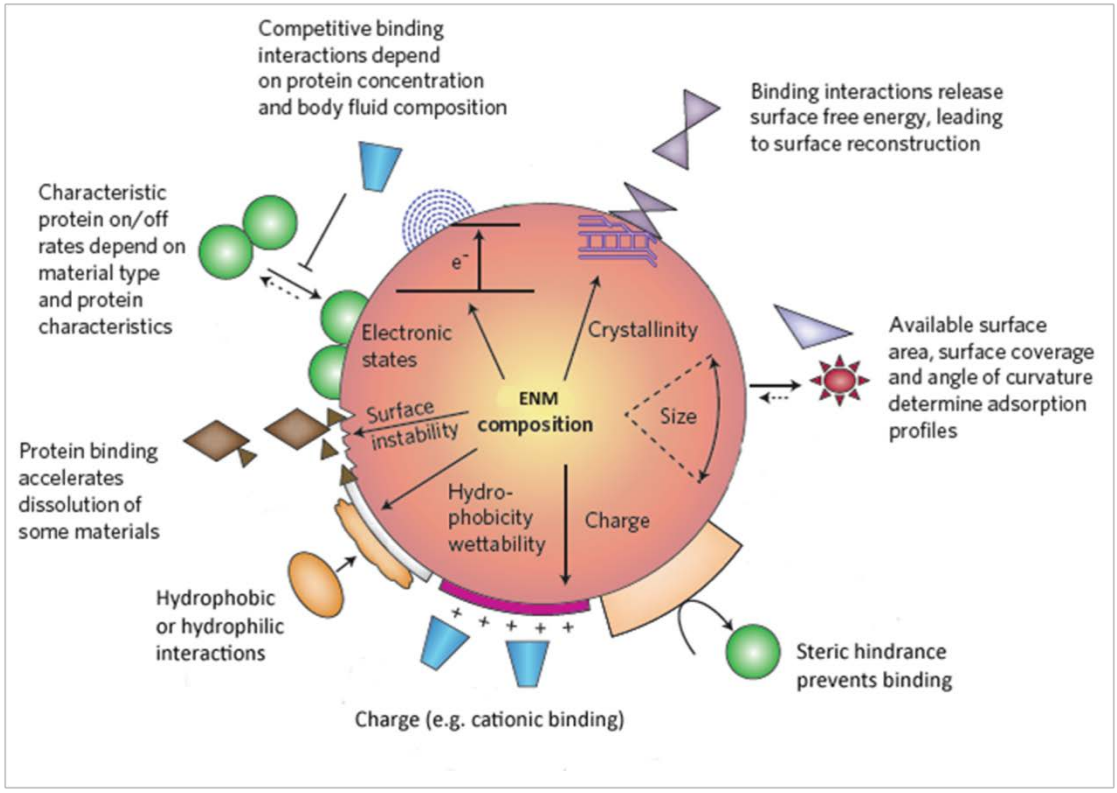


**Figure 2.3a:** Formation of protein corona is dictated by pre-existing properties of ENMs. The colored symbols represent various types of proteins and biomolecules with different physico-chemical properties. [Adapted from (Nel et al. 2009) with copyright permission from Nature Publishing Groups]

The primary nano-bio interface will shape the fate of ENMs as well as they have influence on the structural conformation of proteins forming the corona. For instance, binding of proteins like complement and immunoglobulin to ENM, promotes receptor-mediated phagocytosis clearance of ENMs; polyethylene glycol (Moreira et al.)-coating

hinders ENM interaction with plasma proteins which increases the circulation of PEGylated ENMs and decrease the clearance from body (Owens Iii et al. 2006). The presence of proteins and organic substances facilitates the leaching and solubalization of metal ions from ZnO, CdSe, iron oxide, and aluminum oxide based ENMs (Xia et al. 2008). On the other hand ENM and nano-bio interface may also alter conformations of proteins that form a corona on ENM leading to exposure of new epitopes, alterations in protein function or enzymatic activities (Nel et al. 2009) (Figure 2.3a). An abiotic experiment has shown that ceria, copolymer ENM and CNTs act as a catalyst, exposing protein interaction domains that induce human β-microglobulin fibrillation (Baca et al. 2006). There is no biological evidence available yet; however repetition of same process in the brain could contribute to the neurodegenerative process in Alzheimer disease (Nel et al. 2009). Similarly, possible formation of electron-hole pair or electron confinement on ENM's surface could oxidatively damage covalent bonding and cross-linking of protein-SH domains, e.g. $SiO_2$ ENMs induces unfolding of α-helix, and cause loss of enzyme activity in chicken egg lysosomes (Vertegel et al. 2004). On a similar note, if cryptic epitopes of proteins are exposed on ENM surface, then newly exposed antigen sites may induce auto-immune response (Figure 2.3b) (Nel et al. 2009).

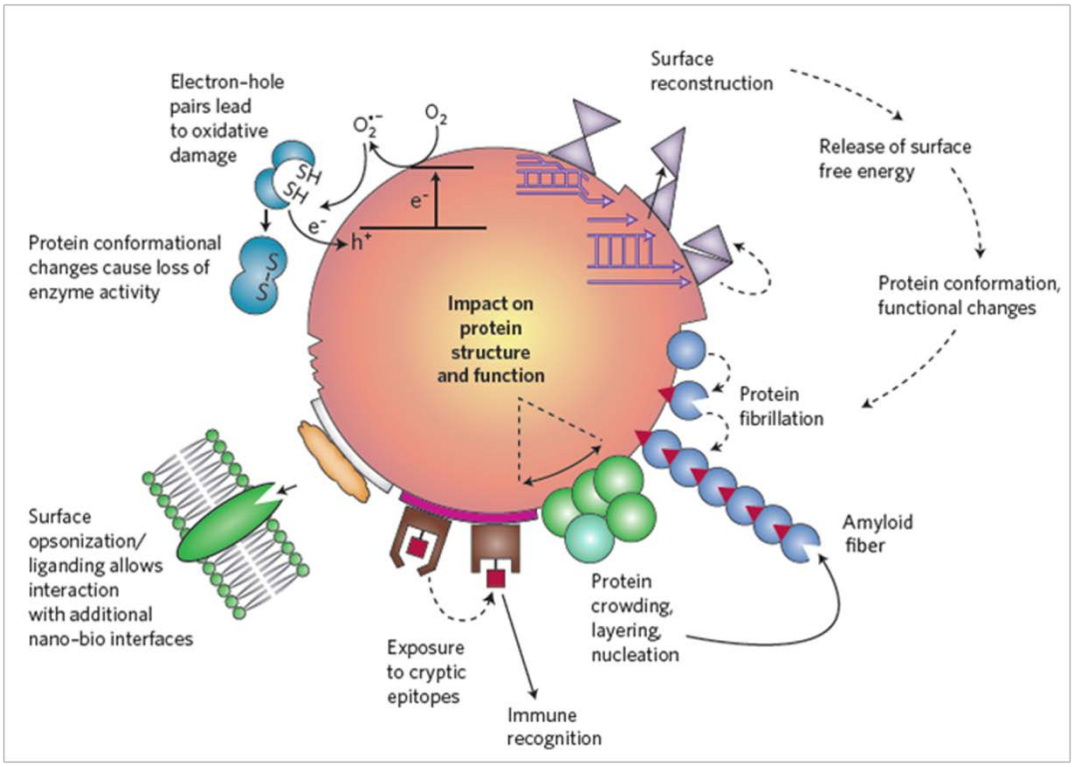


**Figure 2.3b:** Impact of nano-bio interactions on protein structure and function. The colored symbol represents various types of proteins with different physico-chemical properties. [Adapted from (Nel et al. 2009) with copyright permission from Nature Publishing Groups]

### 2.4. Physico-chemical properties and toxicity of ENM

With burgeoning technological growth, intentional or unintentional exposure to any material used in industrial, consumer, medical or research application has always been a major topic of concern. Similarly, from the past decade, researchers are putting efforts in investigation of potential health risk associated with nanomaterial usage. However, compared to the exponential growth of nanotechnology, the efforts in the field of toxicity of nanomaterials are negligible. For example, compare to the number of publications on

nanotechnology from year 1990 to 2005, the research publications on nanotoxicity during that period is less than 0.002% (Buzea et al. 2007; Yokel et al. 2009).

Nanometer sized particles generated from natural activities such as dust storms, forest fires, volcanic eruptions, ocean and water evaporation, organisms-viruses, or as by-products of human activities, like diesel and engine exhaust nanoparticles, cigarette smoke, burning coal or wood, building construction, and cosmetic or other consumer products etc., are known as ambient ultrafine particles (Buzea et al. 2007). A short- or long-term exposure to any of these nano-sized materials is shown to have adverse health effects. This knowledge about toxicity of ambient nanomaterials has helped to form a basis to understand the potential adverse health effects of ENMs (Oberdörster et al. 2005; Buzea et al. 2007). The critical point to consider with ENMs is that they can be manufactured in almost any size and shape with variety of combinations of chemical compositions and surface coatings. These very properties of ENMs that are exploited for diverse applications of ENMs can have detrimental side-effects on health and environment. Therefore, while evaluating the nanotoxicity, it is important to consider the role of physico-chemical properties of ENMs in their toxicity (Oberdörster et al. 1994; Nel et al. 2006; Buzea et al. 2007; Fubini et al. 2010). In this dissertation research we have explored influence of size- and shape or aspect ratio as well as exposure period on the toxicity of ceria ENMs.

The possible conformational and structural changes in protein corona leading to their functional disability can cause potential molecular mechanism of injury that could contribute to disease pathogenesis. The primary nano-bio interactions at lysosome are a key to use ENM in the drug delivery as well as for nanomaterial toxicity, however only

toxicity related points are discussed here. Amino-labeled polystyrene, cationic dendrimers and polymers bind with high affinity to the surface lipid-groups on lysosome, which then is endocytosed in the crowded vesicle. Once entered, amino groups from ENM keep the proton pumps on the lysosome surface in continuously active state, flooding the vesicle with chloride ions and water molecules. Eventually the lysosome swells beyond its capacity and bursts open expelling internal content, triggering intracellular $Ca^{2+}$ release, ultimately causing cytotoxicity (Xia et al. 2007). In another experiment, uptake of ZnO ENM in lysosome accelerates its dissolution due to acidic environment and release of excess zinc ions into the cell can induce cytokine production and cytotoxicity (Xia et al. 2008).

Another review article has summarized possible mechanisms by which ENMs can induce oxidative stress mediated cytotoxicity (Nel et al. 2006) (Figure 2.4). Fullerene or $TiO_2$ based or any other metal oxides based ENMs with discontinuous crystal planes and defects or with semiconductor type compositions or with electron donor groups can reduce biomolecules on their surface. Ambient ultrafine particles, carbon nanotubes or metal based ENMs (Fe) or organic materials (quinone) can facilitate Fenton type chemical reactions or enzymatic reaction. $TiO_2$ based ENMs can act as photo-catalyst and generate electron and hole pair in presence of UV light, so they have applications in cosmetic industries, solar cells, etc. However, when ENM came in contact with biomaterial in UV or natural light, they may cause reduction of biological molecules (Xia et al. 2008). Zinc, cadmium and selenium ions leaching out from ZnO or CdSe or CdTe based ENMs can disrupt cellular metabolism (Kirchner et al. 2004; Zhang et al. 2007; Xia et al. 2008).

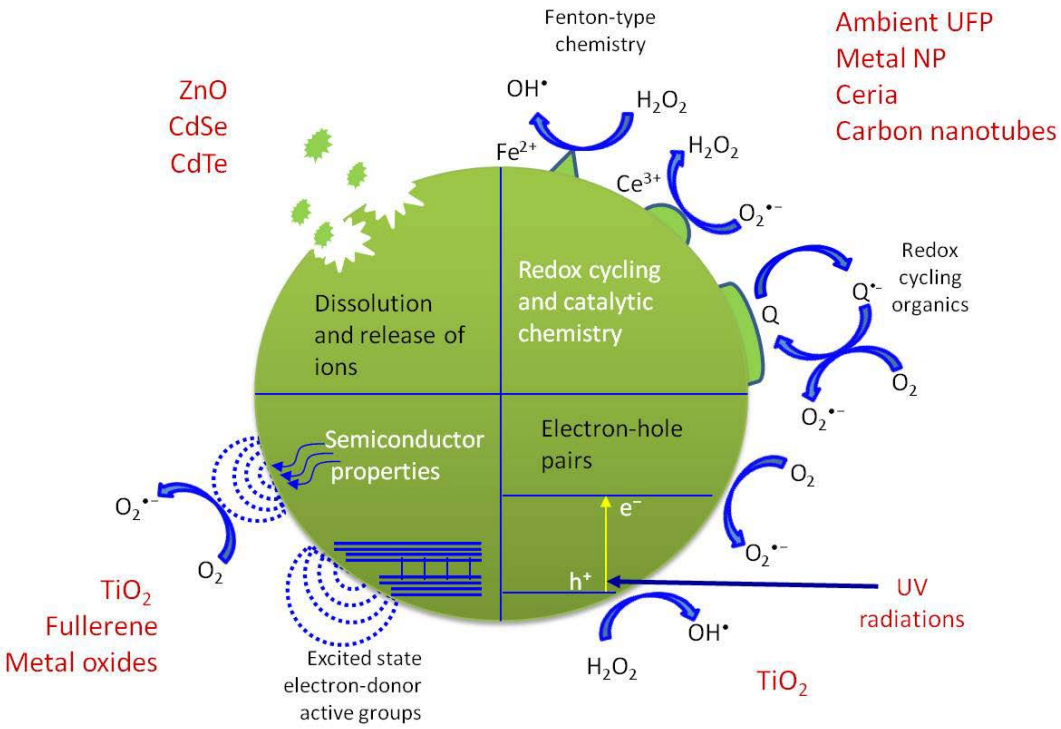


**Figure 2.4:** Oxidative stress mechanism of ENM cytotoxicity and involvement of surface chemistry.

## 2.5. Free radicals, antioxidants and oxidative stress

Oxidative stress is one of the important mechanisms of nanoparticles toxicity. Nanoparticles with metal atoms or ions, or electron donor or acceptor groups, any other redox active groups present on their surface can generate free radicals on their surface in presence of oxygen or ozone (Nel et al. 2006). Further the free radicals can impart toxic effects by reacting with biological molecules and damage them.

**2.5.1. Free radicals:** Free radicals are atoms, molecules or ions with one or more unpaired electrons that render them very labile. To counteract this labile condition, free radicals are strongly impelled to reacts with electron donor or acceptor groups. At the end

of the reaction, free radicals gain or lose an electron and become stable, while the other group or species become labile. This newly form secondary radical then react with some other group to regain the stability and thus a free radical chain reaction propagates. When a radical chain reaction occurs in biological system, it leaves biological molecules proteins, lipids and DNA oxidatively damaged. In aerobic organisms free radicals are generated in and through normal physiological processes. The major source of free radicals is electron transport chain in mitochondria, and some other sources are NADPH oxidase, xanthine oxidase, cytochrome P450 and Haber-Weiss reactions with transition metals (Shigenaga et al. 1994). Although free radicals are highly reactive and potentially damaging, they are also integral part of some cellular processes. Extracellular secretion of free radicals by leucocytes and microphages evoke immune response against bacteria, viruses, degenerated cells and other foreign substances (Simko 2007; Simkó et al. 2011). Intracellular secretion of free radicals stimulates different cell signaling pathways, trigger oxidative stress defense response, as well as apoptosis (Simko 2007; Simkó et al. 2011). Apoptosis or programmed cell death mediated by free radicals is thought to be one of the tumor suppression mechanisms (Simko 2007; Simkó et al. 2011). Because of perilous nature of free radicals, cells have a counter mechanism know as antioxidant defense, to keep the free radical levels under check. Unfortunately, when certain conditions promote the excess production of free radicals or deplete the antioxidant defense that leads the cell to oxidative damage, oxidative stress is said to exist. This can be one consequence of exposure to nanoparticles.

Some of the examples of free radicals are given in the Table 2.5.1. Free radicals much often are reactive oxygen species (ROS), or reactive nitrogen species (RNS) but all ROS

or RNS are not free radicals. Some of the well known ROS and RNS that are particularly discussed in the present dissertation work are superoxide ($O_2^{\bullet-}$), hydrogen peroxide ($H_2O_2$), hydroxyl radical ($OH^{\bullet}$), nitric oxide radical ($NO^{\bullet}$), and peroxynitrite anion ($ONOO^-$).

| Radical species | | Non-Radical Species |
|---|---|---|
| Superoxide, $O_2^{\cdot-}$<br>Hydroxyl, $\cdot OH$<br>Peroxyl, $RO_2\cdot$<br>Alkoxyl, $RO\cdot$<br>Hydroperoxyl, $HO_2\cdot$ | ROS | Hydrogen peroxide, $H_2O_2$<br>Hypochlorous acid, HOCl<br>Ozone, $O_3$<br>Singlet oxygen, $^1\Delta g$<br>Hypobromous acid, HOBr |
| | | |
| Nitric oxide, NO<br>Nitrogen dioxide, $NO_2$ | RNS | Nitrous acid, $HNO_2$<br>Nitrosyl cation, $NO^+$<br>Nitroxyl anion, $NO^-$<br>Dinitrogen tetroxide, $N_2O_4$<br>Dinitrogen trioxide, $N_2O_3$<br>Peroxynitrite,[d] $ONOO^-$<br>Nitronium cation, $NO_2^+$<br>Nitryl chloride, $NO_2Cl$<br>Alkyl peroxynitrates, $ROONO^-$ |

**Table 2.5.1:** Examples of reactive oxygen (ROS) and reactive nitrogen species (RNS)

**2.5.1.1. ROS:** Superoxide radical is formed by one electron reduction of oxygen. Although electron-transport chain at mitochondrial membrane is a highly efficient electron transporter, some electrons can leak and reduce oxygen molecule to form $O_2^{\bullet-}$, and mitochondria serves as a major source of $O_2^{\bullet-}$. Another location of electron-transfer is endoplasmic reticulum, where $O_2^{\bullet-}$ can generate by leakage of electrons from NADPH cytochrome P450 reductase. Some additional sources of $O_2^{\bullet-}$ are xanthine oxidase, phagocytic NADPH oxidase, as well as UV-γ radiation etc.

Superoxide radical is further converted into $H_2O_2$ and oxygen by enzyme superoxide dismutase (SOD). Although both $O_2^{\bullet-}$ and $H_2O_2$ can damage biomolecules, they are only moderately reactive with biomolecules (Kamata et al. 1999). However, both superoxide and hydrogen peroxide can further generate highly potent and notoriously reactive hydroxyl radical. Hydrogen peroxide alone undergoes Fenton type reaction to generate $OH^{\bullet}$ radical in presence of transition metals $Fe^{2+}$ or $Cu^{1+}$ (Kehrer 2000). Whereas, $O_2^{\bullet-}$ and $H_2O_2$ react together in presence of transition metals $Fe^{2+}$ or $Cu^{1+}$, to produce $OH^{\bullet}$ radical, and reaction is known as Haber-Weiss process (Kehrer 2000).

$$H_2O_2 + Fe^{2+} \text{ or } Cu^{1+} \longrightarrow OH^{\bullet} + OH^{-} + Fe^{3+} \text{ or } Cu^{2+}$$ .....Fenton reaction

$$O_2^{\bullet-} + H_2O_2 \xrightarrow{Fe/\ Cu} OH^{\bullet} + OH^{-} + O_2$$ .....Haber-Weiss process

All the above mentioned ROS can oxidize biomolecules proteins, lipid and DNA's and functionally damage them.

**2.5.1.2. RNS:** Nitric oxide ($NO^{\bullet}$ or simply NO) and peroxynitrite ($ONOO^{-}$) are reactive nitrogen species (RNS). NO is produced from amine acid L-arginine by enzymatic action of nitric oxide synthase (NOS) enzymes, as shown below.

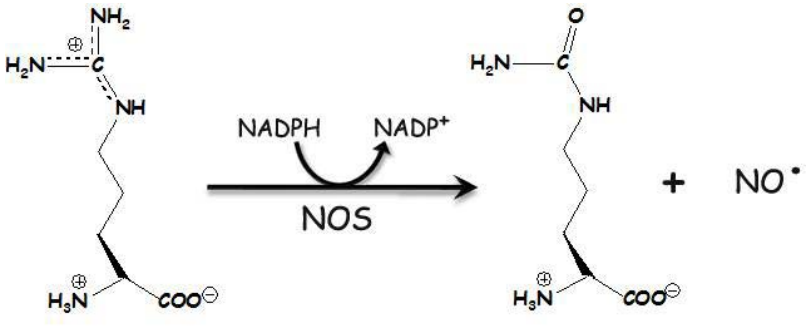


.....NO synthesis

NO exhibits neuroprotective as well neurotoxic effects, depending on cellular redox status (Halliwell et al. 1999; Calabrese et al. 2006; Calabrese 2007). In the presence of $O_2^{\bullet-}$, nitric oxide form peroxynitrite anion, which get rapidly protonated under physiological condition to peroxynitrous acid, a very reactive RNS. Peroxynitrous acid itself can oxidize and nitrate proteins, lipids and DNA's (Radi et al. 1991; Alvarez et al. 2003), as well as it can undergo homolytic fission to form even more reactive $OH^{\bullet}$ (Halliwell 2006).

$NO^{\bullet} + O_2^{\bullet-} \longrightarrow ONOO^-$ …..Formation of peroxynitrite anion

$ONOOH \longrightarrow NO_2^{\bullet} + OH^{\bullet}$ …..Fission of peroxynitrous acid

Peroxynitrite anion can react with carbon dioxide to form nitrogen dioxide radical, which can attack tyrosine amino acid residue of proteins to form protein nitration product known as 3-nitrotyrosine (3NT).

$ONOO^- + CO_2 \longrightarrow ONOOCOO^- \longrightarrow NO_2^{\bullet} + CO_3^{\bullet-}$ ….Nitrogen dioxide formation

**2.5.2. Antioxidants:** To protect biomolecules from detrimental effects of free radicals, the cell produces different antioxidant molecules and enzymes, which together they are known as the antioxidant defense system. According to Halliwell (Halliwell 2007), "antioxidant is any substance that delay, prevents, or remove oxidative damage to a target molecule".

Four very important antioxidant enzymes are superoxide dismutase (SOD), glutathione peroxidase (GPx), glutathione reductase (GR), and catalase and various other low molecular weight antioxidant molecules such as glutathione, ascorbic acid, vitamin-E,

vitamin-C, etc. constitute the cellular defense system. Considering the scope of this dissertation work, this discussion is limited to GPx, GR, SOD, catalase and glutathione antioxidants.

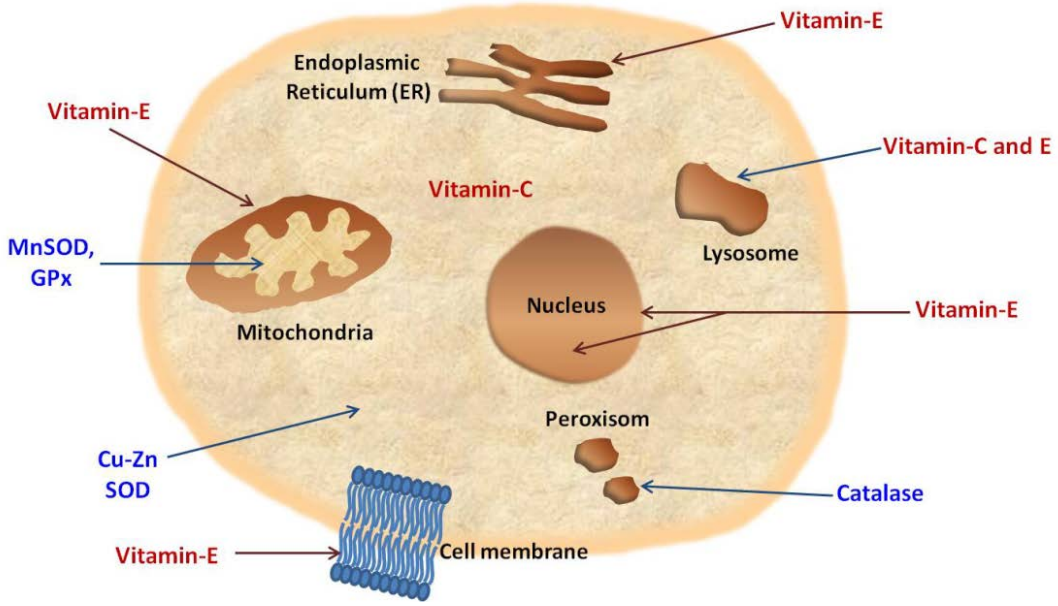


**Figure 2.5.2:** Locations of antioxidant enzymes (blue) and anioxidant molecules (red). SOD stands for superoxide dismutase and GPx for glutathione peroxidase.

**2.5.2.1. Superoxide dismutase (SOD)** converts superoxide radical into hydrogen peroxide and oxygen. Eukaryotic cells have two major isoforms of SOD, copper-zinc (CuZn SOD) localized in cytosol and manganese (MnSOD) localized in mitochondria. The importance of SOD has been exemplified by experiments with MnSOD-knockout mice (Murakami et al. 1998). As well as removing the $O_2^{\bullet-}$ radicals, SOD also generates another ROS- $H_2O_2$. SOD usually works in conjunction with $H_2O_2$- removing enzymes such as GPx or catalase (Evans et al. 1999).

$$O_2^{\bullet-} \xrightarrow{SOD} H_2O_2 + O_2 \qquad \text{.....SOD reaction}$$

**2.5.2.2. Glutathione peroxidase (GPx)** reduces various intracellular peroxides such as $H_2O_2$ and lipid peroxides, using glutathione (GSH) as electron donor. GPx has eight isoforms, identified in humans and GPx1 is the most abundant isoform, localized in cytosol (Muller et al. 2007). GPx has selenium at its active site. A mini review summarizes various oxidative stress effects caused by inactivation of GPx and cellular adaptive response to GPx inactivation (Miyamoto et al. 2003).

$$H_2O_2 + 2GSH \xrightarrow{GPx} 2H_2O + GSSG \qquad \text{…..GPx reaction}$$

**2.5.2.3. Glutathione reductase (GR)** is another GSH related enzyme, which reduces oxidized glutathione GSSG to its reduced form GSH. GR uses NADPH as reducing equivalent to carryout reduction of GSSG. GR is highly conserved in all the kingdoms, including animal, bacteria, yeast, and plants. Age-related decrease in GR activity has seen in mouse erythrocytes, kidney, heart and liver (Hazelton et al. 1980) as well as rat liver, lung, heart, spleen and brain (Blakytny et al. 1992).

$$GSSG + NADPH + H^+ \xrightarrow{GR} 2GSH + NADP^+ \qquad \text{…..GR reaction}$$

**2.5.2.4. Catalase (Cat)** is a very efficient enzyme that scavenges potent ROS hydrogen peroxide. Majority of catalase in localized in peroxisomes. Inhibition of catalase activates compensatory cellular response in goldfish liver in kidney and induces GPx and GST activities (Bagnyukova et al. 2005). Overexpression of catalase HepG2 cells, rescued the cells from cytochrome P450 induced oxidative stress injury (Bai et al. 2001). As well as reduced catalase expression and activity make the cells more susceptible to become carcinogenic (Khan et al. 2010).

$$H_2O_2 \xrightarrow{Catalase} 2H_2O + O_2 \qquad \text{…..Catalase reaction}$$

**2.5.2.5. Glutathione (GSH)** an endogenous abundant antioxidant tri-peptide (Figure 2.5.3.5a) that acts as an antioxidant due to virtue of its amino acid cysteine residue. GSH contains the amino acids glutamate, cysteine, and glycine, with glutamate and cysteine connected via a γ-linkage (Figure 2.6), therefore making the bond less susceptible to protease degradation.

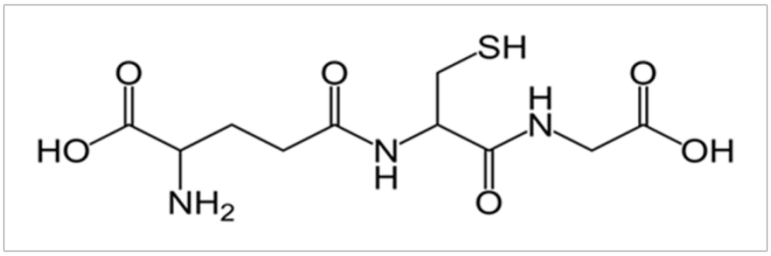


**Figure 2.5.2.5a:** Structure of Glutathione (GSH).

GSH is a versatile antioxidant and its primary role is to provide electrons or H for detoxification of peroxides carried out by GPx. During this reaction GSH forms disulphide bond with another GSH molecule, oxidized glutathione GSSG is recycled back by another enzyme GR, using NADPH as a reducing equivalent (Figure 2.5.2.5b). The ratio of GSH: GSSG is indicative of oxidative stress; ~10:1 is what healthy cells usually have. A decrease in this ratio or depletion in GSH levels triggers various cellular defense responses, known as phase II antioxidant response (Lee et al. 2008; Speciale et al. 2011). In addition to the redox activity GSH can scavenge alpha-beta unsaturated aldehyde or ketone though Michael addition and can form nitroso-thiol to protect against nitrosative stress. As well as GSH can chelate heavy metal ions such as mercury, probably to prevent the metal toxicity mediated by ROS generation (Patrick 2002).

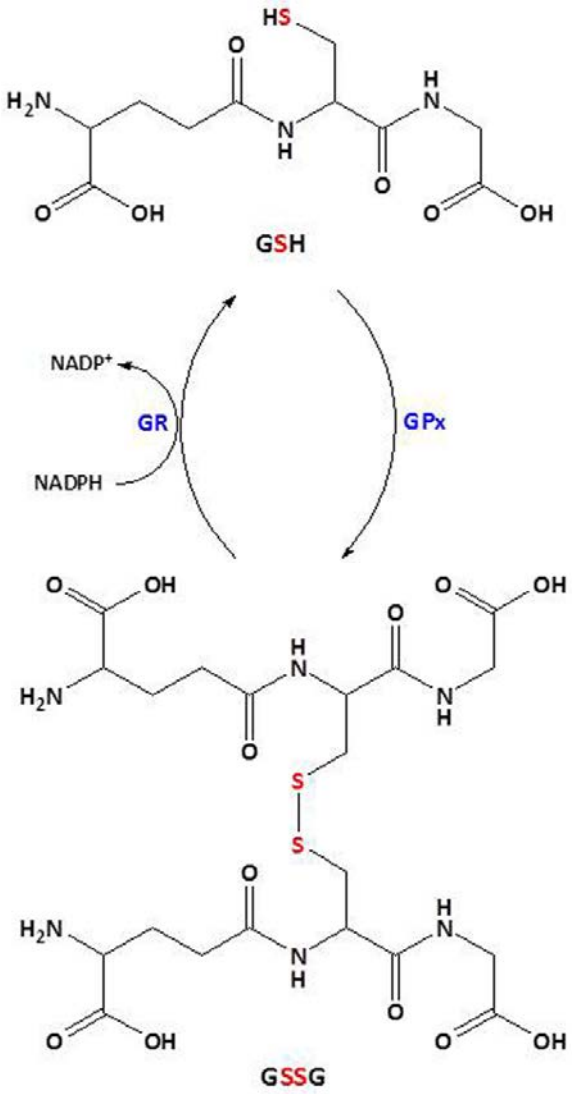


**Figure 2.5.2.5b:** Oxidation and reduction cycle of glutathione. GSH is the reduced form of glutathione which oxidized into GSSG, while scavenging peroxides by glutathione peroxidase (GPx) and then reduced back to original GSH by enzymatic action of glutathione reductase (GR).

**2.5.3. Heat shock proteins:** Heat shock protein (HSPs) is the family of proteins that are of different molecular weight and structure but all functionally related. HSPs are named according to their molecular weight except ubiquitine, whose molecular weight is 8 kDa.

The important function of HSPs is to chaperon other proteins. HSPs play important roles in protein-protein interactions such as protein folding, assisting other proteins in attending proper conformation, and preventing unwanted protein aggregation. HSPs also help to stabilize partially unfolded proteins and escort them across membranes or through organelles within a cell for proteasome degradation. Some house-keeping HSPs are expressed under normal physiological conditions, but as their name suggests, HSPs are induced by temperature, exposure to heavy metals, cytotoxic drugs and other stress including oxidative stress (Calabrese et al. 2000; Calabrese et al. 2000). The HSPs studied in this dissertation work, Hsp70 and Hsp32 (a.k.a. Heme oxygenase-1 or HO-1) can be induced by oxidative stress (Calabrese et al. 2000; Calabrese et al. 2000).

**2.5.4. Oxidative stress:** Is defined as "A disturbance in the pro-oxidant-anti-oxidant balance in favor of the former, leading to potential damage" (Halliwell 2007). Under normal physiological conditions although ROS and RNS are generated, their levels are efficiently regulated by antioxidant-enzymes and -molecules to maintain the cellular redox balance Figure 2.5.4**.** The imbalance in pro- and anti-oxidant can be caused by increased levels of free radical generation and/ or could be result of antioxidant depletion, failure of repair or replacement system (Halliwell et al. 2004; Halliwell et al. 2007). In any case, either both circumstances occurring together or separately, eventually will lead to deleterious modifications of biomolecules, and multitude of downstream consequences. Oxidative stress has been implicated in vast array of conditions including cancer, arthritis, cardiovascular diseases, diabetes, aging, and neurodegenerative disorders.

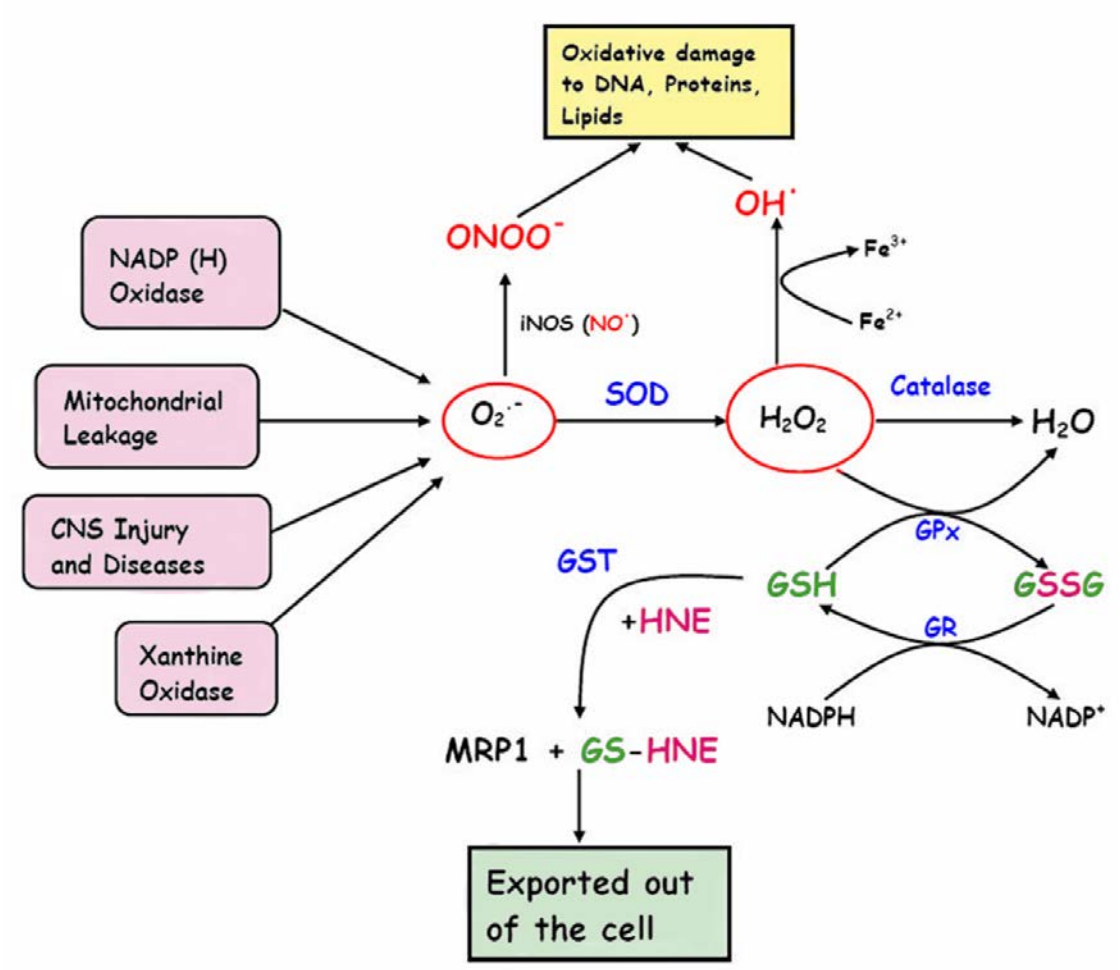


**Figure 2.5.4:** Different endogenous sources for ROS/ RNS, antioxidant defense and clearance of HNE. Where, GST stands for glutathione s-transferase, MRP1 stands for multidrug resistance protein 1 and HNE is one of the end-product of lipid peroxidation. Antioxidant enzymes are shown in blue and antioxidant molecules glutathione in green color. ROS and RNS are in red color.

**2.5.4.1. Oxidation of biomolecules- Protein carbonyls (PC):** The functions of proteins are highly dependent on their tertiary structures and any disruption of this spatial arrangement can have serious consequences on the activities of enzymes and proteins. Increased oxidative stress induces oxidative modification of biological molecules such as

proteins, lipids and nucleic acids. Oxidative modifications such as carbonylation, nitration, s-nitrosylation, glycosylation etc. can severely disrupt spatial arrangement of proteins damaging their functions partially or completely.

Protein carbonylation is one of the most common post-translational oxidative modifications, resulting from and direct cleavage of protein backbone (Figure 2.5.4.1a) and β-scission of the amino-acid side chains (Figure 2.5.4.1b) by ROS or RNS (Butterfield 1997; Stadtman 2006). Protein carbonyls (PC) can also arise from adduction of alkenals like HNE and acrolein to Cys, His, and Lys residues by Michael addition (Figure 2.5.4.1c) and glycoxidation reactions (Butterfield 1997; Stadtman 2006). Studies have shown that protein carbonylation does not depend on amount of proteins but some proteins are more susceptible to carbonylation than the other (Cabiscol et al. 2000; Jana et al. 2002; Choi et al. 2005; Dalle-Donne et al. 2006). Such selective susceptibly is likely due to protein structure and presence of transition metal binding-site (Stadtman 1990; Stadtman 2006). Since protein carbonylation is an irreversible form of oxidative modification, immunochemical detection of protein carbonyl (PC) levels (described in Chapter 3) is a widely recognized way to index global oxidative stress and damaged to proteins in a given biological sample.

Initial studies discovered that primary site of hydroxyl radical attack is alpha carbon of amino acids (Swallow 1960; Garrison et al. 1962; Schuessler et al. 1984; Garrison 1987) as well as aliphatic amino acid side chain (Stadtman et al. 2003). As shown in Figure 2.5.4.1a, abreaction of H• from alpha carbon by hydroxyl radical produces a C-C cross linking in absence of oxygen and peroxyl radical (-COO•) in aerobic conditions. This peroxyl radical can be neutralized by abstraction H• from alpha carbon of adjacent

protein, thus propagating the radical chain reaction. In the presence of transition metal ions like $Fe^{2+}$ or $HO_2$• radical, the alkyl peroxide (ROO•) radical is converted into alkoxyl radical, which will be then lead to protein carbonylation either by α-amidation pathway or by diamide pathway (Figure 2.5.4.1a). In the α-amidation pathway, the alkoxyl radical is reduced to a hydroxyl, which will be eventually forming an N-terminal amide derivative and C-terminal alkyl carbonyl derivative. Alternatively alkoxyl radical can undergo diamide pathway and can form diamide derivative of N-terminal cleavage product and isocyanides derivative of C-terminal of protein after undergoing β-scission. As shown in Figure 2.5.4.1b [adapted from (Bader Lange 2010)], peptide bond of an amino acid residue say valine can directly undergo β-scission after attack of •OH (Stadtman 2006).

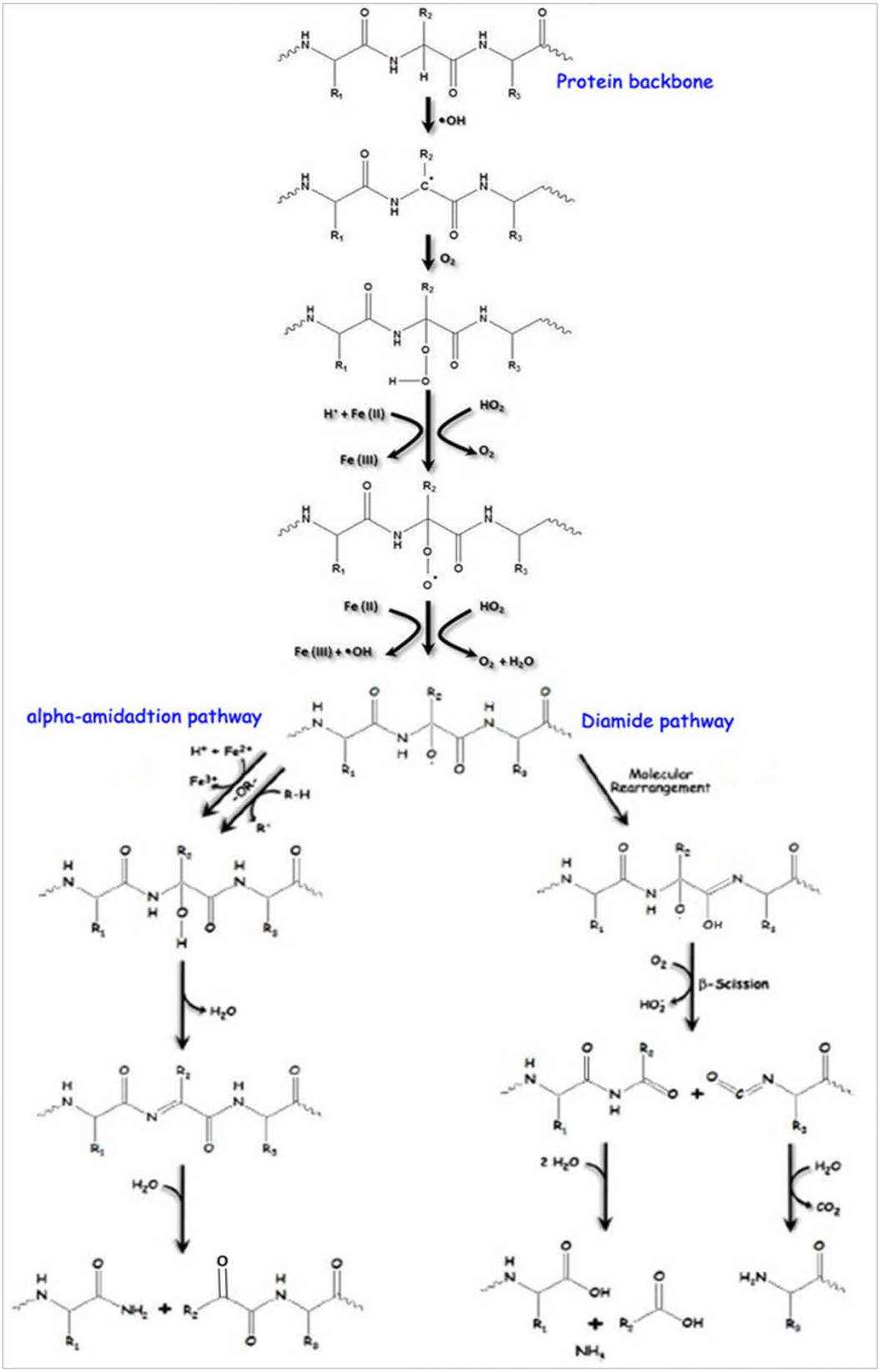


**Figure 2.5.4.1a:** Oxidative cleavage of peptide backbone.

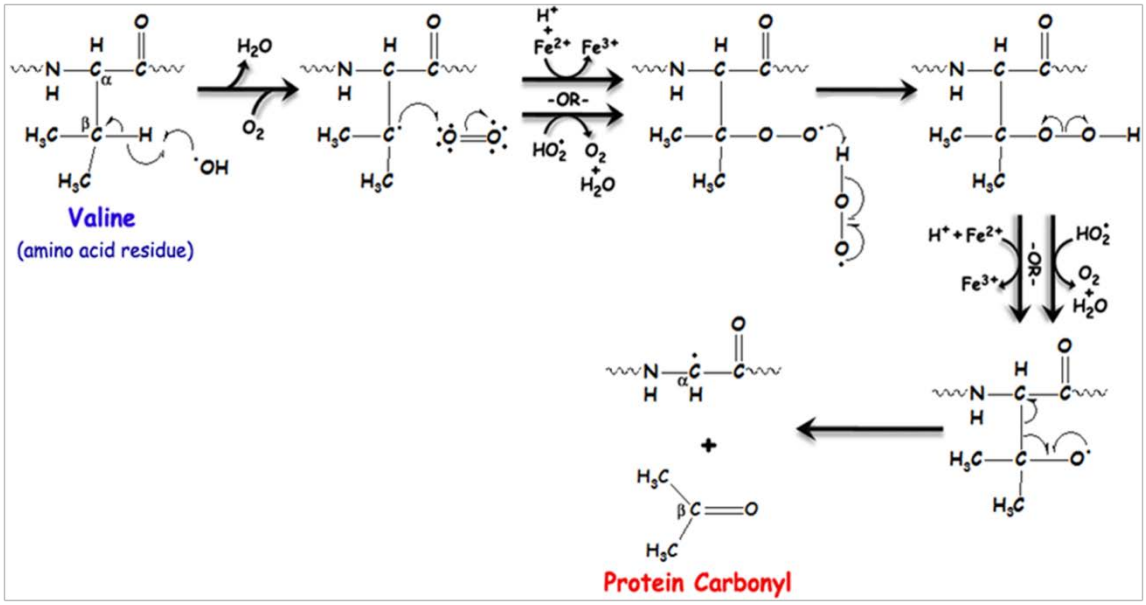


**Figure 2.5.4.1b:** Oxidative cleavage of amino acid side chain- β-scission of valine.

**2.5.4.2. 3-Nitrotyrosine (3NT) and S-nitrosylation:** Nitric oxide (NO•) is an extremely important biological radical, particularly because of its role as a second messenger in vasodilatation (Calabrese 2007).However, in conditions of oxidative stress where excessive production of NO is induced and significant amounts of $O_2^{-\bullet}$ are present, RNS resulting from their interaction can damage proteins. Proteins with tyrosine residue are especially susceptible to RNS attack. The interaction NO and $O_2^{-\bullet}$ forms highly reactive peroxynitrite anion, which in presence of $CO_2$ produces nitrite radical ($NO_2$•) [described in section 2.5.1.2a, taken from (Bader Lange 2010)]. As shown in Figure 2.5.4.2, $NO_2$• attacks the meta- or '3'-position of the tyrosine residue, because of the ortho- and para-directing electron-donating resonance effect of –OH group. The addition of nitrite group on tyrosine can disrupt protein structure as well as bulky nitrite group imposes steric

hindrance to the substitution of –OH group, interfering with the protein function and metabolic processes (Halliwell et al. 1999; Greenacre et al. 2001; Alvarez et al. 2003). Similar to PC, immunochemical detection of 3-nitrotyrosine (3NT) (described in Chapter 3) is another index of protein oxidation and global oxidative stress in a given biological sample.

Nitric oxide can also react with sulfur atom of cysteine and methionine amino acid residues in aerobic conditions (Broillet 1999; Fernhoff et al. 2009), to form S-nitrosylation derivatives of corresponding proteins as shown in the Figure 2.5.4.2b.

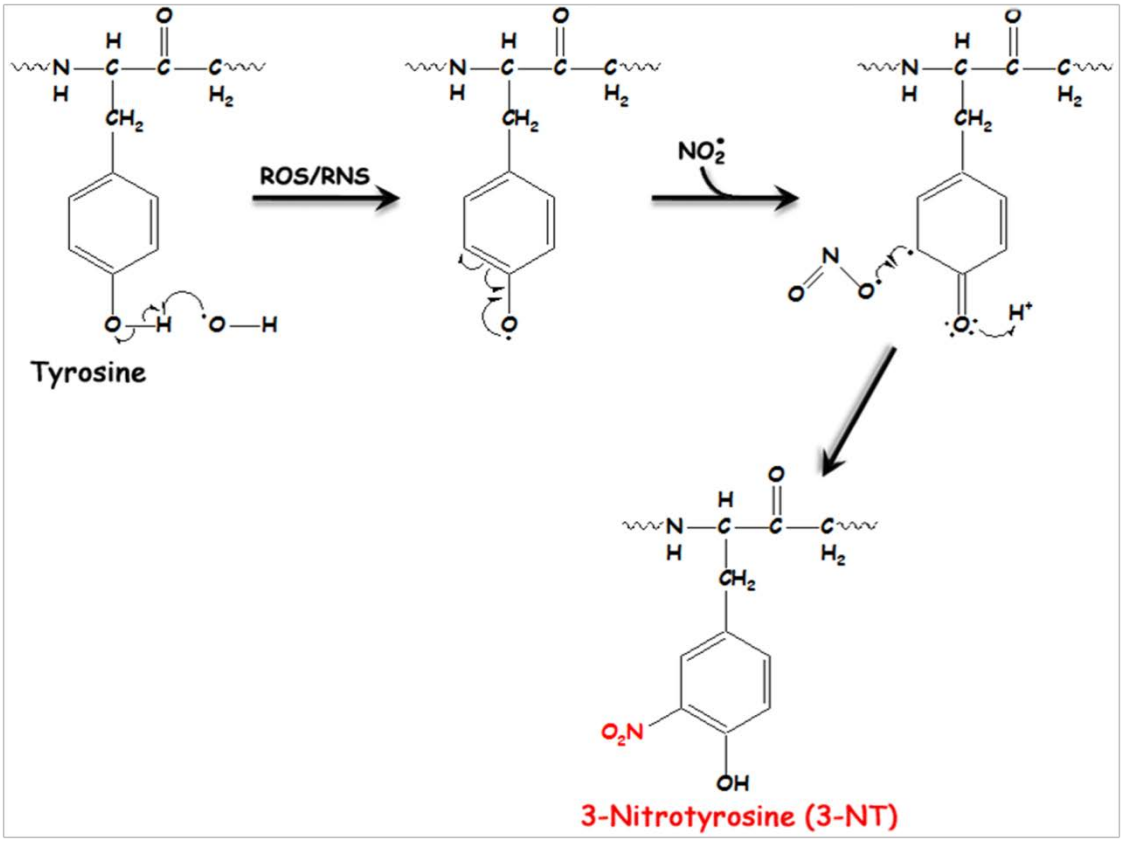


**Figure 2.5.4.2a:** Formation 3-nitrotyrosine (3NT)

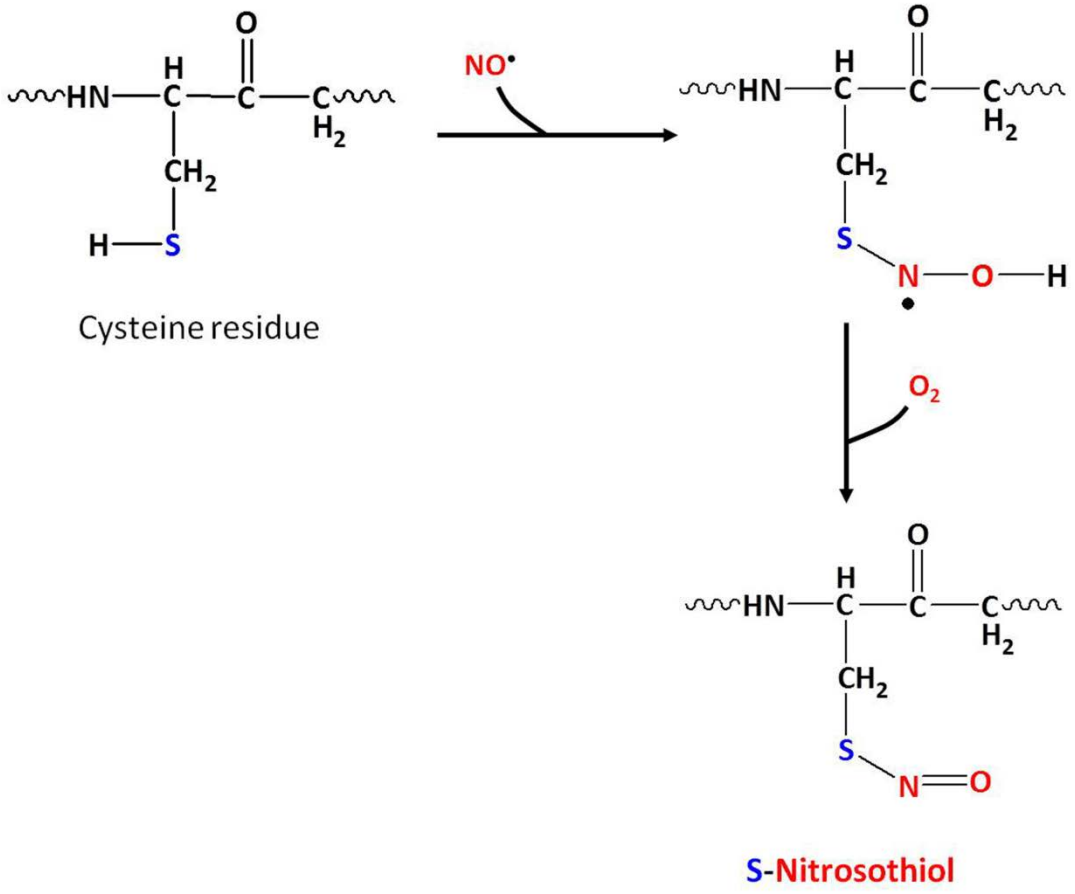


**Figure 2.5.4.2b:** Formation S-nitrosylate derivatives of cysteine in aerobic conditions.

**2.5.4.3 Lipid peroxidation and 4-hydroxy-2-trans nonenal:** Lipids with poly-unsaturated fatty acid chains (PUFA's) are more susceptible to ROS/RNS attack compare to the saturated ones. The brain contains extremely high levels of PUFA, in addition to it brain also consumes high amounts of $O_2$, combining this together makes nervous system extremely vulnerable to oxidative stress. The majority of lipid peroxidation event that occurs within the cell are result of free radical chain reaction. In which allylic hydrocarbons undergo arrack of free radical, forming alkoxyl radical (ROO•) in aerobic conditions, alkoxyl radical can then further propagate the chain reaction unless quenched (Spiteller 2001) as shown below.

$R_1H + X\bullet \longrightarrow R_1\bullet + XH$

$R_1\bullet + O_2 \longrightarrow R_1OO\bullet$

$R_1OO\bullet + R_2H \longrightarrow R_1OOH + R_2\bullet$ ……..Free radical chain reaction propagates.

$R_1OO\bullet + R_2OO\bullet \longrightarrow$ non-radical form + $O_2$ ……Quenching of radical chain reaction.

Oxidative damage to lipids generally results in formation cytotoxic aldehyde and ketone derivatives. Typically free radicals have very short half life; therefore damage caused by them is localized. Unlike free radicals, lipid peroxidation products have longer half life and so they can diffuse into bilayer and can cause oxidative damage away from their site of production. For a given fatty acid, multiple aldehydic or ketonic products can arise as result of lipid peroxidation, depending upon which allylic carbon gets attacked to initiate the chain reaction. 4-Hydroxy-2-trans nonenal (HNE) is such very reactive product of lipid peroxidation. HNE is a product of oxidation of arachiodonic acid an important fatty acid abundantly present in brain. Abstraction of labile H• from $13^{th}$ allylic carbon or oxidation of $11^{th}$ carbon, followed by peroxyl and alkoxyl formation in presence of $O_2$ and transition metal ion $Fe^{2+}$; then cyclization and β-scission results into formation of HNE (Figure 2.5.4.3a). It is also interesting to note that abstraction of same H• from arachidonic caid my yield multiple end products.

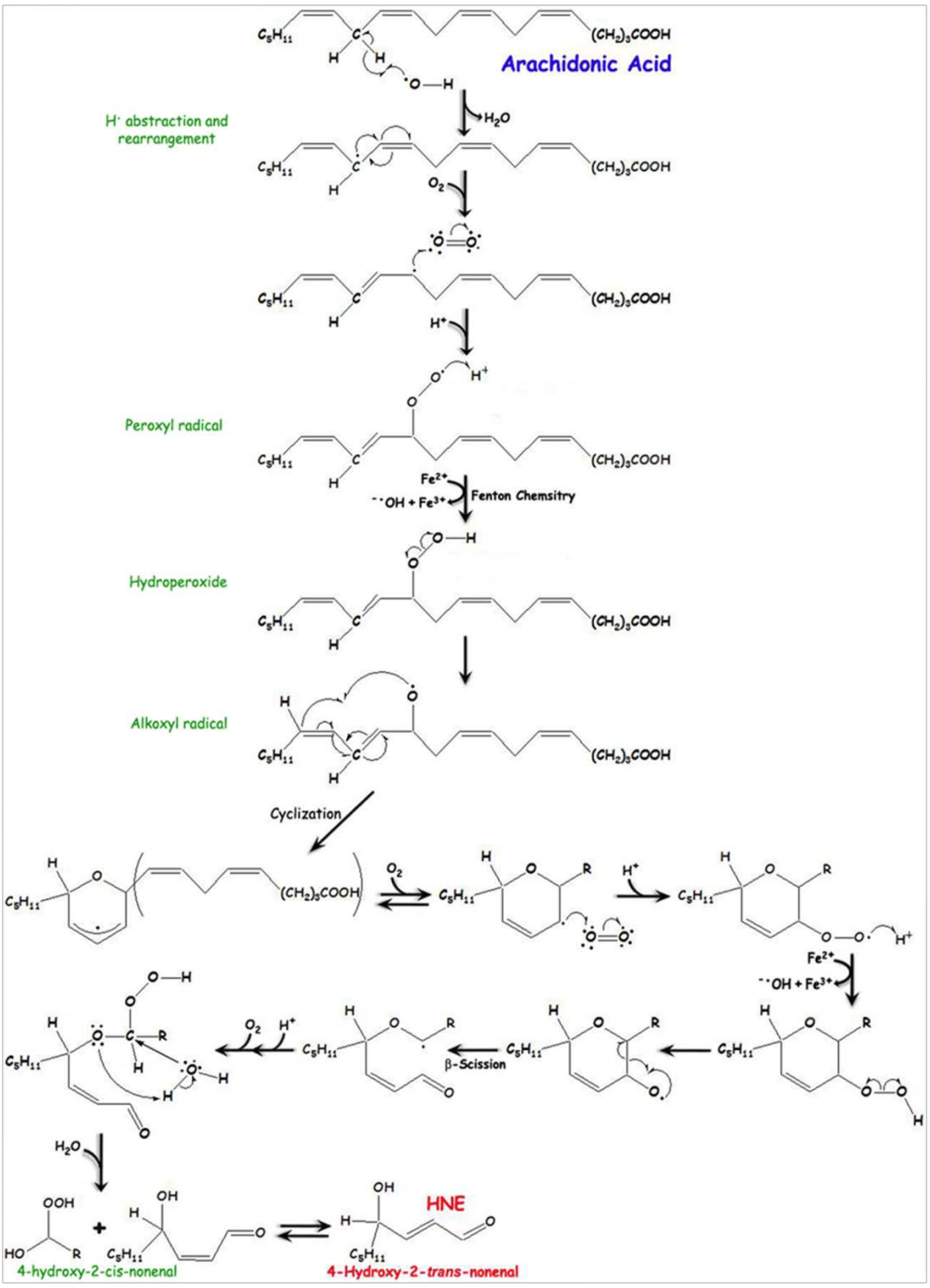


**Figure 2.5.4.3a:** HNE formation from Arachidonic acid.

Although formation of HNE itself is indicative of lipid peroxidation, the downstream products of interaction of HNE with other biomolecules can have serious consequences. HNE and other lipid peroxidation products, although less reactive than free radicals, are capable of migrating long distance from point of origin to attack biomolecules. HNE can covalently modify amino acid residues, such as histidine, cysteine, and lysine, by undergoing Michael addition (Esterbauer et al. 1991; Subramaniam et al. 1997; Schaur 2003; Siems et al. 2003) (Figure 2.4.4.3b). Similar to PC, and 3NT, immunochemical detection of HNE (described in Chapter 3) is an index of lipid peroxidation and overall oxidative stress in a given biological sample (Waeg et al. 1996).

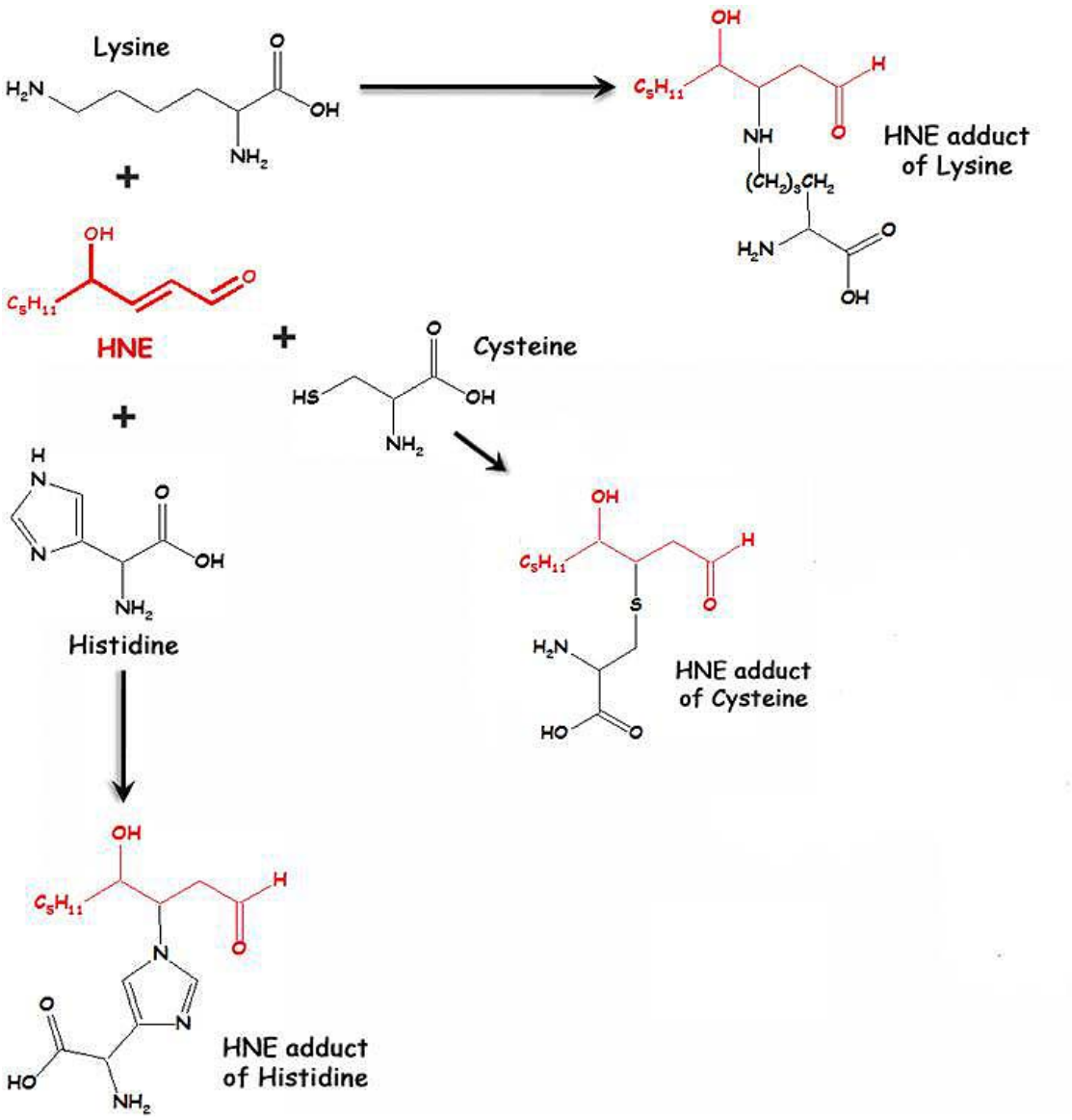


**Figure 2.5.4.3b:** Michael addition of HNE to protein residue.

### 2.6. Oxidative stress paradigm for evaluation of ENM-toxicity

When ENM of different size, shape, aspect ratio, aggregation, crystallinity, surface functionalization and so on come in contact with biological fluids, proteins, lipids, DNA, cell membrane, mitochondria, and lysosomes, can generate vast numbers of biochemical interactions. Such interactions could be biologically inert, beneficial for improvement of

biological function or process or detrimental to biological system and may or may not pose long term adverse health effects. Although many researchers have studied ENM-toxicity, their research is very much case specific and there is a need to have a standard and reliable model or algorithm or template that can be followed to evaluate the toxicity of any ENM or ENM based consumer product (Meng et al. 2009).

The knowledge about induction of oxidative stress and related biological responses such as phase II response, inflammation, apoptosis, necrosis etc. has been around for decades and well studied in case of various disease conditions and disorders. As various in-vitro and in-vivo studies reported that free radical generation can be triggered by ENMs, researcher are now accepting the induction of oxidative stress as a prominent mechanism of ENM-toxicity [as described in section 2.4.]. Based on the basic understanding of oxidative stress mediated biological responses Nel's research group has proposed a hierarchy oxidative stress model for evaluation of ENM-toxicity in cell culture model. Some studies have successfully evaluated ENM-and UFP-toxicity in cell culture media, employing this oxidative stress paradigm.

According to Nel's research (Nel et al. 2006; Nel et al. 2009), as shown in Figure 2.6., at lower levels of oxidative stress (Tier-1), phase-II antioxidant enzymes are induced by nuclear factor (Nrf-2)-signaling pathways to restore cellular redox homeostasis. At intermediate levels of oxidative stress (Tier-2) or up on failure of Tier-1 response, yield to pro-inflammatory response by activation of redox-sensitive mitogen-activated protein kinase (MAPK) and nuclear factor-kappa B (NF-κB) cascade. At the highest levels (Tier-3) of oxidative stress perturbation of mitochondrial inner membrane electron transfer and opening of permeability transition pore can trigger cellular apoptosis and cytotoxicity.

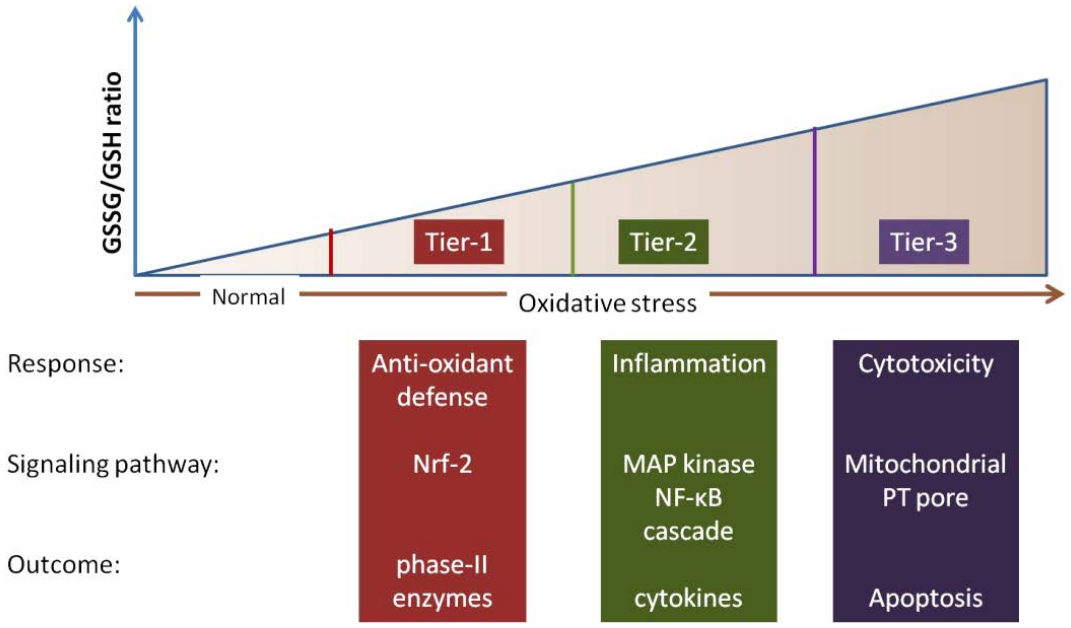


**Figure 2.6:** Hierarchy oxidative stress model proposed by Andre Nel's research group

### 2.7. Susceptibility of brain to oxidative stress and blood brain barrier

Although all aerobic cells are susceptible to oxidative damage, mammalian brain is especially vulnerable (Halliwell 1992). As well reviewed by Halliwell (Halliwell 2006), adult human brain consumes ~20% of basal levels of oxygen due to high turnover of ATP molecules, neuronal membranes are constitutes lipids with highly poly-unsaturated fatty acids side-chains as well as ~60 mg of non-heme iron present within various iron containing proteins, any damage to brain can release iron (as well as copper) ions which may initiate radical formation being the main reasons of vulnerability. Due to the high susceptibility and functional importance, brain and entire central nervous system is somewhat-isolated and protected from harmful xenobiotics and endogenous molecules by blood brain barrier (Bhaskar et al. 2010).

**2.7.1. Blood Brain Barrier (BBB):** Circulating blood is separated from the brain extracellular fluid in central nervous system by the presence of intracellular tight junction endothelial cellular lining inside blood vessels (Reese et al. 1967), Figure 2.7.1. The tight junction endothelial cell lining is present only in brain parenchyma and not the normal circulatory system. The BBB strictly regulates influx or efflux of biomolecules, protects brain from invasion of foreign substances- including viruses, bacteria, drug molecules, and thus help to maintain brain homeostasis (Ghersi-Egea et al. 1996; Shibata et al. 2000; Tanzi et al. 2004; Zlokovic 2005). The cells of adult brain parenchyma are non-degenerative; any damage to these cells including oxidative damage can lead to nonreversible consequences such as neurodegenerative disorders. The BBB provides the brain with privileged immune environment shielding against any inappropriate immune response (Niederkorn 2006; Arck et al. 2008).

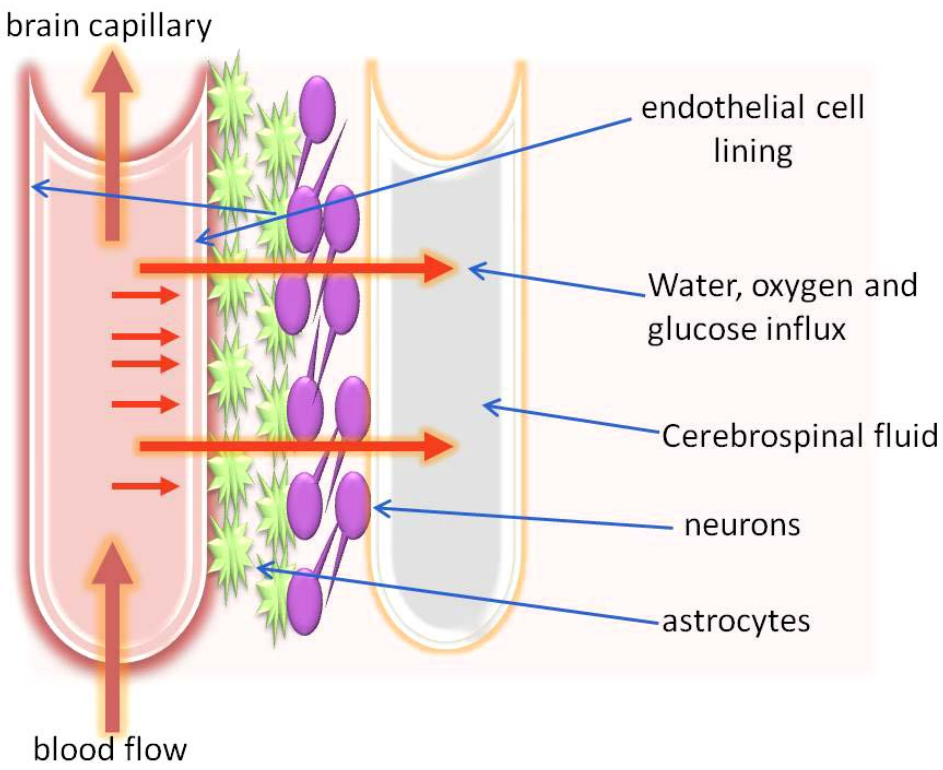


**Figure 2.7.1:** Over simplified presentation of cross-section of brain capillary and blood-brain barrier.

### 2.8. Exposure to ENM and neurological toxicity concerns

With increasing applications of ENMs and ENM-based products in various sectors, eventually these ENMs will come in contact with biological world. The primary anticipated routes of human exposure to ENMs intended for industrial or environmental applications include inhalation exposure, dermal uptake, and oral ingestion with possible subsequent absorption of ENMs into systemic circulation. Although some data exist on the absorption properties and associated toxicities of ENMs after exposure via the pulmonary, oral, and topical routes, little is known about their distribution into the brain once they reach systemic circulation (Luther 2004). Apart from unintentional exposure to ENMs and thereafter the translocation to brain, there is also considerable interest in

ENMs to enhance drug delivery to the brain, as reviewed by Koziara et al. (Koziara et al. 2006). Overcoming the BBB is often a major challenge in designing a suitable drug, therapeutic agents or imaging molecule targeted towards brain for medicinal or medicine related technological applications. ENMs have the potential to revolutionize filed of medicine with their ability to gain access to otherwise inaccessible biological compartments such as cardiovascular, mitochondrion, as well as brain. However, while major medical and pharmacological research is focused on beneficial applications of ENMs, the secondary negative effects are often neglected (Oberdörster et al. 2005; Thomas et al. 2005). It has been shown that ENMs from blood circulation may influence endothelial cell membrane integrity and / or BBB and may gain access to CNS (Chen et al. 2008; Simko et al. 2010). Metal- and metal oxide-based ENMs reviewed in Simko et al. (Simko et al. 2010) did translocate from the point of applications (respiratory tract, skin, and circulatory system) to the brains of the animals. It is well accepted that ENM-induced oxidative stress leading to generations of ROS can disrupt BBB. Some in-vitro studies reviewed in the same report supported the concept that under specific in-vitro conditions, several types of ENMs can influence neuronal redox homeostasis.

Formation of extra-and intra-cellular protein aggregates is one of the hallmarks for several neurodegenerative diseases and some ENMs may enhance this process. $TiO_2$ ENM is shown to trigger and promote formation of beta-amyloid aggregates in solution, which are associated with progression of Alzheimer disease (Wu et al. 2008). As well as some other ENMs [ceria, quantum dots, and carbon nanotubes] are able to stimulate faster formation of fibrils of $\beta_2$-microglobulin protein in solution (Linse et al. 2007).

In-vivo animal studies suggest that although very low but definitely possible translocation of ENMs to brain can occur even after substantial instillation or inhalation (Sharma et al. 2007; Oberdorster et al. 2009; Simko et al. 2010). Therefore, it is feasible that in humans also some such degree of translocation of ENM can occur as a consequence of environmental and / or occupational exposure. Over the time, non-biodegradable and non-excreted ENMs may accumulate in remote biological compartments and can exert hazardous health effects including oxidative stress effects; chronic exposure may also aggravate the ongoing pathological processes (Simko et al. 2010). However, at this point these are only speculations as there is no long term data is available which could stimulate chronic exposure effects.

### 2.9. Why ceria (cerium oxide) ENM?

Cerium (atomic number 58) a member of lanthanide series has electronic configuration [Xe] 4f 5d $6s^2$, is a radox active metal with 4+ and 3+ are most stable oxidative states. Ceria (a.k.a.: CeO2, ceric oxide, Ce dioxide, Ce oxide, CAS # 1306-38-3) is a cerium metal oxide based ENM. Many ENMs are comprised primarily of metals and oxides of Al, Ce, Cu, Au, Fe, Pd, Si, Ag, Ti and Zn. Ceria was selected for this dissertation work to characterize ENM bio-distribution from blood and its effects on oxidative stress endpoints because: (1) It is an insoluble metal oxide that can be readily observed in situ by electron microscopy (EM), making it a useful as an in vivo tracer, (2) it is redox reactive (Zhang et al. 2004), (3) it can be functionalized [e.g. (Qi et al. 2008)], (4) it is available in sizes relevant for uptake across the BBB, one of the most limiting mammalian membranes, (5) it can be produced in a variety of shapes by many different

methods, including nanodisks, nanoplates, nanotubes, nanocubes, nanorods, nanopolyhydra, and

tadpole, comet, and prism shapes (Bai et al. 2001; Mai et al. 2005; Si et al. 2005; Yu et al. 2005; Gao et al. 2006; Han W-Q et al. 2006; Yang et al. 2006), and (6) it has current commercial applications. A major commercial application of ceria is its use as an abrasive for chemical-mechanical planarization of advanced integrated circuits. This application of ENMs accounted for 60% of the $1 billion market for nanomaterials in 2005 (Feng et al. 2006). Another significant application is its use as a catalyst in ENMs that have very small size, large surface area, and thermal stability to 6508C and are stable in humid air (Trovarelli 1996). For example, ceria (10 nm primary particles coated with a dispersant to facilitate its dispersion in fuel liquids) is marketed by Oxonica Ltd. as Envirox®, a diesel fuel catalyst to improve combustion, reduce fuel consumption and decrease exhaust emissions (UK MNT Network). Ceria was also considered to be a good candidate for these studies because it has been reported to have both pro-oxidant and anti-oxidant properties. These properties represent the conundrum enveloping the development of ENMs: There is evidence for both beneficial and toxic effects to the same organ, the brain. Both the ILSIRF/RSI expert working group and the National Cancer Institute Nanotechnology Characterization Laboratory highlighted three key elements for a toxicity screening strategy of ENMs: (1) Physico-chemical characteristics, (2) cellular and non-cellular in vitro assays, and (3) in vivo assays. ‘Tier 1 evaluations’ of these groups included markers of inflammation and oxidant stress in selected remote organs and tissues such as the nervous system (Oberdörster et al. 2005). Nanoscale ceria has been nominated by the NIEHS for toxicological consideration, including toxicokinetic

studies, due to its widespread and expanding industrial uses, limited toxicity data, and a lack of toxicological studies for nanoscale ceria (Inc. 2006).

The interest in ceria as a potential therapeutic agent with SOD- and catalase-enzyme-mimetic properties increases the probability that it will be further studied for medical applications (Celardo et al. 2011). The regenerative redox cycling ability of ceria has shown promising future as radical scavengers and antioxidant therapeutics (Karakoti et al. 2008; Karakoti et al. 2009; Karakoti et al. 2009)as well as its ability to generate ROS can be employed in fight against cancer (Lin et al. 2006; Babu et al. 2010). Ceria has shown to improve the culture of mesenchymal stem cells and growth of cardiac progenitors in biodegradable polymer matrix (Mandoli et al. 2010) and additionally proved to be effective drug carriers for treatment against-tumor (Vincent et al. 2009). Thus the understanding of distribution of ceria ENM from the central compartment (blood) and resultant effects is important. This dissertation research is the first report of the distribution and effects of ceria from the central compartment, after introduction into blood. However, the form of ceria employed in the present study would not be effective as a vehicle for drug delivery to the brain.

Nonetheless we had focused our research on understanding the relationship between physico-chemical properties of ENM and ENM induced oxidative stress mediated biochemical response in rat brain after one-time intravenous injection of ceria ENMs, for both short term as well as chronic exposure with Nel's oxidative stress model as a central guideline.

# CHAPTER 3

# METHODS

## 3.1. Nanomaterial

Ceria ENM: Citrate coated ceria nanomaterials of different sizes and shapes were synthesized and obtained from our collaborators Dr. Eric Grulke (Department of Chemical Engineering, University of Kentucky) and Dr. Uschi Graham (Center for Applied Energy Research, University of Kentucky). A hydrothermal approach was used to synthesize ceria ENM (Schäf et al. 2004) using analytical grade inorganic salts of cerium, viz. cerium chloride or cerium nitrate as starting material. The reaction conditions such as temperature, pH, and time duration for heating cycle were varied to obtain the desired size and shape of the nanomaterial. The ceria ENM was citrate coated (capped) to prevent agglomeration seen with uncoated ceria that occurs in high ionic strength solutions, such as in blood (Xia et al. 2008).

Silver NP: The different sized silver metal nanoparticles (NP) were purchased commercially and provided by our collaborator Dr. Jason Unrine (Department of Plant and Soil Sciences, University of Kentucky).

## 3.2. Nanomaterial characterization

Ceria ENM: The morphology, crystallinity, and particle size distribution of highly diluted samples of the citrate-coated ceria ENM were determined by our collaborators Dr. Eric Grulke (Department of Chemical Engineering, University of Kentucky), Dr. Uschi Graham (Center for Applied Energy Research, University of Kentucky) and Dr. Jason Unrine (Department of Plant and Soil Sciences, University of Kentucky). The ceria nanoparticles were crystalline and highly pure as determined by X–ray diffraction and

scanning transmission electron microscopy (Inc.). The potential presence of contaminating elements/metals was determined by inductively coupled plasma mass spectrometry (ICP-MS). Particle size distribution in aqueous dispersion was determined using dynamic light scattering (DLS). To indicate the stability of the ceria dispersion when infused into the rat, the zeta potential was measured. Analysis with electron energy loss spectroscopy (EELS) was concurrently conducted on the freshly synthesized ceria particles *in vitro* and after its iv infusion in *in vivo*, to determine its M4/M5 or Ce (Owens Iii et al.) vs. Ce(IV) ratio as a measure of its original oxidative signature.

Silver NP: All the characterization was carried out by Dr. Jason Unrine's laboratory members (Department of Plant and Soil Sciences, University of Kentucky).

### 3.3. Ceria administration and BBB integrity assessment

The ceria ENM and saline administration and blood brain barrier (BBB) integrity assessment was performed in our collaborator, Dr. Robert Yokel's research laboratory (College of Pharmacy, University of Kentucky). Ceria dispersion was administered to the male Sprague-Dawley rats prepared with two cannulae, surgically inserted into femoral veins, which terminated in the vena cava. Five minutes before termination, the rats were given BBB integrity markers, anesthetized with ketamine, and decapitated to enable rapid harvest of the brain. The tissue samples were collected rapidly and weighed before freezing them in liquid nitrogen.

The research was conducted in accordance with the Guiding Principles in the Use of Animals in Toxicology.

### 3.4. Light and electron microscopic assessment

Ceria ENM: Light and electron microscopic assessment was carried on thin sections of brain tissue by Dr. Michael Tseng (Department of Anatomical Sciences and Neurobiology, University of Louisville) using TEM and high-resolution transmission electron microscopy (HRTEM).

Silver NP: All the light and electron microscopic assessments were carried out in Dr. Jason Unrine's laboratory (Department of Plant and Soil Sciences, University of Kentucky).

### 3.5. Silver NP administration

Silver NP were first suspended in DI water and then mixed with Yeager sandy loam artificial soil to which young adult earthworms were exposed (Shoults-Wilson et al. 2011). All the preparatory work was carried out in Dr. Jason Unrine's laboratory.

### 3.6. Biological sample preparation

For ceria ENM projects, three brain regions, namely, hippocampus, cortex and cerebellum, were used from each ceria ENM or saline treated rat brain. Frozen brain samples obtained from our collaborator, Dr. Robert Yokel, were separately homogenized using a manual Wheaton glass homogenizer in Media 1 (300-500 µL) buffer containing: 0.32 M sucrose, 0.10 mM Tris-HCl- pH 8.0, 0.10 mM $MgCl_2$, 0.08 mM EDTA, 10 µg/ml leupeptin, 0.5 µg/ml pepstatin, 11.5 µg/ml aprotinin and PMSF 40 µg/ml; pH 8.0. After sample homogenization, protein concentration in brain homogenates was determined by the Pierce Bicinchoninic acid (BCA) assay. However, a small portion of un-homogenized frozen brain tissue from each region of each rat was saved for GSH assay.

For silver NP treated earthworm samples, control and silver NP treated whole earthworms were frozen in liquid nitrogen and then ground using a porcelain mortar and pestle. The frozen powder formed tissue was obtained from our collaborator (Dr. J. Unrine). The powdered samples were thawed, mixed with 300- 400 µL Media 1 buffer and sonicated with a Fischer Scientific 550 Sonic Dismembrator (Fischer Scientific, Pittsburgh, PA) for 10 s at 20 % power. After sample homogenization, samples were centrifuged at 5000 x g for 10 min in a Hettich Mikro 22R Microcentrifuge (Hettich, Beverly, MA) to remove debris. Protein concentration in the supernatant was determined by the BCA assay.

### 3.7. Bicinchoninic acid (BCA) protein estimation assay

All the protein concentrations in this dissertation were determined using the Pierce BCA Protein Estimation Assay (Pierce, Rockford, IL). The Pierce method combines the biuret reaction, chemical reaction used for detection of peptide bonds, by subsequent chelation of $Cu^{1+}$ with BCA molecules results in a violet-colored complex (Smith et al. 1985). In this reaction $Cu^{2+}$ ions are reduced by peptide bonds under basic condition and the presence of cysteine, tryptophan, and tyrosine residues aide the reaction. The resultant $Cu^{1+}$- bicinchoninic acid complex has absorbance maximum at 562 nm (Figure 3.7). This assay follows Beer- Lambert law ($A = \xi l c$); therefore, protein concentration is directly proportional to the intensity or absorbance of the sample. The bovine serum albumin (BSA) was used as a standard and loaded with 3 µL sample on 96-well plate (Evergreen Scientific, Los Angeles, CA). The mixture of solution A and B from Pierce BCA assay kit in the ratio (49:1) was added to standards and protein samples to make an equal final volume 100 µL in each well. The plate was then incubated in oven at 37 ºC for 10 min

and shacked gently before reading the absorbance in a μ-Quant UV plate reader (Bio-Tek, Winooski, VT) at 562 nm.

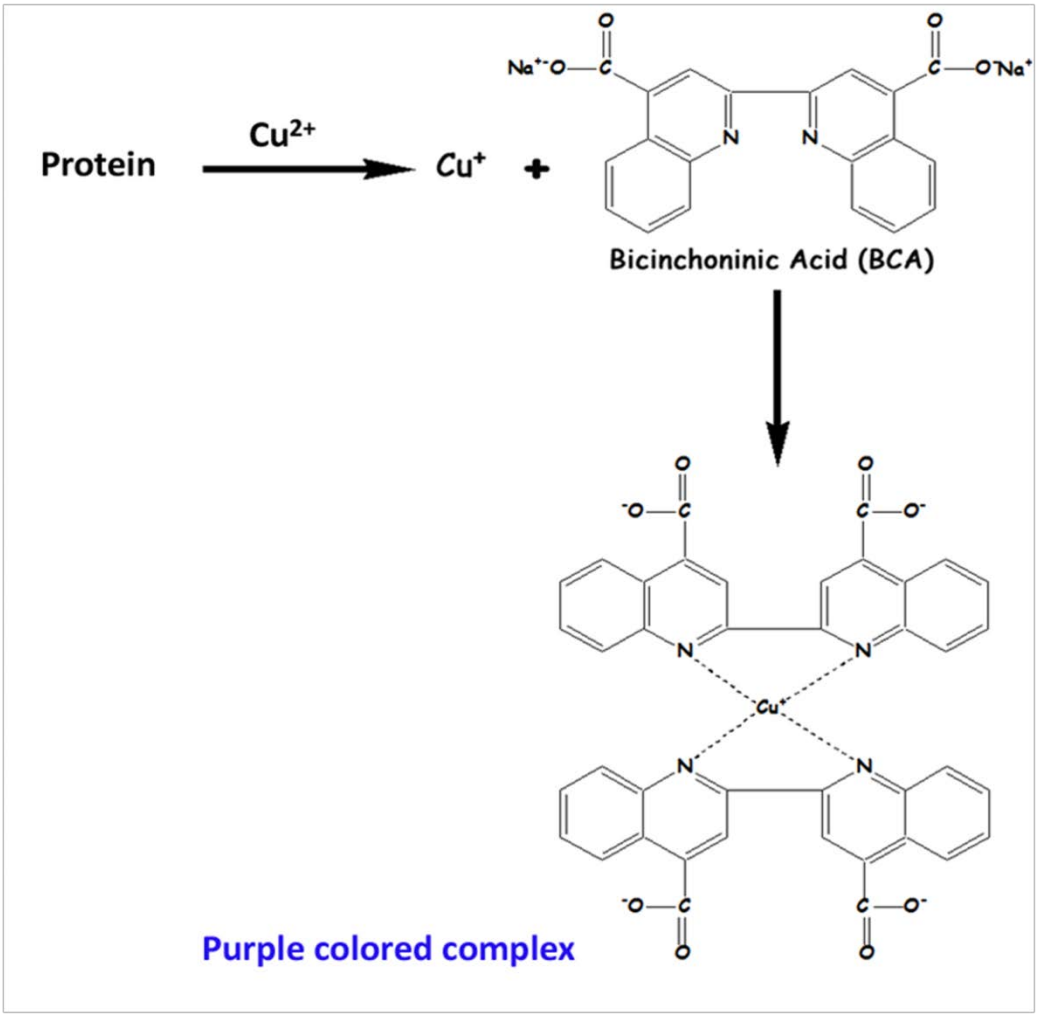


**Figure 3.7:** Formation of $Cu^{+}$-BCA complex upon BCA interaction with $Cu^{+}$ as a result of protein interaction.

### 3.8. Detection of Oxidatively Modified Proteins

#### 3.8.1. Protein Carbonyls (PC)

Protein carbonyls are a global index of protein oxidation. The oxidized proteins contain an abundance of carbonyl groups in the form of conjugated aldehydes or ketones. Addition of carbonyl groups on protein back-bone could be result of either cleavage of protein back-bone or covalent attachment with HNE or acrolein or lipid or sugar oxidation products. As a result the oxidative modification changes the three-dimensional conformation of the protein, subsequently affecting its catalytic activity (Subramaniam et al. 1997). In this dissertation research a sensitivetest used for identification of protein carbonyls is derivatization of carbonyl groups by 2, 4,-dinitrophenylhydrazine (DNPH) to form a hydrazone (Figure 3.8.1), where under acidic conditions carbonyl groups of aldehyde or ketone, react with DNPH to form a Schiff base. The protein bound 2, 4-dinitrophenyhydrazone can be detected using an antibody directed at the hydrazone adduct, which is then detected by immunochemical or fluorescent techniques.

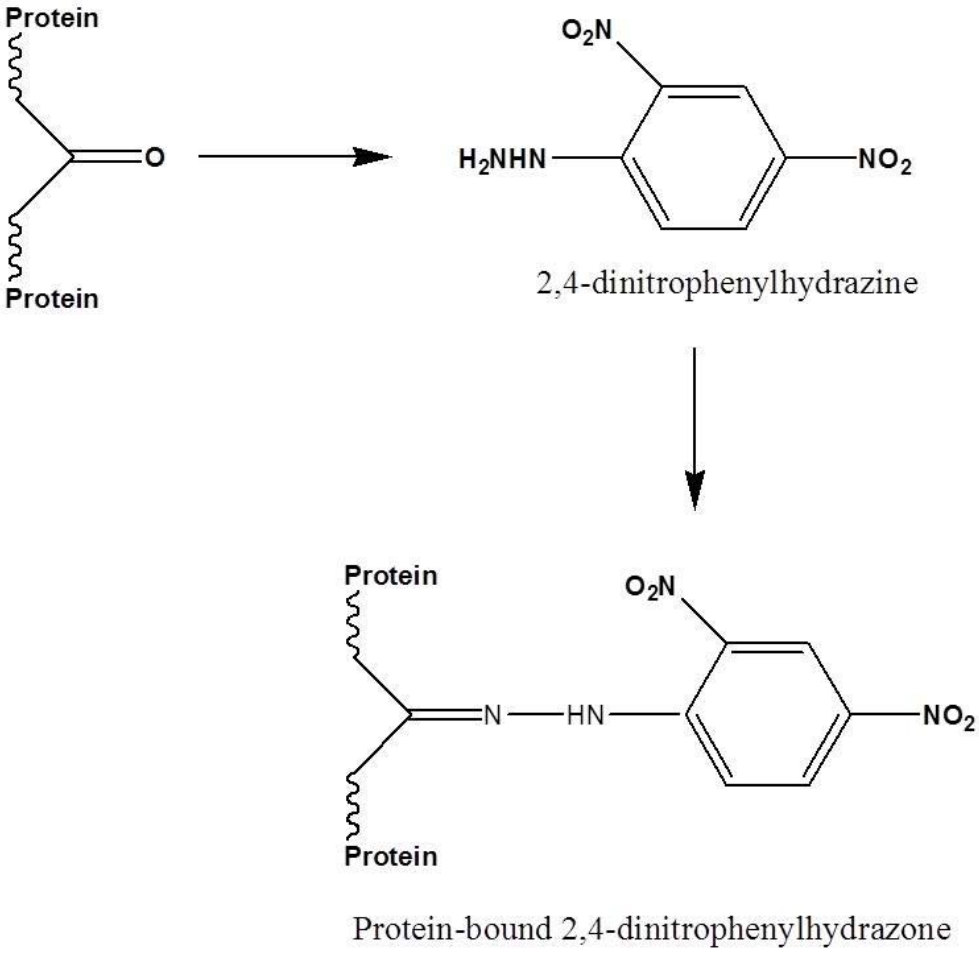


**Figure 3.8.1:** Derivatization of protein carbonyls by DNPH

In brief, each brain sample (5 µL) is derivatized at room temperature by incubation with 5 µL of 12% SDS and 10 µL of 10 mM DNPH solution in 2N HCl for 20 min. After 20 min the sample is neutralized by adding 7.5 µL of neutralization buffer supplied with the OxyBlot Protein Oxidation Detection Kit (Chemicon International Millipore, Temecula, CA). Further, a derivatized sample is diluted with phosphate saline buffer (10 mM, pH 8 with 0.88% NaCl) to obtain a final concentration of 1 µg/ml. A 250 µL aliquot from the

diluted sample is loaded in duplicate onto a nitrocellulose membrane under vacuum pressure using a BioRad slot blot apparatus (BioRad, Hercules, CA).

### 3.8.2. Protein resident 3NT and protein-bound HNE

Protein-resident 3NT is a global index for nitrated proteins, whereas protein-bound HNE is a global index for lipid peroxidation. The biological samples are denatured in sodium dodecyl sulfate (SDS) containing buffer and then 3NT and HNE modifications are detected using separate antibodies directed at the respective 3NT and HNE modification epitopes.

In brief, each brain sample (5 µL) is incubated at RT with 5 µL of 12% SDS and 10 µL of Laemmli buffer (0.125 M Tris pH 6.8, 4% v/v SDS, 20% v/v glycerol) for 20 min. The sample mixture is further diluted with phosphate saline buffer (10 mM, pH 8 with 0.88% NaCl) to obtain a final concentration of 1 µg/ml. A 250 µL aliquot from diluted sample is loaded in duplicate onto a nitrocellulose membrane under vacuum pressure using a BioRad slot blot apparatus (BioRad, Hercules, CA).

### 3.8.3. Slot Blot Technique

Slot blot technique or in some cases known as Dot blot technique, get its name from the shape of the loading wells on the sample template part of the apparatus (Figure 3.8.3). This technique is very useful tool for detection of global levels of a protein modification such as PC or 3NT or HNE. Protein sample is solubalized in SDS containing buffer (in case of PC, later incubated with DNPH) and loaded in equal concentration on the nitrocellulose membrane under vacuum. Nitrocellulose membrane binds to negatively charged protein, owing to sulfate groups on SDS, and any uncharged material is passed though the sub-micron sized pores of nitrocellulose membrane. The protocol is further

standardized so that equal amount of protein is loaded for control as well as treated groups and resulting color intensities after development of membrane by immunochemical technique will be reflective of the global levels of specific protein modification. The advantage of this technique is that very small amount of sample is required (< 1 μg) and multiple samples can be analyzed simultaneously.

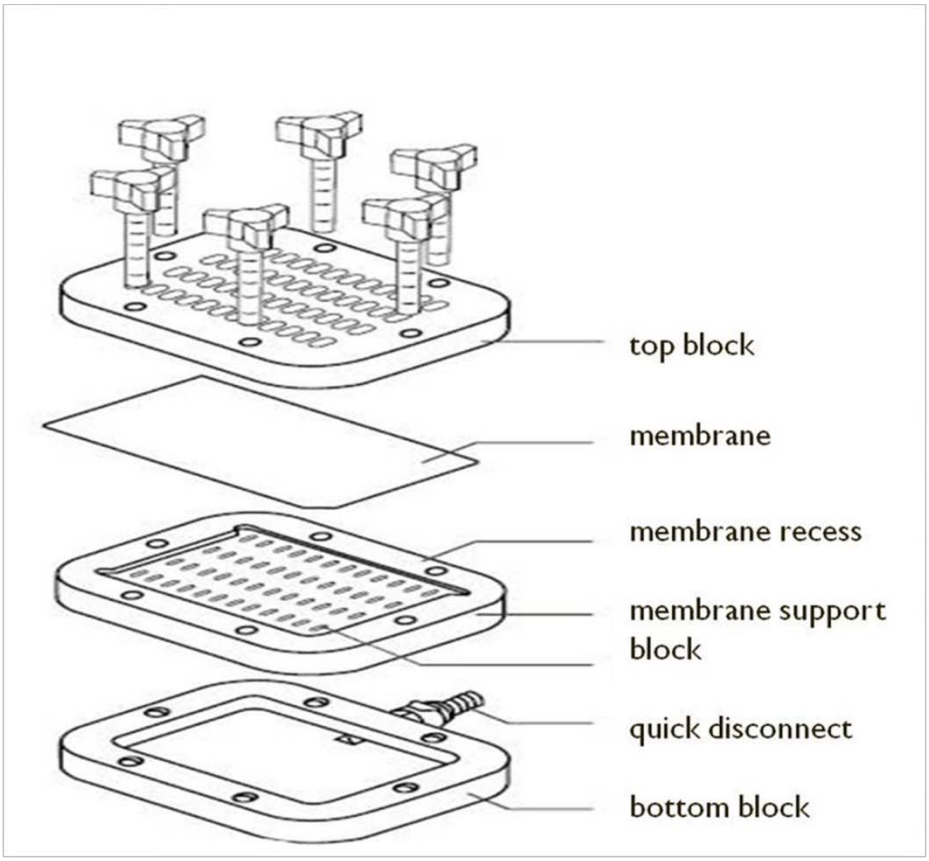


**Figure 3.8.3:** Slot blot apparatus, adapted from Bio-Rad product instruction manual

### 3.9. Enzyme assays

To determine the activity of various antioxidant enzymes, enzyme assays were performed using ready-to-use specific enzyme assay kits from Cayman Chemical Company (Ann Arbor, MI). Briefly, 10-20 μg of homogenized sample was loaded along with standards

provided on a 96-well plate and mixed with the assay buffer provided in the kit. Along with other particular assay related specific reagents, reaction initiator is added to the mixture, such as cumene hydroperoxide used for glutathione peroxidase (GPx) assay, NADPH used for glutathione reductase (GR) assay, hydrogen peroxide used for catalase assay, and xanthine oxidase used for superoxide dismutase (SOD) assay. Typically an initiator is a substrate used during enzymatic reaction. The change in absorbance of the substrate is correlated with the change in concentration of the substrate and the enzyme activity. The change in absorbance can be measured directly or indirectly (using some other chromophore dye) using spectrophometrically in a μ-Quant UV 96-Well plate reader (Bio-Tek, Winooski, VT).

### 3.10. Reduced and oxidized glutathione assay

The ratio of reduced glutathione (GSH) to oxidized glutathione (GSSG) is measure of cellular redox status. GSH and GSSG levels can be measured simultaneously in a fresh tissue using the Hissin-Hiff (Hissin et al. 1976) fluorescence spectroscopic method. In brief, freshly thawed brain tissue is weight rapidly on a weighing balance and homogenized in 25% metaphosphoric acid ($HPO_3$) and 0.1 M sodium phosphate-0.005 EDTA buffer (pH 8.0). The homogenized mixture is centrifuged at 14,000 rpm (10 min, 4 ºC) and supernatant is kept for the assay. For GSH levels, 50 μL of supernatant is diluted with 450 μL of phosphate-EDTA buffer. A 10 μL aliquot of this diluted mixture is loaded along with the 10 μL GSH standard solutions on a 96-well plate. An additional 180 μL of phosphate-EDTA buffer is added followed by 10 μL of o-phthalaldehyde (OPT) solution in methanol. The plate is incubated for 15 min and fluorescence is measure at 420 nm (excited 350 nm). For GSSG levels, 50 μL of supernatant is incubated with 20 μL of 0.04

M N-ethylmaleimide solution in phosphate-EDTA buffer (30 min, RT). After 30 min, mixture is diluted by adding 430 µL of 0.1 N NaOH. A 10 µL of this diluted mixture and 10 µL of GSSG standards are loaded on a 96-well plate and after these same steps are followed as described above for determination of GSH level, except 0.1 N NaOH added instead of phosphate-EDTA buffer.

The GSH to GSSG ratio was determined using GSH and GSSG calibration curve. Student's t-test was used to determined significant difference between normalized GSH: GSSG ratios from treated and control samples with $p < 0.05$.

### 3.11. One-dimensional SDS-PAGE

One-dimensional sodium dodecyl sulfate polyacrylamide gel electrophoresis (SDS-PAGE) separate proteins based on their relative migration rates (Abdelmoez et al.). The sample (75 µg) is solubilized in 4X SDS-containing buffer composed of 0.5 M Tris (pH 6.8), glycerol (40% v/v), SDS (8% wt/v), β-mercaptoethanol (20% v/v), and bromophenol blue (0.01% wt/v). The samples are then denatured by boiling ~100 ºC in water bath for 5 min and cooled immediately on ice before loading on polyacrylamide gel (12% Bis-Tris). Precision Plus Protein ™ All Blue Standards (~4 µL) are loaded in a separate lane along with actual samples on polyacrylamide gel. SDS imparts a net negative charge on the samples, so that samples can migrate from negatively charged anode to positively charged cathode, under the influence of applied electric field (90 V for first 30 min and 120 V till the end). The migration rate $M_r$ is depend on size, molecular weight and shape of the protein, generally proteins with low $M_r$ migrate further in the gel towards the cathode than proteins with higher Mr (Figure 3.11).

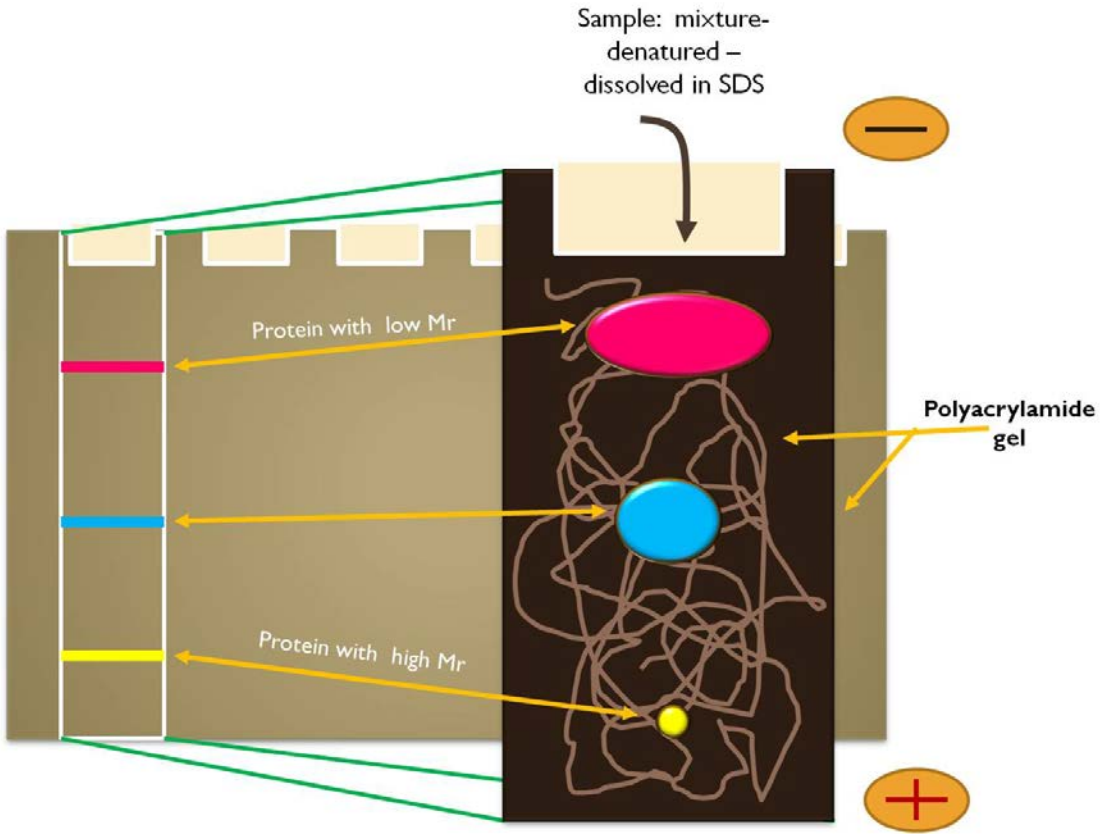


**Figure 3.11:** Separation of protein mixture by SDS-PAGE technique

### 3.12. Isoelectric focusing and two-dimensional gel electrophoresis

Isoelectric focusing (IEF) is a technique in which proteins loaded on an immobilized pH gradient strip (IPG) migrates under the influence of an electric field to a pH in the strip at which they reach their respective isoelectric point (pI) (Figure 3.12). The isoelectric point is the pH where the net charge on a protein is zero.

IEF is also the first dimension of separation of proteins in a 2-D-seperation process, in which 200 µg homogenized protein samples are precipitated by addition of trichloroacetic acid (TCA). Samples are then centrifuged at 14,000 rpm (23,700 x g) for 5 min at 4 ºC in a microcentrifuge (Hettich, Beverly, MA). The pellets are re-suspended in

ethanol-ethyl acetate solution (1:1 v/v) and vortexed to equilibrate. Suspended pellets are re-centrifuged at 14,000 rpm for 1 min at 4 ºC. The cycle of suspension and centrifugation is repeated for 3 more times to ensure removal of any additional salts that may interfere with IEF. After the final cycle, the supernatant is discarded, and pellets are dried at RT for ~7-10 min. After drying, pellets are rehydrated in 200 µL of rehydration buffer composed of 1:1 (v/v) ratio of the Zwittergent solubilization buffer solution (7 M urea, 2 M thiourea, 2% CHAPS, 65 mM DTT, 1% zwittergent, 0.8% 3-10 ampholytes or biolytes, bromophenol blue) and ABS-14 solubilization buffer (7 M urea, 2 M thiourea, 5 mM TCEP, 1% ABS-14, 1% Triton X 100, 0.5% CHAPS, 0.5% 3-10 ampholytes or biolytes) for 2 h, while continuously vortexing at RT (Opii et al. 2007).

The IEF process is begun by actively rehydrating IEF ready strip (pH 3-10) for 17-18 hr at 50 V and 20 ºC. After rehydration IEF is begun at constant temperature 20 ºC and a linearly increasing voltage starting from 300 V going up to 8000 V over the next 24 h. After completion of IEF, the resolved IPG strip can stored at -80 ºC or can be used immediately. For the present work, IPG strops were used immediately without ever freezing them.

To begin 2-D gel or second dimension process, the IPG strip is equilibrated in two different buffer solutions for 15 min each. The first buffer was composed of: 50 mM Tris-HCl (pH 6.8), 6 M urea, 1% SDS w/v, 30% glycerol v/v, and 0.5% dithiothreitol, and the second buffer was composed of everything in the first buffer except 4.5% iodacetamide was used instead of dithiothreitol. Criterion precast linear gradient 8-16% Tris-HCl gels from BioRad are used to perform second dimension electrophoresis, in which proteins are

further resolved based upon their relative $M_r$ (Figure 3.12). Precision Protein Standards (BioRad, CA) are run along with the samples at 200 V for 65 min.

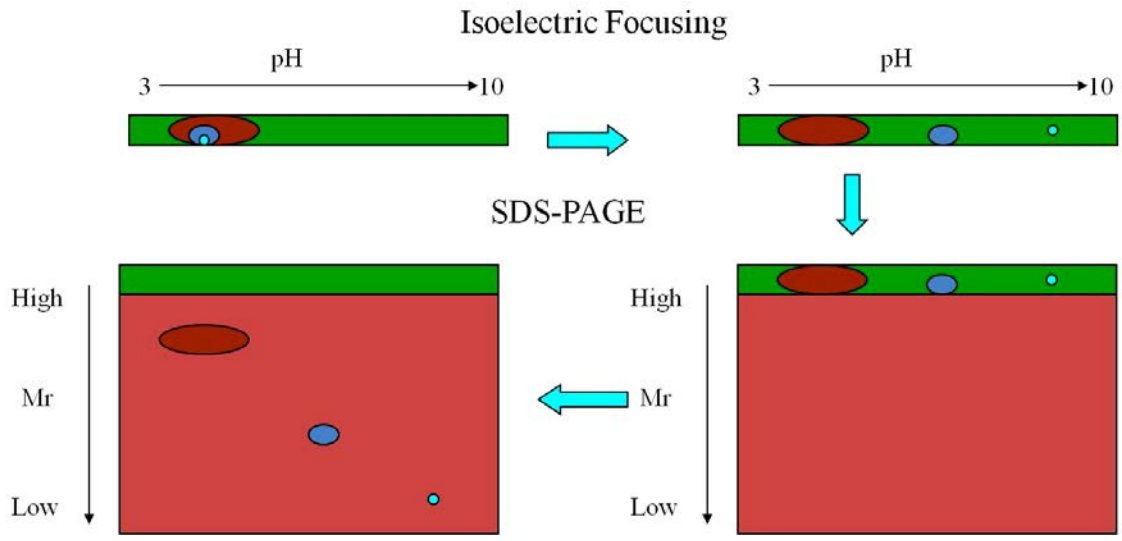


**Figure 3.12:** First-dimension of protein separation using IEF technique is followed by second-dimension SDS-PAGE based separation.

### 3.13. Gel fixation and Sypro-Ruby© in-gel protein staining

After 2D SDS-PAGE, gels are incubated in a fixing solution containing acetic acid (7% v/v) and methanol (10% v/v) in DI water for 45 min- 1 h. Later the gels are transferred into ~50 ml Sypro Ruby Protein Gel Stain (BioRad, Hercules, CA) for overnight incubation on gentle rocking platform. Excess stain is removed by rocking gels in DI water for overnight. The stained gels are visualized using a STORM860 Phosphoimager (GE Healthcare, Piscataway, NJ) (excitation 470 nm and emission 618 nm), and the scanned image is imported and converted into tiff format using Adobe Photoshope 6.0 to be used in either PD-Quest image analysis software (Bio-Rad, Hercules, CA) or ImageQuant image analysis software (GE, Healthcare, Piscataway, NJ).

In-Gel fixation prevents proteins from diffusing out of the gel and sharpens protein band or spots on the gel as well it removes unwanted leftover components from SDS-PAGE. Sypro Ruby is a fluorescent protein stain composed of a proprietary ruthenium-based organometallic compound, which is highly sensitive and does not interfere with mass spectrometry analysis of proteins.

### 3.14. Western blotting

In-gel fixation steps are avoided before Western blotting; instead, after 1D- or 2D-SDS-PAGE gels are directly transferred onto nitrocellulose membrane (0.45 μm). Using a Semi-dry Transfer Cell System (BioRad, Hercule, CA) proteins are transferred from a gel to nitrocellulose membrane in the presence of electric field (20 V). The resultant nitrocellulose membrane blot with protein bound to it can be probed with antibodies raised against specific proteins and can be quantified. To achieve this result, the blot is incubated with a primary antibody for the specific protein and subsequently in with a secondary antibody raised against IgG antibodies (Figure 3.14a). The secondary antibody is conjugated to an enzyme that produces a chemiluminescent or colorimetric product, which can be quantified using ImageQuant image analysis software (GE Healthcare, Piscataway, NJ).

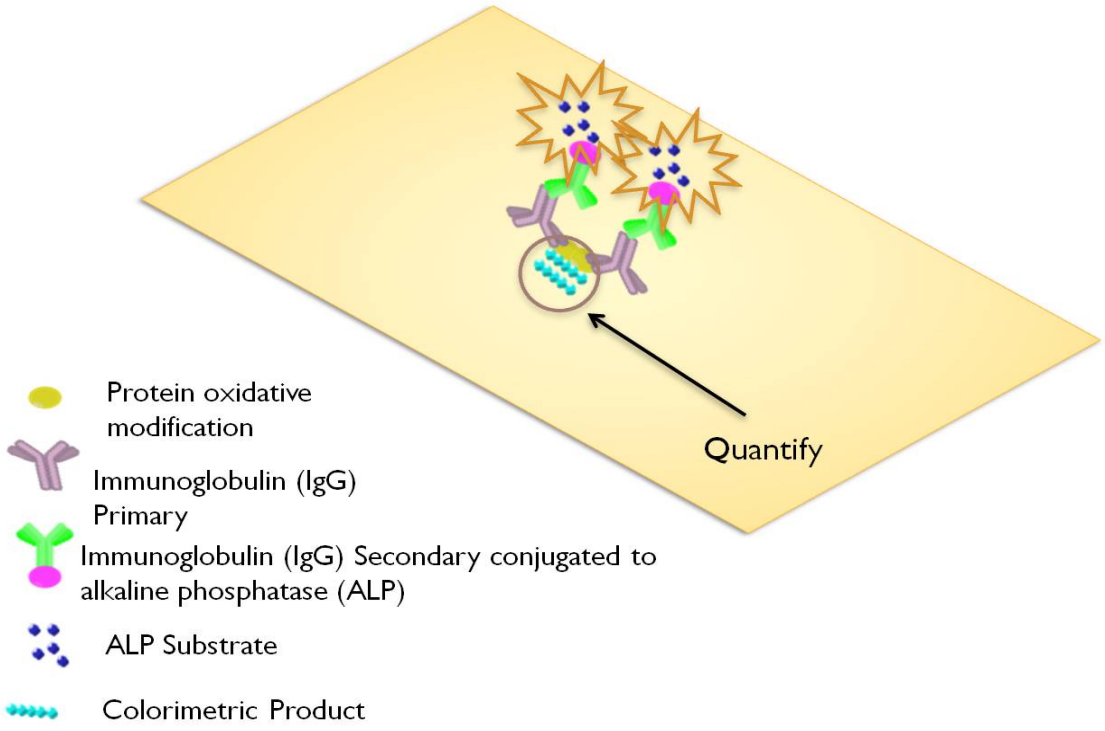


**Figure 3.14a:** Western blotting

Two types of secondary antibodies were used in this dissertation research, one conjugated with alkaline phosphatase (ALP), which reacts with two substrates, 5-bromo-4-chloro-3-indolyl phosphate dipotassium (BCIP) and nitroazolithium blue chloride (NBT) to produce a colorimetric product (Figure 3.14b). The secondary antibody with horseradish peroxidase (HRP) reacts with a substrate luminal PS-3 to form a chemifluorescent product (Figure 3.14c)

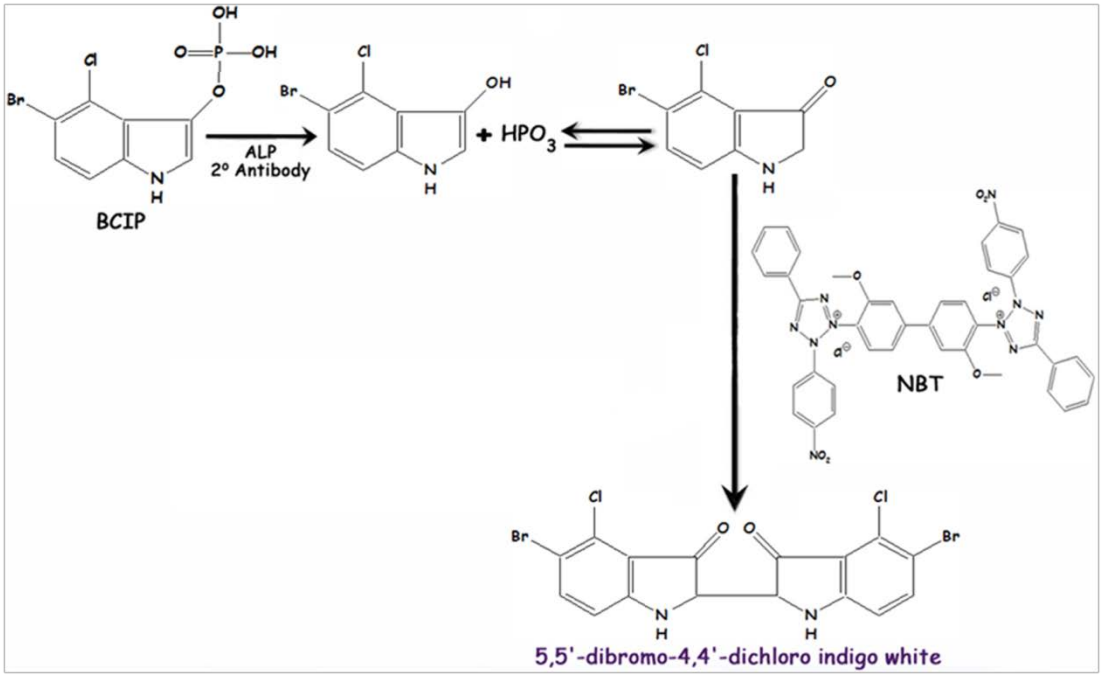


**Figure 3.14b:** Colorimetric method of detection

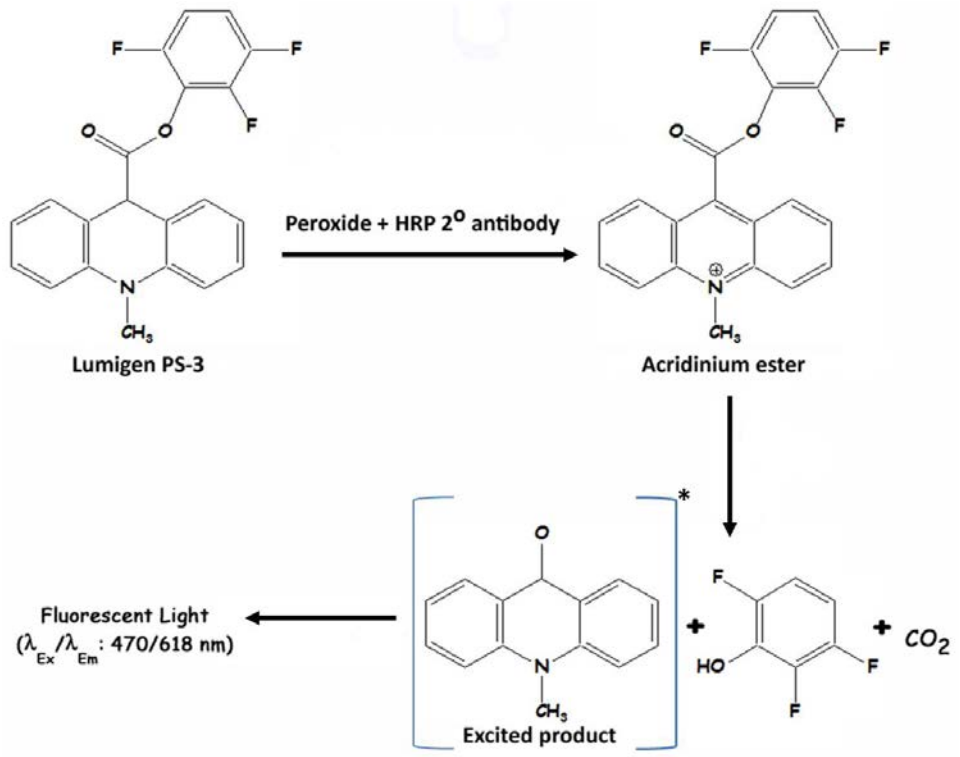


**Figure 3.14c:** Chemifluorescent method of detection

### 3.15. PD-Quest Image analysis software

PD-Quest software is used to compare spot intensities densitometrically from Sypro Ruby stained control and silver NP treated gels. Briefly, a master gel is selected followed by normalization of all the control and treated gels according to the total spot density. Differential expression analysis of protein was then initiated by manually matching common spots that could be visualized in the gels. After obtaining a significant number of matched spots automated matching of all spots is initiated. Automated matching is based on user-defined parameters of the "master" gel, the faintest spot, the largest spot and the largest spot cluster. Based on these parameters the software defines spot centers for the gel. If the software "misses" spots that are obvious to the naked eye, the user can manually assign a spot center. This process generates a large pool of data, however, only spots showing computer-determined significant differential levels between the groups being analyzed are considered for identification. The analysis sets of significant differential levels of proteins are created by the software, which is then compared statistically. A Student's t-test is used to identify significant difference in differential levels of proteins spots from control and treated group with $p < 0.05$. These spots were selected for subsequent mass spectrometric analysis.

### 3.16. ImageQuant software analysis

The densitometric analysis of slot blots and 1D Western blots are performed using ImageQuant software (GE Healthcare, Piscataway, NJ). The nitrocellulose membrane blots are scanned using Microtech Scanmaker 4900 scanner and converted into tiff file format. The ImageQuant software quantified number of pixels present in the desired bands from a tiff image of the blot, which corresponds to an increase/ decrease in protein

level or extent of post-translational modification as PC, 3NT or HNE level. A Student's t-test is used to identify significant difference in intensities of the bands from control and treated group with $p < 0.05$.

### 3.17. In-gel trypsin digestion

Protein spots that are identified as significantly changed from controls were excised from selected gels using a clean micro-pipette tip and placed in separate eppendrof tubes. Spots then are washed with 0.1 M ammonium bicarbonate ($NH_4HCO_3$, 15 min, RT) and incubated with acetonitrile (15 min). The solvent mixture is then removed and gel pieces dried. The dried spots are incubated with 30 µL of 20 mM DTT in 0.1 M $NH_4HCO_3$ (45 min, 56 ºC). The DTT solution is then removed and gel pieces incubated with 30 µL of 55 mM iodacetamide in 0.1 M $NH_4HCO_3$ (30 min, RT). The iodacetamide is removed and replaced with 0.2 ml of 50 mM $NH_4HCO_3$ (15 min, RT), which is again replaced by acetonitrile (15 min). After 15 min the solvent is removed and gel pieces are dried in a flow hood for 30 min. The gel pieces are then hydrated with 10 µL of (20 ng/µL) modified trypsin (Promega, Madison, WI) in 50 mM $NH_4HCO_3$. The gel pieces are incubated overnight at 37 ºC in a shaking incubator. After overnight incubation, the tryptic digest is cleaned with the Zip-Tip (Millipore, Billerica, MA) method to remove any traces of salts, which could interfere with mass spectrometric analysis.

Trypsin is a protease that specifically cleaves proteins at the C-terminal side of lysine and arginine amine acid residue.

### 3.18. Mass Spectrometry

All the mass spectrometric results reported in this dissertation were obtained in the University of Louisville Mass Spectrometry Facility in collaboration with the Department of Pharmacology.

A mass spectrometer (MS) is a mass analyzer that can detect masses of peptides by their respective movements in an electric field. Any MS has three basic components, ionization source, a mass analyzer, and a detector. A Zip-Tip cleaned tryptic digest solution is introduced into a fine capillary containing a high voltage tip in nano-spray or electron spray ionization (ESI) source. While passing through high voltage the peptides become positively charged, eventually the solvent evaporates and subsequently very small charged peptides creates aerosol in the shape of a Taylor cone. The positively charged peptides get pulled into the evaporation chamber by the negative charge imposed on the chamber inlet.

After ionization, positively charged peptides are introduced to orbitrap mass analyzer mass analyzer. An orbitrap type mass analyzer has a spindle shaped central electrode surrounded by a concentric outer electrode. The charged species revolve around the central electrode in various oscillation frequencies. The attraction toward the central electrode is balanced by the centrifugal force of the rotation of the ion. Unlike radial frequency, the axial frequency is independent of energy, angle and position, and it creates an image the form of current that can be detected in order to determine m/z ratio.

The tandem mass spectra generated are searched against Caenorhabditis elegans (*C. elegans*) data base using SEQUEST. This is because there is no existing database for the earthworm proteome. Exact peptide masses (known from the mass spectrum) of the

digested protein are compared with theoretical peptide masses in the database, producing a list of peptide that may possibly match the peptide of interest. The database contains a theoretical MS/MS spectrum of the peptides that have similar masses to the unidentified peptides. The unidentified peptide is then subjected to MS/MS fragmentation and resultant spectrum is then compared with the database. The overlap in fragmentation pattern between the unidentified peptide and database spectra of possible matches is compared using cross correlation analysis, where proteins receive scores based on the quality of overlap. Finally from this data, a protein is identified based on uniqueness of identity and probability of theoretical spectral match from selected organism database.

# CHAPTER 4

# IN VIVO OXIDATIVE STRESS EFFECTS OF A SYSTEMICALLY-INTRODUCED COMMERCIAL CERIA ENGINEERED NANOMATERIAL

## 4.1. Overview of Study

An engineered nanomaterial (ENM) that solves an important problem in the engineering or environmental fields (i.e., ENMs for bioremediation) may have serious consequences after unintended uptake by humans. Inadequate identification of ENM hazards and management of risks from exposure could lead to serious human health problems (Nel et al. 2006). The primary anticipated routes of human exposure to ENMs intended for industrial or environmental applications include inhalation exposure, dermal uptake, and oral ingestion with possible subsequent absorption of ENMs into systemic circulation. Although some data exist on the absorption properties and associated toxicities of ENMs after exposure via the pulmonary, oral, and topical routes, little is known about their distribution into the brain once they reach systemic circulation. There is a need to determine the influence of the physico-chemical properties of ENMs on their distribution into and across the blood-brain barrier (BBB) and into brain cells and their beneficial and/or hazardous effects. Indeed the US Environmental Protection Agency (Shvedova et al.) has nominated ceria ENM as on priority for future study to determine its safety and awarded a STAR Grant RD-833772 to UK to conduct the research.

The objective of this study was to evaluate the effects of nanoscale ceria on oxidative stress endpoints. The intravenous route of exposure was used to assess the potential for the model ENM, after being absorbed by any route and entering systemic circulation, to distribute into organs and produce toxicity. A commercial 5% crystalline ceria dispersion

in water (average particle size~31 ± 4 nm) was infused intravenously into rats (0, 50, 250 and 750 mg/kg), which were terminated 1 or 20 h later. Biodistribution in rat tissues was assessed by microscopy and ICP-AES/MS. Oxidative stress effects were assessed by protein-bound 4-hydroxy 2-trans-nonenal (HNE), 3-nitrotyrosine (3-NT), and protein carbonyls.

## 4.2 Materials and methods

### 4.2.1. Nanomaterial:

A 5% ceria dispersion in water at pH 4.2 (Aldrich #639648; USA) was used. The specifications for this product were: <150 nm and 4.5- 5.5% dispersion. The physical properties of nanoparticles reported by the manufacturer are not always the actual properties of a particular lot. The characterization methods used for research in this chapter HR-SEM, TEM, FTIR XRDICP-MS, Zeta potentiometer, and DLS techniques were performed by our collaborators (Dissertation Section 3.2).

### 4.2.2. Animals:

Nineteen rats were infused with 0 (n=4; 1 infused 0.5 h, 2 infused 2.5 h and 1 infused 7.5 h), 50 (n=5), 250 (n=5) or 750 (n=5) mg ceria/kg and terminated 1h after completion of the infusion and 32 rats were infused with 0 (n=10; two infused 0.5 h, 4 infused 2.5 h and 4 infused 7.5 h), 50 (n=7), 250 (n=7) or 750 (n=8) mg ceria/kg and terminated 20 h after completion of the infusion (Dr. Yokel's lab).

Blood brain barrier integrity assessment (Section 3.3, Dr. Yokel's lab), light and electron microscopic assessment (Section 3.4, Dr. Tseng's lab), tissue homogenization (Section

3.6), BCA protein estimation (Section 3.7), PC, 3NT, protein-bound HNE assays (Section 3.8) were carried out.

### 4.3. Results

Light scattering particle size determinations suggested the mean ceria ENM size was ~30 nm, which correlated with HR-STEM imaging of the dosing material (Figure 4.1). FTIR results showed several peaks between 1300 and 1700 $cm^{-1}$ indicating the ceria ENM was modified with organic molecules, probably either an intentionally added stabilizer or an unintentional contaminant. The exact nature of this organic matter was not determined. The XRD results showed the presence of pure ceria in a cubic shape.

Tissue Ce concentration was ceria dose-dependent. The Ce concentration was highest in the spleen, which was higher than the liver, which was higher than the brain (Table 4.1). In contrast to the significant accumulation of ceria agglomerations in reticuloendothelial organs, much less ceria was seen in the brain (Figure 4.2), consistent with the much lower Ce concentration in this organ compared to the spleen, liver and kidney (Table I). No microscopic evidence of disruption of the BBB was observed.

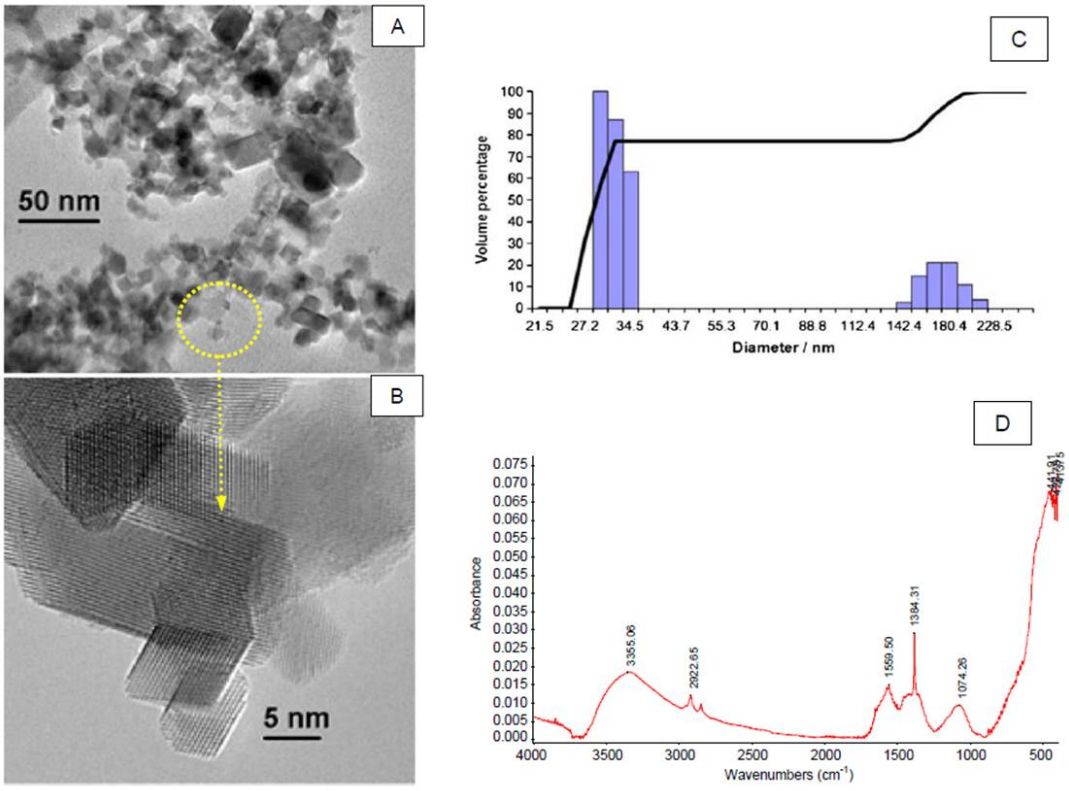


**Figure 4.1:** HRTEM results for the ultra-sonicated 5% ceria ENM dispersion used in this study. Panel A: Lower magnification showing particle size distribution. The upper limit of the particle size range was ~100 nm. Panel B: Higher magnification illustrating that the lower limit of the particle size ranges was ~5 nm. All size fractions of the ceria ENM were highly crystalline. Panel C: The volume-based particle size distribution was bimodal. Panel D: FTIR scan of the powder surface showed the presence of carboxylate groups.

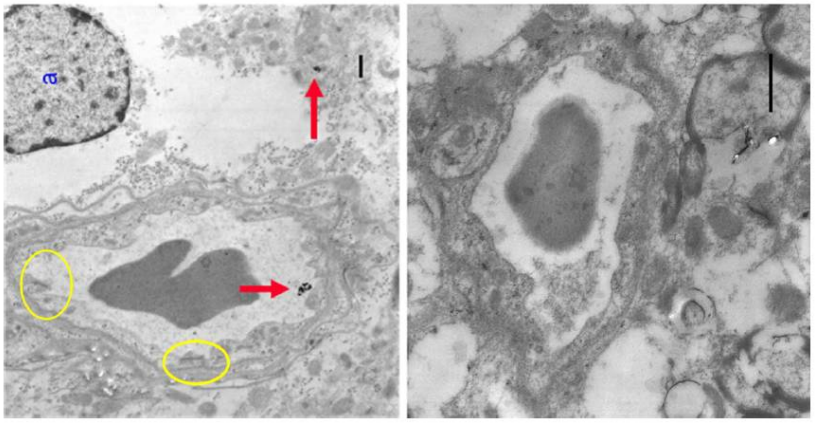


**Figure 4.2:** Left image: Electron micrograph of hippocampus of a rat that received 750 mg ceria/kg and was terminated 20 h after the infusion. Ceria was seen in the vascular lumen (red arrows) and an astrocyte (a). The BBB appeared intact (yellow circles). Scale bar =1 mm. Right image: Electron micrograph of hippocampus of a rat that received 250 mg ceria/kg and was terminated 20 h after the infusion. There is an apparent absence of ceria. Scale bar =1 mm.

**Table 4.1:** Blood and tissue [Ce] concentrations were measured1 and 20 h after completion of intravenous ceria infusion. *All the values were below detection.

| Cerium [mg/L or mg/kg wt weight][a] | | | |
|---|---|---|---|
| **Ceria dose (mg/kg)** | **Blood** | **Brain** | **Liver** |
| **1 h Termination** | | | |
| **0** | 0.032 ± 0.045 | 0.12 ± 0.09 | 0.25 ± 0.31 |
| **50** | 0.56 ± 0.50 | 0.087 ± 0.067 | 390 ± 137 |
| **250** | 1.3 ± 1.4 | 0.15 ± 0.10 | 1632 ± 941 |
| **750** | 41 ± 11 | 1.1 ± 0.3 | 6327 ± 725 |
| **20 h termination** | | | |
| **0** | * | * | * |
| **50** | 1.2 ± 0.1 | 1.0 ± 0.3 | 610 ± 131 |
| **250** | 13 ± 0 | 3.4 ± 1.0 | 3139 ± 1451 |
| **750** | 354 ± 45 | 7.4 ± 1.2 | 9335 ± X |

There were no significant changes in the oxidative stress markers (protein-bound HNE, protein-bound 3-NT and protein carbonyls) in brains from rats terminated 1 h after completion of the ceria infusion (Figure 4.3., upper panel). Rats terminated 20 h after the ceria infusion showed a significant increase of protein-bound HNE in the hippocampus and a decrease of protein carbonyls in the cerebellum (Figure 4.3., lower panel).

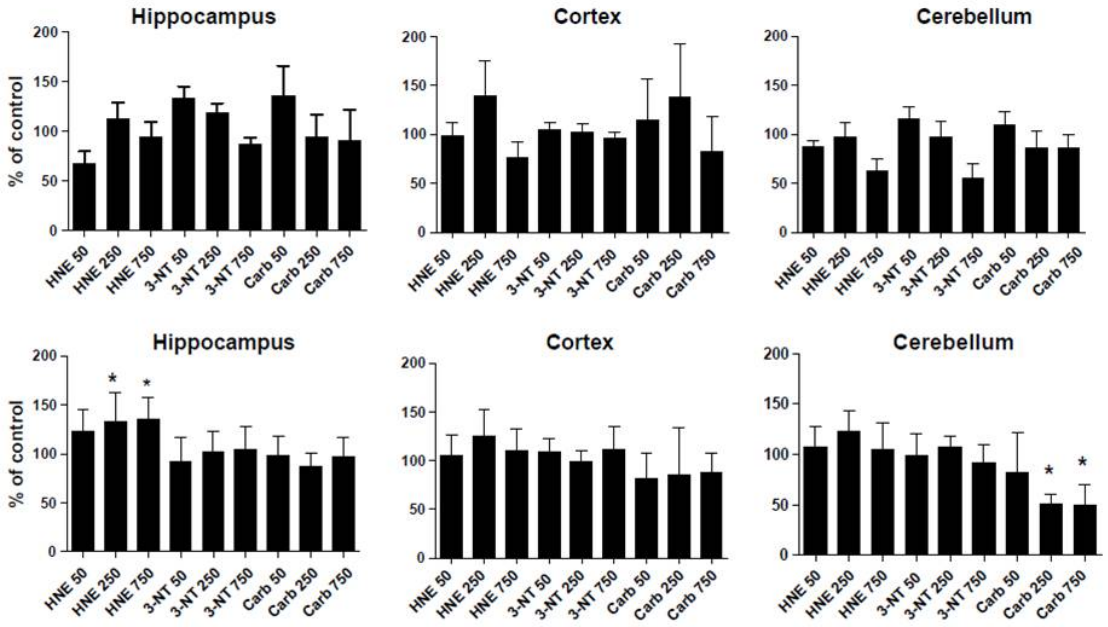


**Figure 4.3:** Protein-bound HNE, protein-bound 3-NTand protein carbonyls were measured in the hippocampus, cortex and cerebellum 1 h (upper panels) and 20 h (lower panels) after completion of intravenous ceria ENM infusion. Results are mean ± SD of 4, 5, 5, and 5 rats that received 0, 50, 250 and 750 mg ceria/kg and were terminated 1 h after the infusion and 8, 5, 5 and 7 rats that received 0, 50, 250 and 750 mg ceria/kg and were terminated 20 h after the infusion. *=Significantly different from control, $p<0.05$.

### 4.4. Discussion

Material characterization results obtained were not fully consistent with the properties of this commercial ENM provided by its supplier. FTIR results suggested it had an unknown, and not revealed (for proprietary purposes), surface stabilizer(s). Surface stabilizers are commonly added to ENM to provide ease of dispersion. However, in an adverse effects assessment, as in this study, the presence of unknown components of the study material is not desired. To avoid this confound in future studies, we are preparing materials to have precise control over surface coating effects in our future studies.

The commercial ceria ENM used in this study was quite pure in regards to other metals. Sonication added little metal to the ceria. The ratio of non-cerium metals to ceria suggests that oxidative stress effects seen in this work are due to the ceria ENM (data not shown). The lack of profound effects on the oxidative stress endpoints in the brain may relate to the limited ceria distribution into the brain. No great BBB disruption was seen 1 and 20 h after completion of the infusion. Much less ceria ENM entered the brain than peripheral organs, suggesting an intact BBB during the infusion and that the BBB is an effective barrier for this crystalline ceria ENM. As it is unknown whether the ceria ENM that did enter the brain did so as administered, or after associating with proteins or other circulating factors in blood, we cannot glean from this study the properties that did enable its limited brain distribution.

Oxidative injury is a common, primary endpoint of ENM toxicity (Unfried et al. 2007). Ceria has been reported to produce toxicity attributed to increased oxidative damage (Brunner et al. 2006; Lin et al. 2006; Thill et al. 2006; Park et al. 2008). On the other hand, ceria ENM were reported to be protective against oxidative-induced injury in cells

from many origins, including the nervous system (Tarnuzzer et al. 2005; Chen et al. 2006; Schubert et al. 2006; Das et al. 2007; Niu et al. 2007; Singh et al. 2007; Xia et al. 2008). This may be a direct anti-oxidant effect of ceria owing to its ability to reversibly change from Ce (Owens Iii et al.) to Ce (IV). However, that effect was only pronounced in acidic environments (Asati et al. 2009). The interest in ceria as a potential therapeutic agent with anti-oxidant properties increases the probability that it will be further studied for medical applications, making the understanding of its distribution from the central compartment (blood) and resultant effects important. The current study is the first report of the distribution and effects of ceria from the central compartment, after introduction into blood. However, the form of ceria employed in the present study would not be effective as a vehicle for drug delivery to the brain.

In this study, indices of protein oxidation (protein carbonyls and protein-bound 3-NT) and lipid peroxidation (protein-bound HNE) were determined. We observed no alterations in any of these oxidative stress markers in brain isolated from rats 1 h after exposure to ceria ENM. Twenty h after exposure to ceria by intravenous infusion, a dose-dependent increase of protein-bound HNE in the hippocampus was observed. The hippocampus is one of the most vulnerable brain regions, and in the most common neurodegenerative disorder, Alzheimer's disease, the hippocampus, the brains area through which initial aspects of memory are formed, is severely damaged by free radicals early in the disease (Butterfield et al. 2007). The highly reactive alkenal HNE can bind to proteins, thereby inducing conformational and functional changes (Aksenov et al. 1997; Subramaniam et al. 1997; Aksenov et al. 2000; Reed et al. 2008). Hence, ceria induced

hippocampal lipid peroxidation could lead to deficits in learning and memory, and consequently dementia (Butterfield 1997; Butterfield et al. 1997; Lauderback et al. 2001).

In the cerebellum, protein carbonylation was decreased compared to controls. Cerebellum is devoid of oxidative damage and other pathology in Alzheimer's disease, and though no explanation for this observation is yet known, speculation suggests that elevated levels of heme oxygenase-1 (which leads to low levels of bilirubin that are highly neuroprotective), coupled to both a different neuronal type than in hippocampus and less amyloid β-peptide (that leads to free radical oxidative stress) accounts for this protection against oxidative stress and neurodegeneration (Poon et al. 2004). Elevated levels of heme oxygenase conceivably might be induced by ceria that lead to neuroprotection against oxidative stress as assessed by protein carbonyl levels. The commercial ceria used in this study was not obviously accumulated in brain, perhaps because of its size as well as its propensity for agglomeration. That, nevertheless, elevated lipid peroxidation was observed in vulnerable hippocampus may reflect two possibilities: (a) Brain-resident ceria ENM induced lipid peroxidation directly, which involves a chain reaction and requires only a modest initiation step to greatly amplify its effect; or (b) ceria-induced pro-inflammatory cytokines, e.g., TNF-a, in the periphery that are well-known to cross the BBB and induce oxidative stress in brain, including lipid peroxidation (Tangpong et al. 2006; Joshi et al. 2007). Further studies will be necessary to distinguish between these or other alternatives. It is interesting to speculate that ceria ENM <10 nm in size, and of defined shape and surface properties, in marked contrast to what was used in the current study, might have accumulated more in brain and led to either more oxidative or more neuroprotective effects. Studies to test this notion are in progress.

In summary, much less ceria entered the BBB cells or the brain. The commercial ceria studied induced oxidative stress and a stress response in the brain. Ceria provides an inert core ENM enabling the study of the effects of size, shape and surface chemistry on the biodistribution, and neurotoxic or neuroprotective potential of metal oxide ENMs. These results provide a foundation to study the impact of physico-chemical properties of ENMs on their brain entry and neurotoxicity or neuroprotection activity.

# CHAPTER 5

# IN VIVO OXIDATIVE STRESS EFFECTS OF A SYSTEMICALLY-INTRODUCED IN-HOUSE ENGINEERED 5 NM CERIA NANOMATERIAL

## 5.1. Overview of Study

Ceria ENM (a.k.a. cerium oxide; $CeO_2$), which is one of the most used ENM employed in different industrial applications (Yokel et al. 2009; Hardas et al. 2010), has been shown to have both anti-inflammatory properties as well as potent toxicity. However, there is no clear understanding of what exactly controls ceria's pro-or anti-oxidant effects. A recently published report summarizes findings of *in vitro* and *in vivo* studies conducted with ceria ENM under basal and induced oxidative stress conditions (Celardo et al. 2011). Ceria exhibited antioxidant properties by scavenging free radicals, by reducing levels of peroxides, iNOS, TNF-α, NF-κβ, and interleukin, promoted cell viability or protected organelles from diesel exhaust and cigarette smoke-induced oxidative stress, ROS generating chemical agents, or side effects of radiation treatment. Ceria is reported to have potential use in the treatment of diabetic cardiomyopathy, cancer, stroke, retinal degradation and Alzheimer's disease as well as to prolong life span (Chen et al. 2006; Rzigalinski et al. 2006; Das et al. 2007; Xia et al. 2008; D'Angelo et al. 2009; Hirst et al. 2009; Babu et al. 2010; Colon et al. 2010; Younce et al. 2010; Estevez et al. 2011; Niu et al. 2011). Antioxidant properties of ceria may be related to its SOD- and catalase-mimetic activity (Korsvik et al. 2007; Pirmohamed et al. 2010) attributed to Ce3+/ Ce4+ redox coupling (Celardo et al. 2011) . In contrast, there are reports of ceria induced pro-oxidant effects under basal conditions. Ceria ENM mediated ROS injury, elevation of the lipid peroxidation marker MDA, as well as the membrane damage marker LDH,

cytokines, IL-8 mRNA levels, GSH depletion, and reduced cell viability (Brunner et al. 2006; Lin et al. 2006; Park et al. 2008; Auffan et al. 2009).

To utilize ceria for therapeutic and non-therapeutic applications, it is important to know the long term effects of intended and un-intended ceria exposure on mammals. Most reports on effects of ceria ENM were on non-mammalian organisms or in cell culture, and they do not address long-term effects or the fate of ceria. In addition to our own previous studies (Yokel et al. 2009) (Yokel et al. 2009; Hardas et al. 2010), a few ceria ENM studies were conducted in intact animals (Chen et al. 2006; Niu et al. 2007; Hirst et al. 2009; Amin et al. 2011; Choi et al. 2011; Hirst et al. 2011; Srinivas et al. 2011; Zhou et al. 2011).

We have shown that iv administration of a commercial ceria ENM induced oxidative stress in rat brain (Yokel et al. 2009). However, this ENM was of larger size than advertised, tended to agglomerate, and had an unknown surface coating. The objectives of the present research were (1) to test the hypothesis that the size of metal oxide ENMs inversely relates to their ability to; cross the BBB and produce immediate (1 h) and later (20 h) pro- and/or antioxidant effects in the brain using ceria as a model metal oxide ENM; and (2) evaluate residual effects of long-term ENM exposure (30 days) on oxidative stress parameters in brain. Toward these goals, the iv route was used to assess the potential for this ENM, after being absorbed by any route and entering systemic circulation, to distribute into the brain and produce effects. Quite large doses were initially studied to likely produce significant effects.

In the current study, 5-nm ceria ENM was synthesized and characterized, and its toxic effects were determined in the cerebellum, cortex, and hippocampus. The levels and activities of the antioxidant enzymes catalase, manganese superoxide dismutase (Mn-SOD), glutathione peroxidase (GPx), and glutathione reductase (GR) were measured along with the ratio of reduced glutathione (GSH) to its oxidized form (GSSG). To understand the extent of changes in cellular redox status, the levels of oxidative stress endpoints, protein carbonyl (PC), 3-nitrotyrosine (3NT), and protein-bound 4- hydroxyl-2-trans-nonenal (HNE), were measured along with heat shock protein (Hsp70) levels.

## 5.2 Materials and Methods

### 5.2.1. Nanomaterial:

Ceria ENM was obtained from our collaborator, which was synthesized in in-house facility (Section 3.1). Nanomaterial characterization was carried out by our collaborators, prior to ceria ENM treatment to the animals (as described in Section 3.2).

### 5.2.2. Animals:

Seven rats were infused with 0 and 11 rats with 100 mg ceria/kg and terminated 1 h after completion of infusion. Eight rats were infused with 0 and 12 rats with 100 mg ceria/kg and terminated 20 h after completion of infusion. Seven rats received 0 and nine rats received 85 mg ceria/kg and terminated 30 days after completion of infusion. After ceria ENM treatments, the BBB integrity assessment (Section 3.3), light and electron microscopic assessment (Section 3.4) and EELS analysis (Section 3.2) were carried out by our collaborators. The brain homogenates were prepared from control and ceria treated rat brain samples (Section 3.6). Total protein content was determined using BCA

assay (Section 3.7) and various biochemical assays were carried out on all the samples (Section 3.8, 3.9, 3.10, 3.11, and 3.14) in our lab.

### 5.3. Results

Ceria composition

HR-TEM/HR-STEM showed the ceria ENM was polyhedral shape (Figure 5.1). The XRD patterns demonstrated the ceria were highly crystalline. Evaluation of a number of TEM images showed that the ceria had a number-average primary particle size of ~ 5 nm. Analysis of the ceria dispersion by ICP-MS showed that the ceria content of the as-synthesized dispersion was 4.35 ± 0.20%.

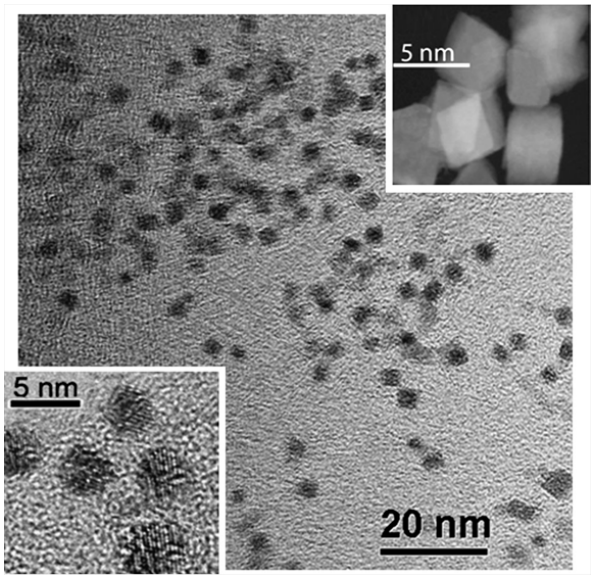


**Figure 5.1:** Ceria ENM imaged using HRTEM and HRSTEM. The ceria were dispersed on a carbon film. Visually they have a narrow size distribution ranging from 4 to 6 nm, the majority 5 nm. The magnified TEM insert at the lower left illustrates that the ceria ENMs are highly crystalline. The insert at the top right is a STEM image showing the morphology of the ceria ENM (taken by Dr. Peng Wu).

Ceria concentration in brain and electron microscope

ICP-MS analysis suggested that a very small amount of ceria was present in the brain parenchyma compared to the peripheral organ liver (Table 5.1). Electron microscopy studies suggested that ceria ENM was not found in the brain, but located on the luminal side of the BBB endothelium. The hippocampus and cerebellum tissues did not show obvious ceria induced injury as no necrotic neurons or elevated gliosis were observed and the BBB was visibly intact (data not shown).

**Table 5.1:** Ceria concentration in blood, brain, and liver expressed as concentration and as a percentage of the 5 nm ceria ENM dose 1h, 20 h and 30 d after the treatment. % dose was based on blood volume of the rat of 7% body weight and brain, and liver ceria concentration x organ weights. *All values were below minimum detection limit.

| **Cerium (mg/l or mg/kg) wet weight and [% of dose][a]** | | | |
|---|---|---|---|
| % dose | **Blood** | **Brain** | **Liver** |
| 1 h termination | | | |
| 0 (n=7) | 0.02 ± 0.03 | 0.09 ± 0.10 | 0.30 ± 0.54 |
| 100 (n=11) | 27 ± 8 | 0.020 ± 0.007 | 22 ± 14 |
| 20 h termonation | | | |
| 0 (n=8) | * | * | * |
| 100 (n=12) | 1 ± 1 | 0.0046 ± 0.0011 | 51 ± 11 |
| 30 d termination | | | |
| 100 (n=9) | 0.01 ± 0.02 | 0.008 ± 0.009 | 44 ± 27 |

EELS results

Electron energy loss spectroscopic measurements on liver tissue were performed as a representative organ. The ratio of Ce(Owens Iii et al.) to Ce(IV) in the aged ceria was evaluated using EELS measurements after locating agglomerates of the 5 nm ceria in tissue 20 h and 30 days after infusion into rat and comparing with synthesized ceria. The high $Ce^{3+}$/ $Ce^{4+}$ ratio that was obtained in the as-synthesized, fresh 5 nm ceria particles seems to have only been altered slightly in individual ceria measured in liver after 30 days *in vivo*. However, this difference was not significant after 20 h as well as 30 d (data not shown).

Oxidative Stress Indices

*Ceria treatment affected catalase levels and activities*

Previously ceria ENM was reported to have $H_2O_2$-producing ability (Korsvik et al. 2007); therefore, the effect of 5 nm ceria ENM on levels and activity of a primary $H_2O_2$ reducing enzyme (catalase) was determined. Catalase activity was significantly increased 20 h later in the hippocampus (~28%, $p<0.05$, Table 5.2a) but, decreased after 1 h in cerebellum (~16%, $p<0.05$, Table 5.2b) and 30 d later in the hippocampus (~18%, $*p<0.05$, Figure 5.2b). Catalase levels were significantly increased 1 h after ceria infusion in the hippocampus (~ 41%, $*p<0.05$, Table 5.2) and decreased 30 d after in the cerebellum (~16%, $*p<0.05$, Figure 5.4a). To determine the influence of ceria treatment on the SOD enzyme or contribution to $H_2O_2$ levels produced from SODs, if any, the level of MnSOD and SOD activity were measured after 1 h, 20 h and 30 d. There were no significant changes observed in the levels and activity of Mn-SOD (data not shown).

**Table 5.2a:** Oxidative stress indices measured in hippocampus after 1 and 20 h of 5 nm ceria treatment. All values are expressed as mean of percentage of controls ± SEM, which were concurrently assayed. The control mean was normalized to 100%. *Statistically significant difference with ($p < 0.05$).

| | 1 h after treatment | | 20 h after treatment | |
|---|---|---|---|---|
| | Control | Ceria treated | Control | Ceria treated |
| **(a) Hippocampus** | | | | |
| **Oxidative stress markers** | | | | |
| PC | 100 ± 2 | 93 ± 3 | 100 ± 8 | 103 ± 3 |
| 3NT | 100 ± 3 | 101 ± 3 | 100 ± 5 | 103 ± 3 |
| Protein-bound HNE | 100 ± 7 | 103 ± 6 | 100 ± 3 | 101 ± 3 |
| **The GSH antioxidant defense system** | | | | |
| GR levels | 100 ± 4 | 99 ± 13 | 100 ± 3 | 109 ± 7 |
| GR activity | 100 ± 7 | 93 ± 5 | 100 ± 6 | 106 ± 5 |
| GPx levels | 100 ± 3 | 97 ± 4 | 100 ± 2 | 102 ± 3 |
| GPx activity | 100 ± 21 | 97 ± 18 | 100 ± 13 | 77 ± 10 |
| **Antioxidant enzymes** | | | | |
| MnSOD levels | 100 ± 8 | 93 ± 8 | 100 ± 6 | 98 ± 9 |
| SOD activity | 100 ± 10 | 93 ± 8 | 100 ± 8 | 76 ± 5 |
| Catalase levels | 100 ± 11 | 141 ± 10* | 100 ± 4 | 91 ± 5 |
| Catalase activity | 100 ± 3 | 101 ± 5 | 100 ± 7 | 128 ± 7* |

**Table 5.2b:** Oxidative stress indices measured in cortex and cerebellum after 1 and 20 h of 5 nm ceria treatment. All values are expressed as mean of percentage of controls ± SEM, which were concurrently assayed. The control mean was normalized to 100%. *Statistically significant difference with ($p < 0.05$).

| | 1 h after treatment | | 20 h after treatment | |
|---|---|---|---|---|
| | Control | Ceria treated | Control | Ceria treated |
| **(a) Cortex** | | | | |
| **Oxidative stress markers** | | | | |
| PC | 100 ± 3 | 102 ± 3 | 100 ± 6 | 102 ± 3 |
| 3NT | 100 ± 3 | 104 ± 4 | 100 ± 6 | 97 ± 4 |
| Protein-bound HNE | 100 ± 16 | 110 ± 9 | 100 ± 4 | 106 ± 5 |
| **Antioxidant enzymes** | | | | |
| Catalase levels | 100 ± 4 | 104 ± 2 | 100 ± 7 | 109 ± 6 |
| Catalase activity | 100 ± 7 | 93 ± 4 | 100 ± 6 | 105 ± 2 |
| **(b) Cerebellum** | | | | |
| **Oxidative stress markers** | | | | |
| PC | 100 ± 3 | 102 ± 3 | 100 ± 5 | 85 ± 3 |
| 3NT | 100 ± 4 | 104 ± 2 | 100 ± 1 | 98 ± 2 |
| Protein-bound HNE | 100 ± 7 | 103 ± 6 | 100 ± 4 | 104 ± 2 |
| **Antioxidant enzymes** | | | | |
| Catalase levels | 100 ± 6 | 105 ± 6 | 100 ± 10 | 91 ± 9 |
| Catalase activity | 100 ± 6 | 84 ± 3* | 100 ± 8 | 104 ± 5 |

*Ceria treatment decreases GPx levels, activity and the GSH-GSSG ratio after 30 d*

GPx reduces $H_2O_2$ along with other peroxides using glutathione (GSH) as a source of reducing equivalents. The activity of GPx was significantly decreased in the hippocampus (~69%, **p<0.001, Figure 5.2b, 30 d) and in cerebellum (~23 %, *p<0.05, Figure 5.4b, 30 d). GPx levels showed a decreasing trend in all brain regions but was significantly decreased only in cerebellum (~27 %, *p<0.05, Figure 5.4a, 30 d). GR levels were significantly decreased (~24%, *p<0.05, Figure 5.3a, 30 d) in the cortex. GR activity did not show any significant change in any of the three brain regions of 30 d samples. A marker of overall cellular redox status was evaluated by comparing the GSH: GSSG ratio of ceria-treated samples. The GSH: GSSG ratio was significantly decreased in the hippocampus (~13%, *p<0.05, Figure 5.2b, 30 d) and cerebellum (~15%, **p<0.01, Figure 5.4b, 30 d) consistent with an increase in oxidative stress seen in brain from ceria ENM-treated animals after 30 d.

GPx and GR activities and levels remained unchanged in 1 h and 20 h samples, whereas GSH and GSSG levels were not measured for these early time points.

*Hsp-70 levels increased 30 d after ceria treatment*

Hsp-70 is a member of the heat shock protein family and inducible by oxidative stress. Hsp-70 levels were significantly increased in the hippocampus (~49%, *p<0.05, Figure 5.2a) and in the cerebellum (~40% *p<0.05, Figure 5.4a), which are consistent with depletion of GSH levels indicated by the decreased GSH: GSSG ratio in those regions. The levels of Hsp70 were not measured in 1 h and 20 h early time-points.

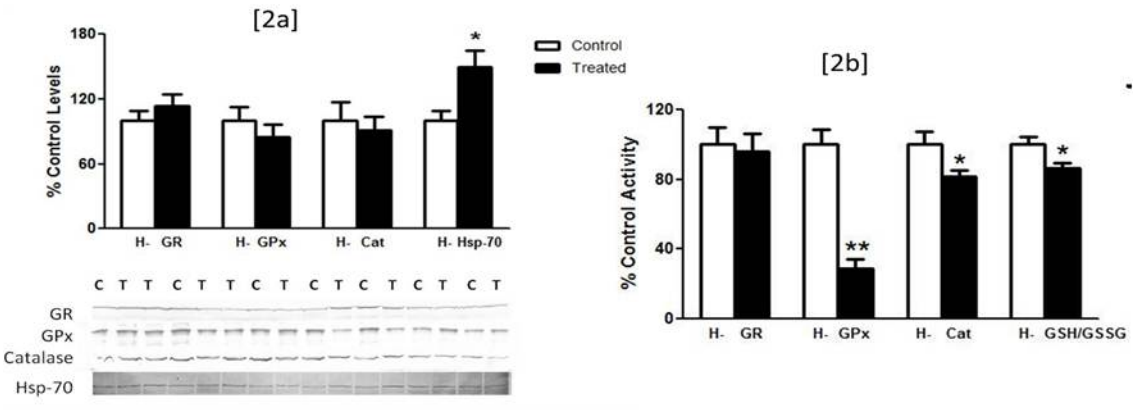


**Figure 5.2:** Antioxidant levels and activities in hippocampus 30 d after 5 nm ceria ENM administration. a) The histograms showing GR, GPx, catalase, antioxidant enzymes and HO-1, Hsp70 heat shock proteins levels and corresponding Western blots showing protein levels in control [C] and treated [T] samples. The intensity of each band was normalized with intensity of corresponding band of β-actin-loading control, and b) GR, GPx catalase antioxidant activities, and GSH: GSSG ratio measured in control and ceria treated samples. The values are calculated as % control for each measurement expressed as mean ± SEM, control n = 7, treated n = 9, *p <0.05, **p < 0.01, compared to control.

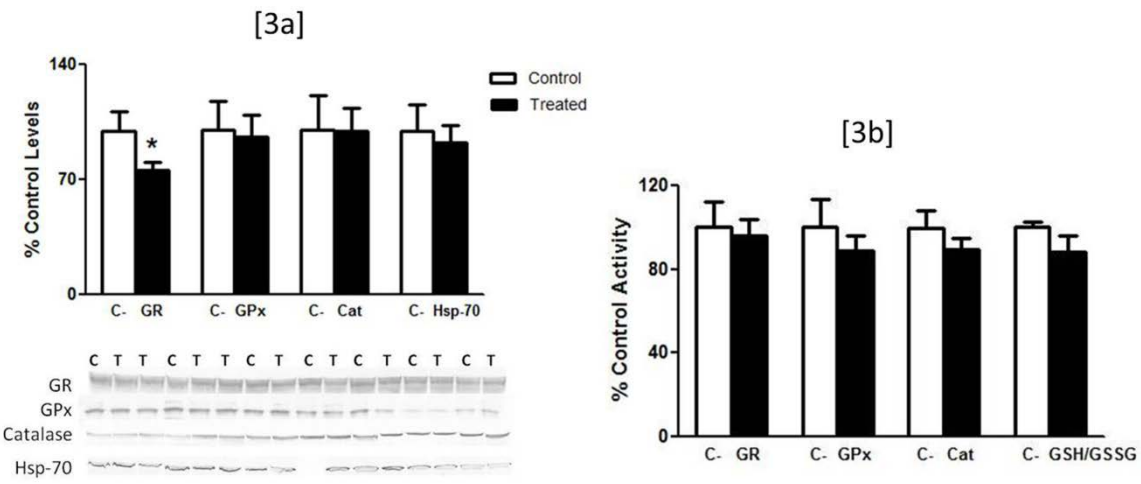


**Figure 5.3:** Antioxidant levels and activities in cortex 30 d after 5 nm ceria ENM administration. a) histograms showing GR, GPx, catalase, antioxidant enzymes and HO-1, Hsp70 heat shock proteins levels and corresponding Western blots showing protein levels in control [C] and treated [T] samples. The intensity of each band was normalized with intensity of corresponding band of β-actin-loading control, and b) GR, GPx catalase antioxidant activities, and GSH: GSSG ratio measured in control and ceria treated samples. The values are calculated as % control for each measurement expressed as mean ± SEM, control n = 7, treated n = 9, *p <0.05, **p < 0.01, compared to control.

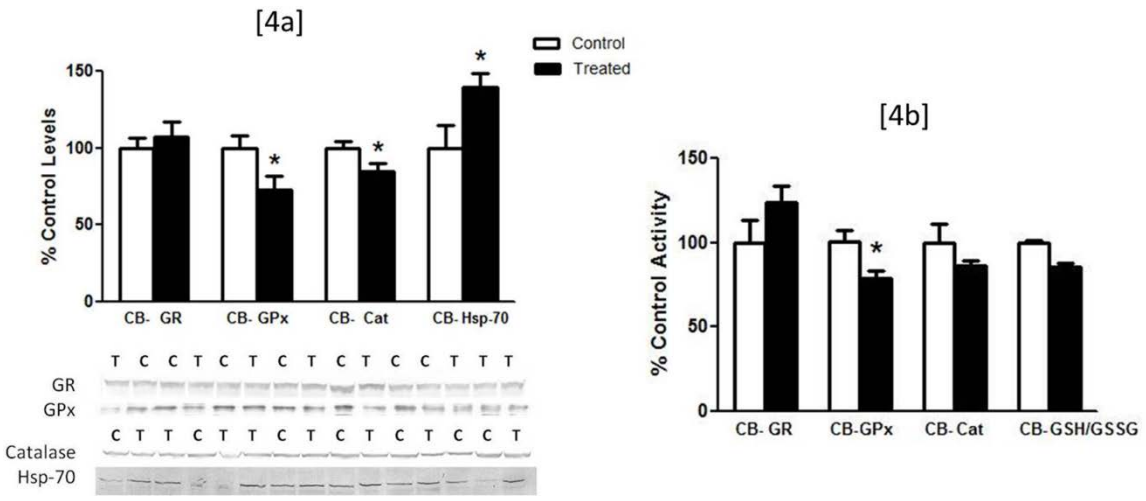


**Figure 5.4:** Antioxidant levels and activities in cerebellum 30 d after 5 nm ceria ENM administration. a) histograms showing GR, GPx, catalase, antioxidant enzymes and HO-1, Hsp70 heat shock proteins levels and corresponding Western blots showing protein levels in control [C] and treated [T] samples. The intensity of each band was normalized with intensity of corresponding band of β-actin-loading control, and b) GR, GPx catalase antioxidant activities, and GSH: GSSG ratio measured in control and ceria treated samples. The values are calculated as % control for each measurement expressed as mean ± SEM, control n = 7, treated n = 9, *p <0.05, **p < 0.01, compared to control.

*Ceria treatment induced protein oxidation after 30 d*

Thirty days after ceria ENM treatment, the levels of PC showed a significant increase in the hippocampus (~ 19%, *p<0.05, Figure 5.5a) and cerebellum (~12 %, *p<0.05, Figure 5.5b) in treated vs. control samples. 3NT levels were significantly increased in the cortex (~20%, *p<0.05, Figure 5.5c). There was no significant change in protein-bound HNE levels in any of the three brain regions. Consistent with increased 3NT levels in cortical region, iNOS levels were increased significantly (~27%, *p<0.05, Figure 5.5d), and there was a positive correlation between 3NT and iNOS levels ($r= 0.67$, $p < 0.05$, Figure 5.5d).

Measurement of oxidative stress parameters (PC, 3NT, and protein-bound HNE) in the hippocampus, cortex, and cerebellum of adult rat brain 1 and 20 h after administration of 100 mg/kg ceria ENM did not reveal any significant difference in control versus treated samples (Table 5.3).

[5a]

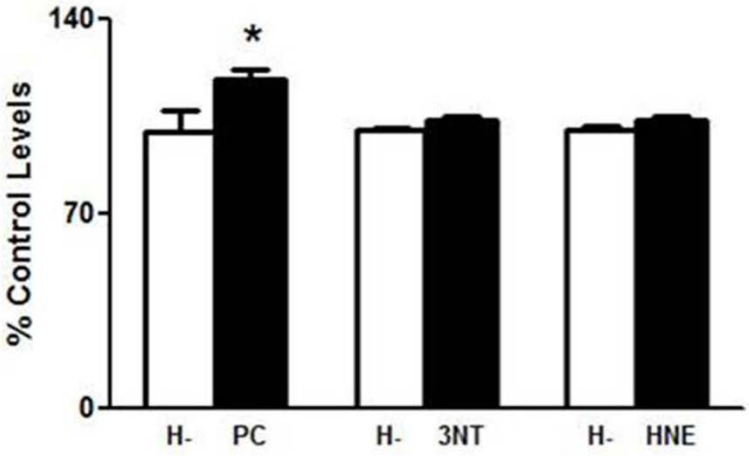


[5b]

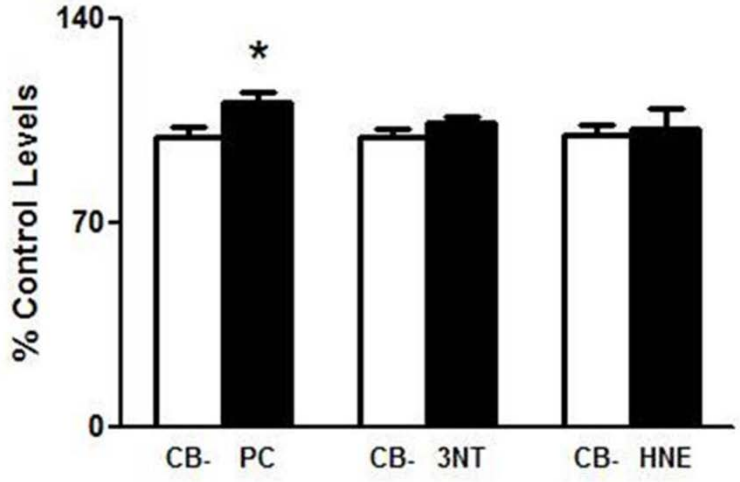


**Figure 5.5a and b:** Protein oxidation and lipid peroxidation markers in hippocampus and cerebellum 30 d after 5 nm ceria administration. a) Oxidative stress markers PC, 3NT and HNE levels in hippocampus, and b) oxidative stress markers PC, 3NT and HNE levels in cerebellum. The values are calculated as % control for each measurement expressed as mean ± SEM, control n = 7, treated n = 9, *p <0.05, **p < 0.01, compared to control.

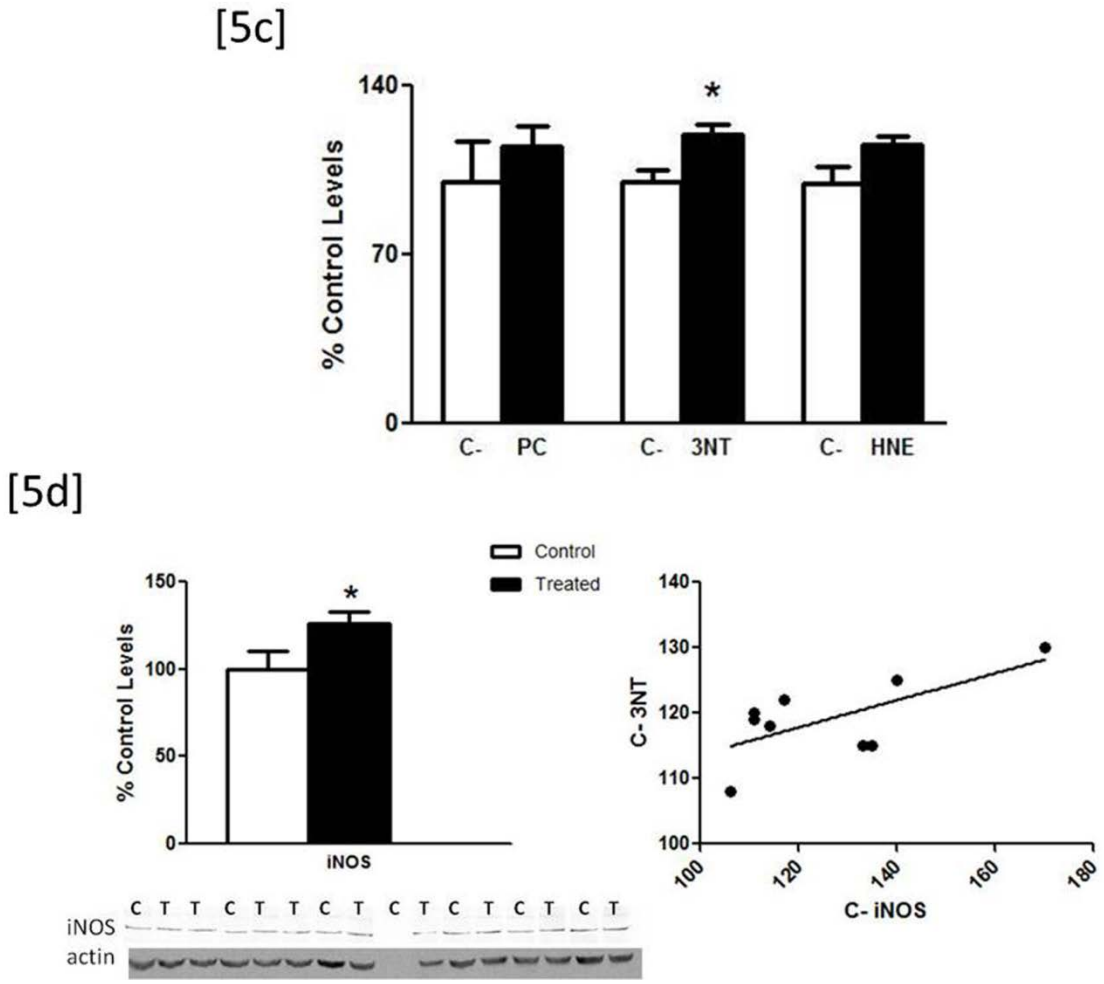


**Figure 5.5c and d:** Protein oxidation and lipid peroxidation markers in cortex 30 d after 5 nm ceria administration. c) Oxidative stress markers PC, 3NT and HNE levels, and d) iNOS levels and correlation between 3NT levels and iNOS levels in ceria treated samples, n=9, r=0.67, $p < 0.05$. The values are calculated as % control for each measurement expressed as mean ± SEM, control n = 7, treated n = 9, *p <0.05, **p < 0.01, compared to control.

### 5.4. Discussion

A decline in the GSH: GSSG ratio (in hippocampus and cerebellum) after 30 d indicates oxidative status of the cellular environment. A similar observation was reported in Park *et al*. in which 30 nm ceria depleted GSH levels in human lung epithelial cells in a dose-dependent manner (Park et al. 2008). Hydroxylated derivatives of fullerenes decreased the GSH: GSSG ratio and induced MDA-lipid peroxidation marker levels (Nakagawa et al. 2011). At the cellular level the GSH: GSSG ratio is dependent on GPx and GR enzymes, and we observed decreased GPx activity (in hippocampus and cerebellum), decreased GPx levels (in cerebellum) and decreased GR levels (cortex) after 30 d. Similarly, 15 nm silver and 90 nm copper ENM down-regulated GPx gene expression (Wang et al. 2009), 25 nm silver ENM (Rahman et al. 2009) and SWCNT (Wang et al. 2011) inhibited GPx activity, and silica ENM reduced GR activity (Akhtar et al. 2010). Thus it may be that after 30 days post exposure, ENM have deleterious effects on brain-rendant enzymes needed for maintenance of the reduced thiol status of the cells. Further inhibition of catalase activity ( after 30 d) along with GPx activity, may lead to accumulation of $H_2O_2$ and ultimately increased production of hydroxyl radicals (OH•). Activity of catalase can be inhibited by hydroxyl radicals (OH•) and that of GPx by $H_2O_2$ and hydroperoxides (Pigeolet et al. 1990). Ceria ENM can produce $H_2O_2$ under abiotic conditions (Korsvik et al. 2007; Xia et al. 2008), and $H_2O_2$ has high membrane permeability (Halliwell 1992). Further $H_2O_2$ can undergo a Fenton-type reaction to produce highly potent OH• radicals as noted above. A lack of change in SOD activity and level in the current study may imply that endogenous SOD does not account for elevated

oxidative stress in brain in this study. Therefore, ceria ENM treatment may have caused induction in ROS that lead to oxidative inhibition of antioxidant enzyme activities, decreased GSH: GSSG ratio and increased in PC and 3NT levels observed after 30 d. Similar augmentation of oxidative stress was seen after exposure to various other ENM such as $TiO_2$ (Hao et al. 2009; Liang et al. 2009; Xiong et al. 2011), SWCNT (Wang et al. 2011), MWCNT (Guo et al. 2011), hematite (Radu et al. 2010), ZnO (Xia et al. 2008).

On the other hand increased levels (1 h) and activity (20 h) of catalase in hippocampus indicates initial oxidative stress defense response to ceria ENM treatment observed at early exposure time-points, which was reinforced by lack of increase in PC, 3NT or HNE levels at 1 and 20 h.

After 30 d, elevated 3NT levels, a marker for increased nitrosive stress, are consistent with elevated levels of inducible nitric oxide synthase (iNOS). iNOS exists at extremely low levels under normal physiological conditions, but is inducible by endotoxin, and inflammatory cytokines among other stresses (Calabrese et al. 2000; Calabrese 2007). We found a correlation between 3NT levels and iNOS levels in the cortical region of rats examined 30 d after ceria ENM treatment. It may indicate that increased 3NT levels are due to increased NO production in the cortex and iNOS levels concurrently may be induced following ceria treatment via increased cytokine production. Electron microscopic analysis showed an intact BBB and an absence of any significant amount of ceria in the brain. However, cobalt-chromium ENMs have damaged DNAs without crossing cellular membranes (Bhabra et al. 2009), and the chemotherapeutic drug doxorubicin lead to neurotoxic effects without ever crossing the BBB (Tangpong et al. 2006). Similarly, it is conceivable that the observed oxidative stress response in brain

regions could be due to the accumulation of 5 nm ceria in peripheral organs and subsequent inflammatory cytokines. Studies to test this notion will be carried out in the future in our laboratory.

Induction of heat shock protein Hsp-70 levels as seen after 30 d is in agreement with other literature reports. Similar to effects of silver ENM (Ahamed et al. 2010) and fullerene C60 (Usenko et al. 2008) treatments, Hsp-70 levels and other oxidative stress markers were induced with concomitant decrease in the GSH: GSSG ratio. In a transgenic mouse model for cardiomyopathy, Hsp-70 levels were increased as an oxidative stress marker of ER stress. Ceria ENM treatment rescued these cells from ER stress and as a result Hsp-70 expression was down regulated (Niu et al. 2007).

These pro-oxidant effects in the brain after 30 days exposure in vivo to ceria ENM indicate some sort of effect of time after long-term retention of ceria ENM in peripheral organs compared to its short term (1 and 20 h) retention, where moderate antioxidant effects were observed. The EELS data suggests that mechanisms other than the switching between $Ce^{4+}$ and $Ce^{3+}$ oxidation states and the possibility to absorb and release oxygen by inducing oxygen vacancies may play a critically important role in pro-oxidant effects of ceria ENM. Therefore, under the conditions of the present study we propose that 5 nm ceria ENM induces in brain initial oxidative stress defense response and upon longer exposure, pro-oxidant effects without crossing the BBB. Ceria ENM indirectly induced ROS production in brain caused depletion of GSH, which initially induced antioxidant levels (1 and 20 h) but over 30 days eventually inhibits $H_2O_2$-scavenging catalase and GPx enzyme activities. This may increase $H_2O_2$ levels and therefore OH• production via Fenton reaction, which may cause protein oxidation and induction of Hsp 70, levels

(Figure 5.6). We speculate that ceria ENM may cause increased iNOS levels in a similar fashion, which leads to increased 3NT levels.

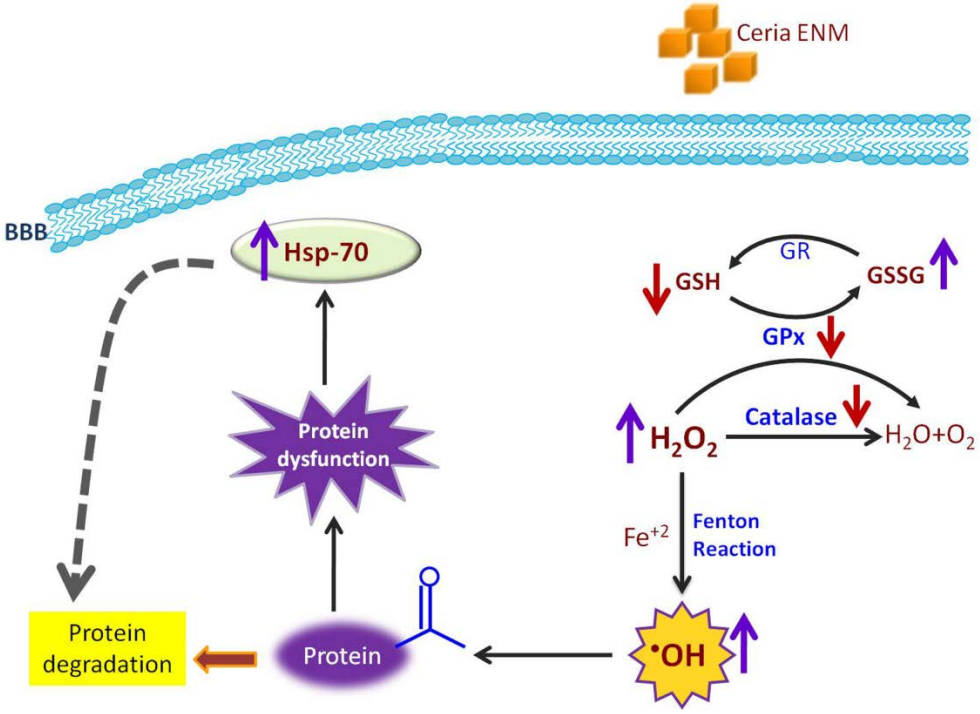


**Figure 5.6:** In this proposed pathway 5 nm ceria ENM induces pro-oxidant effects after 30 d in rat brain without crossing the BBB. Ceria ENM indirectly induces ROS production as indicated by thick downward arrow leading to GSH depletion and inhibition of catalase and GPx enzymes. This inhibition of $H_2O_2$ reducing enzyme activity can induce $H_2O_2$ levels and therefore hydroxyl radicals (OH•) production mediated by Fenton reaction. Increased OH• can further oxidize the proteins and may hamper their regular function. Hydroxyl radicals may also inhibit $H_2O_2$ reducing catalase and GPx activity by way of oxidative modification. These bio-chemical reactions could make cellular environment more oxidizing, triggering a cellular stress response to induce Hsp-70 levels. Hsp-70 is a chaperone protein that can shepherd oxidized protein to proteosomes for degradation for further cellular clearance (shown as dotted arrow). If

timely clearance of oxidized protein takes place then there may not be any change in cellular PC levels. As there was no evidence of the presence of ceria ENM inside the brain, it is further proposed that ceria ENM exert its pro-oxidant effect in the brain secondary to its peripheral effects.

# CHAPTER 6

# SYSTEMIC ADMINISTRATION OF 15 NM CERIA ENM INDUCES PHASE II ANTIOXIDANTRESPONSE IN RAT BRAIN

## 6.1. Overview of the Study

According to the U.S. National Nanotechnology Initiative (NNI) nanoscale material is one which has at least one dimension in the range of 1 to 100 nanometers, with properties that are often unique due to their dimensions (Yokel et al. 2011). As size of particle decreases, its surface area to mass ratio increases concomitantly, the fraction of atoms present on the surface also increases. Due to these factors, nanoparticles behave significantly different than bulk materials of microparticles. The size of nanoparticles not only influences the physico-chemical properties of nanomaterial but also, it's the biological behavior. Upon exposure to biological materials or biological systems, nanomaterials can reach to various small cellular compartments, which are otherwise inaccessible to microparticles. In addition to this, the large surface area of nanaoparticles can be used as a platform or anchor by bio-molecules for different biological processes (Nel et al. 2009; Fubini et al. 2010). As well as due to the high fraction of atoms present on the surface, nanoparticles can take active part and catalyze biological reactions efficiently (Das et al. 2007; Karakoti et al. 2009). Therefore, size becomes an important factor to be considered in determining the nanotoxicity of nanomaterials.

The toxicological studies conducted over past decade have demonstrated that small ENMs (< 100nm), cause adverse respiratory effects, by mainly inducing inflammation than larger particles with same material composition (Donaldson et al. 2003; Oberdörster et al. 2005; Buzea et al. 2007; Kang et al. 2009; Thomassen et al. 2009). Based on

literature findings, ~ 15 to 30 nm is a critical width or diameter for ENMs to have properties different from the solution and bulk chemistry of their components (Jiang et al. 2008; Yokel et al. 2011). The significant change in the physico-chemical properties of ENM is strongly related to the exponential increase in the number of atoms localized on the surface of ENM, making ~ 15 to 30 nm ENM to stand out from microparticles and bulk materials (Auffan et al. 2009; Yokel et al. 2011). Pulmonary toxicity studies with TiO2 ENMs compared two sizes 20 nm and 250 nm (Oberdörster et al. 1994; Oberdörster et al. 2005). A comparison of ultrafine- and fine-TiO2 particle induced revealed increased cytotoxic effects upon untrafine-TiO2 treatment (Kang et al. 2009) as well silica ENM showed size-dependent cytotoxicity (Thomassen et al. 2009). In spite of having same crystal structure, smaller size ENM induced high inflammatory response, showed significantly prolonged retension (up to 1 year), and increased translocation to pulmonary intestitium and persistence. In addition to it, small ENM had adverse effect on cell proliferation, and it impaired alveolar microphage functions (Oberdörster 1988; Buzea et al. 2007).

As explained earlier, oxidative stress effects of ceria ENM are topic of discrepancy. In order to understand the influence of size on the oxidative stress effects of ceria ENM, ceria ENM with different sizes were synthesized. Each of the proceeding chapters focused on one size of ceria ENM and its oxidative stress effects on rat brain evaluated at different time points. In this chapter we discuss oxidative stress effects of 15 nm ceria ENM on rat brain upon systemic administration. Five% dispersion of the material was administered to male rats intravenously (250 mg/kg and 100 mg/kg). The rats that received 250 mg/kg dose were terminated after 1 h and the rat that received 100 mg/kg

dose were terminated after 30d. Three brain regions, hippocampus, cortex and cerebellum from each treatment were harvested from each ceria and saline-control treated rats and frozen rapidly in liquid nitrogen. The levels and activities of the antioxidant enzymes catalase, manganese superoxide dismutase (Mn-SOD), glutathione peroxidase (GPx), and glutathione reductase (GR), were measured along with the ratio of reduced glutathione (GSH) to its oxidized form (GSSG). To understand the extent of changes in cellular redox status, the levels of oxidative stress endpoints, protein carbonyl (PC), 3-nitrotyrosine (3NT), and protein bound 4- hydroxyl-2-trans nonenal (HNE), were measured along with heat shock protein (Hsp70) levels.

## 6.2. Materials and methods

### 6.2.1. Nanomaterial:

Ceria ENM was obtained from our collaborator, which was synthesized in in-house facility (Section 3.1). Nanomaterial characterization was carried out by our collaborators, prior to ceria ENM treatment to the animals (Section 3.2).

### 6.2.2. Animals:

The male Sprague-Dawley rats received either saline or 5% ceria dispersion intravenously. Five rats were infused with 0 and three rats with 250 mg ceria/kg and terminated 1 h after completion of infusion. Five rats were infused with 0 and 5 rats with 100 mg ceria/kg and terminated 30 d after completion of infusion. After ceria ENM treatments, the BBB integrity assessment (Section 3.3), light and electron microscopic assessment (Section 3.4) and EELS analysis (Section 3.2) was carried out by our collaborators. The brain homogenates were prepared from control and ceria treated rat brain samples (Section 3.6). Total protein content was determined using BCA assay

(Section 3.7) and various biochemical assays were carried out on all the samples (Sections 3.8, 3.9, 3.10, 3.11, and 3.14) in our lab.

### 6.3. Results

Ceria composition

HR-TEM/HR-STEM showed the ceria ENM was polyhedral shape (Figure 1). The XRD patterns demonstrated the ceria are highly crystalline. Evaluation of a number of TEM images showed that the ceria had a number-average primary particle size of 15 nm.

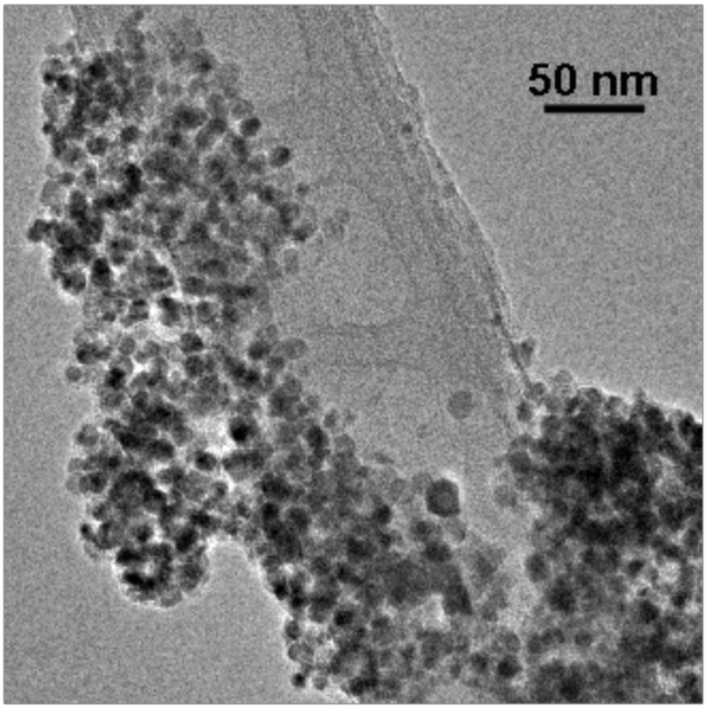


**Figure 6.1:** Ceria ENM imaged using HRTEM and HRSTEM. The ceria were dispersed on a carbon film. Visually they have a size distribution ranging from X to X nm and the majority diameter around 15 nm. The magnified TEM insert at the lower left illustrates that the ceria ENMs are highly crystalline (taken by Dr. Peng Wu).

Ceria concentration in brain and electron microscopy

ICP-MS analysis suggested that a very small amount of ceria was present in the brain parenchyma compare to peripheral organ liver (Table 1). Electron micrographic studies suggested that ceria ENM was not found in the brain, but located on the luminal side of the BBB endothelium. The hippocampus and cerebellum tissues did not show obvious ceria induced injury as no necrotic neurons or elevated gliosis were observed and the BBB was visibly intact (data not shown).

**Table 6.1:** Cerium concentrations in blood, brain, liver, and spleen, expressed as a percent change of 15 nm ceria ENM dose. a) Based on reference volume of blood in the rat (7% of body weight) or weight of the brain, liver x ceria concentration.

| | **Cerium [% of dose][a]** | | |
|---|---|---|---|
| | **Blood** | **Brain** | **Liver** |
| **% dose (1 h)** | 0.59 ± 0.15 | 0.006 ± 0.004 | 32 ± 14 |
| **% dose (30 d)** | 0.0048 ± 0.0011 | 0.0013 ± 0.001 | 22.6 ± 12 |

EELS results

Electron energy loss spectroscopic measurements on liver tissue were performed as a representative organ. The ratio of Ce(Owens Iii et al.) to Ce(IV) in the aged ceria was evaluated using EELS measurements after locating agglomerates of the ceria nanorods in tissue 1 h and 30 days after infusion into rat and comparing with synthesized ceria. The

high $Ce^{3+}$/ $Ce^{4+}$ ratio that was obtained in the as-synthesized, fresh 15 nm ceria seems to have only been altered slightly in individual ceria measured in liver after 30 days *in vivo* (data not shown).

Oxidative Stress Indices

*GSH: GSSG ratio increases in a time dependant manner*

One hour after 250 mg/kg dose of 15 nm ceria, brain redox status was affected as indicated by declined in GSH: GSSG ratios in hippocampus (~ 16%, $^{\xi}p < 0.01$, Figure 6.2), and cortex as well as in cerebellum, although the latter was not significant. Thirty days after administration of 100 mg/kg dose of 15 nm ceria ENM, GSH: GSSG ratio was not significantly changed; however, an increasing trend was observed when compared with the respective controls. The declined trend in GSH: GSSG ratio suggests more oxidized cellular status after 1 h, while the ascending trend of GSH: GSSG ratio may suggest the more reduced redox status of brain after 30 d.

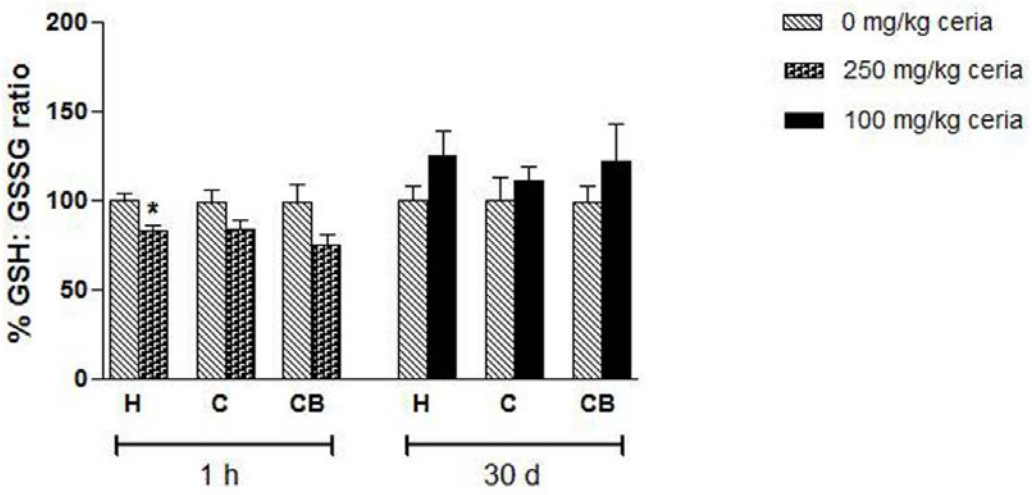


**Figure 6.2:** GSH: GSSG ratios in 3-brain regions 1 h after 250 mg/kg dose and 30 d after 100 mg/kg dose of 15 nm ceria ENM. The histograms represent % control for saline treated controls and ceria treated samples. The values are expressed as mean ± SEM, control n = 5, treated n = 5, *$p < 0.05$, $^{\xi}p < 0.01$, and $^{\Theta}p < 0.001$, compared to mean of respective control samples.

*SOD level and activity spiked up after ceria treatment*

SOD, superoxide dismutase antioxidant enzyme, which converts superoxide radical into $H_2O_2$ and $O_2$, was significantly affected after 15 nm ceria treatment. MnSOD levels were increased significantly in hippocampus (~ 40%, *$p < 0.05$), cortex (~ 53%, $^{\xi}p < 0.01$), and cerebellum (~ 28%, *$p < 0.05$) 1 h after receiving 250 mg/kg dose of 15 nm ceria ENM (Figure 6.3a). However, MnSOD levels remained unaffected 30 days after receiving 100 mg/kg dose of 15 nm ceria. The levels of catalase, $H_2O_2$ reducing antioxidant enzyme, showed slight increase (H and CB) 1 h after administration of higher dose of ceria, and slight decrease (H and CB), 30 d after lower dose of ceria; but neither of the changes were significant (Figure 6.3b). Among two glutathione dependant

enzymes, only GPx levels were significantly elevated in cortex (~ 33%, *$p < 0.05$, Figure 6.3c) 1 h after ceria ENM treatment. GPx levels were decreased in hippocampus, almost unchanged in cortex and slightly increased in cerebellum, 30 d after 100 mg/kg ceria treatment, but none of the changes were significant. GR levels were slightly increased in cortex and decreased in cerebellum after 1 h, and showed no change after 30 d (Figure 6.3d).

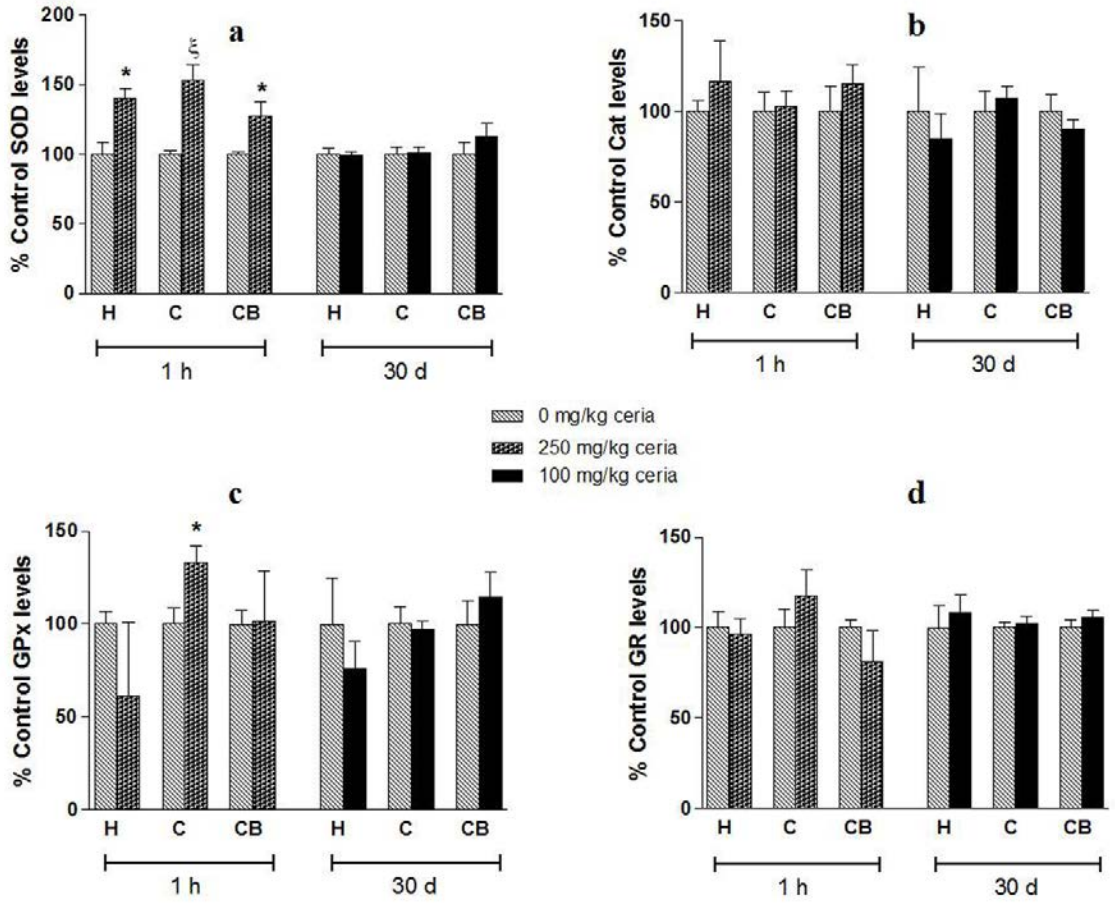


**Figure 6.3a, b, c and d:** The antioxidant enzyme levels in 3-brain regions 1 h after 250 mg/kg dose and 30 d after 100 mg/kg dose of 15 nm ceria ENM. a) The histograms represent % control MnSOD levels measured in saline treated controls and ceria treated samples, b) the histograms represent % control catalase levels measured in saline treated controls and ceria treated samples, c) the histograms represent % control GPx levels measured in saline treated controls and ceria treated samples, d) the histograms represent % control GR levels measured in saline treated controls and ceria treated samples. All the values are expressed as mean ± SEM, control n = 5, treated n = 5, *p <0.05, $^{\xi}$p < 0.01, and $^{\Theta}$p < 0.001, compared to mean of respective control samples.

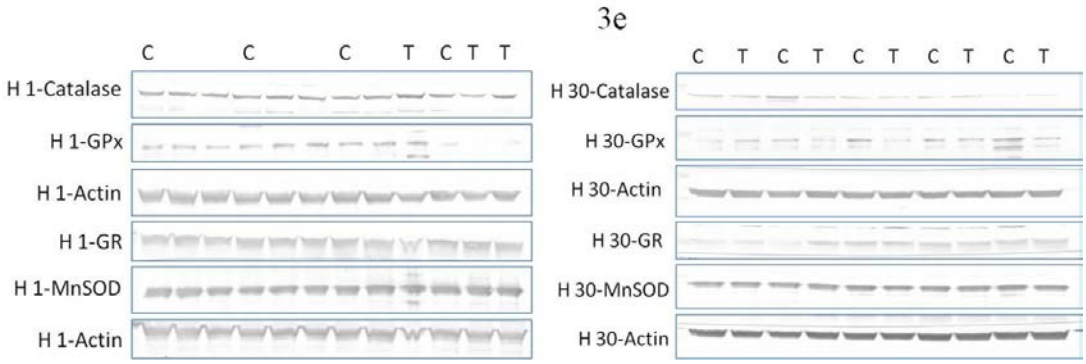


**Figure 6.3e:** Separate Western blots were used to estimate antioxidant protein levels in hippocampus, cortex and cerebellum. However, only representative examples from hippocampus are shown. Protein levels in control [C] n=5, and treated [T] n=3 (1 h, left, consider only labeled bands) and [T] n=5 (30 d, right) 15 nm ceria ENM treatment. The intensity of each antioxidant protein band was normalized with intensity of corresponding band of β-actin-loading control. Similar blots were obtained for cortex and cerebellum regions.

Similar to the antioxidant levels, antioxidant enzyme activities were heavily affected 1 h after 250 mg/kg dose treatment of 15 nm ceria ENM. SOD activity was significantly increased after 1 h in hippocampus (~ 30%, *$p < 0.05$), cortex (~ 26%,*$p < 0.05$), and cerebellum (~ 24%,*$p < 0.05$) but remained unaffected after 30 d (Figure 6.4a). Catalase activities were significantly elevated in hippocampus (~ 24%, $^{\xi}p < 0.01$) and in cerebellum (~ 16%, *$p < 0.05$) after 1 h, cortex region catalase activity was slightly increased (Figure 6.4b). 30 d after 100 mg/kg ceria treatment, catalase activity was slightly declined in cortex, while elevated in cerebellum, but remained unaffected in hippocampus (Figure 6.4b). GPx activity was increased after 1 h in hippocampus (~ 28%, $^{\xi}p < 0.01$) and cortex (~ 33%, *$p < 0.05$), and remained unchanged in cerebellum, while after 30 d GPx activity did not change in any of the brain region (Figure 6.4c). While GR

activity showed some decreasing trend after 1 h (C and CB) and somewhat increasing trend after 30 d (C and CB), the changes were not statistically significant (Figure 6.4d).

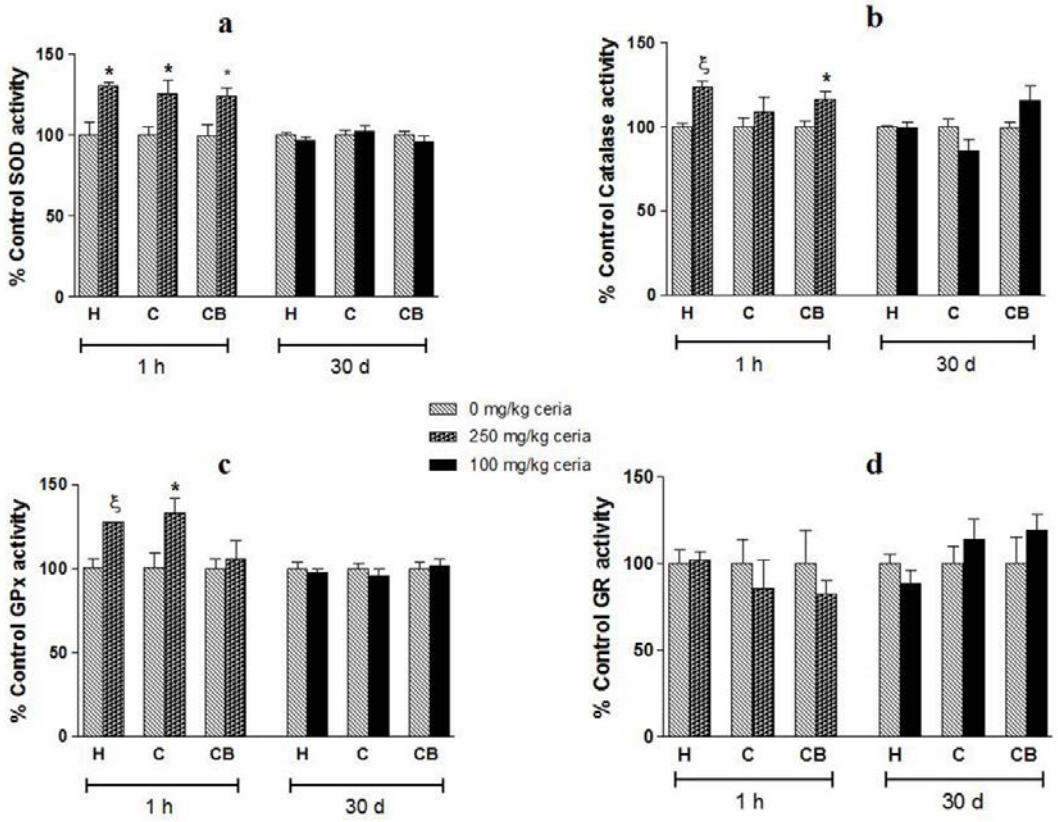


**Figure 6.4:** The antioxidant enzyme activities in 3-brain regions 1 h after 250 mg/kg dose and 30 d after 100 mg/kg dose of 15 nm ceria ENM. a) the histograms represent % control SOD activities measured in saline treated controls and ceria treated samples, b) the histograms represent % control catalase activities measured in saline treated controls and ceria treated samples,c) The histograms represent % control GPx activities measured in saline treated controls and ceria treated samples, d) the histograms represent % control GR activities measured in saline treated controls and ceria treated samples. All the values are expressed as mean ± SEM, control n = 5, treated n = 5, *p <0.05, $^{\xi}$p < 0.01, and $^{\Theta}$p < 0.001, compared to mean of respective control samples.

*PC, 3NT and HNE levels decreased after 1h however, HSP levels increased*

PC, 3NT and HNE levels were affected only after 1 h. PC levels were decreased in hippocampus (~ 30%, *$p < 0.05$) and cerebellum (~ 29%, *$p < 0.05$) (Figure 6.5a). 3NT levels were decreased significantly in hippocampus (~ 69%, $^{\xi}p < 0.01$) and showed decreasing trend in cortex (Figure 6.5b). HNE levels were decreased significantly in hippocampus (~ 38%, $^{\xi}p < 0.01$) and in cerebellum (~ 28%, $^{\xi}p < 0.01$) (Figure 6.5c). There was no effect on the PC, 3NT or HNE levels after 30 d in 3-brain regions (Figure 4a, b and c). The reduction in protein oxidation and lipid peroxidation markers (1 h) is consistent with elevated antioxidant protein levels and activities after 1 h.

The heat shock proteins function as intra-cellular chaperones for other proteins. As a chaperon, they assist in the establishment of proper protein conformation and prevent unwanted protein aggregation. HSPs also help in stabilizing partially folded proteins and transporting proteins across membranes within the cell. The upregulation of heat shock protein is an important cellular stress response and can be induced by oxidative stress. Unlike observed in our other studies, heat shock protein HO-1 and Hsp70 levels were induced after 1 h, even though protein oxidation and lipid peroxidation markers were significantly decreased. Induction in Hsp70 levels was observed in all 3-brain regions; hippocampus (~ 36%, *$p < 0.05$), cortex (~ 33%, *$p < 0.05$) and cerebellum (~ 38%, *$p < 0.05$) after 1 h (Figure 6.6a). Induction of HO-1 levels was seen after 1 h in hippocampus (~ 25%, *$p < 0.05$) and in cerebellum (~ 27%, *$p < 0.05$), whereas decreased in cortex but this change was not significant (Figure 6.6b).

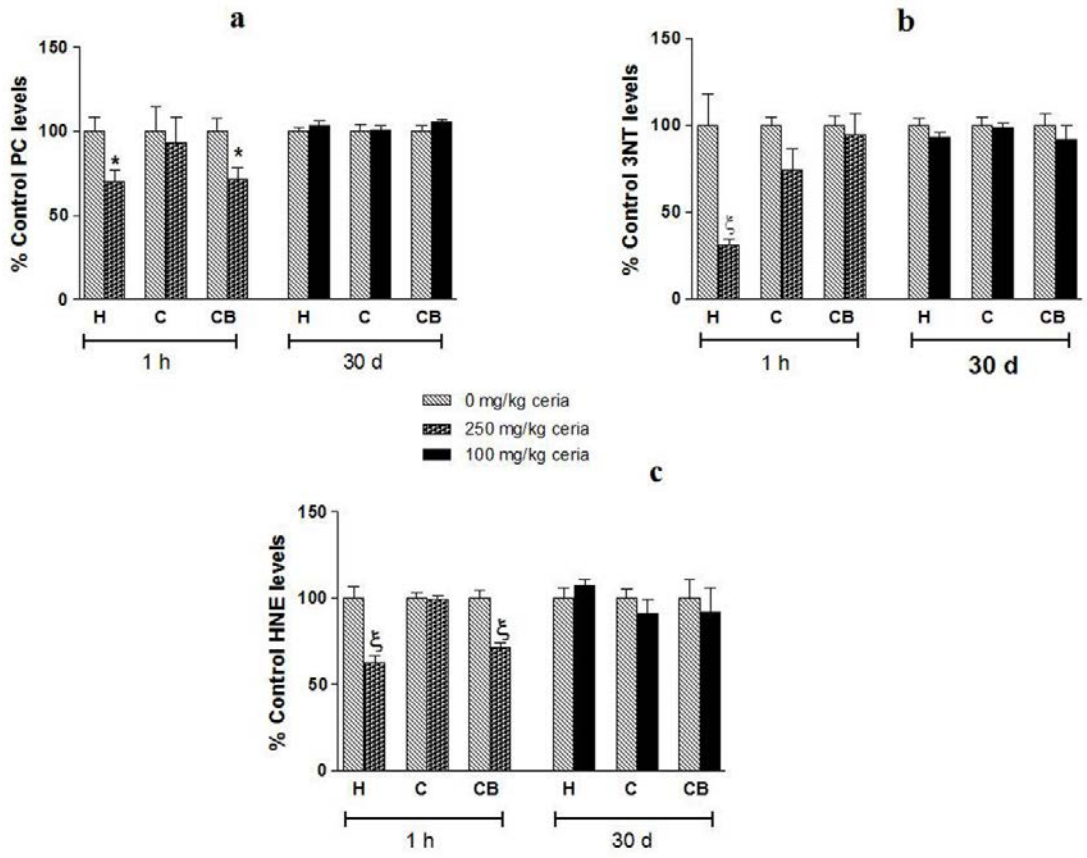


**Figure 6.5:** The oxidative stress marker levels in 3-brain regions 1 h after 250 mg/kg dose and 30 d after 100 mg/kg dose of 15 nm ceria ENM. a) The histograms represent % control PC levels measured in saline treated controls and ceria treated samples, b) the histograms represent % control 3NT levels measured in saline treated controls and ceria treated samples, c) the histograms represent % control HNE levels measured in saline treated controls and ceria treated samples. All the values are expressed as mean ± SEM, control n = 5, treated n = 5, *p <0.05, $^{\xi}$p < 0.01, and $^{\Theta}$p < 0.001, compared to mean of respective control samples

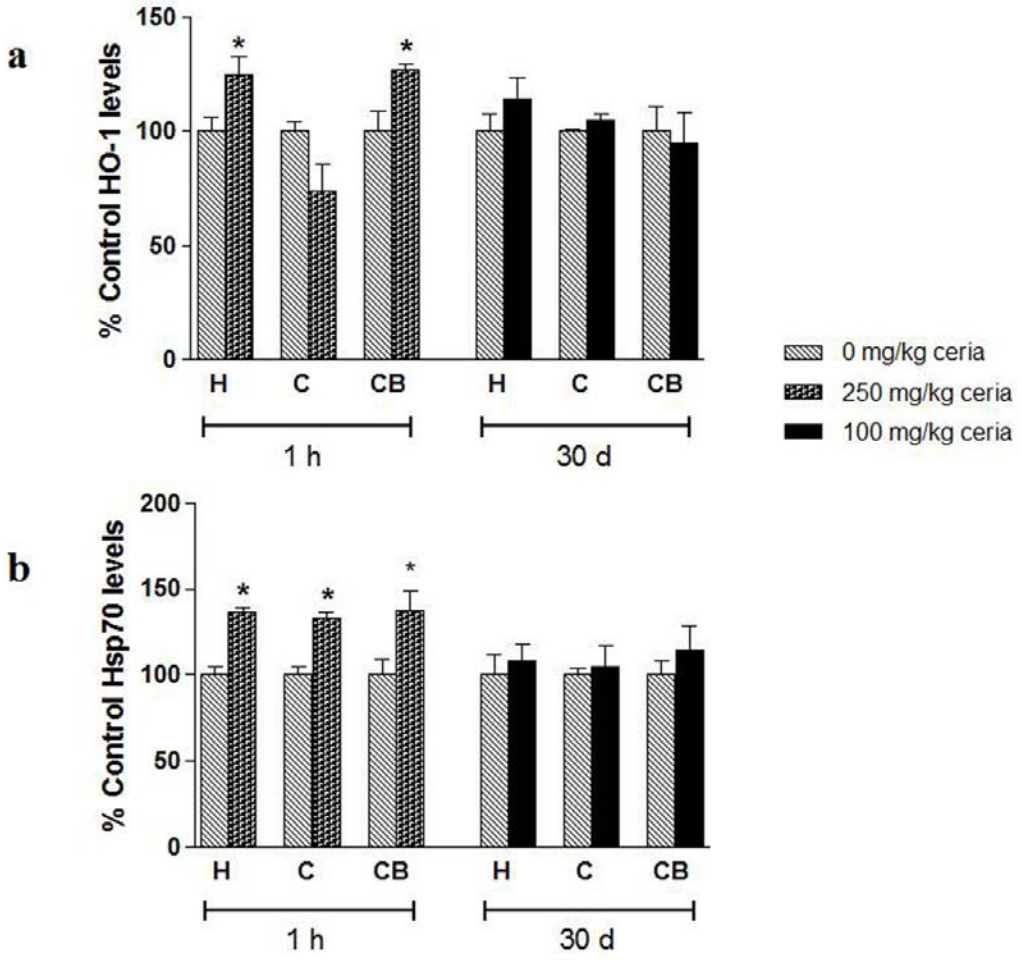


**Figure 6.6a and b:** The heat shock protein levels in 3-brain regions 1 h after 250 mg/kg dose and 30 d after 100 mg/kg dose of 15 nm ceria ENM. a) The histograms represent %control HO-1 levels measured in saline treated controls and ceria treated samples, b) the histograms represent %control Hsp70 levels measured in saline treated controls and ceria treated samples. All the values are expressed as mean ± SEM, control n = 5, treated n = 5, *p <0.05, $^{\xi}$p < 0.01, and $^{\Theta}$p < 0.001, compared to mean of respective control samples.

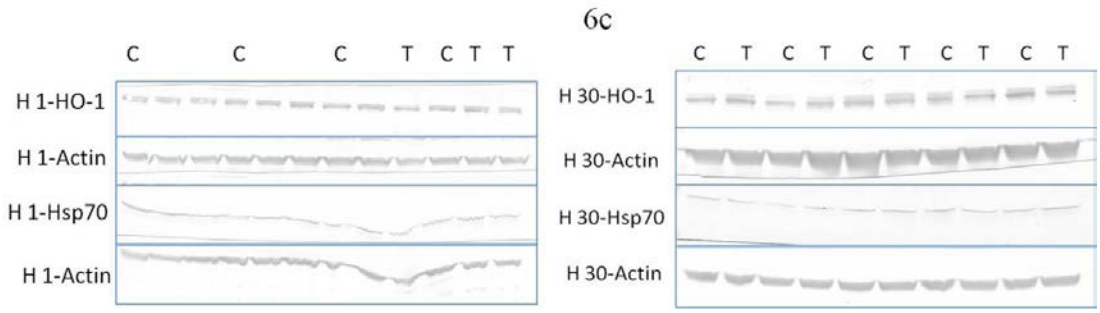


**Figure 6.6c:** Separate Western blots were used to estimate HSPs levels in hippocampus, cortex and cerebellum. However, only representative examples from hippocampus are shown. Protein levels in control [C] n=5, and treated [T] n=3 (1 h, left, consider only labeled bands) and [T] n=5 (30 d, right) 15 nm ceria ENM treatment. The intensity of each antioxidant protein band was normalized with intensity of corresponding band of β-actin-loading control. Similar blots were obtained for cortex and cerebellum regions.

### 6.4. Discussion

The toxicity of nanomaterials is governed by various factors including chemical composition, size, morphology, and surface modifications. According to the ENM toxicity studies from past decade, the smaller the size of ENM, the higher is the toxicity (Lippmann 1990; Buzea et al. 2007). Additionally, based on correlation between surface area and fraction of atoms present on the surface of a particle, ENM with one or more dimensions in the range of ~ 15 to 30 nm exhibits distinctly different physico-chemical behavior (Jiang et al. 2008; Yokel et al. 2011). Therefore, to evaluate the influence of size on the oxidative stress effects of ceria ENM, we synthesized 5 nm, 15 nm 30 nm and 55 nm size ceria ENM. 5% dispersion of each ceria ENM was administered intravenously to the separate groups of male rats. The tissues were harvested at different time intervals

after ceria administration from each saline and ceria ENM treated rats. The oxidative stress effects of ceria ENM on three rat brain regions were evaluated separately.

In the current study the three rats that received higher dose (250 mg/kg) of 15 nm ceria ENM were terminated after 1 h along with five saline-treated rats. Antioxidant enzyme SOD levels were dramatically induced in all the brain regions of ceria treated rats, along with SOD enzyme activity. GPx levels (C) with its activity (H and C) were increased, catalase levels were elevated and activity was increased (H and CB). Such coordinated upregulation of phase II enzymes can be induced by minor increase in oxidative stress caused by external or internal stimuli (Li et al. 2004; Kim et al. 2009). Induction of phase II antioxidant enzymesalso can be seen as a response to GSH depletion or decreased GSH: GSSG ratio (Limón-Pacheco et al. 2007; Lee et al. 2008; Speciale et al. 2011), as observed in the current study after 1 h ceria ENM treatment. Similar cellular response was observed where ceria ENM rescued rat liver from monocrotaline mediated ROS injury (Amin et al. 2011), protected H9c2 cardiomyocytes exposed to cigarette smoke (Niu et al. 2011), human colon cells exposed to radiation (Colon et al. 2010) from induced ROS injury by restoring phase II enzyme activities and / or levels.

The phase II antioxidant enzyme induction is a cellular defense mechanism against increased oxidative stress and to protect protein, lipids and DNA from any further oxidative damage (Li et al. 2004; Limón-Pacheco et al. 2007; Lee et al. 2008; Speciale et al. 2011). Although increased levels and activity of SOD can effectively degenerate super oxide radicals ($O_2^{-\bullet}$), it can also increase levels of $H_2O_2$ (Poon et al. 2004), which can generate OH• radical if not reduced in time by catalase or GPx enzymes. The OH• radical is highly reactive and notorious for causing oxidative damage to proteins and lipids.

However, decreased levels of PC, 3NT and HNE levels suggest additional cellular defense responses that may have protected proteins and lipids from any further ROS injury. HSPs, also known as chaperon proteins; assist the establishment of proper protein conformation and prevents unwanted protein aggregation. HSPs also helps in stabilizing partially folded proteins and transporting proteins across membranes within the cell. The upregulation of heat shock protein is an important cellular stress response and can be induced by heat, chemical toxins or oxidative stress. Inductions of HSPs have shown protection against oxidative stress as well as it prevented protein and lipid peroxidation (Broome et al. 2006; Wang et al. 2006; Shrivastava et al. 2008). In current study, HO-1 (H and CB) and Hsp70 (H, C and CB) levels were significantly induced after 1 h concurrent with increased levels of phase II enzymes and decreased levels of PC (H and CB), 3NT (H) and HNE (H and CB).

Thirty days retention of 15 nm ceria ENM (100 mg/kg dose) in the body did not have any adverse effect on rat brain redox status. The slightly elevated GSH: GSSG suggests favorable reduced status of cellular environment, which was not significantly different than that of saline treated controls. Unlike our pervious study with 5 nm ceria ENM, lack of significant change in levels or activities of phase II enzymes, HSPs and protein or lipid oxidative stress markers (PC, 3NT, HNE) delineate absence of any profound anti- or pro-oxidant effects of 15 nm ceria ENM on rat brain after 30 d. Considering the antioxidant cellular response induced by milder levels of oxidative stress mediated by high dose of 15 nm ceria ENM after 1 h, presumably same 15 nm ceria ENM would have induced similar antioxidant cellular responses after 1 h also at lower dose (100 mg/kg). Thus, absence of any profound anti- or pro-oxidant effect after 30 d, may be due to decreased oxidative

stress or compensation of ceria induced oxidative stress by initial antioxidant defense response at 1 h.

Considering the ENM size-effect on its oxidative stress related effects, smaller sized (5 nm) ceria likely to have more adverse effects on rat brain compared to larger ENMs.

# CHAPTER 7

# MODULATION OF PHASE-II ANTIOXIDANT RESPONSE BY 30 NM CERIA ENM IN RAT BRAIN IN TIME-DEPENDENT MANNER

(30 nm-Size and exposure period – prolong persistence of ceria ENM)

## 7.1. Overview of the study

Engineered nanomaterials (ENMs) have potential to contribute to applications that could produce intended (e.g., drug and gene delivery) or unintended (e.g. occupational and environmental) exposure. Understanding potential ENM toxicity lags behind application development, as is usually the case for new technologies. Insufficient understanding of ENM hazards could lead to human health problems and decreased public acceptance.

Ceria (cerium [Ce] oxide) ENMs have many current and potential commercial applications. Ceria is highly insoluble, including in phagolysosomal fluid at pH 4.5 (He et al. 2010) and abrasive, enabling its use in chemical-mechanical planarization (integrated circuit manufacture) (Feng et al. 2006). Most ceria applications capitalize on its redox activity, including as an oxygen sensor (Molin et al. 2008), diesel fuel catalyst (increases combustion and converts carbon monoxide to carbon dioxide) ((HEI) ; Park et al. 2007), 2001 #659;Cassee, 2011 #177), in fuel cells (Yuan et al. 2009), and for potential medical applications.

Therapeutic ceria ENM applications are generally based on its ability to reduce reactive oxygen species (Dalle-Donne et al. 2006). Using many different cells in culture ceria ENMs have been shown to reduce levels of $H_2O_2$, the superoxide radical, i-NOS, NF-κB, TNF-α, interleukins, and other ROS endpoints. It has been suggested that ceria ENMs have utility in the prevention and/or treatment of cancer, diabetic cardiomyopathy, diesel

exhaust- and cigarette smoke-induced oxidative stress, radiation therapy side effects, retinal degeneration, stroke, and neurodegenerative disorders (Chen et al. 2006; Das et al. 2007; Xia et al. 2008; D'Angelo et al. 2009; Hirst et al. 2009; Babu et al. 2010; Colon et al. 2010; Younce et al. 2010; Estevez et al. 2011; Niu et al. 2011). Ceria mediated ROS reduction may relate to its properties as a SOD mimetic and possessing catalase-like activity (Kagan et al. 1992; Korsvik et al. 2007; Pirmohamed et al. 2010) and is perhaps attributed to Ce (Owens Iii et al.) rather than Ce(IV) (Celardo et al. 2011). Most of these studies were conducted in models of induced oxidative stress.

On the other hand, there are reports of ceria-induced toxicity, indicated by decreased cell viability, lutathione, and DNA content; and increased LDH release, malondialdehyde, and apoptosis (Brunner et al. 2006; Lin et al. 2006; Park et al. 2008; Auffan et al. 2009). Most of these studies were conducted in non-ROS stimulated cells. The reported effects of ceria ENM on non-mammalian organisms have generally been detrimental, including decreased growth, fertility, and survival; and increased lipofuscin accumulation and susceptibility to oxidative stress, shown in *Pseudokirchneriella subcapitata* (green algae), *Synechocystis* PCC6803 and *Anabaena* CPB4337 (cyanobactreria), *E. coli,* Daphnia magna, and *C. elegans* (Roh et al. ; Thill et al. 2006; VanHoecke et al. 2009; Zeyons et al. 2009; Zhang et al. 2010; Rodea-Palomares et al. 2011). All of these studies do not inform about the long-term effects and fate of ceria ENM in the intact mammal, the target of medical applications and a concern about unintended exposures. Nanoscale ceria was identified as an important material for toxicity evaluation by the NIEHS (ILS), 2006 #668) and OECD Environment Directorate ((OECD)), 2010 #669). The need for *in vivo* studies that examine its biokinetics and toxicity w as recently identified (Cassee et al.

2011). A few studies with ceria ENM have been conducted in the intact mammal. Reduced myocardial oxidative stress was seen in transgenic mice that display ischemic cardiomyopathy (Niu et al. 2011). Granulomatous inflammation was seen after pulmonary instillation and inhalation (Cho et al. 2010; Srinivas et al. 2011). Intravitreal injection reduced retinal vascular lesions (Zhou et al. 2011).

Most therapeutic applications of ceria ENM will require systemic or pulmonary administration as its oral absorption is poor (~0.001%) and better from the lung (~0.1 to 1%) (He et al. 2010; Yokel et al. 2012). Translocation can occur from the lung (and potentially other sites of uptake) to blood and ultimately all organs (He et al. 2010). Therefore the fate of ceria that is introduced into, or reaches, blood needs to be better understood.

Our previous research described in this dissertation has shown that, although ceria ENM does not cross BBB and enter brain parenchyma, accumulation and retention of ceria ENM in peripheral organs exerts oxidative stress effects on brain even after 30 d of administration of ENM. The present study was conducted to evaluate the oxidative stress effects on rat brain induced by retention of ceria ENM in peripheral organs for 90 d. In addition we set up our experimental design to test the model for oxidative stress hierarchy model for nanomaterial toxicity proposed by Nel (Nel et al. 2006).

## 7.2. Materials and methods

### 7.2.1. Nanomaterial:

Ceria ENM was obtained from our collaborator, which was synthesized in in-house facility (Section 3.1). Nanomaterial characterization was carried out by our collaborators, prior to ceria ENM treatment to the animals (Section 3.2).

### 7.2.2. Animals:

The male Sprague-Dawley rats received either saline or 5% ceria dispersion intravenously. Five rats were infused with 0 and 5 rats with 100 mg ceria/kg and terminated 1 h after completion of infusion. Five rats were infused with 0 and 5 rats with 100 mg ceria/kg and terminated 20 h after completion of infusion. Three rats with 0 and 3 rats were infused with 100 mg ceria/kg and terminated 1 d after, 3 rats with 0 and 3 rats were infused with 100 mg ceria/kg and terminated 7 d after, 10 rats with 0 and 11 rats were infused with 100 mg ceria/kg and terminated 30 d after, and 6 rats with 0 and 7 rats were infused with 100 mg ceria/kg and terminated 90 d after completion of infusion. After ceria ENM treatments, the BBB integrity assessment (Section 3.3), light and electron microscopic assessment (Section 3.4) and EELS analysis (Section 3.2) was carried out by our collaborators. The brain homogenates were prepared from control and ceria treated rat brain samples (Section 3.6). Total protein content was determined using BCA assay (Section 3.7) and various biochemical assays were carried out on all the samples (Sections 3.8, 3.9, 3.10, 3.11, and 3.14) in our laboratory.

## 7.3. Results

Ceria composition

HR-TEM/HR-STEM showed the ceria ENM was cubic shape (Figure 7.1). The XRD patterns demonstrated the ceria are highly crystalline. Evaluation of a number of TEM images showed that the ceria had a number-average primary particle size of ~31.2 ± 17.1 nm.

Ceria concentration in brain and Electron micrograph

ICP-MS analysis suggested that very small amount of ceria was present in the brain parenchyma compare to peripheral organ liver (Table 7.1). Electron micrograph studies suggested that ceria ENM was not found in the brain, but located on the luminal side of the BBB endothelium. The hippocampus and cerebellum tissues did not show obvious ceria induced injury as no necrotic neurons or elevated gliosis were observed and the BBB was visibly intact (data not shown).

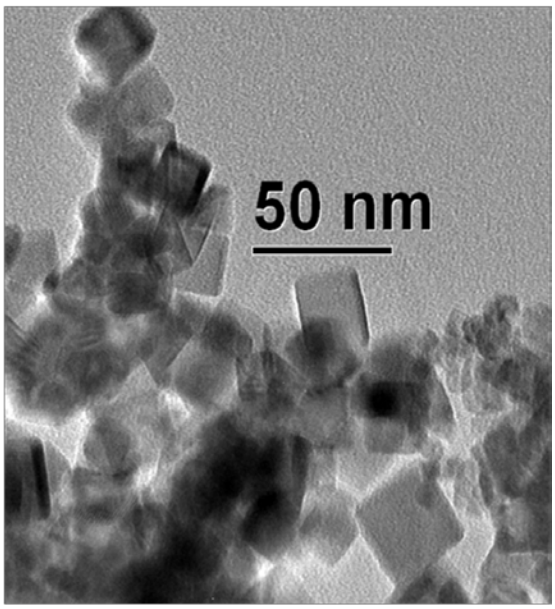


**Figure 7.1:** Ceria ENM imaged using HRTEM and HRSTEM. The ceria were dispersed on a carbon film. Visually they have average size distribution 31.2 ± 17.1 nm (taken by Dr. Peng Wu).

**Table 7.1:** Cerium concentrations in blood, brain, liver, and spleen, expressed as a percent change of the ceria ENM dose. a) Based on reference volume of blood in the rat (7% of body weight) or weight of the brain, liver x ceria concentration.

| | **Cerium [% of dose][a]** | | |
|---|---|---|---|
| | **Blood** | **Brain** | **Liver** |
| **% dose (1 h)** | 0.01 ± 0.009 | 0.0003 ± 0.001 | 40 ± 10 |
| **% dose (30 d)** | 0.0056 ± 0.003 | 0.0056 ± 0.004 | 20.29 ± 6 |

EELS results

Electron energy loss spectroscopic measurements on liver tissue were performed as a representative organ. The ratio of Ce(Owens Iii et al.) to Ce(IV) in the aged ceria was evaluated using EELS measurements after locating agglomerates of the ceria nanorods in tissue 1 h and 30 days after infusion into rat and comparing with synthesized ceria. The high $Ce^{3+}$/ $Ce^{4+}$ ratio that was obtained in the as-synthesized, fresh ceria nanorods seems to have only been altered slightly in individual ceria measured in liver after 30 days *in vivo* (data not shown).

Oxidative Stress Indices

*GSH: GSSG ratio was decreased at all time points- marker of increased oxidative stress*

Glutathione (GSH) is an abundant antioxidant is a part of primary cellular defense against ROS or RNS stress. GSH provides H or electrons for detoxification of free radicals carried out by GPx and in the process get oxidized to form disulfide bond with another GSH molecule. Oxidized glutathione (GSSG) is recycled back to reduced GSH by action of GR enzyme. GSH: GSSG ratio reflects the status of cellular redox state and a decline in GSH: GSSG ratio indicates an oxidative state of the cellular environment, which may activate various downstream signaling pathways. The GSH: GSSG ratio was significantly decreased in hippocampus after 1 h ($^{*}p < 0.05$), 20 h ($^{*}p < 0.05$), 1 d ($^{*}p < 0.05$), 7 d ($^{\xi}p < 0.01$), and 30 d ($^{*}p < 0.05$), in cortex after 1 h ($^{*}p < 0.05$), and in cerebellum after 1 d ($^{*}p < 0.05$), 7 d ($^{*}p < 0.05$), and 30 d ($^{*}p < 0.05$) after 30 nm ceria administration (Figure 7.2). However, there was sudden a spike was observed in GSH: GSSG ratio in 90 d brain samples indicating restoration of cellular redox status.

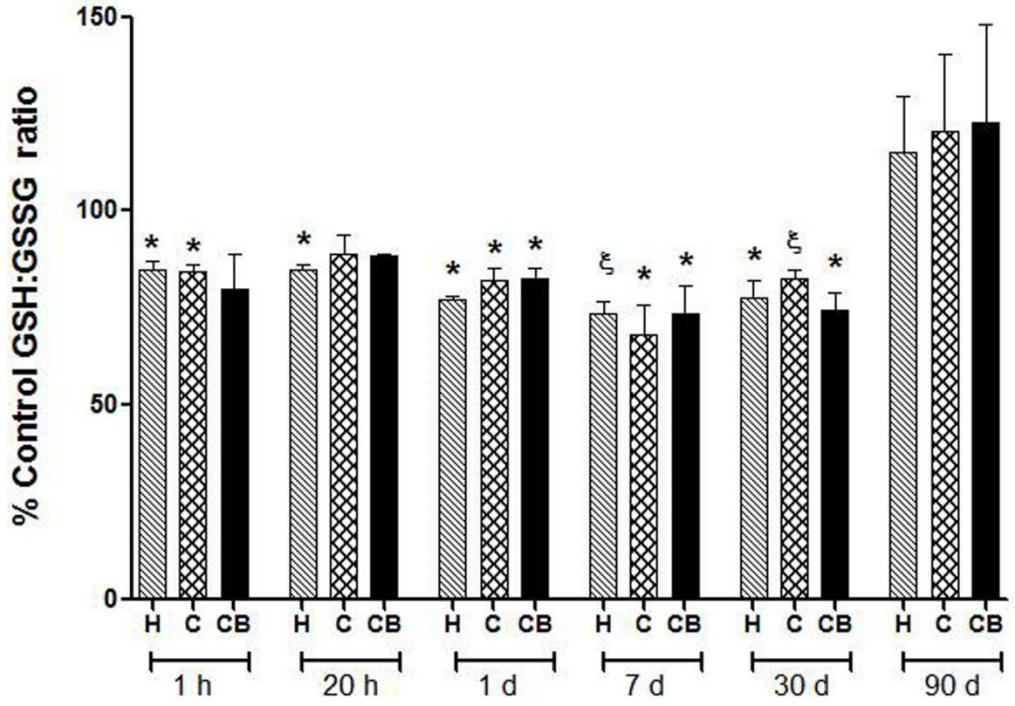


**Figure 7.2:** GSH: GSSG ratios measured in 3-brain regions after 1 h, 20 h, 1 d, 7 d, 30 d and 90 d- 30 nm ceria ENM treatment. The histograms represent %control GSH: GSSG ratio for ceria treated samples normalized with mean of their respective controls. The values are expressed as mean ± SEM of ceria treated samples from, 1 h (n = 5), 20 h (n=5), 1 d (n=3), 7 d (n=3), 30 (n=11), 90 d (n=7). Statistical difference was estimated as *$p < 0.05$, $^{\xi}p < 0.01$, and $^{\Theta}p < 0.001$, compared to mean of respective control samples.

*Induction of Tier 1 oxidative stress response: Phase II antioxidant activities were increased after 1h, 20 h and after 90 d chronic exposure*

An oxidative insult, generation of free radicals, or decline in cellular redox state can activate cellular antioxidant defense response and induction of phase II enzymes. Decline in GSH: GSSG ratio can activate Nrf-2 pathway, which regulates transcription of phase II enzymes like GPx, GR, GST catalase, and SOD (Xiao et al. 2003; Li et al. 2004; Lee et al. 2008; Chia et al. 2010; Speciale et al. 2011). At earlier time points GPx levels were induced in hippocampus (*$p < 0.05$, 1 & 20 h) and cerebellum (*$p < 0.05$, 1 h); Figure 7.3a, and catalase levels in hippocampus (*$p < 0.05$, 1 & 20 h), in cortex (*$p < 0.05$, 1 & 20 h), and in cerebellum ($^{\xi}p < 0.01$, 1 h & $^{\Theta}p < 0.001$, 20 h); Figure 7.4a. However, GR levels were decreased significantly in hippocampus ($^{\Theta}p < 0.001$, 1 h & *$p < 0.05$) Figure 7.5a. Concomitantly activities of phase II enzymes were also increased; GPx activities in hippocampus (*$p < 0.05$, 1 & 20 h), in cortex (*$p < 0.05$, 1 h) and in cerebellum (*$p < 0.05$, 1 h & $^{\xi}p < 0.01$, 20 h); Figure 7.3b, GR activities in cerebellum (*$p < 0.05$); Figure 7.5b, and catalase activities in hippocampus (*$p < 0.05$, 1 & 20 h), in cortex ($^{\xi}p < 0.01$, 20 h), and in cerebellum (*$p < 0.05$, 1 h & $^{\xi}p < 0.01$, 20 h); Figure 7.5b. Glutathione S-transferase (GST) activities remained unaffected at these earlier time points Figure 7.6.

While after 1 d and 7 d although phase II enzyme levels were increased (not all significantly), their activities were reduced. GPx and GR levels showed a increasing trend in hippocampus, cortex and cerebellum after 7 d (Figure 7.3a and 7.5a, respectively) and catalase levels were significantly increased in hippocampus (*$p < 0.05$, 1 d, Figure 7.5a) alone. Exhibiting a inverse trend compare to earlier time points a significant decrease was observed in GPx activities in hippocampus (*$p < 0.05$, 1 & 7 d), in cortex (*$p < 0.05$, 1 d)

and in cerebellum (*$p < 0.05$, 1 d); Figure 7.3b, GR activities in cerebellum (*$p < 0.05$, 1 and 7 d) alone; Figure 7.5b, and catalase activities in hippocampus ($^{\xi}p < 0.01$, 1 d & *$p < 0.05$, 7 d), in cortex ($^{\xi}p < 0.01$, 1 d & *$p < 0.05$, 7 d), and in cerebellum (*$p < 0.05$, 1 & 7 d); Figure 7.5b.

After 30 d, the levels and activities of some phase II enzymes were selectively inhibited. GPx and GR levels were significantly increased in hippocampus ($^{\xi}p < 0.01$ & *$p < 0.05$; respectively) while decreased in cortex (*$p < 0.05$); Figure 7.3a and 7.5a, respectively. Catalase levels were increased in all the brain regions (*$p < 0.05$), Figure 7.5a. Along the line of 1 and 7 days, phase II enzyme activities were significantly decreased; GPx activities in all brain regions (*$p < 0.05$); Figure 7.3b, catalase activities in all brain regions (*$p < 0.05$, H and C, $^{\Theta}p < 0.001$, CB); Figure 7.5b, as well as GST activities were inhibited in all brain regions ($^{\xi}p < 0.01$, H and *$p < 0.05$, C and CB); Figure 7.6. Conversely, GR activities were not inhibited but increased in all brain regions (*$p < 0.05$), Figure 7.5b.

After 90 d, all three phase II enzymes levels were restored to that of control levels and no significant changes were observed in either of brain region, Figure 7.3a, 7.5a, & 7.5a, while activities of phase II enzymes were selectively elevated. GR activities were selectively increased in cerebellum (*$p < 0.05$); Figure 7.3b, catalase activities were increased in all brain regions (*$p < 0.05$, H and CB, $^{\Theta}p < 0.001$, C); Figure 7.5b, while GST activities were selectively increased in hippocampus (*$p < 0.05$) and in cortex (*$p < 0.05$); Figure 7.6. Conversely, GPx activities alone were significantly reduced in hippocampus (*$p < 0.05$), Figure 7.3b.

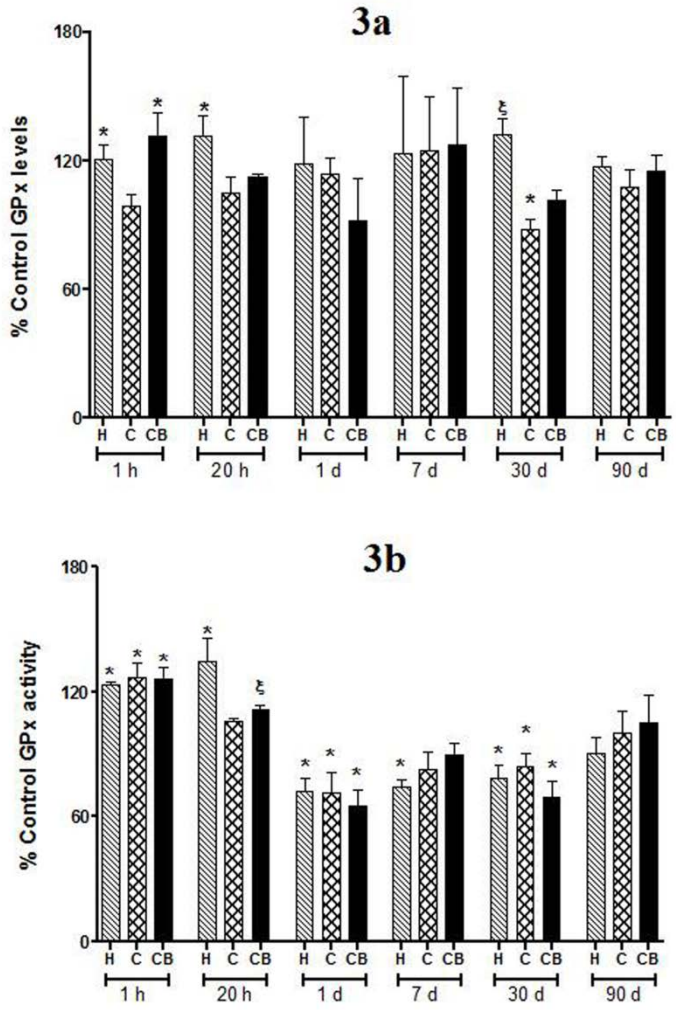


**Figure 7.3a and b:** The GPx antioxidant enzyme levels and activities in 3-brain regions 1 h, 20 h, 1 d, 7 d, 30 d and 90 d after 30 nm ceria ENM treatment. a) The histograms represent %control GPx levels for ceria treated samples normalized with mean of their respective controls, b) The histograms represent %control GPx activities for ceria treated samples normalized with mean of their respective controls. The values are expressed as mean ± SEM of ceria treated samples from, 1 h (n = 5), 20 h (n=5), 1 d (n=3), 7 d (n=3), 30 (n=11), 90 d (n=7). Statistical difference was estimated as *p <0.05, $^{\xi}$p < 0.01, and $^{\Theta}$p < 0.001, compared to mean of respective control samples.

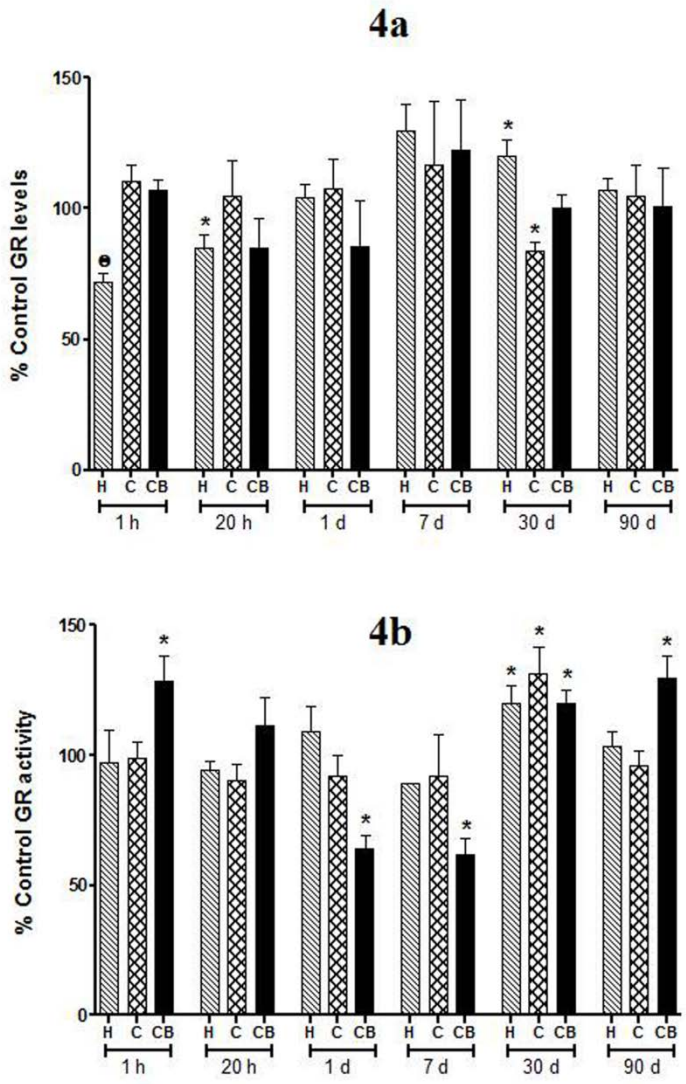


**Figure 7.4a and b:** The GR antioxidant enzyme levels and activities in 3-brain regions 1 h, 20 h, 1 d, 7 d, 30 d and 90 d after 30 nm ceria ENM treatment. a) The histograms represent %control GR levels for ceria treated samples normalized with mean of their respective controls, b) The histograms represent %control GR activities for ceria treated samples normalized with mean of their respective controls. The values are expressed as mean ± SEM of ceria treated samples from, 1 h (n = 5), 20 h (n=5), 1 d (n=3), 7 d (n=3), 30 (n=11), 90 d (n=7). Statistical difference was estimated as *p <0.05, $^{\xi}$p < 0.01, and $^{\Theta}$p < 0.001, compared to mean of respective control samples.

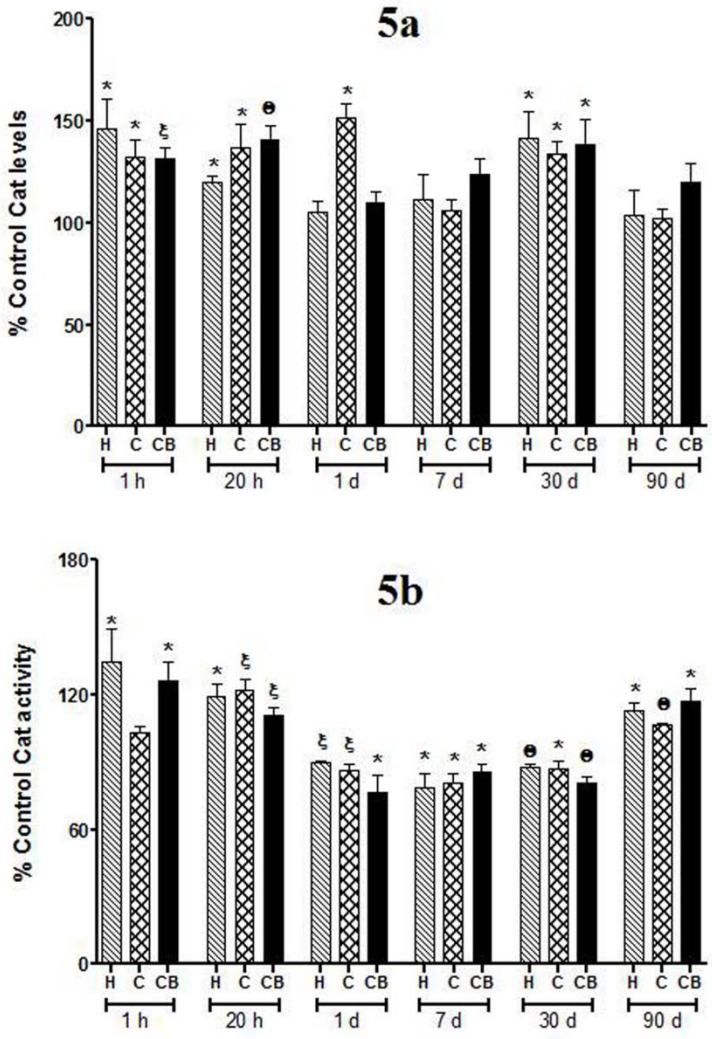


**Figure 7.5a and b:** The catalase antioxidant enzyme levels and activities in 3-brain regions 1 h, 20 h, 1 d, 7 d, 30 d and 90 d after 30 nm ceria ENM treatment. a) The histograms represent %control catalase levels for ceria treated samples normalized with mean of their respective controls, b) The histograms represent %control catalase activities for ceria treated samples normalized with mean of their respective controls. The values are expressed as mean ± SEM of ceria treated samples from, 1 h (n = 5), 20 h (n=5), 1 d (n=3), 7 d (n=3), 30 (n=11), 90 d (n=7). Statistical difference was estimated as *$p < 0.05$, $^{\xi}p < 0.01$, and $^{\Theta}p < 0.001$, compared to mean of respective control samples.

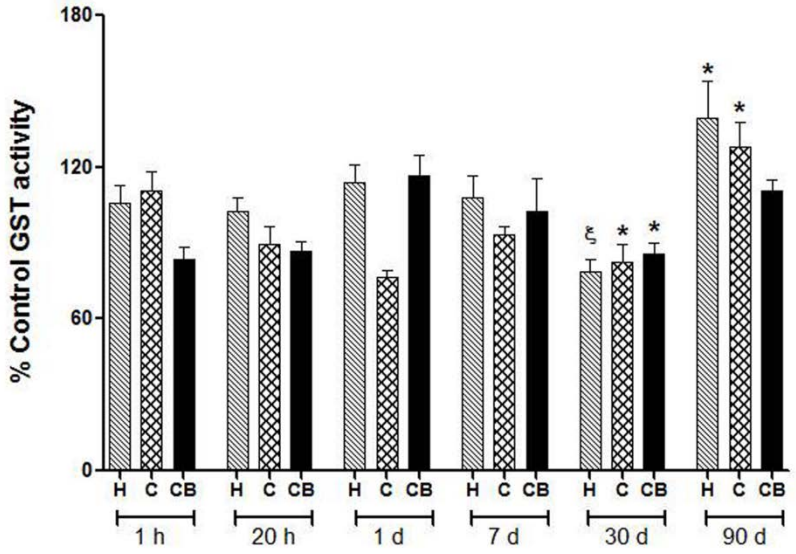


**Figure 7.6:** The GST antioxidant enzyme activities in 3-brain regions 1 h, 20 h, 1 d, 7 d, 30 d and 90 d after 30 nm ceria ENM treatment. The histograms represent %control GST activities for ceria treated samples normalized with mean of their respective controls. The values are expressed as mean ± SEM of ceria treated samples from, 1 h (n = 5), 20 h (n=5), 1 d (n=3), 7 d (n=3), 30 (n=11), 90 d (n=7). Statistical difference was estimated as *$p < 0.05$, $^{\xi}p < 0.01$, and $^{\Theta}p < 0.001$, compared to mean of respective control samples.

*Failure to Tier 1 response: Inhibition of phase II enzyme activities, increased PC, 3NT, HNE levels and HSP levels*

Following the administration of ceria ENM, markers of protein oxidation and lipid peroxidation were decreased at earlier time points were increased later (up to 30 d), suggesting protection against oxidative stress at earlier time points (1 h and 20 h) and failure to antioxidant defense against oxidative stress at later time points (1 d -30 d). Heat

shock proteins are induced under increased oxidative stress conditions, increase in their levels at later time points (1 d to up to 30 d) supports the PC, 3NT and HNE data.

After 1 and 20 h, PC levels were significantly decreased in all brain regions (*$p < 0.05$, 1 & 20 h); Figure 7.7a, 3NT levels decreased in hippocampus (*$p < 0.05$, 1 & 20 h); Figure 7.7b and HNE levels showed a decreasing trend, Figure 7.7c. Along the same line, HO-1 levels were significantly decreased in hippocampus (*$p < 0.05$, 1 h and $^{\xi}p < 0.01$, 20 h), and in cortex ($^{\xi}p < 0.01$, 1 h); Figure 7.9a. Similarly Hsp70 levels were decreased in hippocampus (*$p < 0.05$, 20 h), in cortex (*$p < 0.05$, 1 & 20 h), and in cerebellum (*$p < 0.05$, 1 h); Figure 7.9b.

After 1 and 7 d, PC levels were induced in all brain regions (*$p < 0.05$. 1 d) and (*$p < 0.05$, H & C, $^{\xi}p < 0.01$, CB, 7 d) respectively; Figure 7.7a. 3NT levels were significantly elevated in hippocampus (*$p < 0.05$, 1 d); Figure 7.7b and HNE levels showed some increasing trend, Figure 7.7c. Following the same trend, HO-1 levels were significantly increased in hippocampus (*$p < 0.05$, 1 & 7 d), in cortex (*$p < 0.05$, 1 & 7 d) and in cerebellum (*$p < 0.05$, 1 d); Figure 7.9a. Similarly Hsp70 levels were significantly elevated in cerebellum (*$p < 0.05$, 7 d), Figure 7.9b.

After 30 d, PC levels were induced in all brain regions (*$p < 0.05$. 1 d) and (*$p < 0.05$, H & C, $^{\xi}p < 0.01$, CB, 7 d) respectively; Figure 7.8a. 3NT levels were significantly elevated in hippocampus (*$p < 0.05$, 1 d); Figure 7.8b and HNE levels showed some increasing trend, Figure 7.8c. Following the same trend, HO-1 levels were significantly increased in hippocampus (*$p < 0.05$, 1 & 7 d), in cortex (*$p < 0.05$, 1 & 7 d) and in cerebellum (*$p <$

0.05, 1 d); Figure 7.8a. Similarly Hsp70 levels were significantly elevated in cerebellum (*$p < 0.05$, 7 d), Figure 7.8b.

After 90 d, however, PC levels not only restored by significantly decreased all brain regions (*$p < 0.05$); Figure 7.8a. 3NT levels decreased in hippocampus (*$p < 0.05$) and restored in cortex and cerebellum along with HNE levels; Figure 7.8b & 7.8c. Along the same line, HO-1 levels were restored in hippocampus and significantly decreased in cortex and cerebellum (*$p < 0.05$), Figure 7.8a. Similarly Hsp70 levels were restored in all brain regions, Figure 7.8b.

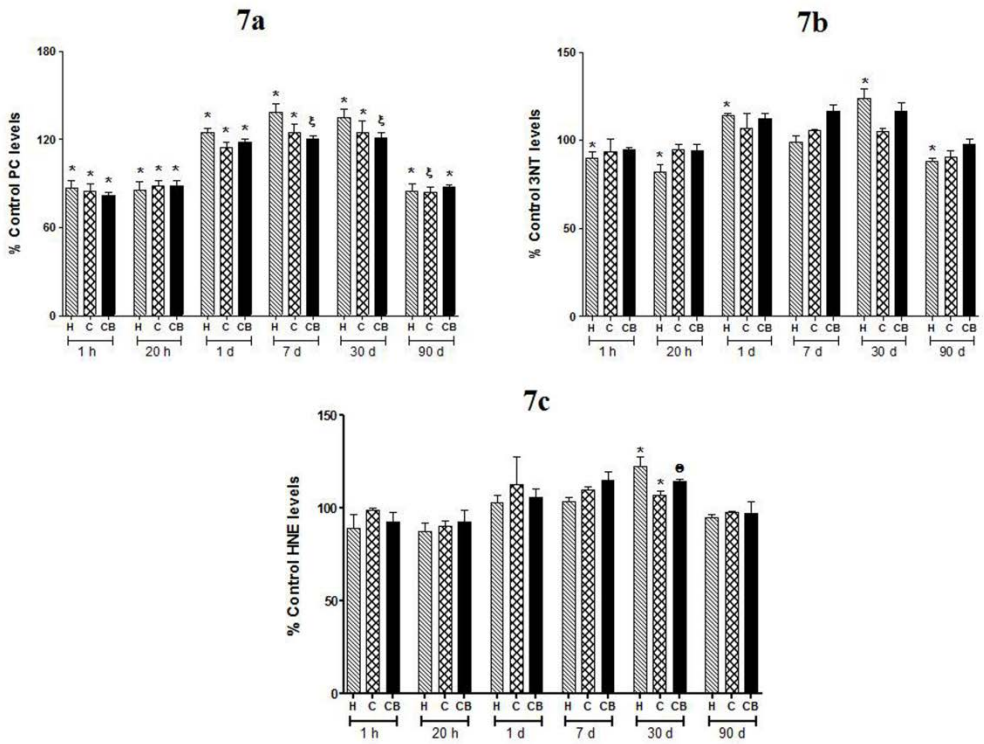


**Figure 7.7:** The oxidative stress marker levels in 3-brain regions 1 h, 20 h, 1 d, 7 d, 30 d and 90 d after 30 nm ceria ENM treatment. a) The histograms represent %control PC levels; b) the histograms represent %control 3NT levels, and c) the histograms represents %control protein-bound HNE levels for ceria treated samples normalized with mean of their respective controls. The values are expressed as mean ± SEM of ceria treated samples from, 1 h (n = 5), 20 h (n=5), 1 d (n=3), 7 d (n=3), 30 (n=11), 90 d (n=7). Statistical difference was estimated as *$p < 0.05$, $^{\xi}p < 0.01$, and $^{\Theta}p < 0.001$, compared to mean of respective control samples.

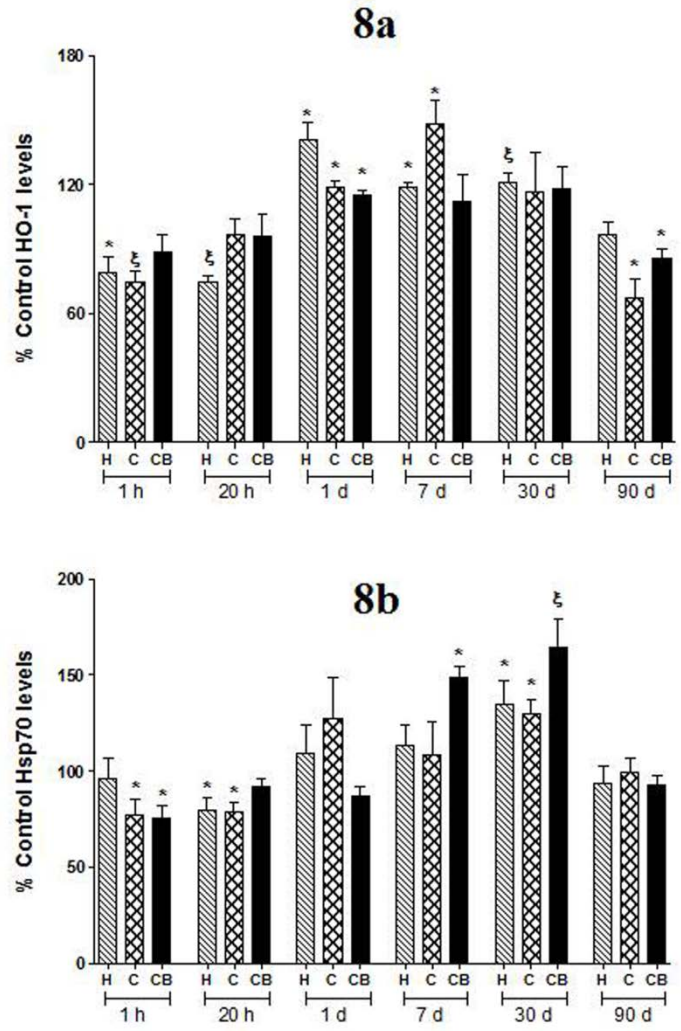


**Figure 7.8:** The heat shock protein levels in 3-brain regions 1 h, 20 h, 1 d, 7 d, 30 d and 90 d after 30 nm ceria ENM treatment. a) The histograms represent %control HO-1 levels, and b) the histograms represent %control Hsp70 levels, for ceria treated samples normalized with mean of their respective controls. The values are expressed as mean ± SEM of ceria treated samples from, 1 h (n = 5), 20 h (n=5), 1 d (n=3), 7 d (n=3), 30 (n=11), 90 d (n=7). Statistical difference was estimated as *$p < 0.05$, $^{\xi}p < 0.01$, and $^{\Theta}p < 0.001$, compared to mean of respective control samples.

*Induction of Tier 2 oxidative stress response: Activation of pro-inflammatory response after 1 d exposure*

In case of failure to phase II antioxidant defense to restore the cellular redox status, elevated oxidative stress further activates cascade of pro-inflammatory response via NF-κB signaling pathway (Hiura et al. 1999; Li et al. 2003; Xiao et al. 2003; Chia et al. 2010). Due to observed inhibition of phase II antioxidant activities concomitant with increased PC, 3NT and HSPs levels at 1 d, 7 d and 30 d time points, hippocampus samples were selected to explore the downstream effects of escaladed oxidative stress. Levels of inflammatory cytokines IL-1β and TNF-α were measured in hippocampus sample for all the time points employing Western blot technique. IL-1β levels did not show any change at earlier time point (1 h and 20 h), but increased after 1 d ($^{*}p < 0.05$, H) and 30 d ($^{\xi}p < 0.01$, H); Figure 7.9a. TNF-α were not significantly increased at either of the time point, but decreased levels of TNF-α after 1 h ($^{\xi}p < 0.01$, H), Figure 7.9b.

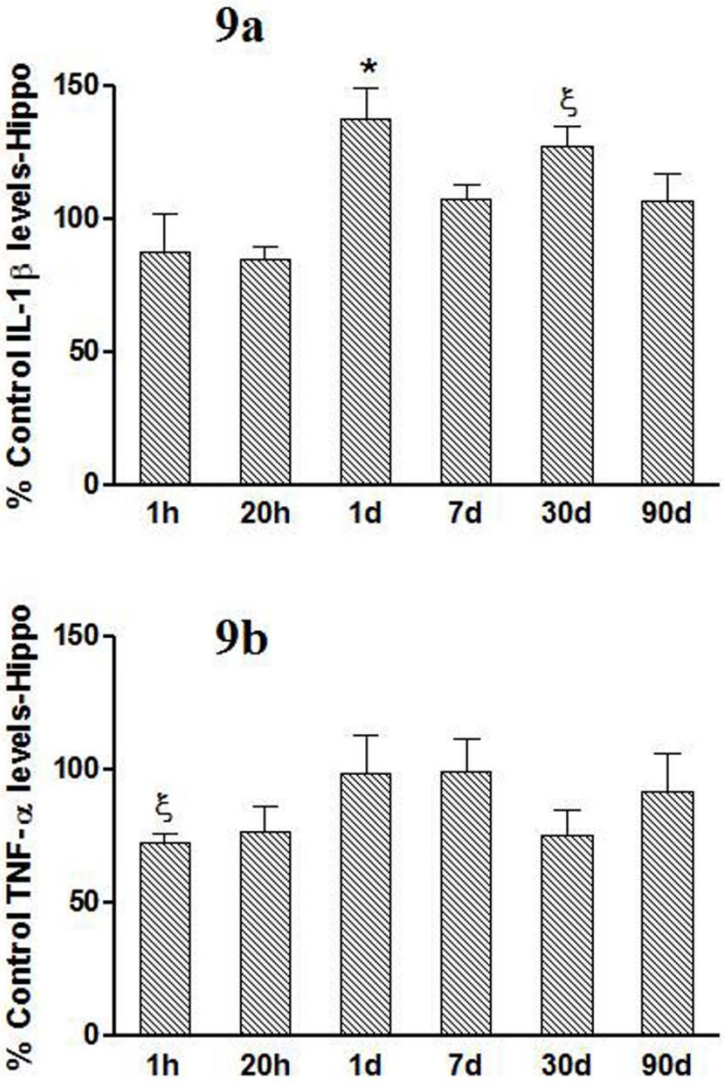


**Figure 7.9:** The inflammatory cytokine levels in hippocampus regions 1 h, 20 h, 1 d, 7 d, 30 d and 90 d after 30 nm ceria ENM treatment. a) The histograms represent %control IL-1β levels, and b) the histograms represent %control TNF-α levels, for ceria treated samples normalized with mean of their respective controls. The values are expressed as mean ± SEM of ceria treated samples from, 1 h (n = 5), 20 h (n=5), 1 d (n=3), 7 d (n=3), 30 (n=11), 90 d (n=7). Statistical difference was estimated as *$p < 0.05$, $^{\xi}p < 0.01$, and $^{\Theta}p < 0.001$, compared to mean of respective control samples.

*Induction of Tier 3 oxidative stress response: Activation of pro-apoptotic response at 30d*

Downstream consequences of activated pro-inflammatory cytokines, activates caspase-3 pro-apoptotic proteins, which can lead cell towards apoptotic pathway (Nesic et al. 2004; Shakibaei et al. 2007). Pro-caspase-3 protein is precursor for caspase-3 and its levels were measured in hippocampus to estimate possibility of activation of caspase-3. Levels of pro-caspase-3 were increased only after 30 d (*$p < 0.05$), suggesting possible increase in caspase-3 levels, Figure 7.10.

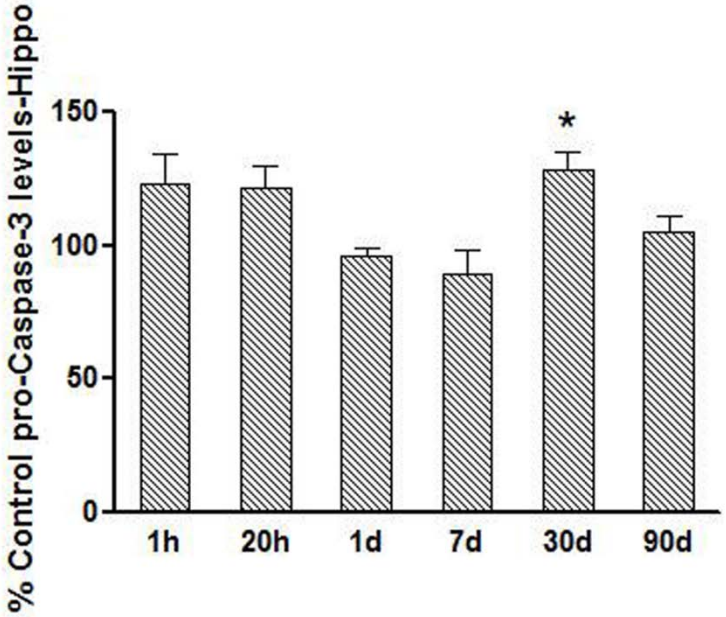


**Figure 7.10:** The apoptosis marker levels in hippocampus regions 1 h, 20 h, 1 d, 7 d, 30 d and 90 d after 30 nm ceria ENM treatment. The histograms represent %control pro-caspase-3 levels, for ceria treated samples normalized with mean of their respective controls. The values are expressed as mean ± SEM of ceria treated samples from, 1 h (n = 5), 20 h (n=5), 1 d (n=3), 7 d (n=3), 30 (n=11), 90 d (n=7). Statistical difference was estimated as *$p < 0.05$, $^{\xi}p < 0.01$, and $^{\Theta}p < 0.001$, compared to mean of respective control samples.

*Autophagy marker appears at 7 d, 30 d and at 90 d*

Escaladed oxidative stress can activate autophagy (Gottlieb et al. 2010; Marambio et al. 2010; Hariharan et al. 2011) to recycle or restored defected macromolecules and organelles. Autophagy marker LC-3AB levels were increased after 7 d (*$p < 0.05$), 30 d ($^{\xi}p < 0.0$), and 90 d (*$p < 0.05$) in hippocampus, Figure 7.11.

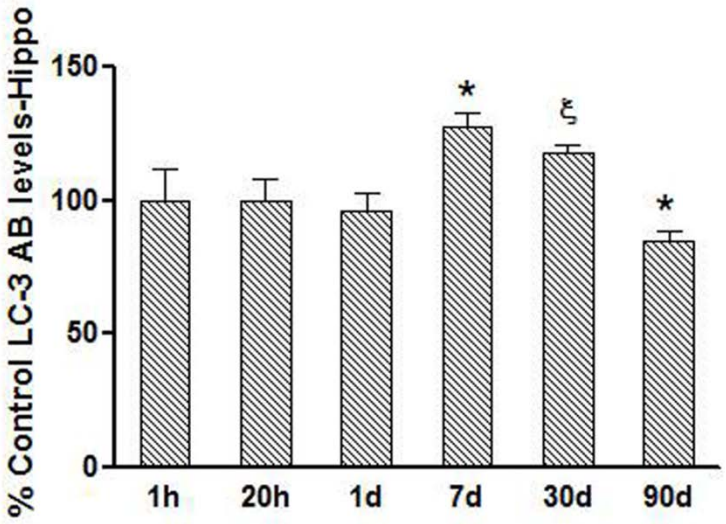


**Figure 7.11:** The autophagy marker levels in hippocampus regions 1 h, 20 h, 1 d, 7 d, 30 d and 90 d after 30 nm ceria ENM treatment. The histograms represent %control LC-3AB levels, for ceria treated samples normalized with mean of their respective controls. The values are expressed as mean ± SEM of ceria treated samples from, 1 h (n = 5), 20 h (n=5), 1 d (n=3), 7 d (n=3), 30 (n=11), 90 d (n=7). Statistical difference was estimated as *$p < 0.05$, $^{\xi}p < 0.01$, and $^{\Theta}p < 0.001$, compared to mean of respective control samples.

### 7.4. Discussion

There are some in vivo and in vitro studies are available on oxidative stress effects of ceria ENM, however they are far from uniform on whether ceria is pro-oxidant or antioxidant (Yokel et al. 2009). This dissertation research is among the first comprehensive in vivo study that addresses mechanisms of oxidative stress effects induced by ceria ENM. This study demonstrates that 30 nm ceria ENM administration induces oxidative stress response and secondary oxidative stimulus in time dependant manner in the brain, without ever crossing BBB.

A review summarizes the evidence available on free radical scavenging ability of ceria ENM under pre-induced oxidative stress condition (Karakoti et al. 2009). However, 30 nm ceria was shown to induce ROS in BEAS-2B cell culture after 24 h incubation in dose-dependent manner in absence of any other external source of ROS. In the same experiment ceria ENM also decreased cell viability in size-independent manner (Park et al. 2008). GSH an important cellular thiol and antioxidant, is known to buffer free radicals and ROS; thus GSH maintains cellular redox balance (Meister et al. 1983; Forman et al. 2003; Rahman et al. 2005). However, in the process GSH gets oxidized to GSSG and decreased levels of this ratio can activate various downstream signaling pathways. We also evaluated cellular redox status by measuring GSH: GSSG ratio in three brain regions. The GSH: GSSG ratio measurements showed continuous decrease in GSH: GSSG ratio at all the time points except after 90 d.

According to the hierarchy of oxidative stress model proposed by Nel's research group (as explained in section 2.6), a mild decrease in GSH: GSSG ratio activates phase II antioxidant response (Tier-1) via Nrf-2 and ARE pathway (Li et al. 2004; Nel et al. 2006;

Lee et al. 2008). In the current study, 30 nm ceria also launched similar Tier-1 response at earlier time points and phase II antioxidant enzymes GPx, GR and catalase levels as well as activities were increased significantly after 1 h and 20 h to protect cell from possible oxidative insult. Concomitantly, the protein oxidation marker-PC, protein nitration marker-3NT, and the lipid peroxidation marker-protein-bound HNE levels, were decreased. As well as heat shock protein HO-1 and Hsp70 levels were decreased after 1 h and 20 h. PC, 3NT and HNE are product of oxidative degradation of biomolecules and both HSPs are induced by elevated oxidative stress (Calabrese et al. 2000; Calabrese et al. 2000), therefore concomitant declined in these parameters indicates cytoprotective environment and success to phase II antioxidant (Tier-1) defense response.

However, unlike earlier time points, phase II antioxidant activities were decreased after 1 d and 7 d, although some of the antioxidant levels were up. As well as after 1 d and 7 d, PC, 3NT and HNE levels were concurrently elevated with HO-1 and Hsp70 levels. Increased levels of oxidative stress suggested by decreased GSH: GSSG ratio after 1 d and 7 d, which may further oxidatively modify phase II antioxidant enzymes (Butterfield 1997; Butterfield 2006). Oxidative modification can disrupt protein- spatial structure and consequently protein function or enzyme activities often get altered either partially or completely (Stadtman et al. 2003; Stadtman 2006). Failure of phase II antioxidant (Tier-1) defense and escaladed oxidative stress, activates NF-κB cascade further inducing pro-inflammatory cytokine levels (Tier-2) (Nel et al. 2006; Meng et al. 2009; Xia et al. 2009). We measured cytokine levels in the current study for all the exposure time periods after ceria ENM treatment. Observed decrease in TNF-α level after 1 h suggested inactivated pro-inflammatory response. Along the same line, decline in cytokine IL-1β levels at

earlier time points and then induction after 1 d, and 30 d suggests activation of pro-inflammatory signaling pathways (Tier-2) at later time points of ceria ENM exposure.

According to Nel, downstream consequences of deactivation or failure of Tier-1 response induces pro-inflammatory Tier-2 response through activation of NF-κB signaling pathway and Tier-3 response by activation of pro-apoptotic signaling cascade (Xiao et al. 2003; Nel et al. 2006). In current study oxidative stress remained elevated up to 30 d as GSH: GSSG ratio remained decreased and phase II antioxidant enzyme activities were inhibited after 1 d; further causing oxidative damage to proteins and lipids. Induction of HSPs did not seem to protect against this elevated oxidative stress at 1 d- 30 d. Therefore to evaluate the possible occurrence of pro-apoptotic / cytotoxic Tier-3 response, levels of pro-caspase-3 were measured. Pro-caspase-3 is the precursor protein for caspase-3 and induction of pro-caspase-3 is definitive marker of activated apoptotic cellular death pathway (Walters et al. 2009). Increased levels of cytokine IL-1β caused transcription of caspase-3 in pig's heart, which further induced pro-caspase-3 levels (Zitta et al. 2010). In addition IL-1β antagonist inhibited activation of caspase-3 and consequent apoptotic pathway in rat spinal cord injury model (Nesic et al. 2004). In current study pro-caspase-3 levels were induced after 30 d alone, concomitant with induction of IL-1β, fostering activation of Tier-3 response. So up to this point all the oxidative stress related observations made in the current study very well fits the oxidative stress hierarchy model of ENM toxicity, proposed by Nel's research group (Li et al. 2003; Xiao et al. 2003; Nel et al. 2006) and ours is the first comprehensive study that has mapped the oxidative stress mechanism of ENM toxicity in animal model for sub-chronic exposure period (30 d).

As we continued pursuing measurement of oxidative stress indices for chronic-exposure period of 90 d, very interesting observations were revealed. Along the line of hierarchy oxidative stress model, we were expecting profound deleterious effects on cellular redox status after 90 d. But quite contrary GSH: GSSG ratio was restored back, phase II antioxidant levels and activities increased again after 90 d, and PC, 3NT and HNE levels were suppressed along with HSP levels; as shown in Figure 7.12. In brief, after 90 d, there was no sign of oxidative stress, let alone damage caused by it. To understand such dramatic change we looked for autophagy marker. Autophagy is a cellular process for bulk degradation of cytosolic proteins and organelles carried out by lysosome (Hariharan et al. 2011). Measurement of autophagy marker LC-3AB levels by Western blot technique revealed increased levels of LC-3AB after 7 d and 30 d, whereas LC-3AB levels were decreased after 90 d; Figure 7.12. Seven days and 30 d are the time points at which possibly ascended oxidative stress induced Tier-2 and Tier-3 response and consecutive oxidation of biomolecules; Figure 7.12.

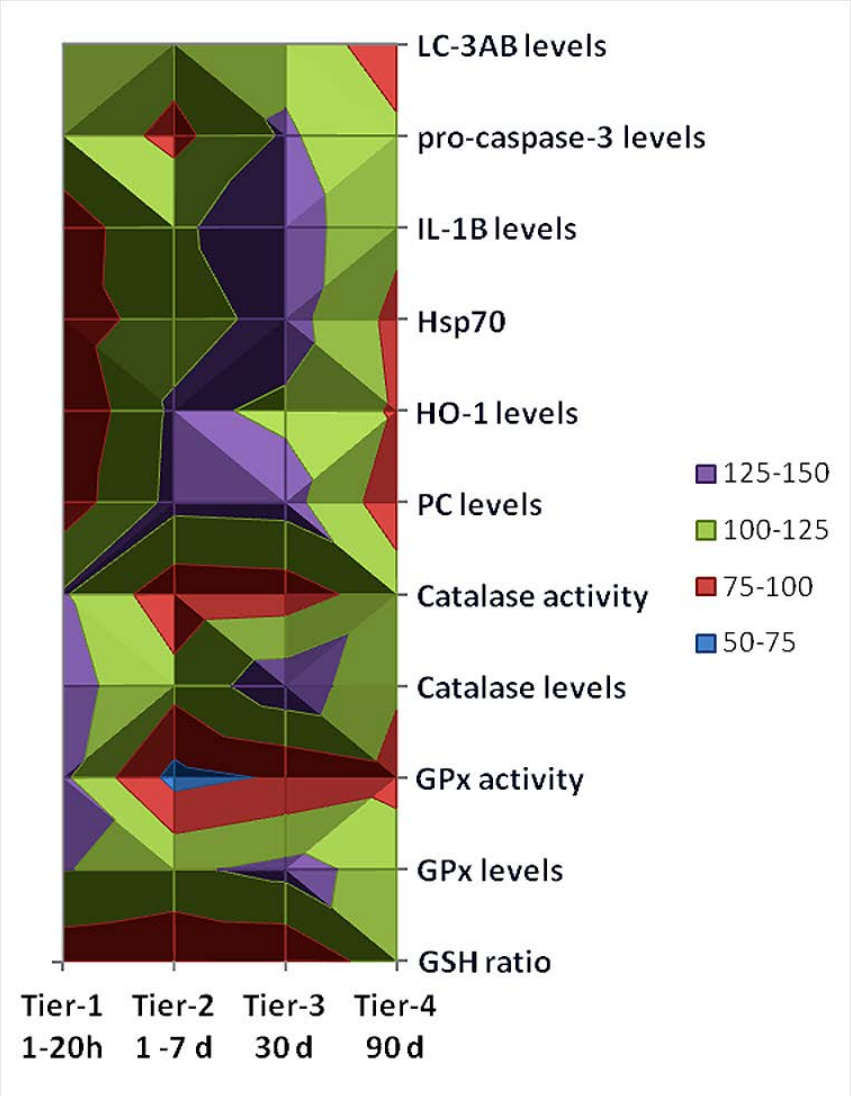


**Figure 7.12:** This demographical presentation summarizes changes in the key oxidative stress indices as observed at different exposure periods in hippocampus, after systemic injection of 30nm ceria ENM. The variation in oxidative stress indices were in good agreement with the hierarchy oxidative stress model proposed by Nel's research group (Nel et al. 2006).

Similar to HSPs (Calabrese et al. 2000; Calabrese et al. 2002), autophagy response can be induced by increased oxidative stress (Marambio et al. 2010; Hariharan et al. 2011). HSPs, especially Hsp70 is a well known chaperon for other proteins and which assist the

establishment that refolds the aggregated proteins as well as aid in transporting damaged proteins across intracellular membranes probably for degradation (Hartl et al. 2002; Young et al. 2003; Calabrese et al. 2004; Mayer et al. 2005; Calabrese et al. 2007). Therefore, observed changes after 90 d are may be a result of early activation of autophagy process (7 d) or induction of HSPs (30 d in H), which might have cleared damaged macromolecules and organelles, and helped the cell to restore its redox balance. We propose that this current trend of data to be termed as Tier-4 response (Figure 7.13 and 7.14), which also fits the description of hormesis (defined as total response of an organism to external stimulus, which includes initial reaction and later adaption).

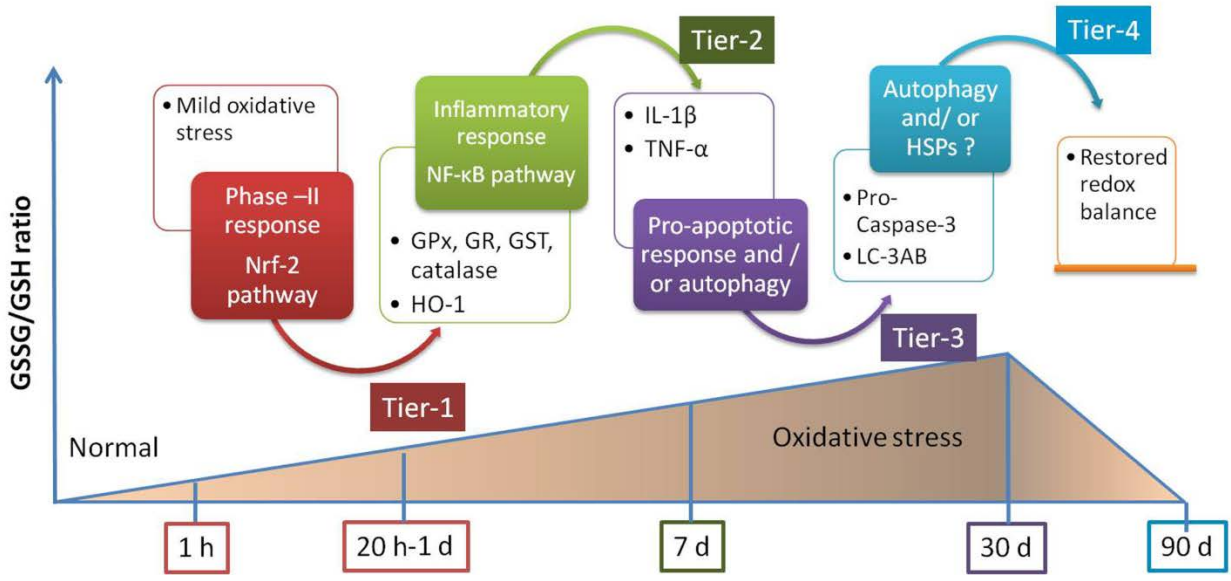


**Figure 7.14:** Modified model for hierarchy oxidative stress mechanism of nanomaterial toxicity based on our finding from 30 nm ceria ENM induced oxidative stress in hippocampus, at different exposure time points.

At this moment we do not have any data in between 30 d to 90 d period, which is a very large time gap for any biochemical or bio-molecular event to occur. Filling some gap of this 60 d period will able to shade some more light on autophagy process or induction of HSPs and their presumable relationship with restoration of redox balance after 90 d in rat brain after 30 nm ceria exposure. Nonetheless, the significance of these observations lies in the choice of the biological model i.e. multicellular organism (rat), which allows expression of adaptation mechanism such as Tier-4 or hormesis unlike cell culture models. These results also emphasize importance of use of *in vivo* models for evaluation of toxicity of nanomaterials as oppose completely relying on *in vitro* models.

CHAPTER 8

# VARIATIONS OF OXIDATIVE STRESS EFFECTS INDUCED BY 55 NM CERIA ENM IN RAT BRAIN IN TIME-AND DOSE-DEPENDENT MANNER

## 8.1. Overview of the Study

The material and chemical properties of ENMs are highly dependent upon two main factors: surface effects related to the fraction of atoms or molecules present on the surface, and quantum effects related to delocalized electrons (Buzea et al. 2007). Both these effects are therefore related to size of the ENMs, as size decreases surface and quantum effects become more predominant (Oberdörster et al. 1994; Nel et al. 2006; Buzea et al. 2007). The size of ENMs also hold key to its biological behavior as due to small size ENMs can get distributed rapidly and may get an easy access to various cellular compartments which are otherwise inaccessible. Due to high surface area, ENMs can interact with or harbor different biomolecules, as well as facilitate bio-reactions with great efficiency (Nel et al. 2009; Fubini et al. 2010). Thus the very properties that make the ENMs popular in various applications may also determine their toxicity. The reports available on size-dependent nanotoxicity are *in vitro* studies with BEAS-2B human lung epithelial cells, which have explored ENM sizes up to 45 nm (Park et al. 2008; Eom et al. 2009) and to our best knowledge, the work presented in this dissertation will be the first study to explore size-dependant toxicity of ceria ENM in multicellular organism. The current chapter of dissertation study focuses on the oxidative stress effects of ~55 nm ceria ENM on rat brain, which will be compared with the findings from Chapters 5 (5 nm ceria ENM), Chapter 6 (15 nm ceria ENM) and Chapter 7 (30 nm ceria ENM) to better understand the role of ENM size in its toxicity.

Apart from size, toxicity of ENM also depends upon composition, aggregation, crystallinity, surface functionality, dose of ENM, exposure period, etc. Dose of ENM is usually defined as the amount or quantity of ENM that will reach a biological system (Buzea et al. 2007). The dose is directly related to exposure or concentration of material in the medium like air, water or food, multiply by the duration of contact (Buzea et al. 2007). Most commonly in a dose-metric study, dose of a substance is determined on the basis of its mass or concentration (Yokel et al. 2011). However, in case of nanomaterials, the choice is not such simple (Oberdörster et al. 1994; Wittmaack 2006; Jiang et al. 2008; Oberdorster et al. 2009; Rushton et al. 2010; Yokel et al. 2011), as nanotoxicity is also co-depend upon matrices like size, surface area, and number of particles etc. Most of the time toxicity mechanism is taken into consideration while determining the appropriate dose matrix and since one is likely to see different mechanism for different materials there will not be a unique choice (Fubini 1997). Nonetheless most studies of ENM have expressed exposure based on dose or concentration.

In current study, the role of dose was evaluated by intravenous administration of two types of bolus doses 50 mg/kg (10 male rats) and 100 mg/kg (5 male rats) of 55 nm ceria ENM. Five rats that received 50 mg/kg ceria ENM were terminated after 1 h with five saline treated control rats. The remaining five rats from 50 mg/kg dose group were terminated with the five rats that received 100 mg/kg of ceria ENM and five saline treated control rats, 20 h after ceria administration. Three brain regions, hippocampus, cortex and cerebellum from each treatment were harvested from each ceria- and saline-control treated rat and frozen rapidly in liquid nitrogen. The levels and activities of the antioxidant enzymes catalase, manganese superoxide dismutase (MnSOD), glutathione

peroxidase (GPx), and glutathione reductase (GR), were measured. To understand the extent of changes in cellular redox status, the levels of oxidative stress endpoints, protein carbonyl (PC), 3-nitrotyrosine (3NT), and protein bound 4- hydroxyl-2-trans nonenal (HNE), were measured along with heat shock protein (Hsp70) levels.

## 8.2. Materials and methods

### 8.2.1. Nanomaterial:

Ceria ENM was obtained from our collaborator, which was synthesized in in-house facility (Section 3.1). Nanomaterial characterization was carried out by our collaborators, prior to ceria ENM treatment to the animals (Section 3.2).

### 8.2.2. Animals:

The male Sprague-Dawley rats received either saline or 5% ceria dispersion intravenously. Five rats were infused with 0 and five rats with 50 mg ceria/kg and terminated 1 h after completion of infusion. Five rats were infused with 0 and 5 rats with 50 mg/kg and 5 more with 100 mg ceria/kg and terminated 20 h after completion of infusion. After ceria ENM treatments, the BBB integrity assessment (Section 3.3), light and electron microscopic assessment (Section 3.4) and EELS analysis (Section 3.2) was carried out by our collaborators. The brain homogenates were prepared from control and ceria treated rat brain samples (Section 3.6). Total protein content was determined using BCA assay (Section 3.7) and various biochemical assays were carried out on all the samples (Sections 3.8, 3.9, 3.10, 3.11, and 3.14) in our laboratory.

## 8.3. Results

Ceria composition

High resolution-TEM/HR-STEM showed the ceria ENM was polyhedral shape (Figure 8.1). The XRD patterns demonstrated the ceria are highly crystalline. Evaluation of a number of TEM images showed that the ceria had a number-average primary particle size of 55 nm.

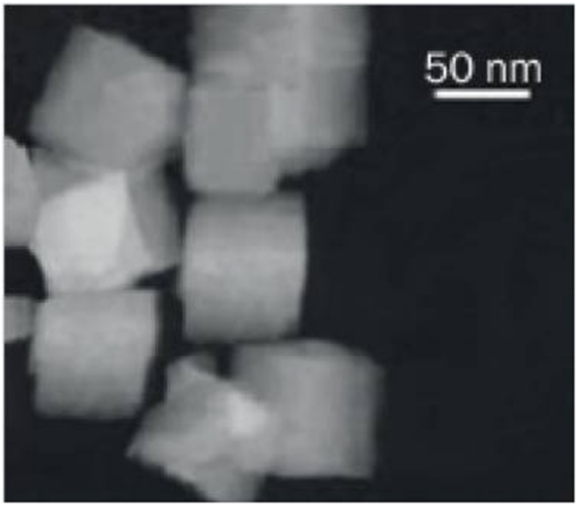


**Figure 8.1:** 55 nm ceria ENM imaged using HRTEM and HRSTEM. The ceria were dispersed on a carbon film. Visually they have a size distribution ranging from X to X nm and the majority diameter around 55 nm. The magnified TEM insert at the lower left illustrates that the ceria ENMs are highly crystalline (taken by Dr. Peng Wu and as published in Dan et.al. 2012).

Ceria concentration in brain and Electron micrograph

ICP-MS analysis suggested that very small amount of ceria was present in the brain parenchyma compare to peripheral organ liver (Table 8.1). Electron micrograph studies suggested that ceria ENM was not found in the brain, but located on the luminal side of

the BBB endothelium. The hippocampus and cerebellum tissues did not show obvious ceria induced injury as no necrotic neurons or elevated gliosis were observed and the BBB was visibly intact (data not shown).

**Table 8.2:** Cerium concentrations in blood, brain, liver, and spleen, expressed as a percent change of 55 nm ceria ENM dose. a) Based on reference volume of blood in the rat (7% of body weight) or weight of the brain, liver x ceria concentration.

| | **Cerium [% of dose][a]** | | |
|---|---|---|---|
| | **Blood** | **Brain** | **Liver** |
| **% dose (1 h)** | 0.0053 ± 0.005 | 0.014 ± 0.01 | 11.6 ± 9 |

EELS results

Electron energy loss spectroscopic measurements on liver tissue were performed as a representative organ. The ratio of Ce(Owens Iii et al.) to Ce(IV) in the aged ceria was evaluated using EELS measurements after locating agglomerates of the ceria nanorods in tissue 1 h and 30 days after infusion into rat and comparing with synthesized ceria. The high $Ce^{3+}$/ $Ce^{4+}$ ratio that was obtained in the as-synthesized, fresh 55 nm ceria seems to have only been altered slightly in individual ceria measured in liver after 20 h *in vivo* (data not shown).

Oxidative Stress Indices

*Phase II antioxidant activities were increased after 1 and 20 h*

Similar to our observation with 15 nm and 30 nm ceria ENM, induction of phase II antioxidant enzymes was observed in different brain regions 1 and 20 h after 55 nm ceria ENM administration. Amongst two glutathione related antioxidant enzymes GPx and GR; only GPx activities and levels were induced after 55 nm ceria ENM treatment at both 1 h and 20 h. GPx activities were induced in hippocampus (~ 19%, *$p < 0.05$, 50 mg/kg) and in cortex (~ 27%, *$p < 0.05$, 50 mg/kg,) after 1 h as well as strongly hiked up after 20 h in hippocampus (~ 43%, *$p < 0.05$, 100 mg/kg) and cortex (~ 49%, *$p < 0.05$, 50 mg/kg and ~ 41%, *$p< 0.05$, 100 mg/kg); Figure 8.2a. Catalase activities were strongly induced in all 3-brain regions after 1 h; in hippocampus (~ 24%, *$p < 0.05$, 50 mg/kg), in cortex (~ 21%, *$p < 0.05$, 50 mg/kg), and in cerebellum (~ 21%, *$p < 0.05$, 50 mg/kg); Figure 8.2c. After 20 h catalase activity followed a trend similar to that as GPx activity and increased only in hippocampus (~ 17%, *$p < 0.05$, 100 mg/kg) and cortex (~ 21%, *$p < 0.05$, 50 mg/kg and ~ 15%, *$p< 0.05$, 100 mg/kg); Figure 8.2c.

A huge upsurge in GPx and catalase levels was observed only after 20 h in hippocampus (~ 56%, $^{\Theta}p < 0.0001$) and (~ 50%, $^{\xi}p < 0.001$) respectively, after administration of 100 mg/kg dose of ceria, Figure 8.3a. GPx and catalase levels in hippocampus measured after 100 mg/kg dose of ceria were significantly increased compared to corresponding levels after 50 mg/kg dose ($^{\Theta}p < 0.001$); Figure 8.3a and c respectively. On the other hand GR and SOD activities and levels remained fairly unaffected from post-treatment effect of ceria administration at smaller and larger doses (Figure 8.2b -8.3b and 8.2d-8.3d, respectively).

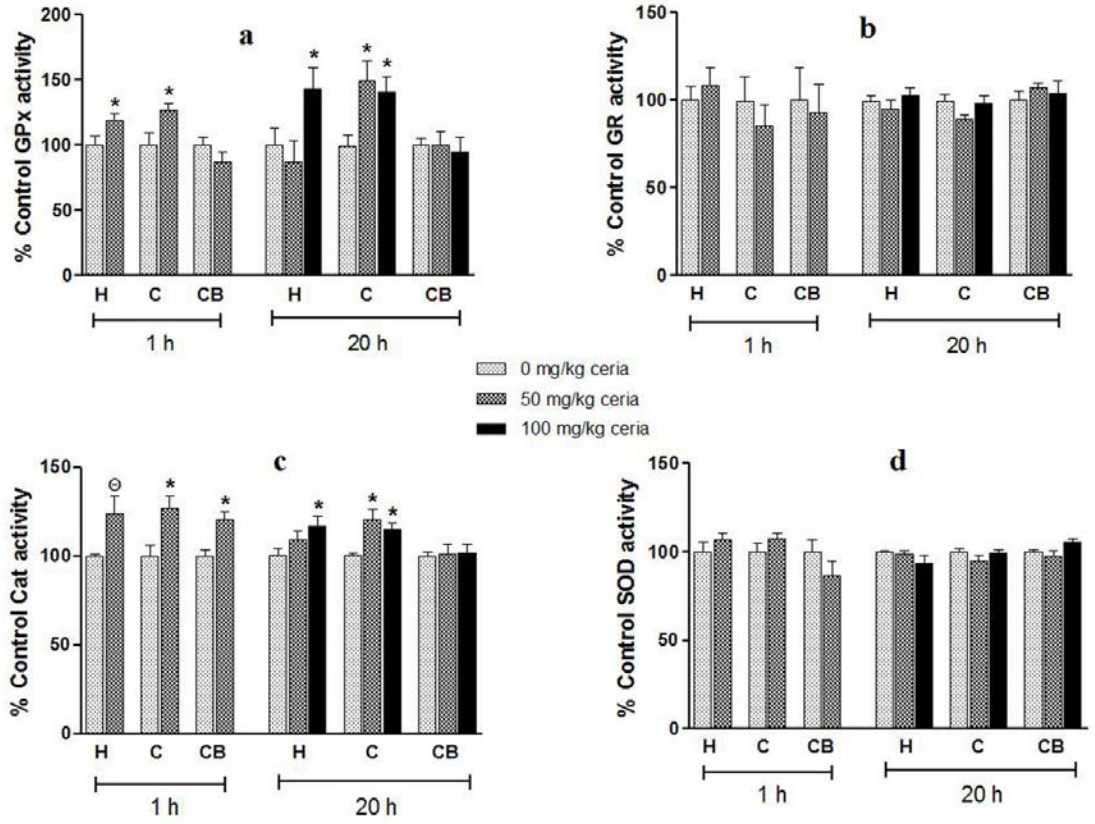


**Figure 8.2:** The antioxidant enzyme activities in 3-brain regions 1 h and 20 h after i.v administration of 50 mg/kg and 100 mg/kg dose 55 nm ceria ENM. a) The histograms represent %control GPx activities measured in saline treated controls and ceria treated samples, b) the histograms represent %control GR activities measured in saline treated controls and ceria treated samples, c) the histograms represent %control catalase activities measured in saline treated controls and ceria treated samples, d) the histograms represent %control SOD activities measured in saline treated controls and ceria treated samples. All the values are expressed as mean ± SEM, control n = 5, treated n = 5, *p <0.05, $^{\xi}p < 0.01$, and $^{\Theta}p < 0.001$, compared to mean of respective control samples.

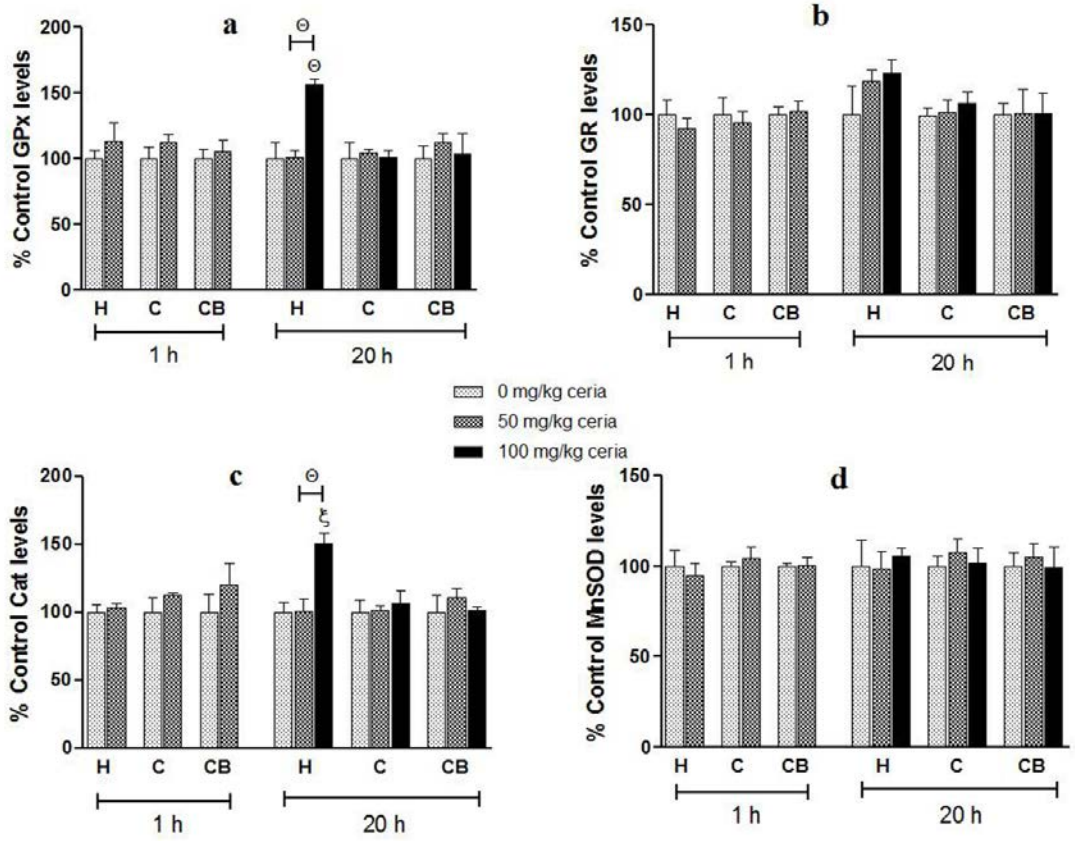


**Figure 8.3a, b, c and d:** The antioxidant enzyme levels in 3-brain regions 1 h and 20 h after i.v administration of 50 mg/kg and 100 mg/kg dose 55 nm ceria ENM. a) The histograms represent %control GPx levels measured in saline treated controls and ceria treated samples, b) the histograms represent %control GR levels measured in saline treated controls and ceria treated samples, c) the histograms represent %control catalase levels measured in saline treated controls and ceria treated samples, d) the histograms represent %control MnSOD levels measured in saline treated controls and ceria treated samples. All the values are expressed as mean ± SEM, control n = 5, treated n = 5, *p <0.05, $^{\xi}p < 0.01$, and $^{\Theta}p < 0.001$, compared to mean of respective control samples.

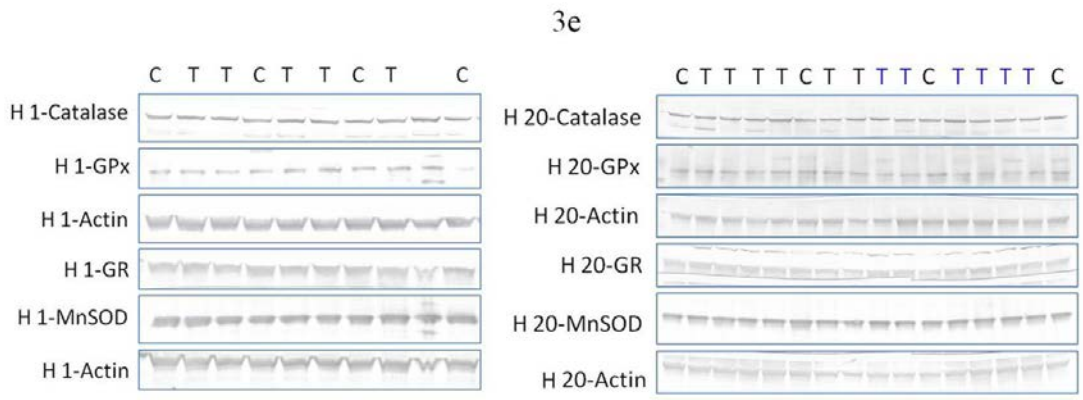


**Figure 8.3e:** Separate Western blots were used to estimate antioxidant protein levels in hippocampus, cortex and cerebellum. However, only representative examples from hippocampus are shown. Protein levels in control [C] n=4, and treated [T] n=5 samples for 1 h (left, consider only labeled bands) and control [C] n=4, treated [T] n=6- black for 50 mg/kg dose and treated [T] n=6- blue for 100 mg/kg dose samples for 20 h 55 nm ceria treatment. The intensity of each antioxidant protein band was normalized with intensity of corresponding band of β-actin-loading control. Similar blots were obtained for cortex and cerebellum regions.

*Reduction in protein oxidation after 1 and 20 h*

Protein oxidation marker-PC levels were decreased in all three brain regions after 1 h, in hippocampus (~ 25%, *$p < 0.05$, 50 mg/kg), in cortex (~ 39%, *$p < 0.05$, 50 mg/kg), and in cerebellum (~ 26%, *$p < 0.05$, 50 mg/kg) Figure 8.4a. PC levels were also decreased after 20 h in hippocampus (~ 13%, *$p < 0.05$, 100 mg/kg) and in cortex (~ 18%, $^{\xi}p < 0.001$, 50 mg/kg and ~ 17%, *$p < 0.05$, 100 mg/kg) Figure 8.4a. PC levels in hippocampus measured after 100 mg/kg dose of ceria were significantly decreased compared to that after 50 mg/kg dose ($^{\xi}p < 0.01$). Protein nitrotyrosine marker-3NT levels were decreased after 1 h in hippocampus (~ 21%, *$p < 0.05$, 50 mg/kg), in cortex

(~ 30%, *p < 0.05, 50 mg/kg) and again after 20 h only in cortex (~ 17%, *p < 0.05, 50 mg/kg and ~ 18%, *p < 0.05, 100 mg/kg) Figure 8.4b.

Both the doses, 50 mg/kg and 100 mg/kg of 55 nm ceria ENM did not have any effect on lipid peroxidation marker-HNE levels in rat brain. HNE levels were unchanged in all three brain regions after 1 and 20 h, Figure 8.4c.

*Reduction in HSPs 20 h after high dose*

HO-1 and Hsp70 levels were fairly unchanged in all three brain regions 1 h after administration of 50 mg/kg dose of 55 nm ceria ENM peripherally, Figure 8.5a and b. Further HO-1 levels were declined after 20 h with significant decrease in hippocampus (~ 21%, *p < 0.05, 100 mg/kg) and in cortex (~ 17%, *p < 0.05, 50 mg/kg and ~ 26%, $^{\xi}$p < 0.001, 100 mg/kg), both after high dosage of ceria, Figure 8.5a. Hsp70 levels were also declined after 1 h with significant decrease in hippocampus (~ 13%, *p < 0.05, 50 mg/kg), and after 20 h in cortex (~ 17%, *p < 0.05, 100 mg/kg), and in cerebellum (~ 23%, *p < 0.05, 100 mg/kg), but decrease in Hsp70 levels was not dose specific, Figure 8.5b. Hsp70 levels in hippocampus measured after 50 mg/kg dose of ceria were significantly decreased compared to that after 100 mg/kg dose (*p < 0.05), Figure 8.5b.

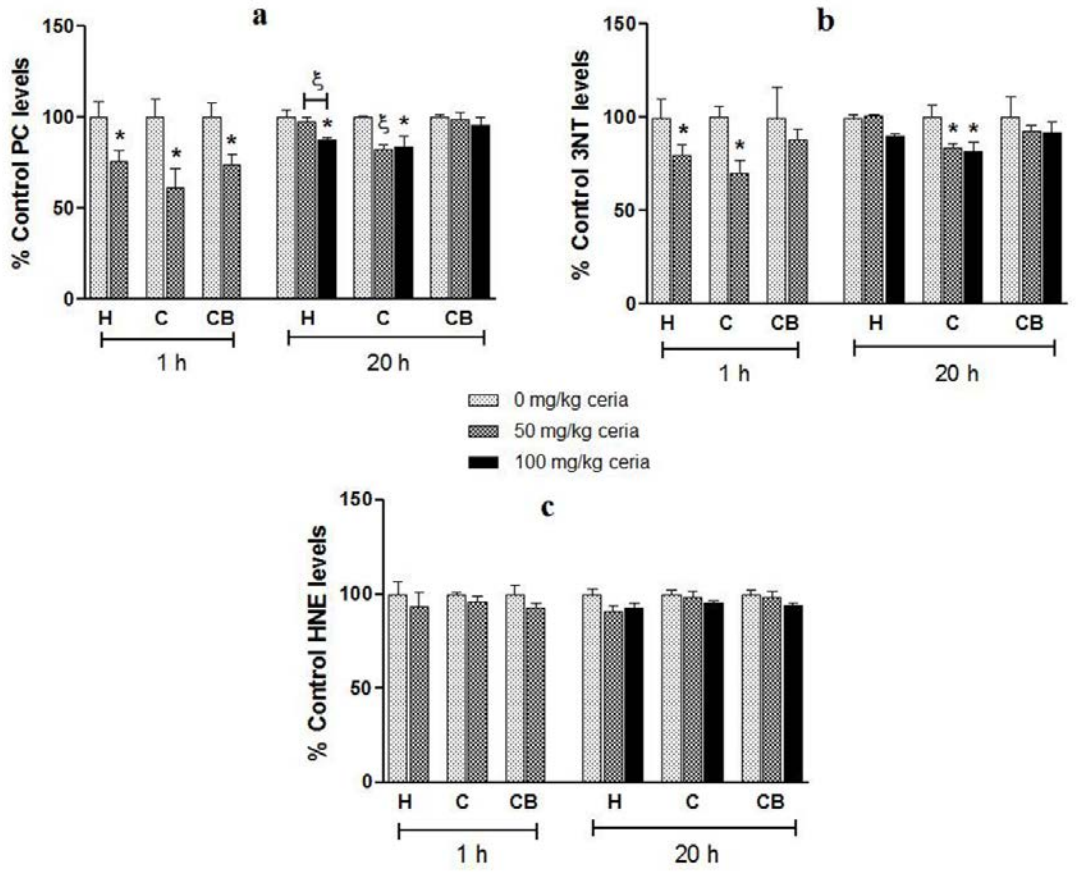


**Figure 8.4:** The oxidative stress marker levels in 3-brain regions 1 h and 20 h after i.v administration of 50 mg/kg and 100 mg/kg dose 55 nm ceria ENM. a) The histograms represent %control PC levels measured in saline treated controls and ceria treated samples, b) the histograms represent %control 3NT levels measured in saline treated controls and ceria treated samples, c) the histograms represent %control HNE levels measured in saline treated controls and ceria treated samples. All the values are expressed as mean ± SEM, control n = 5, treated n = 5, *$p < 0.05$, $^{\xi}p < 0.01$, and $^{\Theta}p < 0.001$, compared to mean of respective control samples.

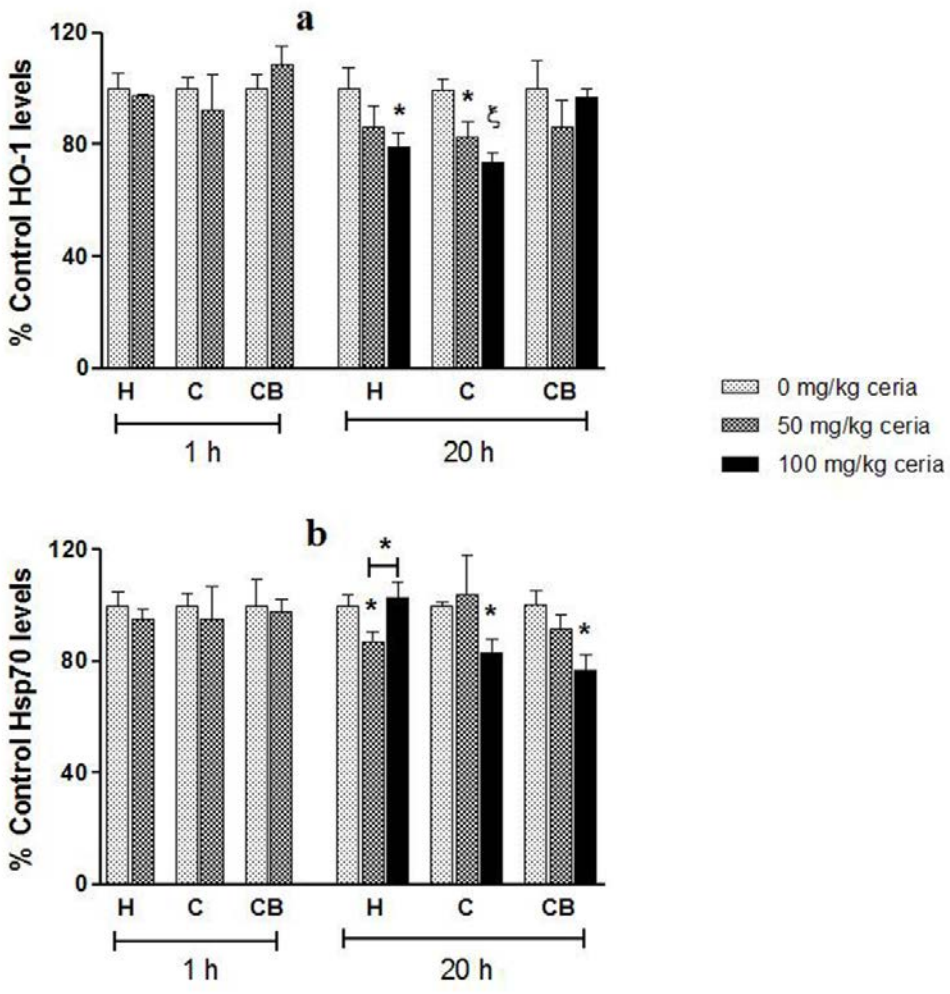


**Figure 8.5a and b:** The heat shock protein levels in 3-brain regions 1 h and 20 h after i.v administration of 50 mg/kg and 100 mg/kg dose 55 nm ceria ENM. a) The histograms represent %control HO-1 levels measured in saline treated controls and ceria treated samples, b) the histograms represent %control Hsp70 levels measured in saline treated controls and ceria treated samples. All the values are expressed as mean ± SEM, control n = 5, treated n = 5, *p <0.05, $^{\xi}$p < 0.01, and $^{\Theta}$p < 0.001, compared to mean of respective control samples.

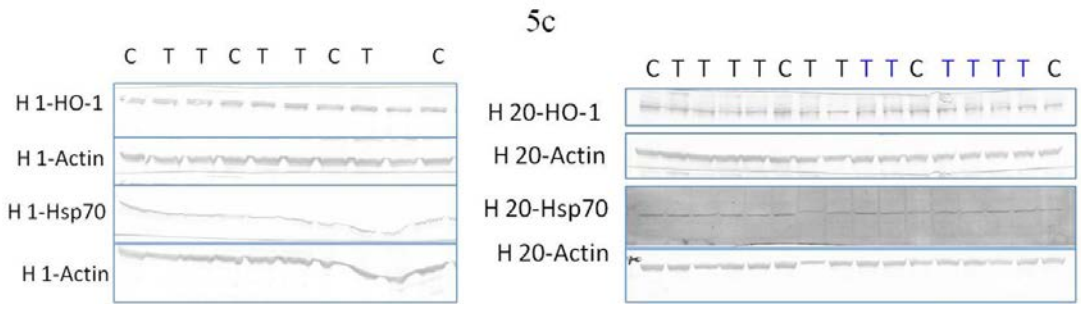


**Figure 8.5c:** Separate Western blots were used to estimate HSPs levels in hippocampus, cortex and cerebellum. However, only representative examples from hippocampus are shown. Protein levels in control [C] n=4, and treated [T] n=5 samples for 1 h (left, consider only labeled bands) and control [C] n=4, treated [T] n=6- black for 50 mg/kg dose and treated [T] n=6- blue for 100 mg/kg dose samples for 20 h 55 nm ceria treatment. The intensity of each antioxidant protein band was normalized with intensity of corresponding band of β-actin-loading control. Similar blots were obtained for cortex and cerebellum regions.

### 8.4. Discussion

The fraction of atoms or molecules present on the surface and therefore the size of ENM, are key to determine not only the material properties but also chemical and biological properties of ENM. In order to understand the role play of size in determining the biological effects of ceria ENM, we prepared the ENMs from size ~ 5nm to ~ 55 nm, with aspect ratio-1. The current study focuses on the oxidative stress effects of 55 nm ceria ENM on rat brain after its systemic administration. The oxidative stress effects were evaluated in terms of changes in the levels of phase II antioxidant enzymes, protein and lipid oxidation markers, heat shock protein response, and phase II antioxidant enzyme activities, when compared with saline treated rats from control groups. In addition to the

size effect, we also examined the dose effect with 50 mg/kg and 100 mg/kg dose of 55 nm ceria ENM.

The 50 mg/kg dose of 55 nm ceria ENM induced cellular antioxidant defense response in time-dependent manner in hippocampus and cerebellum region. The phase II antioxidant enzymes, GPx and catalase activities were elevated after 1 h of 50 mg/kg dose and reduced back to the normal levels after 20 h (H and CB). The induction of phase II enzymes is usually seen at low levels of oxidative stress caused by internal or external stimuli (Talalay et al. 2003; Li et al. 2004; Kim et al. 2009; Speciale et al. 2011) as 50 mg/kg dose of 55 nm ceria ENM administration in current case. The elevated GPx and catalase activities may have caused reduction in PC and 3NT levels after 1 h, although PC and 3NT levels were resorted back to the control levels (H and CB) after 20 h. Various other studies have reported protection against oxidative stress by induction of phase II antioxidant response (Cerutti et al. 1994; Hayes et al. 1999; Talalay et al. 2003; Kim et al. 2009; Speciale et al. 2011). Increased oxidative stress induces HSP levels, therefore lack of change in HO-1 and Hsp70 levels after 1 h and decreasing trend in HO-1 (H, and CB) levels after 20 h suggest reduction in oxidative stress. Decline in oxidative stress can be achieved by either scavenging ROS or by inducing cellular antioxidant enzyme levels and activities. In the current case it was achieved by strong induction of phase II enzyme response, which reduced oxidative stress and oxidative stress indices at initial stage (1 h) and then restored the delicate balance in ROS levels and antioxidant molecules and enzymes, reflected in terms of lack of change in oxidative stress indices as seen after 20 h of 50 mg/kg dose of 55 nm ceria. Also the cortical region showed similar protective antioxidant defense response after 50 mg/kg dose of 55 nm ceria, but levels of

oxidative stress indices did not varyied much with time. Thirty nm ceria treatment also induced similar antioxidant defense-Tier-1 response at 1 and 20 h, but again the variation in the magnitude of oxidative stress indices were not dramatically time dependant (Chapter 7). A time-dependent decrease in cell viability mediated by oxidative stress has been reported by Park in two independent studies with 30 nm ceria and 21 nm $TiO_2$ ENMs (Park et al. 2008; Park et al. 2008).

In addition to time-dependent changes, 55 nm ceria ENM treatment also mediated changes in oxidative stress indices in dose-dependent manner. The dose-dependent changes in the levels and activities of GPx and catalase was observed only in hippocampus region after 20 h where magnitude of change was higher at higher dose of 55 nm ceria ENM (100 mg/ kg). Concomitantly, PC (H), HO-1 (H and C), and Hsp70 (C and CB) levels were decreased to greater magnitude after 100 mg/kg dose of 55 nm ceria ENM compared to 50 mg/kg dose. In slight contrary, Hsp70 levels were decreased to greater magnitude after 50 mg/kg dose of 55 nm ceria ENM compared to 100 mg/kg dose in hippocampus alone. Similar dose-dependency was reported with after treatment of 30 nm ceria (Park et al. 2008) and 21 nm ENM (Park et al. 2008) to human lung epithelial cells, where cell viability was decreased and ROS generation was increased in a dose-dependent manner. A dose-dependent correlation was observed in brain-HNE and PC levels, where hippocampal HNE levels were increased and cerebral PC levels were decreased after 30 nm commercial ceria ENM i.v injections (Yokel et al. 2009). Similarly, some positive dose-dependent correlations in oxidative stress effects were observed in mice brain after systemic delivery of $TiO_2$ (Ma et al. 2010), in lung after inhalation of cobalt containing MWCNTs (Pauluhn 2010). Concentration-dependent

inhibition of murine microphage cell proliferation and lipopolysaccharide-induced COX-2 expression (up to 20 μg/ml), was observed after *in vitro* SWCNT exposure (Dutta et al. 2007). A dose-dependent increase in LDH activity and total protein was seen after intratracheal instillation of MWCNTs (L ~6μm) and after ground MWCNTs (L ~0.7μm) in rat lung bronchoalveolar lavage fluid (Muller et al. 2005).

In the current study, 55 ceria ENM selectively induced the activity of $H_2O_2$ reducing catalase and GPx phase II enzymes. The induction of catalase and GPx is an adaptive cellular response against various ROS insults, which can facilitate clearance of oxidative stress markers (Cerutti et al. 1994; Hayes et al. 1999; Miyamoto et al. 2003; Bagnyukova et al. 2005; Margonis et al. 2007) and exposure to $H_2O_2$ can selectively induce the transcription/ mRNA levels of catalase and GPx gene expression in a feed-back mechanism manner (Wang et al. 2011). Studies in the past have reported the SOD mimetic activity of ceria ENM where it can reduce superoxide radicals to $H_2O_2$ and oxygen (Korsvik et al. 2007; Heckert et al. 2008). Thus may be by causing some increase in cellular oxidative stress, 55 nm ceria ENM induced a strong antioxidant defense response in the brain hippocampal and cortical region. The cellular defense response in hippocampus brain region was varied in the time- as well as dose-dependent manner.

# CHAPTER 9

# ROLE OF ASPECT RATIO (SHAPE) OF ENM IN THE MODULATION OF TOXICITY OF CERIA ENM IN THE RAT BRAIN

## 9.1. Overview of the Study

At emergent of new technologies, creation of nanometer scale functional devices requires the production and handling of component of submicron sizes, which necessitates exploration of development of various nanostructure especially nanofilament (carbon or inorganic nanotubes or nanowires). Nanofilaments (NFs) are envisioned as building blocks of new technologies such as flat panel screens, composite materials, or catalyst supports, expected to be applied in medical diagnosis and imaging (Magrez et al. 2009). NFs are also foreseen as second generation (active) ENMs used in applications like targeted control-release drug delivery systems with some of the popular examples are carbon nanotubes (CNT) and gold nanorods (Lewinski et al. 2008; Yokel et al. 2011). In spite of the promising nature of these NFs, the knowledge on the health effects related to the production, handling and exposure of these materials is essential.

Depending on the aspect ratio (L-length / D-diameter) of a nanofilament, its toxicity is affected, with the higher the aspect ratio, the more toxic the particle (Lippmann 1990). Particles with a length $\leq 1$ μm has a low aspect ratio material, while a particle with a length $> 5$ μm and aspect ratio $\geq 3{:}1$ are high aspect ratio materials or conventionally known as fibers (WHO/EURO et al. 1985; Lippmann 1990). The high aspect ratio morphology includes nanotubes and nanowires, with various shapes like helices, zigzags, belts, with varying diameters and lengths (Buzea et al. 2007). The morphology of low aspect ratio nanomaterials morphology includes spheres, ovals, cubes, prisms, helices,

pillar, wires or rods (Buzea et al. 2007). The long length fibers or high aspect ratio materials (> 20 μm) are cleared less effectively compared to the low aspect ratio material or broken fibers, by alveolar macrophages, therefore leading to pulmonary toxicity ranging from asbestosis, mesothelioma to lung cancer (Lippmann 1990; Buzea et al. 2007). However, even low aspect ratio material, (D < 100 nm, L < 1 μm) may escape phagocyte clearance entering into the vascular system, some of which may end up in various organs including brain, liver, kidney etc., causing adverse health effects (Buzea et al. 2007; Oberdorster et al. 2009; Yokel et al. 2011).

There have been some efforts made to answer the questions on the toxicity of NFs either during the manufacturing process or after short-or long-term exposure. However, as early development was a focus of carbon-based NFs (Iijima 1991) most of the toxicity studies have also exclusively focused on carbon based NFs (Shvedova et al. 2003; Lam et al. 2004; Maynard et al. 2004; Warheit et al. 2004; Monteiro-Riviere et al. 2005; Panessa-Warren et al. 2006; Helland et al. 2007). The toxicity of inorganic materials (Soenen et al. 2011) such as iron oxides, titanium oxides, zinc oxide, gold, silver, has been investigated, but is limited to their isotropic forms (aspect ratio 1) with a few exceptions as asbestos fibers and gold nanorods (Lewinski et al. 2008; Stern et al. 2008). Unfortunately, toxicity of NFs cannot be predicted from their known toxicity in different structural forms for example, “benine” silicates renders highly toxic effects in their fiber form known as asbestos (Magrez et al. 2009). There is only one study available on metal oxide, where $TiO_2$ based nanotubes and nanowires exposed to human lung tumor cells strongly affected cell proliferation and caused cell death (Magrez et al. 2009).

Considering the increasing applications of ceria ENM in various fields including biomedical applications and discrepancy in the oxidative stress related effects (as explained in earlier chapters), the current study was designed to evaluate the influence of aspect ratio on the neuro-nanotoxicity of ceria ENM.

To fulfill the objective, 10 nm ceria nanorods with an aspect ratio 5 to 60, were synthesized, and 5% dispersion of the material was administered to male rats intravenously. The rats were terminated 1 h and 30 d after the ceria treatment. Three brain regions, hippocampus, cortex and cerebellum, were harvested from each ceria- and saline-treated rats and frozen rapidly in liquid nitrogen. The levels and activities of the antioxidant enzymes catalase, manganese superoxide dismutase (Mn-SOD), glutathione peroxidase (GPx), and glutathione reductase (GR), were measured along with the ratio of reduced glutathione (GSH) to its oxidized form (GSSG). To understand the extent of changes in cellular redox status, the levels of oxidative stress endpoints, protein carbonyl (PC), 3-nitrotyrosine (3NT), and protein bound 4- hydroxyl-2-trans nonenal (HNE), were measured along with heat shock protein (Hsp70) levels.

## 9.2. Materials and methods

### 9.2.1. Nanomaterial:

Ceria ENM was obtained from our collaborator, which was synthesized in in-house facility (Section 3.1). Nanomaterial characterization was carried out by our collaborators, prior to ceria ENM treatment to the animals (Section 3.2).

### 9.2.2. Animals:

The male Sprague-Dawley rats received either saline or 5% ceria dispersion intravenously. Five rats were infused with 0 and 5 rats with 20-50 mg ceria/kg and terminated 1 h after completion of infusion. Five rats were infused with 0 and 5 rats with 100 mg ceria/kg and terminated 30 d after completion of infusion. After ceria ENM treatments, the BBB integrity assessment (Section 3.3), light and electron microscopic assessment (Section 3.4) and EELS analysis (Section 3.2) was carried out by our collaborators. The brain homogenates were prepared from control and ceria treated rat brain samples (Section 3.6). Total protein content was determined using the BCA assay (Section 3.7), and various biochemical assays were carried out on all the samples (Section 3.8, 3.9, 3.10, 3.11, and 3.14) in our laboratory.

## 9.3. Results

Ceria composition

HR-TEM/HR-STEM showed the ceria ENM was polyhedral shape (Figure 9.1). The XRD patterns demonstrated the ceria are highly crystalline. Evaluation of a number of TEM images showed that the ceria had a number-average primary particle size of ~ 10 nm with aspect ratio (length/ diameter) 5-60.

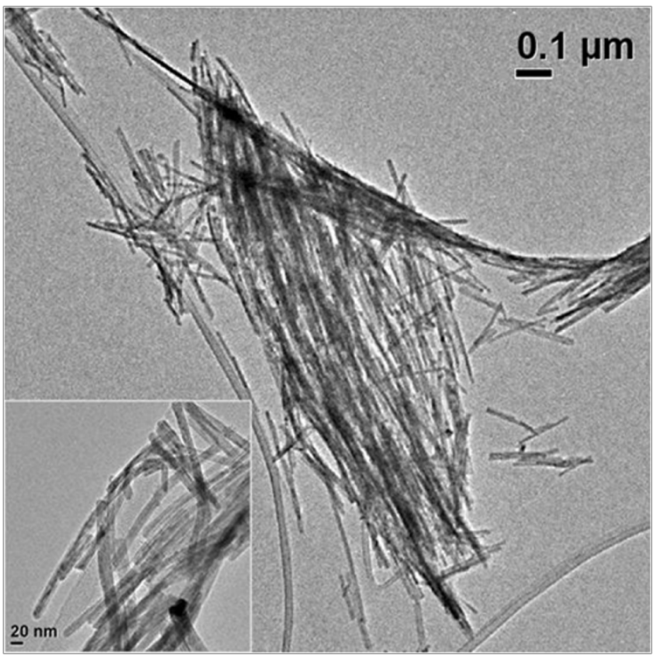


**Figure 9.1:** Ceria ENM nanorods were imaged using HRTEM and HRSTEM. The ceria nanorods were dispersed on a carbon film. Visually they have a size distribution ranging from 50 to 600 nm in length and the majority diameter around 10 nm. The magnified TEM insert at the lower left illustrates that the ceria ENMs are highly crystalline (taken by Dr. Peng Wu).

Ceria concentration in brain and Electron micrograph

ICP-MS analysis suggested that very small amount of ceria was present in the brain parenchyma compare to peripheral organ liver (Table 9.1). Electron micrograph studies suggested that ceria ENM was not found in the brain, but located on the luminal side of the BBB endothelium. The hippocampus and cerebellum tissues did not show obvious ceria induced injury as no necrotic neurons or elevated gliosis were observed and the BBB was visibly intact (data not shown).

**Table 9.1:** Cerium concentrations in blood, brain, liver, and spleen, expressed as a percent change of the ceria ENM dose. a) Based on reference volume of blood in the rat (7% of body weight) or weight of the brain, liver x ceria concentration.

| | **Cerium [% of dose][a]** | | |
|---|---|---|---|
| | **Blood** | **Brain** | **Liver** |
| **% dose (1 h)** | 0.47 ± X | 0.013 ± X | 42 ± X |
| **% dose (30 d)** | 0.018 ± X | 0.001 ± X | 7.1 ± X |

EELS results

Electron energy loss spectroscopic measurements on liver tissue were performed as a representative organ. The ratio of Ce(Owens Iii et al.) to Ce(IV) in the aged ceria was evaluated using EELS measurements after locating agglomerates of the ceria nanorods in tissue 1 h and 30 days after infusion into rat and comparing with synthesized ceria. The high $Ce^{3+}$/ $Ce^{4+}$ ratio that was obtained in the as-synthesized, fresh ceria nanorods seems to have only been altered slightly in individual ceria measured in liver after 30 days *in vivo* (data not shown).

Oxidative Stress Indices

*Decrease in GSH: GSSG ratio in time dependant manner*

One hour after treatment of ceria nanorods, GSH: GSSG ratio showed a decreasing trend in cortex. However, decline in the ratio was statistically significant after 30 d in the

hippocampus (~ 28%, $^{\xi}p < 0.01$, Figure 9.2), in the cortex (~ 18%, *p < 0.05, Figure 9.2) and in the cerebellum (~ 17%, *p < 0.05, Figure 9.2), when compared with the respective control samples. GSH: GSSG ratio is a reflector of the cellular redox status, thereby a decline in the ratio suggest the oxidative nature of the cellular environment, which can affect various signal transduction pathways.

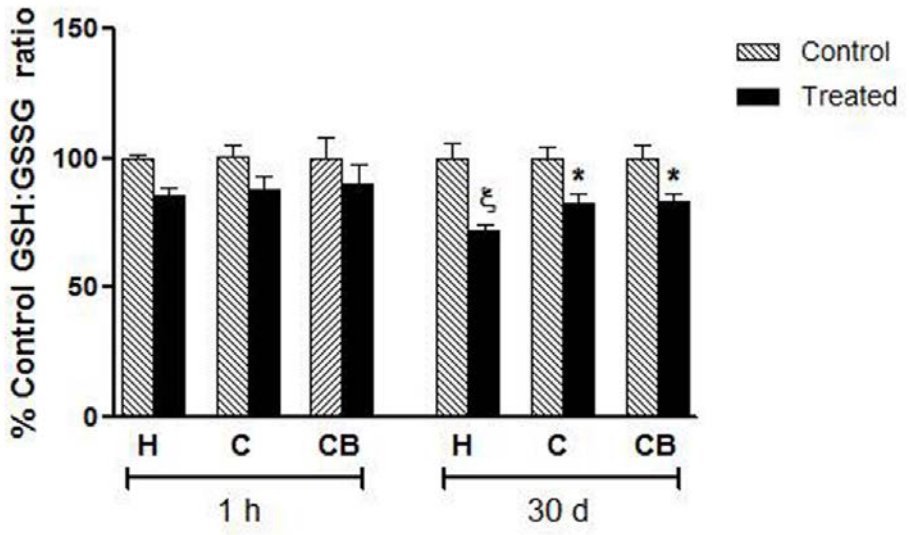


**Figure 9.2:** GSH: GSSG ratios in 3-brain regions measured 1 h and 30 d after ceria ENM nanorod treatment. The histograms represent %control for saline treated controls and ceria treated samples. The values are expressed as mean ± SEM, control n = 5, treated n = 5, *p <0.05, $^{\xi}p < 0.01$, and $^{\Theta}p < 0.001$, compared to mean of respective control samples.

*After initial increase, antioxidant enzyme activities were decreased at 30 d*

Glutathione (GSH) dependant antioxidant enzymes GPx and GR activities showed a trend for increased values after 1 h in the hippocampus, the cortex and the cerebellum as an initial response to ceria nanorods treatment. However, after 30 d GPx activity was significantly decreased in the hippocampus (~ 22%, *p < 0.05, Figure 9.3a), in the cortex

(~ 28%, *p < 0.05, Figure 9.3a), and in the cerebellum (~ 19%, *p < 0.05, Figure 9.3a). Similarly, a non-significant trend was seen in GR activity in three brain regions, Figure 9.3b. Following the trend of GPx and GR, catalase activity was increased significantly in the hippocampus (~ 23%, *p < 0.05, Figure 9.3c), the cortex (~ 17%, $^{\xi}$p < 0.01, Figure 9.3c), and the cerebellum (~ 20%, *p < 0.05, Figure 9.3c) at 1 h, it was significantly decreased after 30 d in the hippocampus (~ 17%, *p < 0.05, Figure 9.3c), and the cerebellum (~ 17%, *p < 0.05, Figure 9.3c). In similar way, SOD activity was significantly increased after 1 h in the hippocampus (~ 19%, $^{\xi}$p < 0.01, Figure 9.3d) and in the cerebellum (~ 21%, *p < 0.05, Figure 9.3d) and significantly decreased after 30 d in the hippocampus (~ 11%, *p < 0.05, Figure 9.3d) alone.

GPx, GR, catalase and SOD levels were affected by ceria nanorods treatment; however, the change in the levels was not statistically significant when compared with the respective controls for both the time points, Figure 9.4.

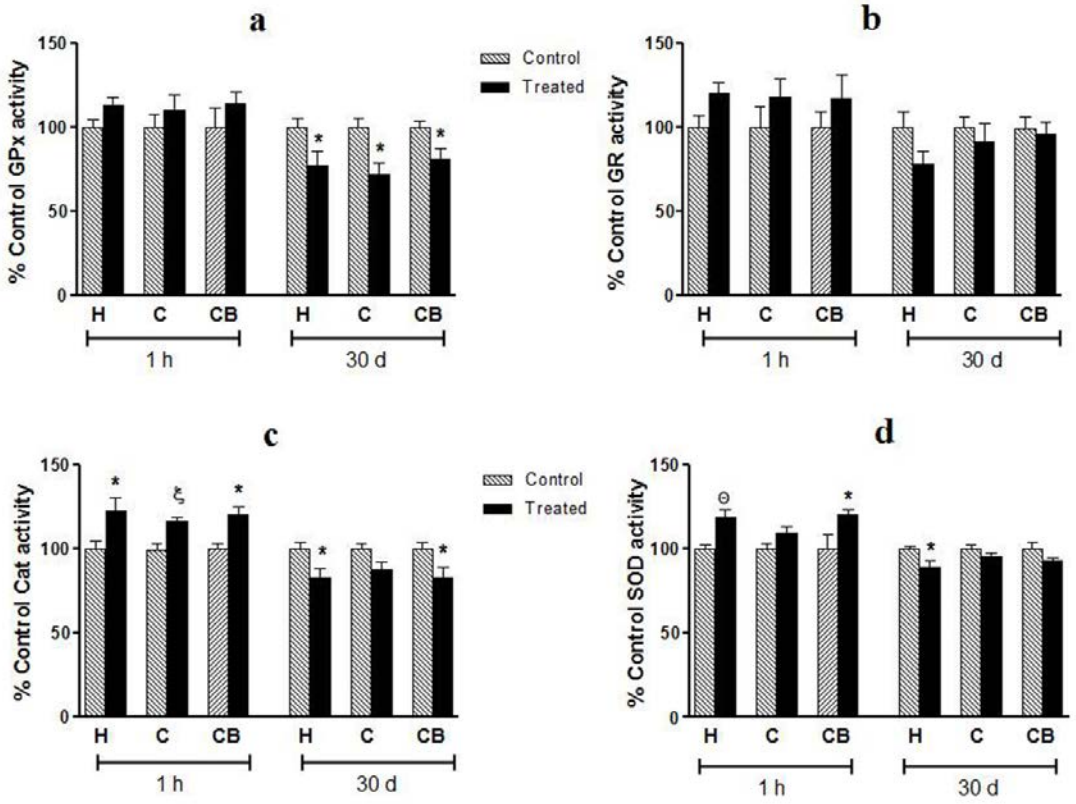


**Figure 9.3:** The antioxidant enzyme activities in 3-brain regions 1 h and 30 d after ceria nanorod treatment. a) The histograms represent %control GPx activities measured in saline treated controls and ceria treated samples, b) the histograms represent %control GR activities measured in saline treated controls and ceria treated samples, c) the histograms represent %control catalase activities measured in saline treated controls and ceria treated samples, d) the histograms represent %control SOD activities measured in saline treated controls and ceria treated samples. All the values are expressed as mean ± SEM, control n = 5, treated n = 5, *$p < 0.05$, $^{\xi}p < 0.01$, and $^{\Theta}p < 0.001$, compared to mean of respective control samples.

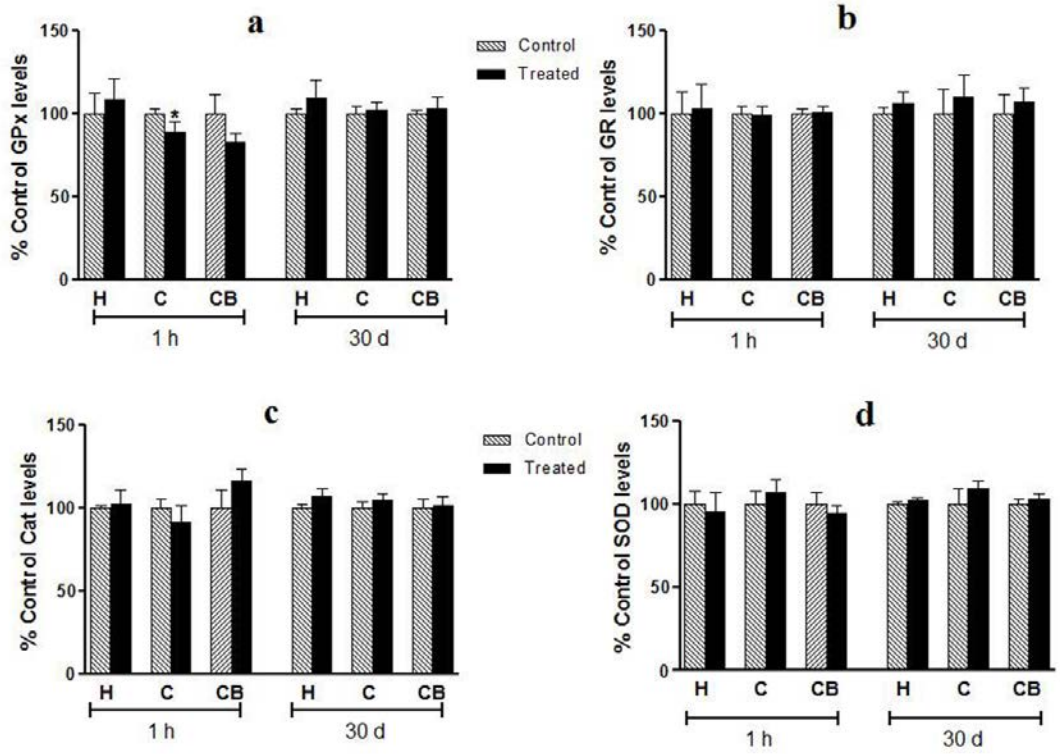


**Figure 9.4a, b, c and d:** The antioxidant enzyme levels in 3-brain regions 1 h and 30 d after ceria nanorod treatment. a) The histograms represent %control GPx levels measured in saline treated controls and ceria treated samples, b) the histograms represent %control GR levels measured in saline treated controls and ceria treated samples, c) the histograms represent %control catalase levels measured in saline treated controls and ceria treated samples, d) the histograms represent %control MnSOD levels measured in saline treated controls and ceria treated samples. All the values are expressed as mean ± SEM, control n = 5, treated n = 5, *p <0.05, $^{\xi}$p < 0.01, and $^{\Theta}$p < 0.001, compared to mean of respective control samples.

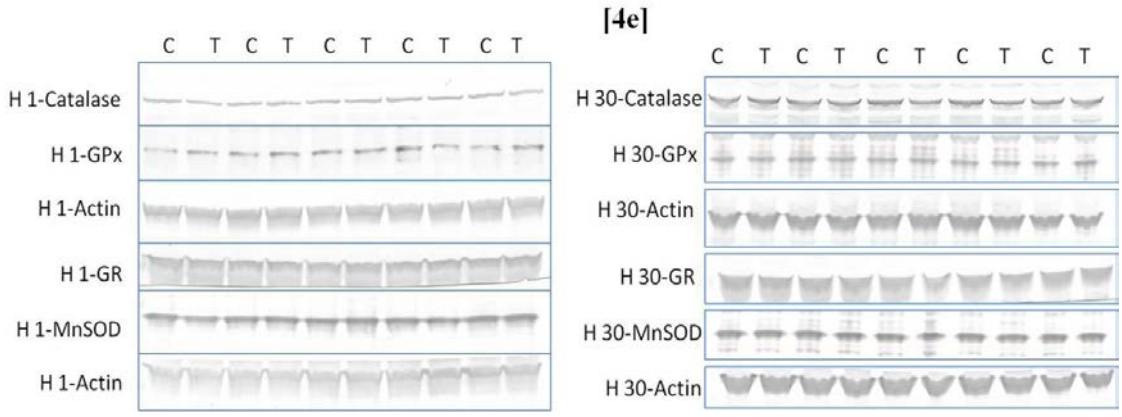


**Figure 9.4e:** Separate Western blots were used to estimate antioxidant protein levels in hippocampus, cortex and cerebellum. However, only representative examples from hippocampus are shown. Protein levels in control [C] n=5, and treated [T] n=5 samples for 1 h (left) and control [C] n=5, treated [T] n=5 for 30 d (Bhabra et al.) ceria nanorod treatment. The intensity of each antioxidant protein band was normalized with intensity of corresponding band of β-actin-loading control. Similar blots were obtained for cortex and cerebellum regions.

*Ceria nanorods reduce protein oxidation at early time point but increases later, similar effect on HSP's*

An inverse correlation was seen in between antioxidant activities and that of PC levels at 1 h and 30 d time points. Concomitant with increased antioxidant activities 1 h after Ceria nanorods treatment, PC levels were significantly decreased in the hippocampus (~ 27%, $^{*}p < 0.05$, Figure 9.5a) and in the cortex (~ 22%, $^{*}p < 0.05$, Figure 9.5a) regions. On the other hand, PC levels were significantly increased after 30 d in the hippocampus (~ 36%, $^{*}p < 0.05$, Figure 9.5a) and in the cortex (~ 27%, $^{\xi}p < 0.01$, Figure 9.5a) concomitant

with significant decrease in the antioxidant activities. 3NT and HNE levels did not show any significant change after 1 h or 30 d.

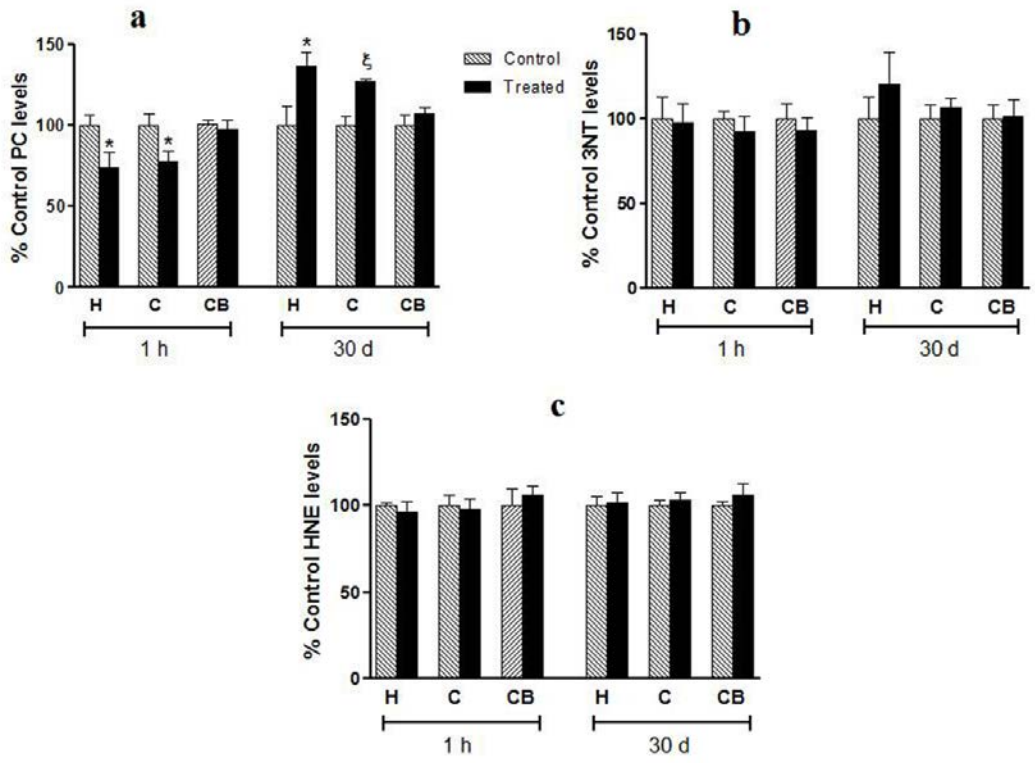


**Figure 9.5:** The oxidative stress marker levels in 3-brain regions 1 h and 30 d after ceria nanorod treatment. a) The histograms represent %control PC levels measured in saline treated controls and ceria treated samples, b) the histograms represent %control 3NT levels measured in saline treated controls and ceria treated samples, c) the histograms represent %control HNE levels measured in saline treated controls and ceria treated samples. All the values are expressed as mean ± SEM, control n = 5, treated n = 5, *p <0.05, $^{\xi}p < 0.01$, and $^{\Theta}p < 0.001$, compared to mean of respective control samples

Furthermore, induction of HSP levels was directly related with changes in PC levels and inversely related with changes in antioxidant enzyme activities. HO-1 levels showed a decreasing trend in all 3-brain regions after 1 h, however, HO-1 was significantly induced after 30 d in the hippocampus (~ 30%, *$p < 0.05$, Figure 9.6a), and in the cortex (~ 23%, *$p < 0.05$, Figure 9.6b). Hsp70 followed a decreasing trend after 1 h and an increasing one after 30 d; however, the changes were not significant in either of the three brain regions.

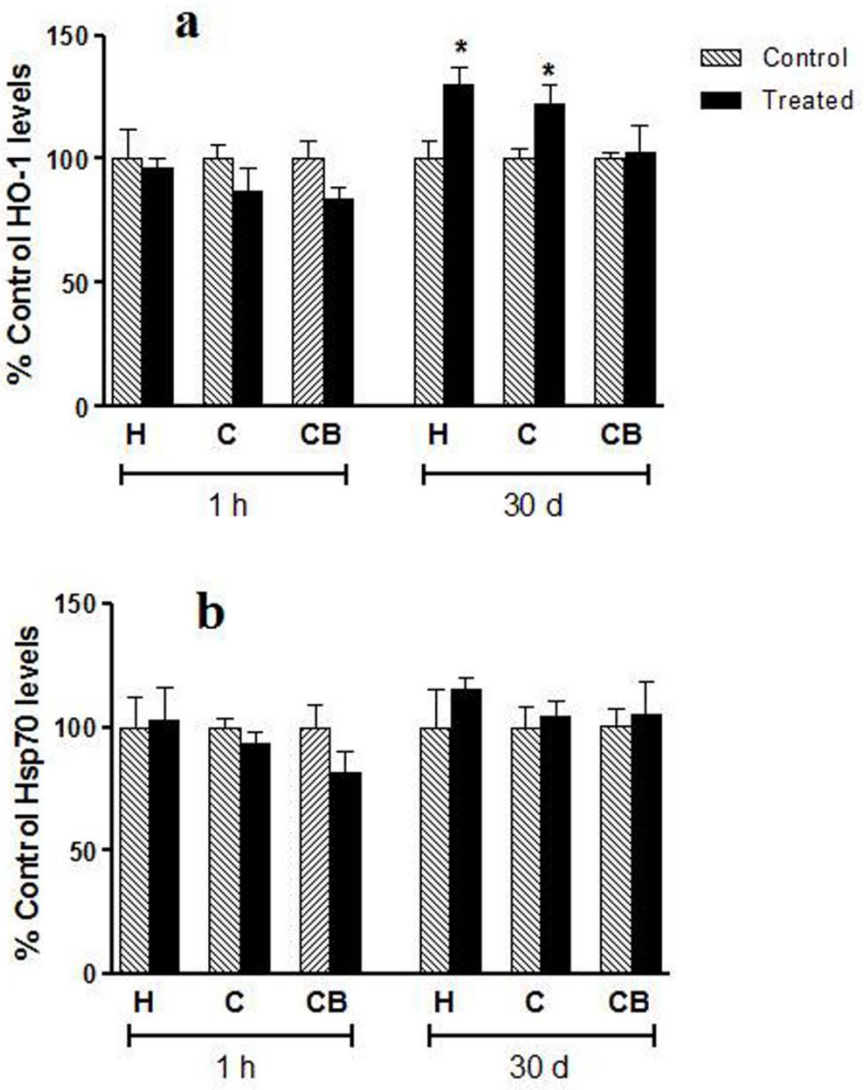


**Figure 9.6a and b:** The heat shock protein levels in 3-brain regions 1 h and 30 d after ceria nanorod treatment. a) The histograms represent %control HO-1 levels measured in saline treated controls and ceria treated samples, b) the histograms represent %control Hsp70 levels measured in saline treated controls and ceria treated samples. All the values are expressed as mean ± SEM, control n = 5, treated n = 5, *p <0.05, $^{\xi}$p < 0.01, and $^{\Theta}$p < 0.001, compared to mean of respective control samples.

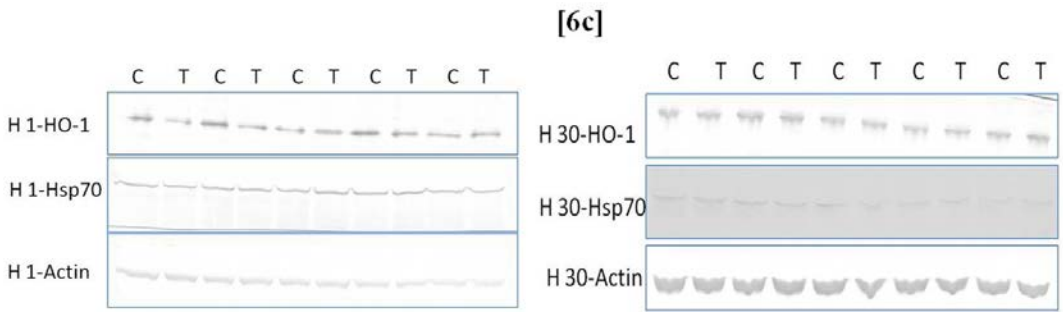


**Figure 9.6c:** Separate Western blots were used to estimate HSPs levels in hippocampus, cortex and cerebellum. However, only representative examples from hippocampus are shown. Protein levels in control [C] n=5, and treated [T] n=5 samples for 1 h (left) and control [C] n=5, treated [T] n=5 for 30 d (Bhabra et al.) ceria nanorod treatment. The intensity of each antioxidant protein band was normalized with intensity of corresponding band of β-actin-loading control. Similar blots were obtained for cortex and cerebellum regions.

### 9.4. Discussion

The toxicity of nanomaterials is governed by various factors including chemical composition, size, morphology, and surface modifications of nanomaterials. The morphology of nanomaterials can be sub-categorized as high aspect ratio nanomaterials and low aspect ratio nanomaterials. The classification of aspect ratio (length to diameter) is a relative terminology. Typically, nanomaterials with length ≤ 1 μm is consider as low aspect ratio material, length >1 μm is considered as high aspect ratio material (Yokel et al. 2011). High aspect ratio material with length > 5μm and diameter ≥ 100 nm is considered highly toxic, regardless of its chemical composition (Buzea et al. 2007; Lewinski et al. 2008). However, studies with long SWCNT's and MWCNT's with

diameter < 100 nm were reported to produce significant pulmonary toxicity compared to short length or spherical nanomaterials (Lam et al. 2004; Warheit et al. 2004; Muller et al. 2005; Bottini et al. 2006; Kostarelos 2008; Kim et al. 2010). The ceria nanorods used in present work were highly crystalline with average diameter 10 nm and length has wide distribution over 50-600 nm range, thus the aspect ratio is 5-60. This aspect ratio is much lower compare to most of the SWCNTs and MWCNTs used in various applications. SWCNTs and MWCNTs have high aspect ratio owing to their long length (>1 – 5 μm).

Compared to CNTs, not much work has been done on toxicological evaluation of metal oxide-based nanotubes or nanowires. Only one such study has been done, which is on pulmonary toxicity of $TiO_2$ nanofilaments to human lung tumor cells (Magrez et al. 2009). Four days after exposure to $TiO_2$ based nanotubes (D-12 nm) and nanowires (D-75 nm), the fragments from both the nanofilaments were found around and inside the nucleus. Both nanotubes and nanowires affected cell proliferation and cell death in dose-dependent manner (Magrez et al. 2009). However, in the current study, although a very small fraction of ceria nanorods was seen in the vascular compartment of brain, brain redox status had profound impact of the ceria treatment.

After earlier exposure (1 h) to ceria nanorods, a significant increase in catalase (3-regions) and SOD (hippocampus and cerebellum) activities and an increasing trend in GPx and GR activities (3-regions) indicated activation of phase II enzymes. A slight decline in GSH: GSSG ratio in 3-regions suggested slight increase in oxidative stress. Induction of phase II enzymes was seen as an antioxidant response induced by small increment of oxidative stress, such as decline in GSH: GSSG ratio (Li et al. 2008; Xia et al. 2008; Xia et al. 2009). Similar augmentation of phase II antioxidant enzymes was

reported after exposure to ceria ENM with aspect ratio one. Catalase levels and activities were increased in hippocampus 1 h after 5 nm ceria exposure (Chapter 5), GPx, GR and catalase activities and levels were increased in hippocampus, and cerebellum concomitant with declined GSH: GSSG ratio; 1 -20 h after 30 nm ceria exposure (Chapter 7), GPx, SOD, catalase, GR and GST activities were increased with decreased GSH levels; 48 and 72 h after hematite NP exposure to human lung cell line (Radu et al. 2010) (also increased MDA and Lipid perx). Concurrent administration of >25 nm ceria ENM (multiple doses before and after) with monocrotaline (MCT, single dose) rescued rat liver from MCT induced ROS injury by restoring GSH levels and GR-GPx activities (Amin et al. 2011).

Unlike hematite NP (24 h, 48 h and 72 h) and hydroxylated fullerene (2-3 h, rat liver) exposure where lipid peroxidation markers MDA and LDH levels were increased (Radu et al. 2010; Nakagawa et al. 2011), PC, 3NT or HNE levels were decreased in hippocampus and cortex 1 h after the treatment in the current study. Additionally absence of any significant change in oxidative stress induced heat shock proteins HO-1 and Hsp70 suggests that there was no oxidative damage to cellular proteins. In a separate study with different metal oxide based ENM, 8 nm ceria ENM exhibited antioxidant behavior and HO-1 levels were not induced in RAW 264.7 and BEAS-2B cells after ceria treatment (Xia et al. 2008).

Unlike initial oxidative stress response after 1h, dramatic changes in the oxidative stress indices 30 d after ceria nanorod exposure were observed. Concurrent decrease in GSH: GSSG ratio (H, C, and CB), GPx (H, C and CB), catalase (H, CB) and SOD (H) activities with increased PC (H, C) and HO-1 levels (H, C) indicated failure of phase II antioxidant

defense response due to increased or persistent oxidative stress. Similar augmentation of oxidative stress is reported by toxicity studies on high aspect ratio materials such as SWCNTs and MWCNTs as well as time-dependent toxicity studies with ceria ENM, aspect ratio-1 (Chapter 5 and 9). In a comparison study, both short-SWCNTs (D~ 1-2 nm, L~ 0.5-2 μm) and long-SWCNTs (D~ 1-2 nm, L~ 20 μm) reduced GSH levels, induced lipid peroxidation marker levels, inhibited catalase, SOD and GPx activity, after 24 and 48 h in PC-12 cells in dose-dependent manner. Although both decreased cell viability and cell proliferation, the long-SWCNTs were more toxic (Wang et al. 2011). MWCNTs exposure to human umbilical vein endothelial cells decreased cell viability in dose- and time-dependant manner (up to 24 h) (Guo et al. 2011). MWCNTs promoted ROS levels just after 2 h exposure, inhibited SOD and GPx activity as well as induced lipid peroxidation (MDA), thus causing cytotoxicity (Guo et al. 2011). Another report on comparative toxicity of MWCNTs (D~ 10-15 nm) with low aspect ratio (L~ 192 nm) and high aspect ratio (L~ 0.5- 1 μm), showed that both MWCNTs inhibited cell growth and cell proliferation of normal human embryonic cell at 24 h, 48 h and 72 h after exposure, as well as increased LDH levels in dose-dependent manner (Kim et al. 2010). Comparison of $TiO_2$ based aspect ratio-1, low and high aspect ratio ENM revealed, aspect ratio-dependant cytotoxicity and induction of inflammatory cytokines at high aspect ratio in alveolar microphages (Hamilton et al. 2009).

As with ceria ENM with aspect ratio-1, changes in oxidative stress indices 30 d after exposure to ceria nanorods are analogous with that observed 30 d after exposure to 5 nm as well 30 nm ceria ENM (Chapter 5 and 9). In a separate study, 24 h after exposure to 15 and 100 nm silver ENM depleted GSH levels, decreased mitochondrial membrane

potential and increased lipid peroxidation levels (LDH) in a dose-dependent manner (Hussain et al. 2005). In a similar fashion, ceria ENM with different sizes and with aspect ratio-1 decreased cell viability in time- and dose-dependent manner (Park et al. 2008). Further ceria and $TiO_2$ ENM with aspect ratio-1 ceria induced ROS under *in vitro* condition, reduced GSH levels, and induced pro-apoptosis marker (Park et al. 2008; Park et al. 2008).

Thus ceria nanorods, a low aspect ratio metal based material, behave as aspect ratio-1 material at the initial exposure period; however at longer exposure it has oxidative stress effects similar to high aspect ratio CNTs. In addition, ceria nanorods have similar oxidative stress impact as that of 5 nm and 30 nm ceria ENM, than do 15 nm ceria ENM. Thus, based on findings from our lab it may propose that aspect ratio of ENM plays a major role in modulation of ENM toxicity compared to its aspect ratio. However, similar experiments should be repeated with a high aspect ratio ceria ENM to solidify this hypothesis.

# CHAPTER 10

# CONCLUSIONS AND FUTURE STUDIES

## 10.1 Conclusions

The work presented in this dissertation examined the ceria-ENM induced oxidative stress effects in hippocampus, cortex and cerebellum of the rat brain. Specifically the influence of size, aspect ratio (shape) and exposure period on ceria ENMs induced oxidative stress was determined *in vivo*. Furthermore, a mechanism of oxidative stress in the brain, induced by systemically injected ceria ENMs was elucidated.

Overall results of oxidative stress analysis of brain revealed a pattern (Figure 10.1) where at early exposure time points (1 h and 20 h) after systemic administration of ceria ENM, showed either no effect (Chapter 5) on oxidative stress end points or showed anti-oxidant effects (Chapter 6-9). At 1 h and 20 h, levels and activities of the phase II antioxidants were induced and markers of protein oxidation and lipid peroxidation were suppressed. However, at later exposure time points (1 d, 7 d, and 30 d), ceria ENM showed pro-oxidant effects (Chapter 5, 7, and 9), except after treatment of 15 nm ceria ENM (Chapter 6). The phase II antioxidant activities were inhibited after 1 d-30 d, although their levels were increased; concomitantly markers of protein oxidation, lipid peroxidation and HSP levels were induced in almost all three brain regions. Interestingly enough, at very late exposure time point (90 d), levels and activities of phase II antioxidant enzymes were restored and there was no sign of protein oxidation or lipid peroxidation was left, as well as HSPs levels were lowered to below control-levels.

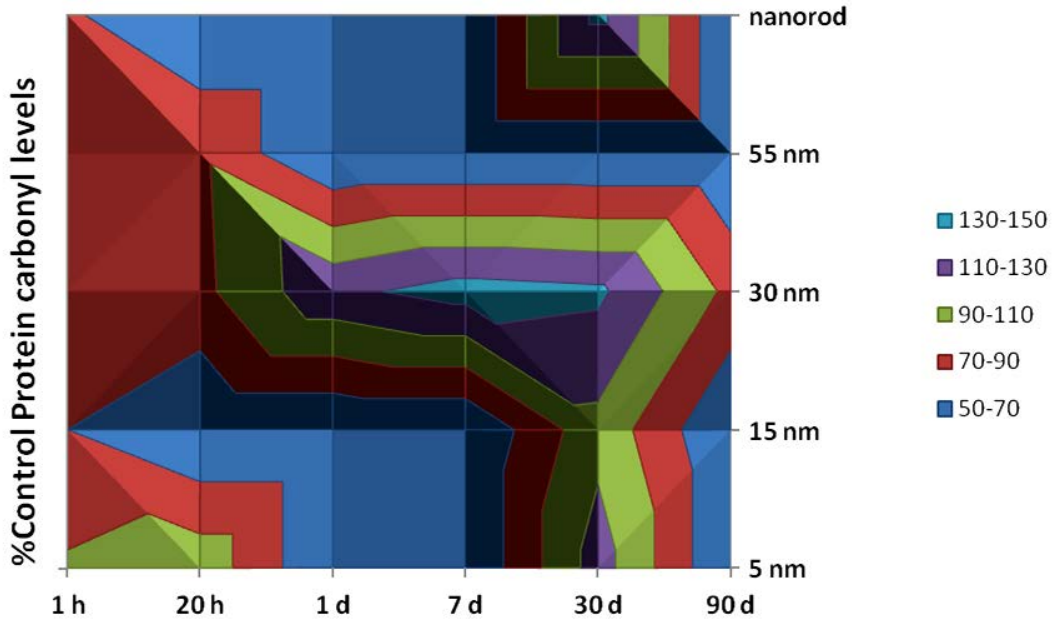


| Mean % Control Protein carbonyl levels | | | | | | |
|---|---|---|---|---|---|---|
| | **1 h** | **20 h** | **1 d** | **7 d** | **30 d** | **90 d** |
| **5 nm** | 93 | 103 | -- | -- | 119 | -- |
| **15 nm** | 70 | -- | -- | -- | 104 | -- |
| **30 nm** | 87 | 85 | 125 | 138 | 134 | 85 |
| **55 nm** | 75 | 87 | -- | -- | -- | -- |
| **nanorod** | 73 | -- | -- | -- | 136 | -- |

**Figure 10.1:** a) Upper left figure represents the demographic depiction of the pattern followed by a representative oxidative stress end point, protein carbonyl levels after treatment of different size ceria ENM at various exposure time points. Red and green color areas represent antioxidant effects, while purple and light blue areas represent pro-oxidant effects. Dark blue color (50-70) covers the points where no data was collected for the specific ceria ENM treatment. b) The table inserted bellow the chart shows the corresponding values expressed as mean % control protein carbonyl levels, taken from corresponding chapters.

Furthermore, the results of oxidative stress end-points measured at earlier time points such as 1 h and/or 20 h and after 30 d, revealed the size-effect of ceria ENM treatment. As shown (as a representative example) in Figure 10.1, 5 nm ceria ENM did not have any significant impact on oxidative stress at 1 h and 20 h (Chapter 5), as opposed to 15 nm, 30 nm, and 55 nm which induced significant tier-1 protective effects in the brain (Chapters 6, 7, and 9 ). After 30 days, 15 nm ceria did not show any pro-oxidant effects suggesting success of tier-1 effects (Chapter 6). Whereas, 5 nm, and 30 nm lead to failure of tier-1 defense and induced downstream pro-oxidant effects in the brain (Chapters 5, 7). A comparison of ultrafine–and fine-$TiO_2$ particles revealed increased cytotoxic effects upon untrafine-$TiO_2$ treatment (Kang et al. 2009) as well as silica ENM showed size-dependent cytotoxicity (Thomassen et al. 2009). On contrary, literature studies have also reported lack of any size-effect on ceria ENM induced toxicity and nickel-ferrite ENM induced toxicity (in absence of oleic acid coating) (Yin et al. 2005; Park et al. 2008; Eom et al. 2009). As for the shape-effect or more precisely the aspect ratio-effect, it is more logical to compare nanorod ceria ENM with 5 nm and 15 nm ceria ENM (aspect ratio-1) as diameter of nanorod was ~10 nm, although nanorod were of varied length (50 nm- 600 nm). The oxidative stress results of 5 nm, 15 nm and nanorod ceria ENM treatments, followed a trend which was very similar at the initial (1 h) time point. All three ceria ENMs induced antioxidant (Tier-1) effects in the brain (Chapter 5, 6, 9). On the other hand, both nanorod and 5 nm ceria treatment lead to failure of tier-1 defense response after 30 d (Chapter 9 and 5 resp.), however, ceria nanorod induced pro-oxidant effects at much smaller dose (20-50 mg/kg) compare to 5 nm or 30 nm ceria ENM. Additionally, the oxidative stress effects induced by nanorod were also in complete agreement with the

findings of 30 nm (1 h and 30 d) and 55 nm (1 h) ceria ENM treatments (Chapter 7 and 8).

In Chapter 7, we examined the dose-effect of 55 nm ceria ENM induced oxidative stress at 20 h. The larger dose 100 mg/kg of 55 nm ceria ENM induced more significant tier-1 antioxidant effects after 20 h compared to the half of dose (50 mg/kg). Similarly, 30 nm ceria and 21 nm $TiO_2$ ENM induced antioxidant tier-1 and apoptotic tier-3 effects in dose-dependent manner in BEAS-2B (Park et al. 2008; Park et al. 2008). In addition to the dose and aspect ratio-effects, we had selected three different brain regions in order to deduce any region-effects of ceria treatment. However, no such differential effects were observed, although overall the hippocampus showed oxidative stress for most of the time points and cerebellum showed for the least, there were no distinct preferences observed.

The major findings of this dissertation work, includes elucidation of the mechanism of oxidative stress based on an oxidative stress hierarchy model of nanomaterial toxicity. Additionally, as we could extend and modify the existing model for in vivo toxicity of ceria ENM (Figure 10.2). The systemic injection of ceria ENM induced phase II antioxidant – tier-1 response in the brain without crossing or disrupting BBB and decreased GSH: GSSG ratio at 1 h and 20 h- exposure time points. In all the cases, except 15 nm ceria ENM, with increasing exposure period (≥ 1 d), the loss of GSH: GSSG ratio was not recovered and as a consequence of escalading oxidative stress activated downstream signaling pathways. These signaling pathways induced tier-2 and tier-3 oxidative stress response in the brain. However, after 90 d, GSH: GSSG ratio improved favorably with phase II antioxidant levels and activities. Thus, the brain redox imbalance was reversed to normal by 90 d. At present we are not sure about what happened in the

last 30 d period where redox balance was restored, but it may be that HSPs or autophagy response together or separately might have cleared damaged macromolecules and thus helped to restored cellular redox status.

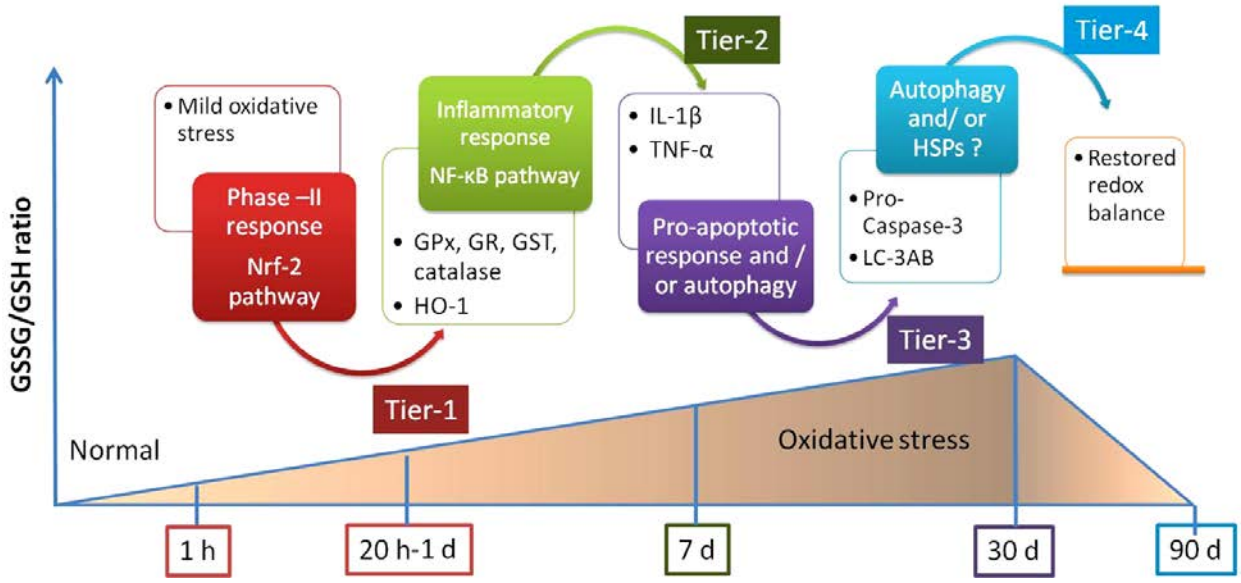


**Figure 10.2:** The modified version of oxidative stress hierarchy model of nanotoxicity. Addition of Tier-4 response is a result of our finding from 30 nm ceria treatment after 90 d exposure period.

This work was the first attempt where the literature-proposed oxidative stress model was tested on multicellular organism. As well as this was the first attempt where the "Tier" responses explained in the model were tested and connected with ENM treatment exposure period. Thus, this work also helps us to understand and clear the fog of discrepancy around oxidative stress effects of ceria ENM treatment. Based on our experience it can be hypothesized that, the antioxidant effects of ceria ENM (in absence

of pre-existing or external source ROS or oxidative stress) reported in literature are result of Tier-1 response induced by initial oxidative stress stimuli generated by ceria ENM. Depending upon this initial oxidative stress insult and "strength" of Tier-1 response, the secondary oxidative stress represented as Tier-2 and Tier-3 may or may not be seen.

### 10.2. Future studies

Based on the results in this dissertation, the following experiments may warrant future investigation:

1. After examining the oxidative stress effects of ceria ENM at considerably high dose, it will be useful to study the pharmacokinetics and corresponding oxidative stress effects at lower dosage curve (10 and 100 times) and at different exposure period.
2. The oxidative stress effects of ceria treatment observed in this dissertation work were induced by ceria ENM in brain but without crossing or disrupting BBB. Therefore, it is important to investigate the mechanism of peripheral effects of ceria ENM and measurement of circulatory cytokine levels in blood or plasma might shade some light.
3. After deducting the size and time-effect of ceria ENM treatment, current work can be extended to investigate role more surface properties like surface charge, surface coating, hydrophobicity etc.
4. Based on the finding of results of nanorod ceria ENM treatment, where ceria nanorods behaved as aspect ratio-1 ENM at initial exposure period (1 h), and similar to high aspect ratio ENM such as CNT's at longer exposure (30 d) time

points. Therefore, it will be interesting to investigate the role of aspect ratio in detail with high aspect ratio ceria ENM.

# APPENDIX A

## OXIDATIVE STRESS EFFECTS INDUCED BY SILVER NANOPARTICLES IN EARTHWORMS (*Eisenia fetida*) AND PROTEOMICS ANALYSIS OF DIFFERENTIALLY EXPRESSED PROTEINS

With the rapid growth of nanotechnology, there is a constant demand for research and production of new engineered nanomaterials (ENM). However, once used in consumer, industrial and medical goods, these ENM will be released into the environment intentionally or accidentally. After released into ecosystem ENMs can enter into wastewater stream and eventually end up in the terrestrial ecosystem-an ultimate sink. Silver metal is known for its antibacterial properties and by virtue it Ag-ENMs are used in medical devices, food-storage containers, soap and sanitizers, wound dressings, and fabrics (Luoma 2008). Thus increasing use of Ag-ENM will contribute to the anthropogenic accumulation of ENM in ecosystem (Blaser et al. 2008). Although some studies are available on aquatic toxicity as reviewed by (Shoults-Wilsona et al. 2010; Shoults-Wilson et al. 2011) however, very little is known about their environmental fate, potential effects especially on terrestrial environment (Klaine et al. 2008; Unrine et al. 2008). The previous studies conducted primarily in cell culture, have reported that smaller Ag-ENMs have greater toxicological effects than larger Ag-ENMs; summarized in (Shoults-Wilson et al. 2011). However, there is very little known about Ag-ENM size-effect toxicity towards fully developed multicellular organisms in terrestrial environmentally realistic exposure scenarios (Shoults-Wilson et al. 2011).

The objective of present study was to compare 1) oxidative stress effects of Ag-ENMs with two different sizes and with toxicity of Ag ions exposed to earthworm *Eisenia fetida* at different exposure period, 2) identify the differential expressed proteins in earthworms

after exposure to Ag-ENM and Ag ions, through artificial soil media. This is a very first proteomics (described in Chapter 3) study on earthworm *Eisenia fetida* conducted ever.

**a] PC levels**

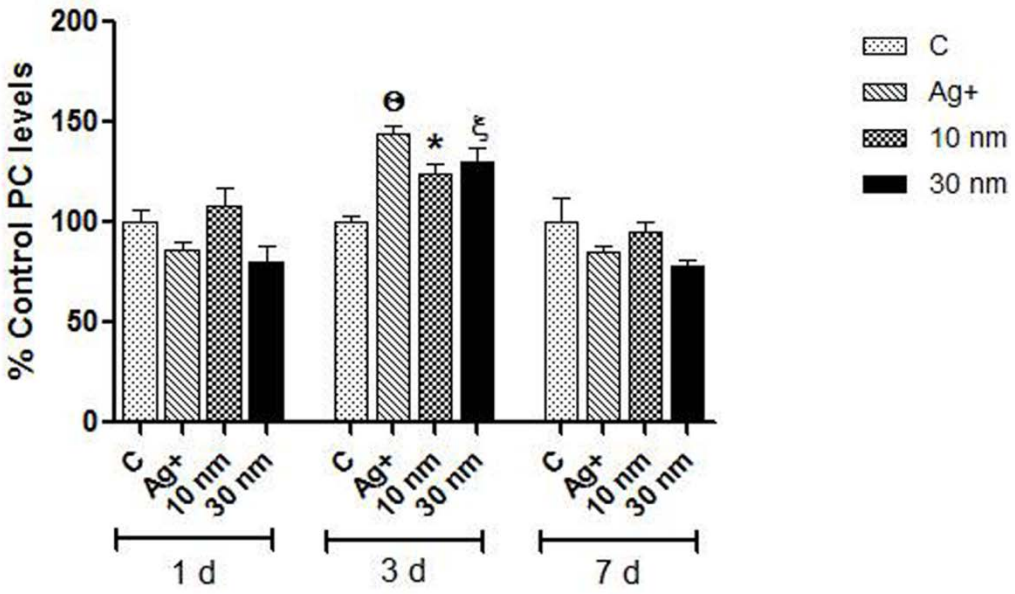


**Figure A.1a:** The oxidative stress marker levels measured in whole earthworm 1 d, 3 d and 7 d after exposure to $AgNO_3$, 10 nm Ag-ENM and 30-50 nm Ag-ENM. a) The histograms represent % control PC levels measured in control and treated samples. All the values are expressed as mean ± SEM, control n = 4, treated n = 4 for each group and each exposure period, *$p < 0.05$, $^{\xi}p < 0.01$, and $^{\Theta}p < 0.001$, compared to mean of respective control samples.

**b] 3NT levels**

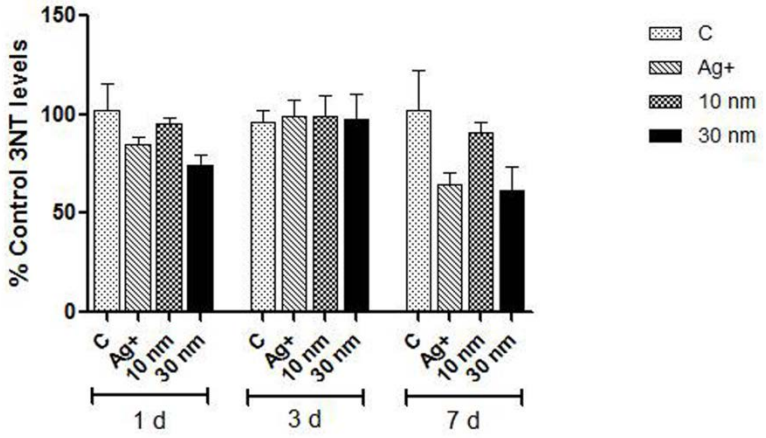


**c] HNE levels**

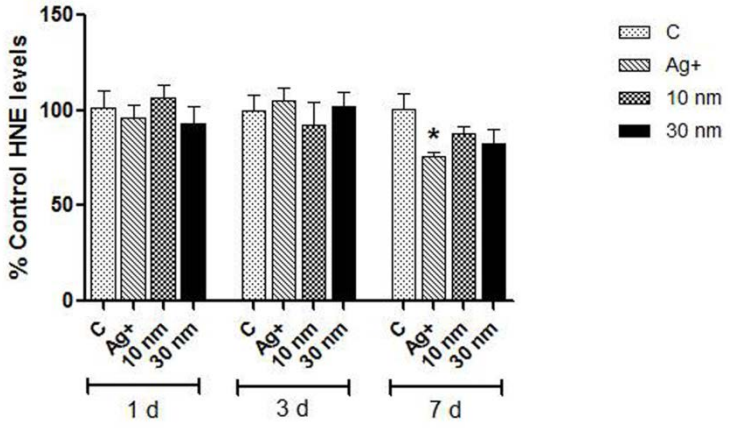


**Figure A.1b and c:** The oxidative stress marker levels measured in whole earthworm 1 d, 3 d and 7 d after exposure to $AgNO_3$, 10 nm Ag-ENM and 30-50 nm Ag-ENM. b) The histograms represent % control 3NT levels measured in control and treated samples, c) the histograms represent % control HNE levels measured in control and treated samples. All the values are expressed as mean ± SEM, control n = 4, treated n = 4 for each group and each exposure period, *$p < 0.05$, $^{\xi}p < 0.01$, and $^{\Theta}p < 0.001$, compared to mean of respective control samples.

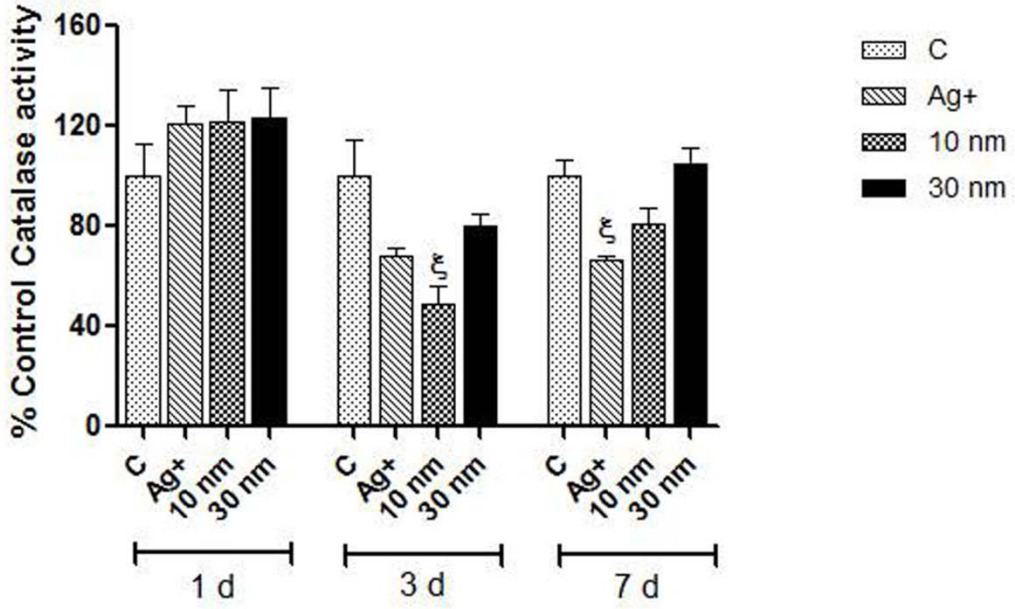


**Figure A.2:** The antioxidant catalase activity measured in whole earthworm 1 d, 3 d and 7 d after exposure to $AgNO_3$, 10 nm Ag-ENM and 30-50 nm Ag-ENM. a) The histograms represent % control catalase activity measured in control and treated samples. All the values are expressed as mean ± SEM, control n = 4, treated n = 4 for each group and each exposure period, *$p < 0.05$, $^{\xi}p < 0.01$, and $^{\Theta}p < 0.001$, compared to mean of respective control samples.

**Table A.1:** Description of proteins identified by MS/MS in four treatment groups, continue on next page……..

| Protein | Description | SwissProt No. | MWt kDa | pI | Peptide hits |
|---|---|---|---|---|---|
| | | | | | |
| P54812 | Transitional endoplasmic reticulum ATPase homolog 2 | C41C4.8 | 89.6 | 5.39 | 3(5) |
| Q9XXK1 | ATP synthase subunit alpha, mitochondrial | H28O16.1c | 54.1 | 9.06 | 2(3) |
| P91427 | pgk-1/ phosphoglycerate kinase | T03F1.3 | 44.1 | 7.02 | 3(4) |
| P91427 | pgk-1/ phosphoglycerate kinase | T03F1.3 | 44.1 | 7.02 | 3(4) |
| P46563 | Fructose-bisphosphate aldolase 2 | F01F1.12a | 38.8 | 7.88 | 3(11) |
| Hsp-70A | Heat shock 70 kDa protein A | F26D10.3 | 69.7 | 5.64 | 2(4) |
| Actin-5 | embryo development ending in birth or egg hatching | T25C8.2 | 41.8 | 5.68 | 5 (14) |
| Actin-4c | ATP-binding | M03F4.2c | 40.4 | 5.83 | 7 (15) |
| Actin-5 | embryo development ending in birth or egg hatching | T25C8.2 | 41.8 | 5.68 | 3 (9) |
| Actin-4b | ATP-binding | M03F4.2b | 37.3 | 5.55 | 4 (7) |
| Actin-2 | cytokinesis after mitosis, embryo development | T04C12.5 | 41.8 | 5.48 | 13 (76) |
| Actin-5 | embryo development ending in birth or egg hatching | T25C8.2 | 41.8 | 5.68 | 10 (64) |
| Actin-4c | ATP-binding | M03F4.2c | 40.4 | 5.83 | 6 (14) |
| Actin-5 | embryo development ending in birth or egg hatching | T25C8.2 | 41.8 | 5.68 | 5 (11) |
| Hsp-70A | Heat shock 70 kDa protein A | F26D10.3 | 69.7 | 5.64 | 2 (5) |
| Actin-4b | ATP-binding | M03F4.2b | 37.3 | 5.55 | 3 (4) |
| Actin-4c | ATP-binding | M03F4.2c | 40.4 | 5.83 | 3 (4) |
| Actin-4c | ATP-binding | M03F4.2c | 40.4 | 5.83 | 3 (5) |
| Hsp-70A | Heat shock 70 kDa protein A | F26D10.3 | 69.7 | 5.64 | 2 (7) |
| Actin-4c | ATP-binding | M03F4.2c | 40.4 | 5.83 | 5 (9) |
| P91427 | pgk-1/ phosphoglycerate kinase | T03F1.3 | 44.1 | 7.02 | 3 (9) |
| Hsp-70A | Heat shock 70 kDa protein A | F26D10.3 | 69.7 | 5.64 | 2 (4) |
| Hsp-70A | Heat shock 70 kDa protein A | F26D10.3 | 69.7 | 5.64 | 2 (5) |

**Table A.1 *continued*:** Description of proteins identified by MS/MS in four treatment groups.

| Protein | Description | SwissProt No. | MWt kDa | pI | Peptide hits |
|---|---|---|---|---|---|
| Actin-4c | ATP-binding | M03F4.2c | 40.4 | 5.83 | 3 (3) |
| Hsp-70A | Heat shock 70 kDa protein A | F26D10.3 | 69.7 | 5.64 | 2 (2) |
| GAPDH-4 | Glyceraldehyde-3-phosphate dehydrogenase 4 | F33H1.2 | 36.4 | 7.88 | 2 (6) |
| GAPDH-4 | Glyceraldehyde-3-phosphate dehydrogenase 4 | F33H1.2 | 36.4 | 7.88 | 2 (5) |
| Aldose-isoform b | Aldolase (Fructose bisphosphate aldolase) protein 2 | F01F1.12b | 28.0 | 7.05 | 2 (4) |
| mec-7 beta tubulin | | ZK154.3 | 49.2 | 5.01 | 2 (3) |
| Actin-4c | ATP-binding | M03F4.2c | 40.4 | 5.83 | 7 (29) |
| Actin-5 | embryo development ending in birth or egg hatching | T25C8.2 | 41.8 | 5.68 | 5 (17) |
| Actin-4b | ATP-binding | M03F4.2b | 37.3 | 5.55 | 3 (4) |
| Actin-4b | ATP-binding | M03F4.2b | 37.3 | 5.55 | 5 (21) |
| Actin-5 | embryo development ending in birth or egg hatching | T25C8.2 | 41.8 | 5.68 | 4 (21) |
| Actin-5 | embryo development ending in birth or egg hatching | T25C8.2 | 41.8 | 5.68 | 2 (6) |
| Actin-4b | ATP-binding | M03F4.2b | 37.3 | 5.55 | 2 (3) |
| FTT-2 | 14-3-3-like protein 2 | F52D10.3a | 28.0 | 4.91 | 2 (3) |
| Actin-4b | ATP-binding | M03F4.2b | 37.3 | 5.55 | 4 (6) |
| ATP-2 | ATP synthase subunit beta, mitochondrial | C34E10.6 | 57.5 | 5.77 | 2 (3) |

**a]**

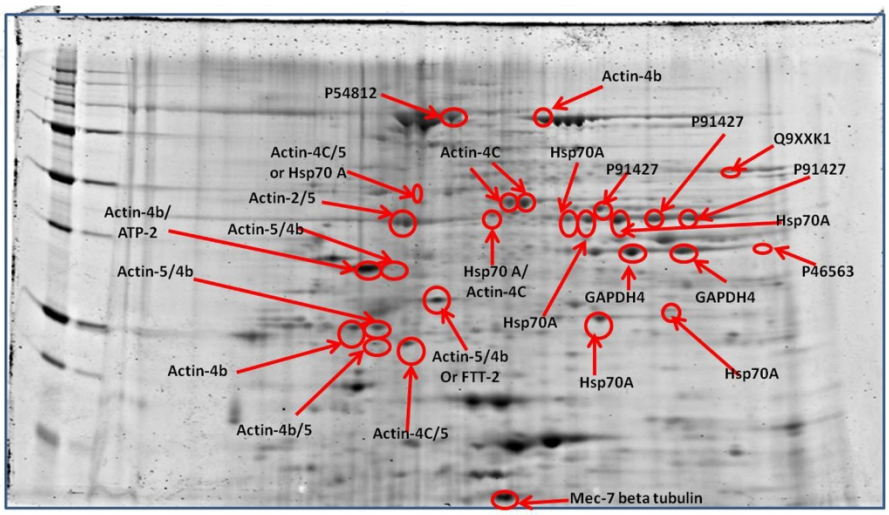


**b]**

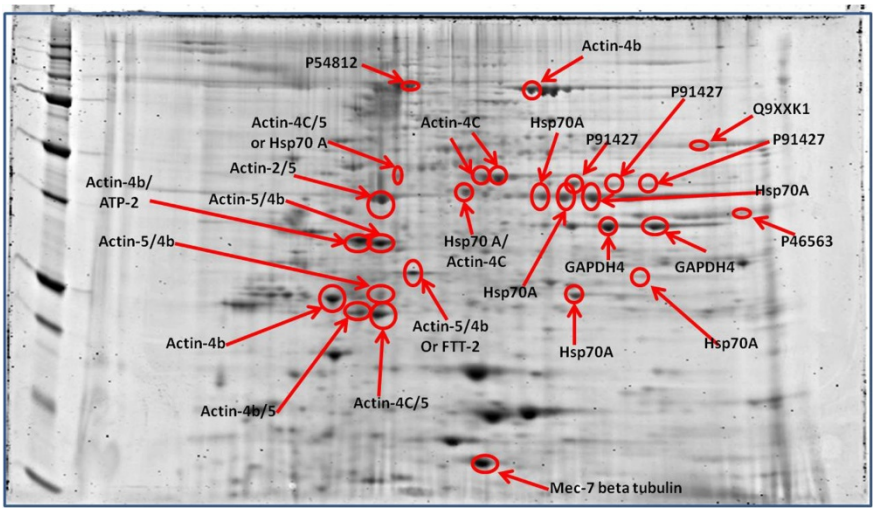


**Figure A.3a and b:** 2-D gel map of proteins identified from control and $AgNO_3$ treated groups using proteomics among the four groups at 3 d exposure period. a) Representative gel from control group of earthworm samples, and d) Representative gel from $AgNO_3$ treated group of earthworm samples. Protein spots were identified by MS/MS and labeled with their corresponding identification.

**c]**

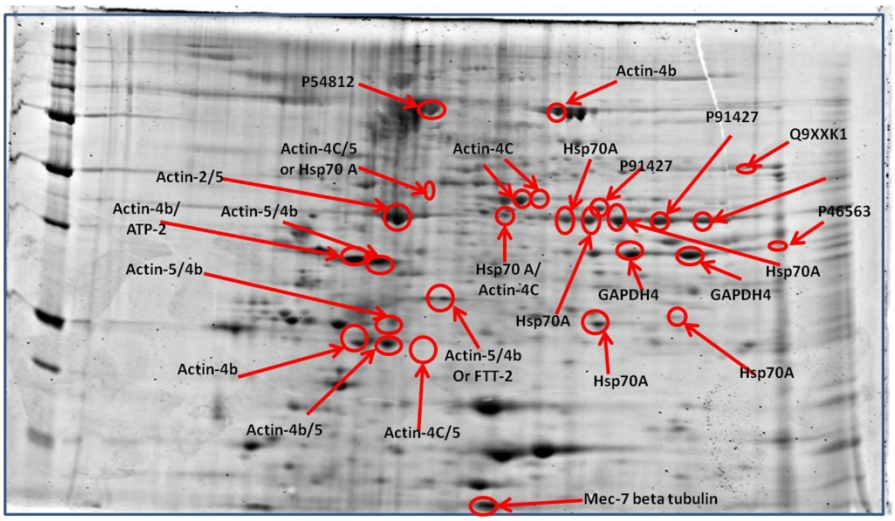


**d]**

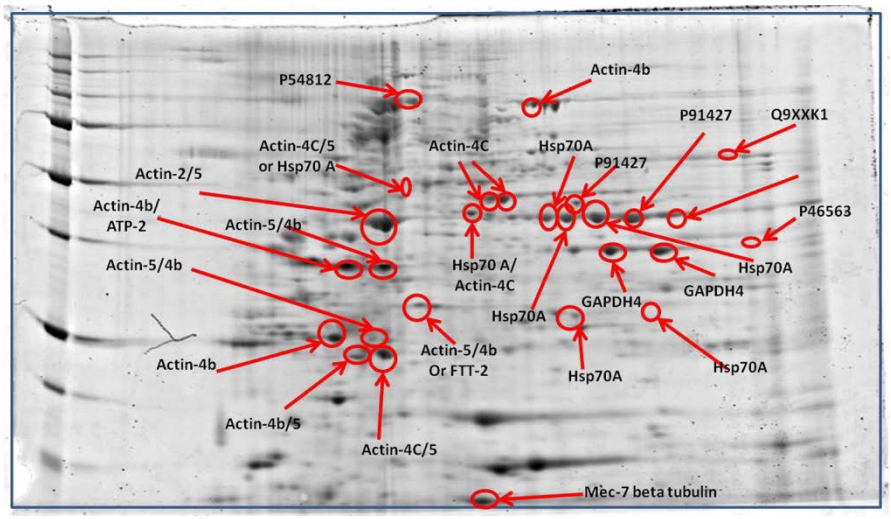


**Figure A.3c and d:** 2-D gel map of proteins identified using proteomics among 10 nm AgNP and 30-50 nm AgNP treated groups at 3 d exposure period, c) Representative gel from 10 nm Ag-ENM treated groups of earthworm samples, and d) Representative gel from 30-50 nm Ag-ENM treated group of earthworm samples. Protein spots were identified by MS/MS and labeled with their corresponding identification.

APPENDIX B

OXIDATIVE MODIFICATION OF LIPOIC ACID IN ALZHEIMER DISEASE BRAIN

Lipoic acid is an important cofactor for multi-enzyme complexes such as α-ketoglutarate dehyede (KGDH), pyruvate dehydrogenase (PDH), branched oxo acid or α-ketoacid dehydrogenase complex, and glycine decarboxylase complex or glycine cleavage system (Kagan et al. 1992). Lipoic acid is also unique endogenous antioxidant, which can scavenge free radicals in aqueous as well as in lipid or membrane phase (Kagan et al. 1992). Lipoic acid is endogenously present in its native form in the body and remains inactive unless reduced to dihydrolipoic acid (DHLA). Lipoamide dehydrogenase is one of the main enzyme that catalyzes this reaction in the presence of a reducing equivalent NADPH (Biewenga et al. 1996) Figure B.1. The antioxidant and functional activity of lipoic acid as a cofactor is attributed to its reduced form DHLA (Kagan et al. 1992). The sulfhydryl groups on DHLA act similar to –SH group from glutathione or cysteine and help in reduction of free radicals by providing –H or an electron.

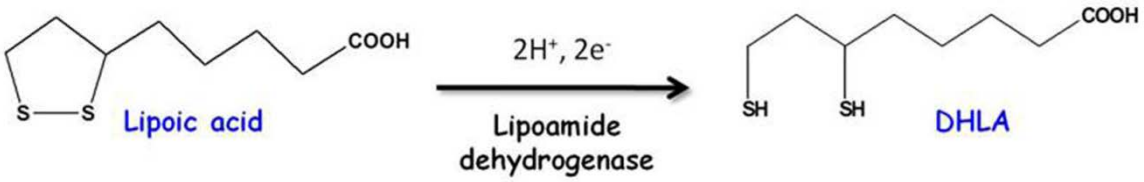


**Figure B.1**: Reduction of Lipoic acid (LA) to dihydrolipoic acid (DHLA) by enzymatic action of lipoamide dehydrogenase in presence of reducing equivalent.

Apart from acting as an antioxidant itself, lipoic acid can also reinforce other water-or lipid-soluble antioxidants such as ascorbate and vitamin E by scavenging their radicals in DHLA form (Kagan et al. 1992). Treatment with lipoic acid can reduce lipid peroxide marker-HNE and apoptotic markers in patients with Alzheimer disease. This was noted in

a study that investigated fibroblast in cell culture. In the same study, co-treatment of cells with N-acetyl cysteine showed much better protection from oxidative stress than lipoic acid or N-acetyl cysteine alone (Moreira et al. 2007). A study from our lab has shown that pretreatment of cortical neurons with acetyl L-carnitine and lipoic acid, plays a protective role against HNE-mediated oxidative stress and neurotoxicity by inducing GSH levels and reducing protein and lipid oxidation (Hafiz et al. 2007). When rat mitochondria were treated with HNE, selective inhibition of KGDH and PDH was observed. The same study further reported that loss of enzyme activity of KGDH and PDH in mitochondria in presence of a reducing equivalent such as NADPH was closely related to the HNE modification of lipoic acid. These findings were also confirmed by results from the experiments with purified enzymes (Humphries et al. 1998); Figure B.2. Similarly inactivation of KGDH and PDH was observed in human HepG2 cells after HNE treatment. However, successive treatment with lipoic acid and other thiol supplements protected these complexes from HNE modification. Further the same study reported that inhibition of PDH was observed when sulfahydryl groups on lipoic acid were in reduced form (Korotchkina et al. 2001). Inhibition was observed at its subunit E2E3-BP and the damage was more in presence of subunit E3-dihydrolipoamide dehydrogenase and NADPH.

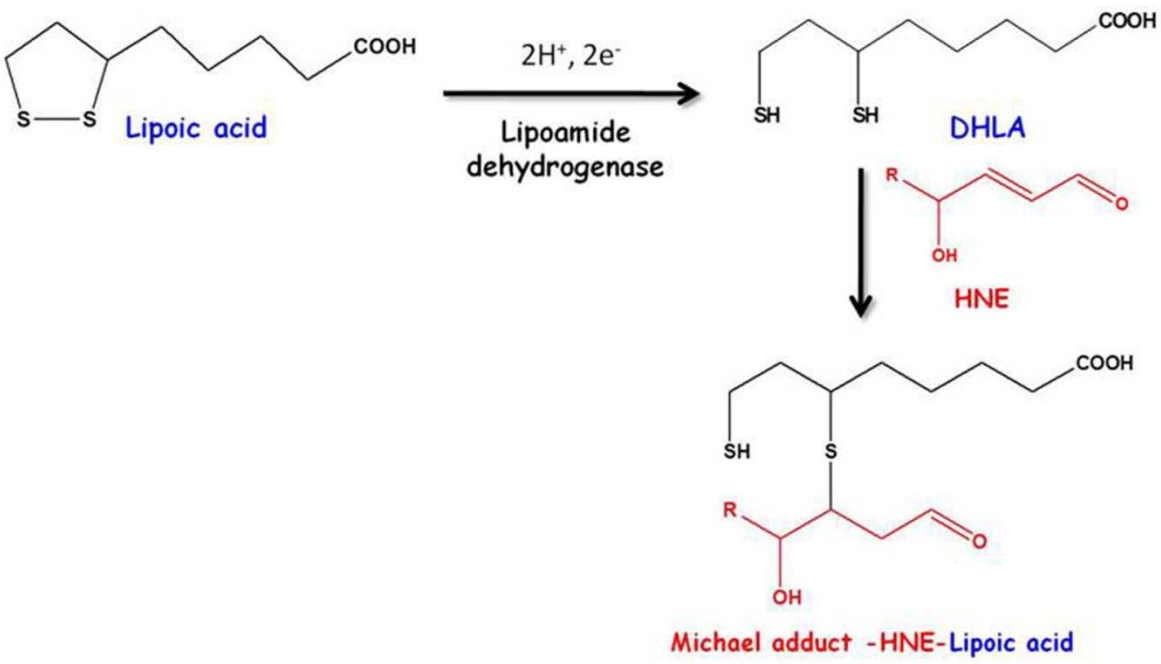


**Figure B.2**: HNE can form Michael adduct with only reduced form of lipoic acid i.e. DHLA.

In this dissertation research, levels of HNE-bound lipoic acid (HNE-LA) were detected using specialized antibody against HNE-LA modification (courtesy to Dr. Szweda's Lab) in IPL region of Alzheimer disease (AD). Brain samples from AD-IPL groups were compared with group of age matched controls for the purpose of this study. We observed significant decrease in HNE-LA levels in AD samples (Figure B.3.).

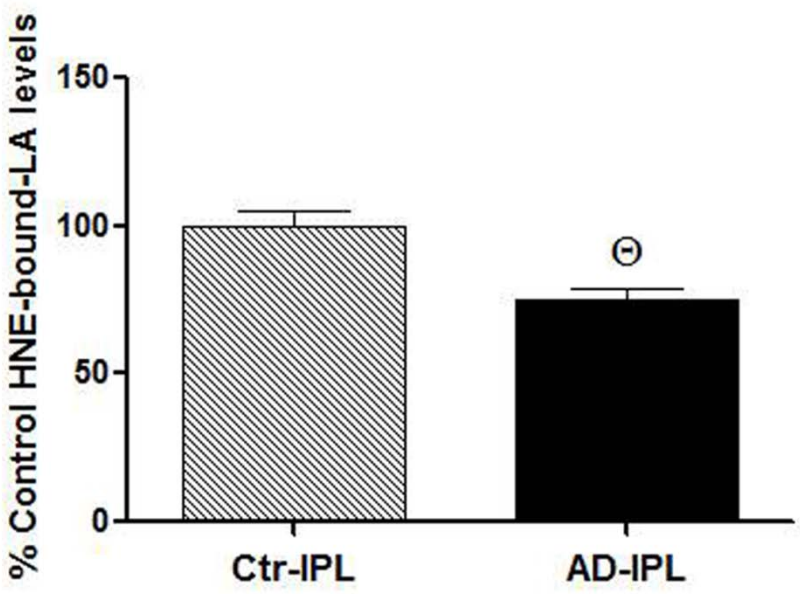


**Figure B.3:** HNE-LA levels were measured in IPL brain region of control (n=10) and AD (n=12) samples by dot blot technique. All the values are expressed as mean ± SEM, *$p < 0.05$, $^{\xi}p < 0.01$, and $^{\Theta}p < 0.001$, compared to mean of respective control samples.

Alzheimers disease is characterized by increased free radical production and HNE modification to proteins (Beal 1995; Markesbery 1997; Markesbery et al. 1998). However we found lower levels of HNE bound lipoic acid in AD-IPL samples compared to age-matched controls. HNE can only react with a reduced form of lipoic acid DHLA (Humphries et al. 1998). As the enzyme responsible for reduction LA to DHLA is lipoamide dehydrogenase, we measured activities and levels of lipoamide dehydrogenase (LADH) in AD and control brain-IPL region. Both levels and activities of LADH were significantly reduced in AD-IPL as compared to age-matched controls (Figure B.4 a-b). Similar reduction in LADH levels and activity was observed in the temporal cortex, parietal cortex and in hippocampus of AD patients (Mastrogiacomo et al. 1996). Similar to LA, LADH is also shared by four multi-enzyme complexes α-keto- glutaraldehyde

dehydrogenase (KGDH), pyruvate dehydrogenase (PDH), the branched oxo acid or α-ketoacid dehydrogenase complex, and the glycine decarboxylase complex or glycine cleavage system (Hunter et al. 1986; Lindsay 1989; Mastrogiacomo et al. 1996) . Inhibition of the levels and activity of LADH may reflect on the loss of enzyme activity of the multi-enzyme complexes in AD.

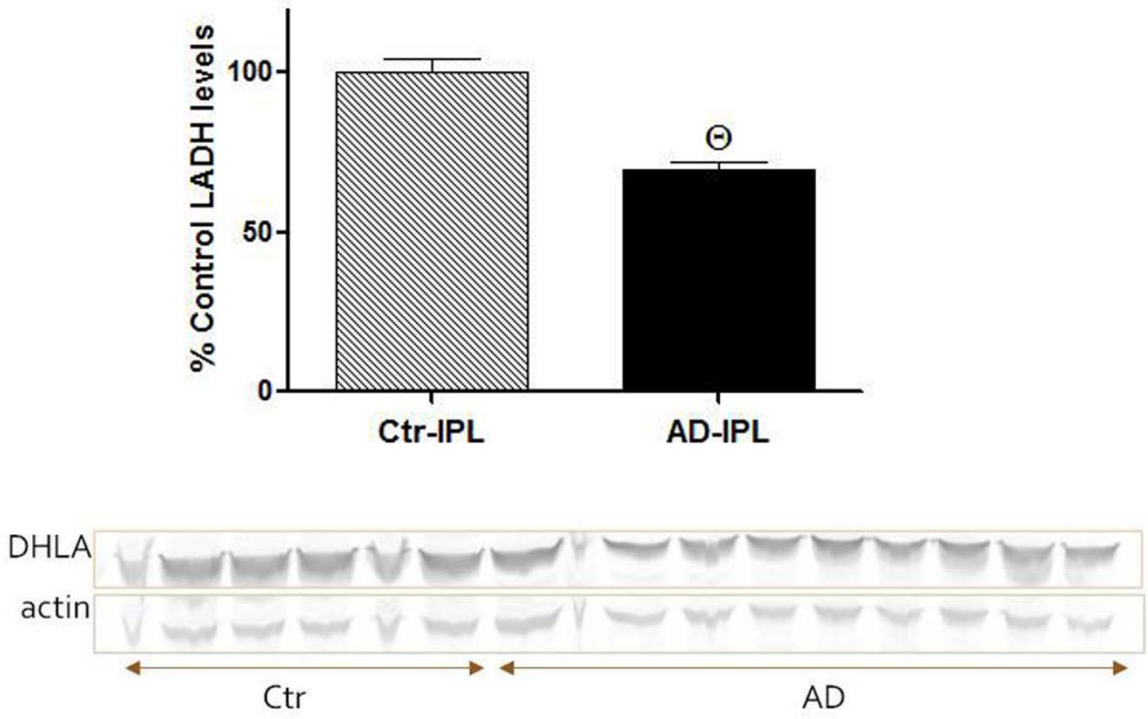


**Figure B.4a]** The histograms represent %control Lipoamide dehydrogenase (LADH) levels measured in IPL region from AD and age-matched control samples. The histograms are accompanying Western blot band of LADH and actin, which was used as loading control and intensity of each band was normalized to loading control. All the values are expressed as mean ± SEM for control (n=6) and AD (n=10), statistical significance was considered at *$p < 0.05$, $^{\xi}p < 0.01$, and $^{\Theta}p < 0.001$, compared to mean of respective control samples.

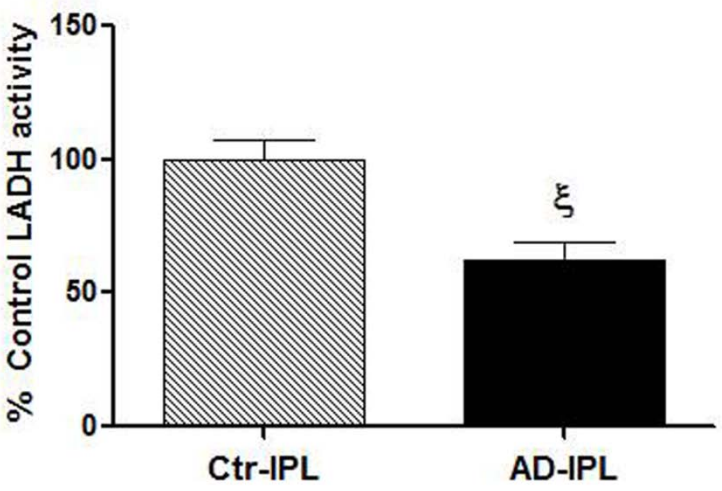


**Figure B.4b]** The lipoamide dehydrogenase (LADH) activity in IPL-brain regions. The histograms represent % control LADH activity measured in control and AD samples. All the values are expressed as mean ± SEM, control n = 10, treated n = 12, *p <0.05, $^{\xi}$p < 0.01, and $^{\Theta}$p < 0.001, compared to mean of respective control samples.

APPENDIX C
DATA TO SUPPLEMENT FIGURES

Figure 5.5

| **Hippocampus-PC** | | | **Cortex-PC** | | |
|---|---|---|---|---|---|
| **%Control** | **Avg** | **Stdev** | **%Control** | **Avg** | **Stdev** |
| 99 | | | 123 | | |
| 111 | | | 134 | | |
| 111 | | | 125 | | |
| 107 | | | 56 | | |
| 71 | 100 | 17 | 63 | 100 | 37 |
| | | 8 | | | 17 |
| 125 | | | 132 | | |
| 122 | | | 133 | | |
| 126 | | | 91 | | |
| 110 | | | 113 | | |
| 111 | 119 | 8 | 106 | 115 | 18 |
| | | 4 | | | 8 |
| | 0.050874 | | | 0.439208 | |

| **Cerebellum-PC** | | |
|---|---|---|
| **%Control** | **Avg** | **Stdev** |
| 89 | | |
| 97 | | |
| 101 | | |
| 111 | | |
| 101 | 100 | 8 |
| | | 3 |
| 102 | | |
| 104 | | |
| 116 | | |
| 116 | | |
| 120 | 112 | 8 |
| | | 4 |
| | 0.046587 | |

| H-3NT | | | C-3NT | | | CB-3NT | | |
|---|---|---|---|---|---|---|---|---|
| %Control | Avg | Stdev | %Control | Avg | Stdev | %Control | Avg | Stdev |
| 96.8966 | | | 104.9575 | | | 90.13022 | | |
| 99.8012 | | | 106.2048 | | | 105.2564 | | |
| 102.235 | | | 100.4067 | | | 101.115 | | |
| 101.436 | | | 80.73482 | | | 104.2953 | | |
| 99.6300 | 100 | 2.053695 | 107.6961 | 100 | 11.10878 | 99.20306 | 100 | 6.028484 |
| | | 0.91844 | | | 4.967997 | | | 2.69602 |
| 103.6729 | | | 121.6649 | | | 104.0808 | | |
| 102.0335 | | | 115.0669 | | | 100.3457 | | |
| 96.67728 | | | 108.2204 | | | 99.04425 | | |
| 104.9948 | | | 124.887 | | | 105.7906 | | |
| 108.7716 | 103.23 | 4.426903 | 130.3733 | 120.0425 | 8.621867 | 111.7635 | 104.205 | 5.029635 |
| | | 1.979771 | | | 3.855816 | | | 2.249321 |
| | | | | TTEST | 0.012861 | | | |

| H-HNE | | | C-HNE | | | CB-HNE | | |
|---|---|---|---|---|---|---|---|---|
| %Control | Avg | Stdev | %Control | Avg | Stdev | %Control | Avg | Stdev |
| 100.7464 | | | 123.1721 | | | 89.28452 | | |
| 100.5379 | | | 104.0495 | | | 99.65474 | | |
| 104.4698 | | | 84.92688 | | | 111.2736 | | |
| 93.73723 | | | 98.4252 | | | 99.131 | | |
| 100.5087 | 100 | 3.882874 | 89.42632 | 100 | 14.95682 | 100.6562 | 100 | 7.797761 |
| | | 1.736474 | | | 6.688895 | | | 3.487265 |
| 105.3371 | | | 125.9843 | | | 119.8924 | | |
| 106.1794 | | | 119.2351 | | | 112.8197 | | |
| 103.9445 | | | 109.1114 | | | 102.8475 | | |
| 104.3656 | | | 107.1429 | | | 83.24255 | | |
| 99.24113 | 103.8135 | 2.699412 | 118.1102 | 115.9168 | 7.753578 | 94.03178 | 102.5668 | 14.59152 |
| | | 1.207214 | | | 3.467506 | | | 6.525528 |
| | | | | 0.067601 | | | | |
| | | | | | | | | 0.737604 |

Figure 5.2a hippocampus antioxidant levels

Hippo-h1-blot 1

| Sr.No | Catalase | Actin | Ratio | Avg | Catalase %Control | Avg | Stdev | SEM |
|---|---|---|---|---|---|---|---|---|
| L1 | 13681.58 | 21964.27 | 0.622902 | | 87.84458 | | | |
| L3 | 36604 | 33025.11 | 1.108369 | | 156.3075 | | | |
| L4 | 39430.56 | 34293.52 | 1.149796 | | 162.1498 | | | |
| L6 | 29967.62 | 38255.5 | 0.783355 | | 110.4724 | | | |
| L7 | 17670.41 | 34466 | 0.512691 | | 72.30215 | | | |
| L11 | 17388.95 | 36866 | 0.47168 | | 66.51856 | | | |
| L16 | 13688.05 | 43471.5 | 0.314874 | 0.709095 | 44.40506 | 100 | 45.22081 | 17.09186 |
| L2 | 30136.5 | 31811.84 | 0.947336 | | 133.5979 | | | |
| L5 | 26170.13 | 32677.08 | 0.800871 | | 112.9427 | | | |
| L8 | 25145.16 | 34859.5 | 0.721329 | | 101.7252 | | | |
| L9 | 35506.64 | 36212.13 | 0.980518 | | 138.2773 | | | |
| L10 | 27623.02 | 38022.04 | 0.7265 | | 102.4545 | | | |
| L12 | 22143.07 | 38681 | 0.572453 | | 80.73012 | | | |
| L13 | 20972 | 37297.5 | 0.56229 | | 79.29679 | | | |
| L14 | 13676.63 | 40731.5 | 0.335775 | | 47.35264 | | | |
| L15 | 7581.49 | 50010.5 | 0.151598 | 0.644297 | 21.37907 | 90.86181 | 38.35993 | 12.78664 |

1 1

| GPx | Actin | Ratio | Avg | GPx %Control | Avg | Stdev | SEM |
|---|---|---|---|---|---|---|---|
| 29513.1 | 21964.27 | 1.343687 | | 126.2357 | | | |
| 49330 | 33025.11 | 1.493712 | | 140.3302 | | | |
| 39309 | 34293.52 | 1.146252 | | 107.6872 | | | |
| 41564.2 | 38255.5 | 1.08649 | | 102.0727 | | | |
| 42076 | 34466 | 1.220797 | | 114.6906 | | | |
| 24195 | 36866 | 0.656296 | | 61.6572 | | | |
| 21899 | 43471.5 | 0.503755 | 1.064427 | 47.32644 | 100 | 33.7607 | 12.76035 |
| 45952.5 | 31811.84 | 1.444509 | | 135.7077 | | | |
| 40434.5 | 32677.08 | 1.237396 | | 116.25 | | | |
| 36264.5 | 34859.5 | 1.040305 | | 97.73378 | | | |
| 36647 | 36212.13 | 1.012009 | | 95.07548 | | | |
| 43415.46 | 38022.04 | 1.14185 | | 107.2737 | | | |

| | | | | | | | |
|---|---|---|---|---|---|---|---|
| 17226.44 | 38681 | 0.445346 | | 41.83907 | | | |
| 20949 | 37297.5 | 0.561673 | | 52.76765 | | | |
| 32630 | 40731.5 | 0.8011 | | 75.26115 | | | |
| 22816.91 | 50010.5 | 0.456242 | 0.904492 | 42.86273 | 84.97458 | 33.68938 | 11.22979 |
| | | | | | TTEST | 0.391521 | |

| GR | Actin | Ratio | Avg | %Control | Avg | Stdev | SEM |
|---|---|---|---|---|---|---|---|
| 15363.61 | 57683.42 | 0.266344 | | 91.68718 | | | |
| 20787.17 | 51144.96 | 0.406436 | | 139.9133 | | | |
| 12595.34 | 44782.05 | 0.281259 | | 96.82161 | | | |
| 10346.35 | 43472 | 0.238 | | 81.93018 | | | |
| 20064.59 | 38364.11 | | | | | | |
| 13143.73 | 42877.61 | 0.306541 | | 105.5248 | | | |
| 11320.45 | 46324.99 | 0.24437 | 0.290492 | 84.12299 | 100 | 21.36069 | 8.07358 |
| | | | | | | | |
| 20372.63 | 47699.69 | 0.427102 | | 147.0273 | | | |
| 22120.91 | 50910 | 0.43451 | | 149.5775 | | | |
| 13233.13 | 50594.93 | 0.261551 | | 90.03719 | | | |
| 10316.63 | 48622.94 | 0.212176 | | 73.04038 | | | |
| 10939.73 | 43952.91 | 0.248897 | | 85.68116 | | | |
| 18597.96 | 41693.21 | 0.446067 | | 153.5558 | | | |
| 17612.52 | 44140.17 | 0.399013 | | 137.358 | | | |
| 10879.04 | 44062.79 | 0.246899 | | 84.99335 | | | |
| 10921.2 | 38497.22 | 0.283688 | 0.328878 | 97.65789 | 113.2143 | 32.8321 | 10.94403 |

| MnSOD | Actin | Ratio | Avg | %Control | Avg | Stdev | SEM |
|---|---|---|---|---|---|---|---|
| 102129.2 | 57683.42 | 1.770511 | | 68.18338 | | | |
| 131354 | 51144.96 | 2.568269 | | 98.90546 | | | |
| 138627 | 44782.05 | 3.095593 | | 119.213 | | | |
| 129830.9 | 43472 | 2.986541 | | 115.0134 | | | |
| 93277.9 | 38364.11 | 2.431384 | | 93.63397 | | | |
| 114608.5 | 42877.61 | 2.672922 | | 102.9357 | | | |
| 122836 | 46324.99 | 2.651614 | 2.596691 | 102.1151 | 100 | 16.64159 | 6.289929 |
| | | | | | | | |
| 116981.7 | 47699.69 | 2.452463 | | 94.4457 | | | |
| 123949 | 50910 | 2.434669 | | 93.76046 | | | |

| | | | | | | | |
|---|---|---|---|---|---|---|---|
| 133487 | 50594.93 | 2.638347 | | 101.6042 | | | |
| 137423 | 48622.94 | 2.8263 | | 108.8424 | | | |
| 129562 | 43952.91 | 2.947746 | | 113.5193 | | | |
| 105851.1 | 41693.21 | 2.538808 | | 97.77091 | | | |
| 97393 | 44140.17 | 2.206448 | | 84.97155 | | | |
| 113757.5 | 44062.79 | 2.581714 | | 99.42322 | | | |
| 115608.5 | 38497.22 | 3.003035 | 2.625503 | 115.6485 | 101.1096 | 9.989166 | 3.329722 |

| Hsp-32 | Actin | Ratio | Avg | %Control | Avg | Stdev | SEM |
|---|---|---|---|---|---|---|---|
| 64318.07 | 46962.56 | 1.369561 | | 92.86544 | | | |
| 81797.02 | 42429.5 | 1.927834 | | 130.7201 | | | |
| 66480.24 | 48021.2 | 1.384394 | | 93.87121 | | | |
| 60135.11 | 43563.62 | 1.380397 | | 93.60025 | | | |
| 72071.98 | 34717.35 | 2.075964 | | 140.7644 | | | |
| 58150.94 | 41854.14 | 1.389371 | | 94.20874 | | | |
| 40857.7 | 51332.85 | 0.795937 | 1.47478 | 53.96987 | 100 | 28.54001 | 10.78711 |
| | | | | | | | |
| 66455.43 | 39487 | 1.68297 | | 114.1167 | | | |
| 80521.2 | 37894.21 | 2.124895 | | 144.0822 | | | |
| 74043.96 | 45481.09 | 1.628016 | | 110.3905 | | | |
| 66760.29 | 46810.58 | 1.42618 | | 96.70458 | | | |
| 63037.95 | 46179.25 | 1.365071 | | 92.56101 | | | |
| 65311.18 | 42108.44 | 1.551024 | | 105.1698 | | | |
| 69778.09 | 41433 | 1.684119 | | 114.1946 | | | |
| 45166.6 | 48268.71 | 0.935732 | | 63.44897 | | | |
| 58018.87 | 46069.5 | 1.259377 | 1.517487 | 85.39425 | 102.8958 | 22.41296 | 7.470986 |

| Hsp-70 | Actin | Ratio | Avg | %Control | Avg | Stdev | SEM |
|---|---|---|---|---|---|---|---|
| 10183.79 | 22055.34 | | | | | | |
| 8749.68 | 25421.34 | | | | | | |
| 5107.65 | 27733.84 | 0.184167 | | 91.53341 | | | |
| 4120.04 | 29507.65 | 0.139626 | | 69.39614 | | | |
| 5355.29 | 24279.2 | 0.220571 | | 109.6269 | | | |
| 7204.17 | 29934.98 | 0.240661 | | 119.6117 | | | |
| 6965.96 | 31522.53 | 0.220984 | 0.201202 | 109.8319 | 100 | 19.88869 | 7.517217 |
| | | | | | | | |
| 9116.13 | 22969.78 | 0.396875 | | 197.2524 | | | |

| | | | | | | | |
|---|---|---|---|---|---|---|---|
| 10272.81 | 23865.39 | 0.430448 | | 213.9386 | | | |
| 7268.11 | 22543.74 | 0.3224 | | 160.2375 | | | |
| 9445.25 | 26047.45 | 0.362617 | | 180.2257 | | | |
| 5975.45 | 27634.01 | 0.216235 | | 107.472 | | | |
| 6612.86 | 23623.12 | 0.279932 | | 139.1299 | | | |
| 9829.99 | 28663.66 | 0.342943 | | 170.4472 | | | |
| 7416.05 | 35386.02 | 0.209576 | | 104.162 | | | |
| 4455.05 | 31021.72 | 0.143611 | 0.300515 | 71.3765 | 149.3602 | 47.38579 | 15.79526 |
| | | | | | TTEST | 0.048768 | |

Figure 5.2b hippocampus antioxidant activities

Catalase activity

| **Hippo Abs** | **blank minus** | **Formaldehyde uM** | **Catalase activity** | **Avg** | **%Control** | **Avg %Cotrol** | **STDEV** | **SEM** |
|---|---|---|---|---|---|---|---|---|
| 0.243 | 0.143 | 13.25 | 2.76 | | 118 | | | |
| 0.241 | 0.141 | 13.06 | 2.72 | | 117 | | | |
| 0.217 | 0.117 | 10.86 | 2.26 | | 97 | | | |
| 0.184 | 0.084 | 7.83 | 1.63 | | 70 | | | |
| 0.245 | 0.145 | 13.43 | 2.80 | | 120 | | | |
| 0.22 | 0.12 | 11.14 | 2.32 | | 99 | | | |
| 0.195 | 0.095 | 8.84 | 1.84 | 2.33 | 79 | 100 | 20 | 7 |
| | | | | | | | | |
| 0.205 | 0.105 | 9.76 | 2.03 | | 87 | | | |
| 0.194 | 0.094 | 8.75 | 1.82 | | 78 | | | |
| 0.217 | 0.117 | 10.86 | 2.26 | | 97 | | | |
| 0.224 | 0.124 | 11.50 | 2.40 | | 103 | | | |
| 0.19 | 0.09 | 8.39 | 1.75 | | 75 | | | |
| 0.195 | 0.095 | 8.84 | 1.84 | | 79 | | | |
| 0.184 | 0.084 | 7.83 | 1.63 | | 70 | | | |
| 0.188 | 0.088 | 8.20 | 1.71 | | 73 | | | |
| 0.187 | 0.087 | 8.11 | 1.69 | | 72 | 82 | 12 | 4 |
| | | | | | | | | |
| | | | | | TTEST | 0.035 | | |

GPx activity

| Hippo 5nm, 30d | Sample id | Slope | Backgd minus | GPx activity | | | | | |
|---|---|---|---|---|---|---|---|---|---|
| | Backgd | 0.004 | | | | | | | |
| | Positive C | 0.059 | | | Avg | %Control | | | |
| c | 128 | 0.006 | 0.0017 | 4.457 | | 72 | | | |
| c | 133 | 0.007 | 0.0028 | 7.004 | | 113 | | | |
| c | 135 | 0.0075 | 0.0033 | 8.277 | | 133 | | | |
| c | 138 | 0.006 | 0.0018 | 4.457 | | 72 | | | |
| c | 141 | 0.007 | 0.0028 | 7.004 | | 113 | | | |
| c | 191 | 0.006667 | 0.0024 | 6.155 | | 99 | | | |
| c | 197 | 0.006667 | 0.0024 | 6.155 | 6.216 | 99 | 100 | 22 | 8 |
| | 130 | 0.005 | 0.0008 | 1.910 | | 31 | | | |
| | 137 | 0.005 | 0.0008 | 1.910 | | 31 | | | |
| | 142 | 0.0055 | 0.0013 | 3.184 | | 51 | | | |
| | 146 | 0.0055 | 0.0013 | 3.184 | | 51 | | | |
| | 147 | 0.005 | 0.0008 | 1.910 | | 31 | | | |
| | 192 | 0.0045 | 0.0003 | 0.637 | | 10 | | | |
| | 193 | 0.0045 | 0.0003 | 0.637 | | 10 | | | |
| | 195 | 0.005 | 0.0008 | 1.910 | | 31 | | | |
| | 196 | | | | | | 31 | 15 | 5 |
| | | | | | | TTEST | 8.85284E-06 | | |

SOD activity

| Hippo | SOD activity No Inhibitor | SOD activity LR (NInh) | in 230 ul (U/ml) | in 1ml (U/ml) | Avg | %Control | Avg %Cotrol | STDEV | SEM |
|---|---|---|---|---|---|---|---|---|---|
| 128 | 0.107 | 3.70 | 6.57 | 28.55 | | 85 | | | |
| 133 | 0.105 | 3.77 | 6.73 | 29.28 | | 87 | | | |
| 135 | 0.099 | 3.99 | 7.28 | 31.66 | | 94 | | | |
| 138 | 0.081 | 4.88 | 9.41 | 40.92 | | 122 | | | |
| 141 | 0.107 | 3.70 | 6.57 | 28.55 | | 85 | | | |
| 191 | 0.09 | 4.39 | 8.24 | 35.83 | | 107 | | | |
| 197 | 0.082 | 4.82 | 9.27 | 40.30 | 33.58 | 120 | 100 | 16 | 6 |
| 130 | 0.097 | 4.08 | 7.48 | 32.52 | | 97 | | | |
| 137 | 0.09 | 4.39 | 8.24 | 35.83 | | 107 | | | |
| 142 | 0.093 | 4.25 | 7.90 | 34.35 | | 102 | | | |
| 146 | 0.096 | 4.12 | 7.58 | 32.96 | | 98 | | | |
| 147 | 0.087 | 4.55 | 8.60 | 37.41 | | 111 | | | |
| 192 | 0.084 | 4.71 | 8.99 | 39.10 | | 116 | | | |

| | | | | | | | | |
|---|---|---|---|---|---|---|---|---|
| 193 | 0.08 | 4.94 | 9.56 | 41.56 | 124 | | | |
| 195 | 0.083 | 4.77 | 9.13 | 39.70 | 118 | | | |
| 196 | 0.086 | 4.60 | 8.73 | 37.96 | 113 | 110 | 9 | 3 |

Figure 6.5 PC, 3NT and HNE levels at 1h

| H-PC % Control | Avg | Stdev | SEM | H-3NT % Control | Avg | Stdev | SEM |
|---|---|---|---|---|---|---|---|
| 115.2389 | | | | 138.1351 | | | |
| 113.9401 | | | | 125.5992 | | | |
| 86.81741 | | | | 70.34177 | | | |
| 84.00359 | 100 | 16.89395 | 8.446974 | 65.92392 | 100 | 37.19496 | 18.59748 |
| 67.04916 | | | | 24.59238 | | | |
| 61.015 | | | | 36.12666 | | | |
| 83.09716 | 70.38711 | 11.41323 | 6.589431 | 31.61503 | 30.77802 | 5.812512 | 3.355855 |
| | 0.048579 | | | | 0.026238 | | |

| C-PC % Control | Avg | Stdev | SEM | C-3NT % Control | Avg | Stdev | SEM |
|---|---|---|---|---|---|---|---|
| 126.6366 | | | | 104.3041 | | | |
| 95.59929 | | | | 89.52255 | | | |
| 77.76407 | 100 | 24.73169 | 12.36585 | 106.1733 | 100 | 9.121743 | 4.560871 |
| 91.04401 | | | | 54.66773 | | | |
| 66.5392 | | | | 72.42078 | | | |
| 121.0881 | 92.89045 | 27.3213 | 15.77396 | 96.7018 | 74.59677 | 21.10135 | 12.18287 |
| | | | | | 0.128156 | | |

| CB-PC % Control | Avg | Stdev | SEM | CB-3NT % Control | Avg | Stdev | SEM |
|---|---|---|---|---|---|---|---|
| 88.27506 | | | | | | | |
| 121.7598 | | | | 110.3297 | | | |
| 90.23623 | | | | 90.60685 | | | |
| 99.72892 | 100 | 15.34457 | 7.672283 | 99.06349 | 100 | 9.8947 | 4.94735 |
| 70.94958 | | | | 91.46195 | | | |
| 59.25218 | | | | 76.20689 | | | |
| 84.46077 | 71.55418 | 12.61517 | 7.28337 | 117.0125 | 94.89377 | 20.61812 | 11.90388 |
| | 0.04815 | | | | 0.718651 | | |

H-HNE

| % Control | Avg | Stdev | SEM |
|---|---|---|---|
| 117.5759 | | | |
| 86.32789 | | | |
| 95.08233 | | | |
| 101.0139 | 100 | 13.17891 | 6.589455 |
| | | | |
| 56.68427 | | | |
| 70.17125 | | | |
| 60.33173 | 62.39575 | 6.976373 | 4.027811 |
| | 0.006846 | | |

C-HNE

| % Control | Avg | Stdev | SEM |
|---|---|---|---|
| 93.18681 | | | |
| 103.8506 | | | |
| | | | |
| 102.9626 | 100 | 5.917079 | 2.95854 |
| | | | |
| 94.83874 | | | |
| 100.9569 | | | |
| 101.612 | 99.13587 | 3.735813 | 2.156873 |

CB-HNE

| % Control | Avg | Stdev | SEM |
|---|---|---|---|
| 112.3505 | | | |
| 99.7939 | | | |
| 97.59298 | | | |
| 90.26259 | 100 | 9.186744 | 4.593372 |
| | | | |
| 76.70967 | | | |
| 68.18113 | | | |
| 70.36443 | 71.75174 | 4.430293 | 2.557831 |
| | 0.004731 | | |

Figure 6.5 PC, 3NT and HNE levels at 30 d

| 30d H-PC % Control | Avg | Stdev | SEM |
|---|---|---|---|
| 103.0257 | | | |
| 104.6668 | | | |
| 93.38355 | | | |
| 95.68135 | | | |
| 103.2426 | 100 | 5.095991 | 2.278996 |
| | | | |
| 102.4429 | | | |
| 109.0037 | | | |
| 109.4238 | | | |
| 102.6856 | | | |
| 95.63705 | 103.8386 | 5.666042 | 2.533931 |

| 30d H-3NT % Control | Avg | Stdev | SEM |
|---|---|---|---|
| 90.67567 | | | |
| 107.3649 | | | |
| 89.88203 | | | |
| 105.8369 | | | |
| 106.2405 | 100 | 8.896228 | 3.978514 |
| | | | |
| 100.5348 | | | |
| 92.58814 | | | |
| 96.2243 | | | |
| 81.5213 | | | |
| 92.68926 | 92.71157 | 7.049481 | 3.152624 |

| C-PC % Control | Avg | Stdev | SEM |
|---|---|---|---|
| 111.1513 | | | |
| 92.03296 | | | |
| 100.5166 | | | |
| 90.18315 | | | |
| 106.1159 | 100 | 8.970342 | 4.011659 |
| | | | |
| 104.8909 | | | |
| 108.7897 | | | |
| 95.6071 | | | |
| 99.91757 | | | |
| 94.4798 | 100.737 | 6.087709 | 2.722506 |

| C-3NT % Control | Avg | Stdev | SEM |
|---|---|---|---|
| 85.30942 | | | |
| 95.5334 | | | |
| 99.91671 | | | |
| 103.1536 | | | |
| 116.0869 | 100 | 11.23057 | 5.022463 |
| | | | |
| 89.79133 | | | |
| 94.36081 | | | |
| 103.3282 | | | |
| 99.07351 | | | |
| 106.5021 | 98.61118 | 6.719106 | 3.004876 |

| CB-PC % Control | Avg | Stdev | SEM |
|---|---|---|---|
| 108.7496 | | | |
| 104.866 | | | |
| 100.4875 | | | |
| 89.87346 | | | |
| 96.02347 | 100 | 7.396463 | 3.307799 |

| CB-3NT % Control | Avg | Stdev | SEM |
|---|---|---|---|
| 112.8306 | | | |
| 92.64751 | | | |
| 84.24907 | | | |
| 89.24858 | | | |
| 121.0243 | 100 | 16.00303 | 7.156771 |

| | | | | | | | | |
|---|---|---|---|---|---|---|---|---|
| 107.3743 | | | | 88.48933 | | | | |
| 106.2667 | | | | 119.3624 | | | | |
| 107.271 | | | | 100.3695 | | | | |
| 99.91896 | | | | 82.95852 | | | | |
| 107.6843 | 105.703 | 3.276818 | 1.465438 | 70.49614 | 92.33517 | 18.53831 | 8.290586 | |

30d

H-HNE

| % Control | Avg | Stdev | SEM |
|---|---|---|---|
| 90.32718 | | | |
| 116.5991 | | | |
| 113.3989 | | | |
| 91.74345 | | | |
| 87.93135 | 100 | 13.80623 | 6.174332 |
| | | | |
| 113.4102 | | | |
| 96.71498 | | | |
| 104.3548 | | | |
| 107.3411 | | | |
| 117.1061 | 107.7854 | 7.953531 | 3.556927 |

C-HNE

| % Control | Avg | Stdev | SEM |
|---|---|---|---|
| 89.00226 | | | |
| 98.57678 | | | |
| 98.25274 | | | |
| 93.84699 | | | |
| 120.3212 | 100 | 12.00876 | 5.370479 |
| | | | |
| 75.34036 | | | |
| 88.14213 | | | |
| 81.80681 | | | |
| 91.84791 | | | |
| 119.6234 | 91.35213 | 17.00961 | 7.606928 |

CB-HNE

| % | Avg | Stdev | SEM |
|---|---|---|---|

| | | | | |
|---|---|---|---|---|
| Control | | | | |
| 134.7228 | | | | |
| 90.22144 | | | | |
| 82.48256 | | | | |
| 78.26838 | | | | |
| 114.3048 | 100 | 23.90107 | 10.68888 | |
| | | | | |
| 72.75657 | | | | |
| 128.8882 | | | | |
| 122.2757 | | | | |
| 76.64967 | | | | |
| 57.20455 | 91.55495 | 31.98842 | 14.30566 | |

Figure 6.3 antioxidant enzyme levels at 30 d

| **H1-catalase** | **H1-actin** | **Ratio** | **Avg** | **% Control** | **Avg** | **Stdev** | **SEM** |
|---|---|---|---|---|---|---|---|
| H1-catalase | H1-actin | | | | | | |
| 19670 | 130863 | 15 | | 147 | | | |
| 26923 | 101779 | | | | | | |
| 10988 | 121446 | 9 | | 88 | | | |
| 7876 | 118909 | 7 | | 65 | | | |
| 3926 | 129694 | | 10 | | 100 | 42 | 19 |
| | | | | | | | |
| 15404 | 117794 | 13 | | 128 | | | |
| 11628 | 118020 | 10 | | 96 | | | |
| 7911 | 129505 | 6 | | 60 | | | |
| 11075 | 121904 | 9 | | 89 | | | |
| 5970 | 118711 | 5 | | 49 | 84 | 31 | 14 |
| | | | | | | | |
| | | | | | 0.326951 | | |

| H1-GPx | H1-actin | Ratio | Avg | % Control | Avg | Stdev | SEM |
|---|---|---|---|---|---|---|---|
| H1-GPx | H1-actin | | | | | | |
| 6792 | 130863 | 5 | | 35 | | | |
| 14095 | 101779 | 14 | | 94 | | | |
| 27588 | 121446 | 23 | | 155 | | | |
| 20139 | 118909 | 17 | | 115 | | | |
| 40846 | 129694 | | 15 | | 100 | 50 | 22 |
| | | | | | | | |
| 14619 | 117794 | 12 | | 85 | | | |
| 7767 | 118020 | 7 | | 45 | | | |
| 7564 | 129505 | 6 | | 40 | | | |
| 20108 | 121904 | 16 | | 112 | | | |
| 17300 | 118711 | 15 | | 99 | 76 | 32 | 15 |
| | | | | | | | |
| | | | | | 0.436519 | | |

| H2-MnSOD | H2-actin | Ratio | Avg | % Control | Avg | Stdev | SEM |
|---|---|---|---|---|---|---|---|
| H2-MnSOD | H2-actin | | | | | | |
| 81463 | 192625 | 42 | | 90 | | | |
| 84606 | 166926 | 51 | | 108 | | | |
| 97480 | 186581 | 52 | | 111 | | | |
| 91883 | 211039 | 44 | | 92 | | | |
| 102766 | 219221 | 47 | 47 | 99 | 100 | 9 | 4 |
| | | | | | | | |
| 81019 | 170587 | 47 | | 101 | | | |
| 96632 | 190440 | 51 | | 108 | | | |
| 84821 | 188020 | 45 | | 96 | | | |
| 103873 | 223648 | 46 | | 99 | | | |
| 103823 | 241744 | 43 | | 91 | 99 | 6 | 3 |
| | | | | | | | |
| | | | | | 0.765421 | | |

| H3-Hsp-32 | H3-actin | Ratio | Avg | % Control | Avg | Stdev | SEM |
|---|---|---|---|---|---|---|---|
| H3-Hsp-32 | H3-actin | | | | | | |
| 28022 | 108615 | 26 | | 97 | | | |
| 22931 | 106205 | 22 | | 81 | | | |
| 38787 | 122781 | 32 | | 119 | | | |
| 31097 | 114136 | 27 | | 103 | | | |
| 50144 | 120262 | | 27 | | 100 | 16 | 7 |
| | | | | | | | |
| 40857 | 111974 | 36 | | 137 | | | |
| 27796 | 125820 | 22 | | 83 | | | |
| 36577 | 133465 | 27 | | 103 | | | |
| 37600 | 120378 | 31 | | 118 | | | |
| 38450 | 112232 | 34 | | 129 | 114 | 22 | 10 |
| | | | | | | | |
| | | | | | 0.53582 | | |

| H4-Hsp-70 | H4-actin | Ratio | Avg | % Control | Avg | Stdev | SEM |
|---|---|---|---|---|---|---|---|
| H4-Hsp-70 | H4-actin | | | | | | |
| 9626 | 63828 | 15 | | 98 | | | |
| 5361 | 59015 | 9 | | 59 | | | |
| 10031 | 66722 | 15 | | 98 | | | |
| 13620 | 68227 | 20 | | 130 | | | |
| 11889 | 67272 | 18 | 15 | 115 | 100 | 26 | 12 |
| | | #DIV/0! | | | | | |
| 7358 | 57312 | 13 | | 84 | | | |
| 9499 | 59346 | 16 | | 104 | | | |
| 13092 | 71472 | 18 | | 119 | | | |
| 10346 | 70949 | 15 | | 95 | | | |
| 16362 | 76815 | 21 | | 139 | 108 | 21 | 10 |
| | | | | | | | |
| | | | | | 0.398782 | | |

Figure 6.4 enzyme activities

Catalase activity at 1h

| %Control | Avg %Cotrol | STDEV | SEM | |
|---|---|---|---|---|
| 96 | | | | |
| 104 | | | | |
| 100 | 100 | 4 | 2 | |
| 129 | | | | |
| 118 | | | | |
| 125 | 124 | 6 | 3 | 0.003198 |
| 112 | | | | |
| 93 | | | | |
| 87 | | | | |
| 108 | 100 | 12 | 5 | |
| 95 | | | | |
| 125 | | | | |
| 107 | 109 | 15 | 9 | 0.42176 |
| 92 | | | | |
| 109 | | | | |
| 96 | | | | |
| 103 | 100 | 8 | 3 | |
| 115 | | | | |
| 125 | | | | |
| 109 | 116 | 8 | 5 | 0.041831 |

Catalase activity at 30 d

| %Control | Avg %Cotrol | STDEV | SEM |
|---|---|---|---|
| 101 | | | |
| 101 | | | |
| 96 | | | |
| 101 | | | |
| 101 | 100 | 2 | 1 |
| 100 | | | |
| 96 | | | |
| 110 | | | |
| 104 | | | |
| 87 | 99 | 8 | 4 |
| | 0.897349 | | |
| 81 | | | |
| 109 | | | |
| 97 | | | |
| 104 | | | |
| 109 | 100 | 12 | 5 |
| 84 | | | |
| 76 | | | |
| 78 | | | |
| 81 | | | |
| 112 | 86 | 15 | 7 |
| | 0.1428 | | |
| 111 | | | |
| 99 | | | |
| 99 | | | |
| 99 | | | |
| 91 | 100 | 7 | 3 |
| 141 | | | |
| 120 | | | |
| 126 | | | |
| 100 | | | |
| 94 | 116 | 19 | 9 |
| | 0.118556 | | |

GPx activity at 1h

| %Control | Avg %Control | Stdev | SEM | |
|---|---|---|---|---|
| 106 | | | | |
| 83 | | | | |
| 106 | | | | |
| 106 | 100 | 11 | 6 | |
| 128 | | | | |
| 128 | | | | |
| 128 | 128 | 0 | 0 | 0.008282 |
| 72 | | | | |
| 111 | | | | |
| 107 | | | | |
| 111 | 100 | 19 | 9 | |
| 150 | | | | |
| 130 | | | | |
| 120 | 133 | 15 | 9 | 0.0536 |
| 88 | | | | |
| 106 | | | | |
| 106 | 100 | 11 | 5 | |
| 106 | | | | |
| 125 | | | | |
| 88 | 106 | 19 | 11 | 0.64333 |

GPx activity at 30 d

| %Control | Avg %Control | Stdev | SEM | |
|---|---|---|---|---|
| 106 | | | | |
| 106 | | | | |
| 96 | | | | |
| 86 | | | | |
| 106 | 100 | 9 | 4 | |
| 106 | | | | |
| 96 | | | | |
| 96 | | | | |
| 96 | | | | |
| 96 | 98 | 5 | 2 | 0.667 |
| 100 | | | | |
| 111 | | | | |
| 89 | | | | |
| 100 | | | | |
| 100 | 100 | 8 | 3 | |
| 111 | | | | |
| 100 | | | | |
| 89 | | | | |
| 89 | | | | |
| 89 | 96 | 10 | 4 | 0.455 |
| 108 | | | | |
| 98 | | | | |
| 87 | | | | |
| 98 | | | | |
| 108 | 100 | 9 | 4 | |
| 98 | | | | |
| 108 | | | | |
| 108 | | | | |
| 108 | | | | |
| 87 | 102 | 9 | 4 | 0.724 |

SOD activities at 1 h

| %Control | Avg %Cotrol | STDEV | SEM | |
|---|---|---|---|---|
| 80 | | | | |
| 114 | | | | |
| 112 | | | | |
| 94 | 100 | 16 | 7 | |
| 128 | | | | |
| 128 | | | | |
| 135 | 130 | 4 | 3 | 0.025484 |
| 90 | | | | |
| 110 | | | | |
| 108 | | | | |
| 92 | 100 | 10 | 4 | |
| 116 | | | | |
| 118 | | | | |
| 143 | 126 | 15 | 9 | 0.040366 |
| 88 | | | | |
| 88 | | | | |
| 107 | | | | |
| 116 | 100 | 14 | 6 | |
| 133 | | | | |
| 116 | | | | |
| 123 | 124 | 9 | 5 | 0.049328 |

SOD activities at 30d

| %Control | Avg %Cotrol | STDEV | SEM |
|---|---|---|---|
| 99 | | | |
| 99 | | | |
| 99 | | | |
| 107 | | | |
| 97 | 100 | 4 | 2 |
| 97 | | | |
| 99 | | | |
| 93 | | | |
| 92 | | | |
| 104 | 97 | 5 | 2 |
| | | | |
| 109 | | | |
| 90 | | | |
| 101 | | | |
| 100 | | | |
| 100 | 100 | 7 | 3 |
| 104 | | | |
| 104 | | | |
| 93 | | | |
| 100 | | | |
| 112 | 102 | 7 | 3 |
| | | | |
| 97 | | | |
| 95 | | | |
| 97 | | | |
| 104 | | | |
| 107 | 100 | 5 | 2 |
| 101 | | | |
| 106 | | | |
| 89 | | | |
| 87 | | | |
| 97 | 96 | 8 | 3 |

Figure 7.3a, 7.4a, 7.5a western blot data- antioxidant levels and HSP levels

**Catalase**

| **20hr** | Codes | H1-Catalase | H1-Actin | Ratio | Avg | % Control | Avg | Stdev | SEM |
|---|---|---|---|---|---|---|---|---|---|
| **c** | **199** | **14928** | **38257** | **39** | | **92** | | | |
| c | 200 | 19385 | 38411 | 50 | | 119 | | | |
| c | 203 | 18543 | 40074 | 46 | | 109 | | | |
| c | 206 | 15584 | 45407 | 34 | 43 | 81 | 100 | 17 | 8 |
| c | 207 | 15935 | 40413 | 39 | | 100 | 100 | 15 | 7 |
| | | | | | | | | | |
| | 198 | 19621 | 38826 | 51 | | 119 | | | |
| | 201 | 15792 | 30586 | 52 | | 121 | | | |
| | 202 | 17496 | 35664 | 49 | | 115 | | | |
| | 204 | 18286 | 37226 | 49 | | 116 | 118 | 3 | 1 |
| | 205 | 23017 | 45428 | 51 | | 129 | 120 | 5 | 2 |
| | | | | | | | | | |
| | | | | | | TTEST | 0.050943 | | |
| **1hr** | | | | | | | | | |
| c | 216 | 19207 | 42322 | | | | | | |
| c | 217 | 15667 | 44542 | 35 | | 108 | | | |
| c | 220 | 14967 | 49775 | 30 | | 93 | | | |
| c | 223 | 14943 | 46553 | 32 | 32 | 99 | 100 | 8 | 4 |
| c | 224 | 32362 | 42359 | 76 | | 100 | 100 | 6 | 3 |
| | | | | | | | | | |
| | 218 | 23802 | 44910 | 53 | | 163 | | | |
| | 219 | 26011 | 42670 | 61 | | 188 | | | |
| | 221 | 23594 | 50964 | 46 | | 143 | | | |
| | 222 | 20401 | 47046 | 43 | | 134 | 157 | 24 | 12 |
| | 225 | 27951 | 36316 | 77 | | 101 | 146 | 33 | 15 |
| | | | | | | | | | |
| | | | | | | TTEST | 0.029872 | | |

**GR**

| **20hr** | Codes | H3-GR | H3-actin | Ratio | Avg | % Control | Avg | Stdev | SEM |
|---|---|---|---|---|---|---|---|---|---|
| **c** | **199** | **33258** | **32964** | **101** | | **94** | | | |
| c | 200 | 35646 | 32477 | 110 | | 103 | | | |
| c | 203 | 43340 | 29045 | | | | | | |
| c | 206 | 33658 | 30558 | 110 | 107 | 103 | 100 | 5 | 2 |
| c | 207 | 34292 | 40374 | 85 | | 100 | 100 | 4 | 2 |
| | | | | | | | | | |
| | 198 | 24270 | 33495 | 72 | | 68 | | | |
| | 201 | 27094 | 29127 | 93 | | 87 | | | |
| | 202 | 29722 | 33659 | 88 | | 83 | | | |
| | 204 | 25887 | 25310 | 102 | | 96 | 83 | 12 | 6 |
| | 205 | 31824 | 40712 | 78 | | 92 | 85 | 11 | 5 |
| | | | | | | | | | |
| | | | | | | TTEST | 0.0355 | | |
| | | | | | | | | | |
| c | 216 | 27321 | 18087 | 151 | | 91 | | | |
| c | 217 | 35469 | 19713 | 180 | | 109 | | | |
| c | 220 | 32238 | 19469 | 166 | | 100 | | | |
| c | 223 | 21756 | 13174 | 165 | 165 | 100 | 100 | 7 | 4 |
| c | 224 | 29376 | 26663 | 110 | | 100 | 100 | 6 | 3 |
| | | | | | | | | | |
| | 218 | 21546 | 18258 | 118 | | 71 | | | |
| | 219 | 23008 | 19660 | 117 | | 71 | | | |
| | 221 | 29361 | 26895 | 109 | | 66 | | | |
| | 222 | 29950 | 26933 | 111 | | 67 | 69 | 3 | 1 |
| | 225 | 22581 | 24194 | 93 | | 85 | 72 | 7 | 3 |
| | | | | | | | | | |
| | | | | | | TTEST | 0.0002 | | |

| | | GPx | | | | | | |
|---|---|---|---|---|---|---|---|---|
| **20hr** | H3-GPx | H3-actin | Ratio | Avg | % Control | Avg | Stdev | SEM |
| | **11290** | **32964** | **34** | | **66** | | | |
| | 20523 | 32477 | 63 | | 122 | | | |
| | 23162 | 39045 | 59 | | 115 | | | |
| | 15314 | 30558 | 50 | 52 | 97 | 100 | 25 | 12 |
| | 40374 | 40374 | 100 | | 100 | 100 | 22 | 10 |
| | | | | | | | | |
| | 19854 | 33495 | 59 | | 115 | | | |
| | 21151 | 27127 | 78 | | 151 | | | |
| | 24946 | 30659 | 81 | | 157 | | | |
| | 14953 | 25310 | 59 | | 114 | 134 | 23 | 12 |
| | 48121 | 40012 | 120 | | 120 | 131 | 21 | 9 |
| | | | | | | | | |
| | | | | | | | | 0.047 |
| **1hr** | | | | | | | | |
| | 4296 | 18087 | | | | | | |
| | 6288 | 9713 | 65 | | 102 | | | |
| | 11125 | 19469 | 57 | | 90 | | | |
| | 9007 | 13174 | 68 | 63 | 108 | 100 | 9 | 5 |
| | 26663 | 26663 | 100 | | 100 | 100 | 7 | 3 |
| | | | | | | | | |
| | 15570 | 18258 | 85 | | 134 | | | |
| | 8163 | 9660 | 85 | | 133 | | | |
| | 11960 | 17895 | 67 | | 105 | | | |
| | 13861 | 16933 | 82 | | 129 | 126 | 14 | 7 |
| | 24194 | 24194 | 100 | | 100 | 120 | 16 | 7 |
| | | | | | | | | 0.039 |

**Hsp-32**

| | H5-Hsp-32 | H5-Hsp-32-actin | Ratio | Avg | % Control | Avg | Stdev | SEM |
|---|---|---|---|---|---|---|---|---|
| 199 | 10059 | 28491 | 35 | | 79 | | | |
| 200 | 13441 | 25957 | 52 | | 116 | | | |
| 203 | 12100 | 27988 | 43 | | 97 | | | |
| 206 | 13163 | 27610 | 48 | 44 | 107 | 100 | 16 | 8 |
| 207 | 14977 | 34776 | 43 | | 100 | 100 | 14 | 6 |
| | | | | | | | | |
| 198 | 11886 | 32728 | 36 | | 82 | | | |
| 201 | 6788 | 20216 | 34 | | 75 | | | |
| 202 | 8887 | 29757 | 30 | | 67 | | | |
| 204 | 13402 | 37733 | 36 | | 80 | 76 | 6 | 3 |
| 205 | 11251 | 37791 | 30 | | 69 | 75 | 6 | 3 |
| | | | | | | | | |
| | | | | | TTEST | 0.0056 | | |
| 216 | 11167 | 30369 | 37 | | 116 | | | |
| 217 | 11121 | 40483 | 27 | | 86 | | | |
| 220 | 11753 | 41532 | 28 | | 89 | | | |
| 223 | 13356 | 38477 | 35 | 32 | 109 | 100 | 15 | 7 |
| 224 | 15059 | 43345 | 35 | 31 | 100 | 100 | 10 | 5 |
| | | | | | | | | |
| 218 | 9125 | 43973 | 21 | | 65 | | | |
| 219 | 7388 | 39392 | 19 | | 59 | | | |
| 221 | 13205 | 43174 | 31 | | 96 | | | |
| 222 | 11159 | 38509 | 29 | | 91 | 78 | 18 | 9 |
| 225 | 14060 | 48145 | 29 | | 84 | 79 | 17 | 8 |
| | | | | | | | | |
| | | | | | TTEST | 0.0526 | | |

| H7-Hsp-70 | H7-Hsp-70-actin | Ratio | Avg | % Control | Avg | Stdev | SEM |
|---|---|---|---|---|---|---|---|
| 4669 | 27940 | 17 | | 100 | | | |
| 6472 | 42600 | 15 | | 91 | | | |
| 8831 | 44079 | 20 | | 120 | | | |
| 5792 | 38394 | 15 | 17 | 90 | 100 | 14 | 7 |
| 10648 | 19484 | 55 | | 100 | 100 | 12 | 5 |
| | | | | | | | |
| 4691 | 44506 | 11 | | 63 | | | |
| 5799 | 40041 | 14 | | 86 | | | |
| 6431 | 42894 | 15 | | 89 | | | |
| 7183 | 45798 | 16 | | 94 | 83 | 14 | 7 |
| 7131 | 19892 | 36 | | 66 | 80 | 14 | 6 |
| | | | TTEST | 0.039847 | | | |
| | | | | | | | |
| 5456 | 27872 | 20 | | 102 | | | |
| 4623 | 33931 | 14 | | 71 | | | |
| 6917 | 31024 | 22 | | 116 | | | |
| 5555 | 25852 | 21 | 19 | 112 | 100 | 20 | 10 |
| 7909 | 22833 | 35 | | 100 | 100 | 18 | 8 |
| | | | | | | | |
| 6043 | 37004 | 16 | | 85 | | | |
| 4357 | 35381 | 12 | | 64 | | | |
| 5051 | 23296 | 22 | | 113 | | | |
| 5895 | 25686 | 23 | | 119 | 95 | 26 | 13 |
| 6405 | 18300 | 35 | | 101 | 96 | 22 | 10 |
| | | | TTEST | 0.781933 | | | |

30nm- 30d western blot data- antioxidant levels and HSP levels

| H-2-GR | H-2-actin | Ratio | Avg | % Control | Avg | Stdev | SEM |
|---|---|---|---|---|---|---|---|
| 33083 | 26839 | 123 | | | | | |
| 27868 | 20566 | 136 | | 123 | | | |
| 27374 | 32726 | 84 | | 76 | | | |
| 27344 | 26131 | 105 | | 95 | | | |
| 41734 | 37510 | 111 | | 101 | | | |
| 41710 | 39238 | 106 | | 96 | | | |
| 34116 | 28376 | 120 | | 109 | | | |
| 44094 | 21272 | | 110 | | 100 | 16 | 6 |
| 29218 | 19029 | 154 | | 139 | | | |
| 31437 | 23302 | 135 | | 122 | | | |
| 33345 | 26343 | 127 | | 115 | | | |
| 25483 | 22147 | 115 | | 104 | | | |
| 34177 | 28920 | 118 | | 107 | | | |
| 39114 | 36281 | 108 | | 98 | | | |
| 33421 | 23302 | 143 | | 130 | | | |
| 34320 | 21028 | 163 | | 148 | 120 | 18 | 6 |
| | | | | | 0.044321 | | |

| **H-2-GPx** | **H-2-actin** | **Ratio** | **Avg** | **% Control** | **Avg** | **Stdev** | **SEM** |
|---|---|---|---|---|---|---|---|
| 10141 | 26839 | 38 | | | | | |
| 19430 | 20566 | 94 | | 107 | | | |
| 36011 | 32726 | 110 | | 124 | | | |
| 17984 | 26131 | 69 | | 78 | | | |
| 20818 | 27510 | 76 | | 86 | | | |
| 36603 | 39238 | 93 | | 105 | | | |
| 25102 | 28376 | 88 | | 100 | | | |
| 35287 | 21272 | | 88 | | 100 | 17 | 6 |
| 42960 | 29029 | 148 | | 167 | | | |
| 45420 | 33302 | 136 | | 154 | | | |
| 25621 | 26343 | 97 | | 110 | | | |
| 22843 | 22147 | 103 | | 117 | | | |
| 29781 | 28920 | 103 | | 116 | | | |
| 43039 | 36281 | 119 | | 134 | | | |
| 29266 | 23302 | 126 | | 142 | | | |
| 21751 | 21028 | 103 | | 117 | 132 | 21 | 7 |
| | | | | | 0.009038 | | |

| H-3-catalase | H-3-actin | Ratio | Avg | % Control | Avg | Stdev | SEM |
|---|---|---|---|---|---|---|---|
| 24964 | 66890 | 37 | | | | | |
| 17247 | 59313 | 29 | | 87 | | | |
| 17917 | 55328 | 32 | | 97 | | | |
| 20332 | 66801 | 30 | | 91 | | | |
| 21747 | 62742 | 35 | | 104 | | | |
| 25387 | 57725 | 44 | | 132 | | | |
| 23842 | 66560 | 36 | | 107 | | | |
| 18691 | 67562 | 28 | 33 | 83 | 100 | 16 | 6 |
| 20109 | 59565 | 34 | | 101 | | | |
| 23821 | 72268 | 33 | | 99 | | | |
| 30866 | 66330 | 47 | | 139 | | | |
| 21517 | 64175 | 34 | | 100 | | | |
| 31732 | 59959 | 53 | | 158 | | | |
| 24870 | 47017 | 53 | | 158 | | | |
| 21512 | 34274 | 63 | | 188 | | | |
| 25155 | 39959 | 63 | | 188 | 141 | 38 | 13 |

0.019249

| H-3-Hsp-32 | H-3-actin | Ratio | Avg | % Control | Avg | Stdev | SEM |
|---|---|---|---|---|---|---|---|
| 15120 | 66890 | 23 | | | | | |
| 15578 | 59313 | 26 | | 90 | | | |
| 19970 | 65328 | 31 | | 105 | | | |
| 16297 | 66801 | 24 | | 84 | | | |
| 22153 | 69742 | 32 | | 109 | | | |
| 21213 | 69725 | 30 | | 105 | | | |
| 21132 | 66560 | 32 | | 109 | | | |
| 19232 | 67562 | 28 | 29 | 98 | 100 | 10 | 4 |
| 19598 | 59565 | 33 | | 113 | | | |
| 19506 | 60268 | 32 | | 111 | | | |
| 21996 | 66330 | 33 | | 114 | | | |
| 19632 | 61175 | 32 | | 110 | | | |
| 19078 | 53959 | 35 | | 122 | | | |
| 21059 | 57017 | 37 | | 127 | | | |
| 21606 | 54274 | 40 | | 137 | | | |

| | | | | | | | |
|---|---|---|---|---|---|---|---|
| 7851 | 19979 | 39 | | 135 | 121 | 11 | 4 |

0.001615

| **H-4-Hsp-70** | **H-4-actin** | **Ratio** | **Avg** | **% Control** | **Avg** | **Stdev** | **SEM** |
|---|---|---|---|---|---|---|---|
| 2969 | 31558 | 9 | | | | | |
| 5562 | 49740 | 11 | | 101 | | | |
| 4563 | 37606 | 12 | | 110 | | | |
| 5778 | 42027 | 14 | | 125 | | | |
| 4108 | 39522 | 10 | | 94 | | | |
| 2067 | 26267 | 8 | | 71 | | | |
| 2234 | 20518 | 11 | | 99 | | | |
| 4152 | 21532 | | 11 | | 100 | 18 | 7 |
| 5689 | 45097 | 13 | | 114 | | | |
| 4631 | 36545 | 13 | | 115 | | | |
| 4226 | 31020 | 14 | | 123 | | | |
| 5126 | 40319 | 13 | | 115 | | | |
| 4655 | 35785 | 13 | | 118 | | | |
| 5198 | 21886 | 24 | | 215 | | | |
| 2677 | 16348 | 16 | | 148 | | | |
| 2968 | 20506 | 14 | | 131 | 135 | 34 | 12 |

0.042776

30nm-90d western blot data- antioxidant levels and HSP levels

| | H-1-1 catalase | H-1-1-actin | Normalized ratio | Avg | | | Stdev | SEM | |
|---|---|---|---|---|---|---|---|---|---|
| 1dc | 21762 | 34858 | 81 | | 105 | | | | |
| 1dc | 25230 | 40256 | 81 | | 106 | | | | |
| 1dc | 33046 | 43472 | 68 | 77 | 89 | 100 | 10 | 6 | |
| 1d | 22494 | 33718 | 86 | | 113 | | | | |
| 1d | 20143 | 31519 | 83 | | 108 | | | | |
| 1d | 43168 | 53930 | 72 | 80 | 94 | 105 | 10 | 6 | 0.58808 |
| 1wc | 14852 | 24141 | 80 | | 93 | | | | |
| 1wc | 21697 | 23849 | 118 | | 138 | | | | |
| 1wc | 32067 | 48353 | 59 | 86 | 69 | 100 | 35 | 20 | |
| 1w | 21136 | 27506 | 99 | | 116 | | | | |
| 1w | 32322 | 37540 | 111 | | 130 | | | | |
| 1w | 36104 | 43382 | 75 | 95 | 87 | 111 | 22 | 13 | 0.660974 |
| 1mc | 23773 | 26841 | 115 | | 116 | | | | |
| 1mc | 10409 | 15822 | 85 | | 86 | | | | |
| 1mc | 37970 | 35367 | 96 | 99 | 98 | 100 | 15 | 9 | |
| 1m | 26351 | 26730 | 128 | | 129 | | | | |
| 1m | 19682 | 19633 | 130 | | 131 | | | | |
| 1m | 41900 | 45424 | 119 | 126 | 121 | 127 | 6 | 3 | 0.042585 |
| 3mc | 11061 | 13984 | 102 | | 131 | | | | |
| 3mc | 17845 | 25030 | 92 | | 118 | | | | |
| 3mc | 38958 | 47191 | 74 | | 95 | | | | |
| 3mc | 32964 | 44334 | 67 | | 86 | | | | |
| 3mc | 25873 | 33119 | 70 | | 90 | | | | |
| 3mc | 21860 | 31768 | 62 | 78 | 79 | 100 | 20 | 8 | |
| 3m | 17298 | 18634 | 120 | | 154 | | | | |
| 3m | 13410 | 21940 | 79 | | 102 | | | | |
| 3m | 46125 | 37445 | 110 | | 142 | | | | |
| 3m | 37995 | 42820 | 80 | | 102 | | | | |
| 3m | 21436 | 30365 | 63 | | 81 | | | | |
| 3m | 18660 | 33593 | 50 | | 64 | | | | |
| 3m | 21005 | 30778 | 61 | 81 | 79 | 103 | 33 | 13 | 0.831894 |

| | H-1-1-Hsp-32 | H-1-1-actin | Normalized ratio | Avg | | | Stdev | SEM | |
|---|---|---|---|---|---|---|---|---|---|
| 1dc | 29175 | 34858 | 63 | | 97 | | | | |
| 1dc | 42725 | 44256 | 73 | | 112 | | | | |
| 1dc | 24701 | 43472 | 59 | 65 | 90 | 100 | 7 | 4 | |
| 1d | 40086 | 33718 | 90 | | 138 | | | | |
| 1d | 42293 | 31519 | 102 | | 156 | | | | |
| 1d | 43102 | 53930 | 83 | 92 | 127 | 140 | 9 | 5 | 0.018671 |
| | | | | | | | | | |
| 1wc | 34349 | 24141 | 108 | | 102 | | | | |
| 1wc | 35294 | 23849 | 112 | | 107 | | | | |
| 1wc | 44695 | 48353 | 96 | 105 | 91 | 100 | 8 | 5 | |
| 1w | 46553 | 27506 | 128 | | 122 | | | | |
| 1w | 46066 | 27540 | 127 | | 120 | | | | |
| 1w | 50099 | 43382 | 120 | 125 | 114 | 119 | 5 | 3 | 0.023561 |
| | | | | | | | | | |
| 1mc | 28856 | 26841 | 81 | | 100 | | | | |
| 1mc | 15941 | 15822 | 76 | | 94 | | | | |
| 1mc | 51173 | 45367 | 85 | 81 | 105 | 100 | 5 | 3 | |
| 1m | 35273 | 26730 | 100 | | 123 | | | | |
| 1m | 22696 | 15633 | 110 | | 136 | | | | |
| 1m | 49084 | 49424 | 103 | 104 | 127 | 129 | 5 | 3 | 0.004255 |
| | | | | | | | | | |
| 3mc | 19560 | 13984 | 106 | | 96 | | | | |
| 3mc | 38131 | 25030 | 115 | | 104 | | | | |
| 3mc | 50783 | 47191 | 112 | | 101 | | | | |
| 3mc | 47198 | 44334 | 110 | | 100 | | | | |
| 3mc | 39820 | 33119 | 125 | | 112 | | | | |
| 3mc | 29707 | 31768 | 97 | 111 | 87 | 100 | 9 | 4 | |
| 3m | 17334 | 18634 | 70 | | 64 | | | | |
| 3m | 30257 | 21940 | 105 | | 94 | | | | |
| 3m | 56415 | 47445 | 123 | | 111 | | | | |
| 3m | 42872 | 42820 | 104 | | 94 | | | | |
| 3m | 35955 | 32365 | 115 | | 104 | | | | |
| 3m | 40063 | 34593 | 120 | | 108 | | | | |
| 3m | 35955 | 32778 | 114 | 107 | 103 | 97 | 18 | 7 | 0.671076 |

| | H-2-1-Hsp-70 | H-2-1-actin | Normalized ratio | Avg | | | Stdev | SEM | |
|---|---|---|---|---|---|---|---|---|---|
| 1dc | 1632 | 31815 | 72 | | 92 | | | | |
| 1dc | 2287 | 42450 | 76 | | 97 | | | | |
| 1dc | 1949 | 28017 | 88 | 79 | 111 | 100 | 10 | 6 | |
| 1d | 2446 | 36724 | 94 | | 119 | | | | |
| 1d | 1927 | 42621 | 64 | | 81 | | | | |
| 1d | 2279 | 28575 | 101 | 86 | 128 | 109 | 25 | 14 | 0.575769 |
| 1wc | 2647 | 41727 | 90 | | 103 | | | | |
| 1wc | 1138 | 27580 | 58 | | 67 | | | | |
| 1wc | 2171 | 24110 | 114 | 87 | 130 | 100 | 32 | 18 | |
| 1w | 2783 | 34777 | 113 | | 130 | | | | |
| 1w | 2539 | 35534 | 101 | | 116 | | | | |
| 1w | 2558 | 38915 | 83 | 99 | 95 | 114 | 17 | 10 | 0.553244 |
| 1mc | 2902 | 35595 | 115 | | 131 | | | | |
| 1mc | 1723 | 30856 | 79 | | 89 | | | | |
| 1mc | 2248 | 40271 | 70 | 88 | 80 | 100 | 27 | 16 | |
| 1m | 2412 | 39939 | 85 | | 97 | | | | |
| 1m | 2387 | 34456 | 98 | | 111 | | | | |
| 1m | 3428 | 37923 | 128 | 104 | 145 | 118 | 25 | 14 | 0.453024 |
| 3mc | 2331 | 41283 | 80 | | 101 | | | | |
| 3mc | 2676 | 44052 | 86 | | 109 | | | | |
| 3mc | 2127 | 44714 | 60 | | 76 | | | | |
| 3mc | 2468 | 35959 | 87 | | 110 | | | | |
| 3mc | 3000 | 50045 | 76 | | 96 | | | | |
| 3mc | 2434 | 36438 | 84 | 79 | 107 | 100 | 13 | 5 | |
| 3m | 2134 | 36381 | 83 | | 105 | | | | |
| 3m | 1918 | 33652 | 80 | | 102 | | | | |
| 3m | 2291 | 42142 | 69 | | 87 | | | | |
| 3m | 2284 | 37399 | 77 | | 98 | | | | |
| 3m | 2950 | 39611 | 94 | | 119 | | | | |
| 3m | 2102 | 34382 | 77 | | 98 | | | | |
| 3m | 1334 | 47213 | 36 | 74 | 45 | 94 | 23 | 9 | 0.566166 |

| | H-2-1-GPx | H-2-1-actin | Normalized ratio | Avg | | | Stdev | SEM | |
|---|---|---|---|---|---|---|---|---|---|
| 1dc | 13844 | 31815 | 49 | | 109 | | | | |
| 1dc | 9590 | 42450 | 25 | | 57 | | | | |
| 1dc | 17123 | 28017 | 60 | 45 | 134 | 100 | 18 | 10 | |
| 1d | 15011 | 36724 | 46 | | 103 | | | | |
| 1d | 15646 | 42621 | 41 | | 92 | | | | |
| 1d | 20934 | 28575 | 72 | 53 | 161 | 118 | 16 | 10 | 0.586023 |
| | | | | | | | | | |
| 1wc | 6650 | 41727 | 18 | | 42 | | | | |
| 1wc | 9041 | 27580 | 37 | | 86 | | | | |
| 1wc | 18267 | 24110 | 74 | 43 | 173 | 100 | 29 | 17 | |
| 1w | 25125 | 34777 | 81 | | 189 | | | | |
| 1w | 15781 | 35534 | 50 | | 116 | | | | |
| 1w | 11152 | 38915 | 28 | 53 | 65 | 123 | 27 | 15 | 0.681157 |
| | | | | | | | | | |
| 1mc | 15665 | 35595 | 49 | | 102 | | | | |
| 1mc | 16899 | 30856 | 61 | | 127 | | | | |
| 1mc | 14308 | 40271 | 35 | 48 | 72 | 100 | 13 | 8 | |
| 1m | 20973 | 39939 | 59 | | 121 | | | | |
| 1m | 12846 | 34456 | 42 | | 86 | | | | |
| 1m | 19097 | 37923 | 49 | 50 | 102 | 103 | 9 | 5 | 0.878345 |
| | | | | | | | | | |
| 3mc | 25987 | 41283 | 62 | | 104 | | | | |
| 3mc | 16142 | 44052 | 36 | | 61 | | | | |
| 3mc | 19442 | 44714 | 43 | | 72 | | | | |
| 3mc | 28768 | 35959 | 78 | | 132 | | | | |
| 3mc | 29270 | 50045 | 57 | | 97 | | | | |
| 3mc | 29579 | 36438 | 79 | 59 | 134 | 100 | 18 | 7 | |
| 3m | 25184 | 36381 | 68 | | 114 | | | | |
| 3m | 24863 | 33652 | 72 | | 122 | | | | |
| 3m | 33027 | 42142 | 77 | | 130 | | | | |
| 3m | 25200 | 37399 | 66 | | 111 | | | | |
| 3m | 32496 | 39611 | 80 | | 136 | | | | |
| 3m | 23144 | 34382 | 66 | | 111 | | | | |
| 3m | 23389 | 41213 | 56 | 69 | 94 | 117 | 8 | 3 | 0.208601 |

| | H-3-1-GR | H-3-1-actin | Normalized ratio | Avg | | | Stdev | SEM | |
|---|---|---|---|---|---|---|---|---|---|
| 1dc | 113799 | 15566 | 112 | | 104 | | | | |
| 1dc | 109647 | 16934 | 99 | | 92 | | | | |
| 1dc | 67516 | 33766 | 112 | 108 | 104 | 100 | 7 | 4 | |
| 1d | 108693 | 15174 | 110 | | 102 | | | | |
| 1d | 92973 | 13550 | 105 | | 97 | | | | |
| 1d | 82482 | 37854 | 122 | 112 | 114 | 104 | 8 | 5 | 0.537041 |
| 1wc | 104577 | 19243 | 83 | | 111 | | | | |
| 1wc | 86084 | 19603 | 67 | | 89 | | | | |
| 1wc | 66552 | 46821 | | 75 | | 100 | 15 | 9 | |
| 1w | 89815 | 15324 | 90 | | 119 | | | | |
| 1w | 97441 | 13183 | 113 | | 150 | | | | |
| 1w | 69514 | 43100 | 91 | 98 | 121 | 130 | 18 | 10 | 0.144608 |
| 1mc | 102412 | 13587 | 115 | | 121 | | | | |
| 1mc | 98470 | 15744 | 96 | | 101 | | | | |
| 1mc | 54874 | 41443 | 74 | 95 | 78 | 100 | 22 | 12 | |
| 1m | 101519 | 15961 | 97 | | 102 | | | | |
| 1m | 107597 | 17761 | 93 | | 97 | | | | |
| 1m | 72377 | 39430 | 103 | 98 | 108 | 103 | 5 | 3 | 0.843167 |
| 3mc | 76842 | 48167 | 90 | | 86 | | | | |
| 3mc | 95886 | 46047 | 117 | | 112 | | | | |
| 3mc | 77152 | 42386 | 102 | | 98 | | | | |
| 3mc | 82273 | 42043 | 110 | | 105 | | | | |
| 3mc | 80615 | 44295 | 102 | | 98 | | | | |
| 3mc | 75505 | 39677 | 107 | 105 | 102 | 100 | 9 | 4 | |
| 3m | 75847 | 30867 | 138 | | 132 | | | | |
| 3m | 74341 | 36240 | 115 | | 110 | | | | |
| 3m | 88186 | 47780 | 104 | | 99 | | | | |
| 3m | 80396 | 45155 | 100 | | 96 | | | | |
| 3m | 76353 | 41196 | 104 | | 99 | | | | |
| 3m | 76366 | 40511 | 106 | | 101 | | | | |
| 3m | 77710 | 37647 | 116 | 112 | 111 | 107 | 12 | 5 | 0.28211 |

Figure 7.3a, 7.4b, 7.5b, 7.6 antioxidant enzyme activities

| 30nm 1-20h | Catalase activity | Avg | %Control | Avg %Cotrol | STDEV | SEM | |
|---|---|---|---|---|---|---|---|
| 216 | 14.04 | | 109 | | | | |
| 217 | 11.60 | | 90 | | | | |
| 220 | 11.11 | | 87 | | | | |
| 223 | 13.55 | | 106 | | | | |
| 224 | 13.88 | 12.84 | 108 | 100 | 11 | 5 | |
| 218 | 22.65 | | 176 | | | | |
| 219 | 14.36 | | 112 | | | | |
| 221 | 13.88 | | 108 | | | | |
| 222 | 20.86 | | 163 | | | | |
| 225 | 14.69 | | 114 | 135 | 32 | 14 | 0.051775 |
| 199 | 12.41 | | 120 | | | | |
| 200 | 9.16 | | 89 | | | | |
| 203 | 9.33 | | 90 | | | | |
| 206 | 10.14 | | 98 | | | | |
| 207 | 10.63 | 10.33 | 103 | 100 | 13 | 6 | |
| 198 | 13.55 | | 131 | | | | |
| 201 | 10.46 | | 101 | | | | |
| 202 | 12.90 | | 125 | | | | |
| 204 | 12.90 | | 125 | | | | |
| 205 | 11.76 | | 114 | 119 | 12 | 5 | 0.038111 |

| 30nm 30 days | Catalase activity | Avg | %Control | Avg %Cotrol | STDEV | SEM |
|---|---|---|---|---|---|---|
| 209 | 12.58 | | 88 | | | |
| 225 | 15.66 | | 110 | | | |
| 227 | 13.39 | | 94 | | | |
| 228 | 14.69 | | 103 | | | |
| 231 | 13.88 | | 98 | | | |
| 233 | 15.34 | | 108 | | | |
| 235 | 14.04 | 14.22 | 99 | 100 | 8 | 3 |
| 210 | 12.90 | | 91 | | | |
| 211 | 12.09 | | 85 | | | |
| 212 | 13.06 | | 92 | | | |
| 213 | 12.90 | | 91 | | | |
| 214 | 12.41 | | 87 | | | |
| 230 | 11.60 | | 82 | | | |
| 232 | 11.93 | | 84 | | | |
| 234 | 12.74 | | 90 | 87 | 4 | 2 |
| | | | | 0.001278 | | |

| | 30nm 90 days | Catalase activity | Avg | %Control | Avg %Cotrol | STDEV | SEM | |
|---|---|---|---|---|---|---|---|---|
| 1dc | 260 | 13.39 | | 102 | | | | |
| 1dc | 261 | 13.06 | | 100 | | | | |
| 1dc | 270 | 12.74 | 13.06 | 98 | 100 | 2 | 1 | |
| 1d | 259 | 11.93 | | 91 | | | | |
| 1d | 271 | 11.76 | | 90 | | | | |
| 1d | 272 | 11.60 | | 89 | 90 | 1 | 1 | 0.003448 |
| 1wc | 268 | 12.09 | | 98 | | | | |
| 1wc | 269 | 13.39 | | 109 | | | | |
| 1wc | 281 | 11.52 | 12.33 | 93 | 100 | 8 | 4 | |
| 1w | 278 | 10.63 | | 86 | | | | |
| 1w | 279 | 10.30 | | 84 | | | | |
| 1w | 280 | 8.03 | | 65 | 78 | 11 | 7 | 0.053226 |
| 1mc | 263 | 15.18 | | 101 | | | | |
| 1mc | 265 | 14.20 | | 95 | | | | |
| 1mc | 282 | 15.53 | 14.97 | 104 | 100 | 5 | 3 | |
| 1m | 264 | 13.71 | | 92 | | | | |
| 1m | 266 | 13.39 | | 89 | | | | |
| 1m | 267 | 13.55 | | 91 | 91 | 1 | 1 | 0.025606 |
| 3mc | 246 | 13.06 | | 89 | | | | |
| 3mc | 248 | 14.85 | | 101 | | | | |
| 3mc | 251 | 14.85 | | 101 | | | | |
| 3mc | 254 | 16.47 | | 112 | | | | |
| 3mc | 256 | 15.01 | | 102 | | | | |
| 3mc | 258 | 14.04 | 14.71 | 95 | 100 | 8 | 3 | |
| 3m | 247 | 15.01 | | 102 | | | | |
| 3m | 249 | 18.59 | | 126 | | | | |
| 3m | 250 | 16.80 | | 114 | | | | |
| 3m | 252 | 15.66 | | 106 | | | | |
| 3m | 253 | 15.66 | | 106 | | | | |
| 3m | 255 | 18.42 | | 125 | | | | |
| 3m | 257 | 16.15 | | 110 | 113 | 10 | 4 | 0.022437 |

**Hippo**
**30nm** **GPx**
**1-20h** **activity**

| | | Avg | %Control | Avg %Control | Stdev | SEM |
|---|---|---|---|---|---|---|
| 216 | 25.47 | | 88 | | | |
| 217 | 33.96 | | 118 | | | |
| 220 | 25.47 | | 88 | | | |
| 223 | 25.47 | | 88 | | | |
| 224 | 33.96 | 28.87 | 118 | 100 | 16 | 7 |
| 218 | 36.38 | | 126 | | | |
| 219 | 36.38 | | 126 | | | |
| 221 | 36.38 | | 126 | | | |
| 222 | 33.96 | | 118 | | | |
| 225 | 33.96 | | 118 | 123 | 5 | 2 |
| | | | | 0.016355 | | |
| 199 | 25.47 | | 115 | | | |
| 200 | 16.98 | | 77 | | | |
| 203 | 25.47 | | 115 | | | |
| 206 | 16.98 | | 77 | | | |
| 207 | 25.47 | 22.07 | 115 | 100 | 21 | 9 |
| 198 | 8.49 | | | | | |
| 201 | 25.47 | | 115 | | | |
| 202 | 25.47 | | 115 | | | |
| 204 | 33.96 | | 154 | | | |
| 205 | 33.96 | | 154 | 135 | 22 | 10 |
| | | | | 0.047945 | | |

| **Hippo 30nm 30 days** | **GPx activity** | | | | | |
|---|---|---|---|---|---|---|
| | | **Avg** | **%Control** | **Avg %Control** | **Stdev** | **SEM** |
| 209 | 25 | | 98 | | | |
| 225 | 17 | | 65 | | | |
| 227 | 28 | | 107 | | | |
| 228 | 25 | | 98 | | | |
| 231 | 25 | | 98 | | | |
| 233 | 36 | | 137 | | | |
| 235 | 25 | 26 | 98 | 100 | 21 | 8 |
| 210 | 15 | | 59 | | | |
| 211 | 15 | | 59 | | | |
| 212 | 15 | | 59 | | | |
| 213 | 25 | | 98 | | | |
| 214 | 23 | | 88 | | | |
| 230 | 25 | | 98 | | | |
| 232 | 25 | | 98 | | | |
| 234 | 18 | | 68 | 78 | 19 | 7 |
| | | | | 0.053098 | | |

| | Hippo 30nm 90 days | GPx activity | | | | | | |
|---|---|---|---|---|---|---|---|---|
| | | | Avg | %Control | Avg %Control | Stdev | SEM | |
| 1dc | 260 | 38 | | 93 | | | | |
| 1dc | 261 | 38 | | 93 | | | | |
| 1dc | 270 | 47 | 41 | 114 | 100 | 12 | 7 | |
| 1d | 259 | 25 | | 62 | | | | |
| 1d | 271 | 34 | | 83 | | | | |
| 1d | 272 | 30 | | 72 | 72 | 10 | 6 | 0.039021 |
| 1wc | 268 | 47 | | 106 | | | | |
| 1wc | 269 | 47 | | 106 | | | | |
| 1wc | 281 | 38 | 44 | 87 | 100 | 11 | 6 | |
| 1w | 278 | 21 | | 48 | | | | |
| 1w | 279 | 21 | | 48 | | | | |
| 1w | 280 | 38 | | 87 | 61 | 22 | 13 | 0.055041 |
| 1mc | 263 | 38 | | 100 | | | | |
| 1mc | 265 | 38 | | 100 | | | | |
| 1mc | 282 | 38 | 38 | 100 | 100 | 0 | 0 | |
| 1m | 264 | 30 | | 78 | | | | |
| 1m | 266 | 25 | | 67 | | | | |
| 1m | 267 | 30 | | 78 | 74 | 6 | 4 | 0.002192 |
| 3mc | 246 | 25 | | 66 | | | | |
| 3mc | 248 | 42 | | 113 | | | | |
| 3mc | 251 | 42 | | 113 | | | | |
| 3mc | 254 | 30 | | 81 | | | | |
| 3mc | 256 | 42 | | 113 | | | | |
| 3mc | 258 | 42 | 37 | 113 | 100 | 21 | 9 | |
| 3m | 247 | 47 | | 125 | | | | |
| 3m | 249 | 42 | | 113 | | | | |
| 3m | 250 | 30 | | 79 | | | | |
| 3m | 252 | 30 | | 79 | | | | |
| 3m | 253 | 30 | | 79 | | | | |
| 3m | 255 | 30 | | 79 | | | | |
| 3m | 257 | 30 | | 79 | 91 | 20 | 7 | 0.425164 |

| **30nm 1-20h** | GR activity nmol/min/ml | Avg | % Control | Avg | Stdev | SEM |
|---|---|---|---|---|---|---|
| 216 | 110 | | 123 | | | |
| 217 | 84 | | 94 | | | |
| 220 | 97 | | 109 | | | |
| 223 | 84 | | 94 | | | |
| 224 | 71 | 89 | 80 | 100 | 16 | 7 |
| 218 | 97 | | 109 | | | |
| 219 | 122 | | 137 | | | |
| 221 | 59 | | 66 | | | |
| 222 | 84 | | 94 | | | |
| 225 | 71 | | 80 | 97 | 27 | 12 |
| 199 | 84 | | 86 | | | |
| 200 | 84 | | 86 | | | |
| 203 | 110 | | 113 | | | |
| 206 | 97 | | 99 | | | |
| 207 | 112 | 97 | 115 | 100 | 14 | 6 |
| 198 | 102 | | 105 | | | |
| 201 | 88 | | 91 | | | |
| 202 | 88 | | 91 | | | |
| 204 | 97 | | 99 | | | |
| 205 | 84 | | 86 | 94 | 7 | 3 |
| | | | | 0.448515 | | |

| **30nm 30 days** | GR activity nmol/min/ml | Avg | % Control | Avg | Stdev | SEM |
|---|---|---|---|---|---|---|
| 209 | 97 | | 98 | | | |
| 225 | 84 | | 85 | | | |
| 227 | 110 | | 111 | | | |
| 228 | 110 | | 111 | | | |
| 231 | 110 | | 111 | | | |
| 233 | | | | | | |
| 235 | 84 | 99 | 85 | 100 | 13 | 5 |
| 210 | 148 | | 149 | | | |
| 211 | 122 | | 124 | | | |
| 212 | 135 | | 136 | | | |
| 213 | 88 | | 89 | | | |
| 214 | 102 | | 103 | | | |
| 230 | 122 | | 124 | | | |
| 232 | 109 | | 110 | | | |
| 234 | 122 | 119 | 124 | 120 | 19 | 6 |

0.047001

| | GR activity nmol/min/ml | Avg | % Control | Avg | Stdev | SEM | |
|---|---|---|---|---|---|---|---|
| 1dc | 71 | | 93 | | | | |
| 1dc | 71 | | 93 | | | | |
| 1dc | 88 | 77 | 115 | 100 | 13 | 7 | |
| 1d | 84 | | 109 | | | | |
| 1d | 97 | | 126 | | | | |
| 1d | 71 | | 93 | 109 | 17 | 10 | 0.488251 |
| 1wc | 84 | | 105 | | | | |
| 1wc | 71 | | 89 | | | | |
| 1wc | 84 | 80 | 105 | 100 | 9 | 5 | |
| 1w | 71 | | 89 | | | | |
| 1w | 71 | | 89 | | | | |
| 1w | 71 | | 89 | 89 | 0 | 0 | 0.116117 |
| 1mc | 84 | | 111 | | | | |
| 1mc | 71 | | 94 | | | | |
| 1mc | 71 | 76 | 94 | 100 | 10 | 6 | |
| 1m | 71 | | 94 | | | | |
| 1m | 97 | | 128 | | | | |
| 1m | 97 | | 128 | 117 | 19 | 11 | 0.250815 |
| 3mc | 110 | | 124 | | | | |
| 3mc | 84 | | 95 | | | | |
| 3mc | 97 | | 110 | | | | |
| 3mc | 59 | | 66 | | | | |
| 3mc | 71 | | 81 | | | | |
| 3mc | 110 | 88 | 124 | 100 | 24 | 10 | |
| 3m | 84 | | 95 | | | | |
| 3m | 84 | | 95 | | | | |
| 3m | 110 | | 124 | | | | |
| 3m | 97 | | 110 | | | | |
| 3m | 97 | | 110 | | | | |
| 3m | 71 | | 81 | | | | |
| 3m | 97 | | 110 | 103 | 14 | 5 | |

| Hippo-PC 1h | % Control | Avg | Stdev | SEM | Hippo-PC-20h | % Control | | Avg | Avgavg |
|---|---|---|---|---|---|---|---|---|---|
| 216 | 103 | | | | 199 | 96 | | | |
| 217 | 104 | | | | 200 | 102 | | | |
| 220 | 95 | | | | 203 | 103 | | | |
| 223 | 98 | | | | 206 | 94 | | | |
| 224 | 101 | 100 | 4 | 2 | 207 | 105 | 100 | 5 | 2 |
| | | | | | | | | | |
| 218 | | | | | 198 | 90 | | | |
| 219 | 78 | | | | 201 | 96 | | | |
| 221 | 77 | | | | 202 | 96 | | | |
| 222 | 94 | | | | 204 | 79 | | | |
| 225 | 98 | 87 | 11 | 5 | 205 | 65 | 85 | 13 | 6 |
| | TTEST | 0.037 | | | | TTEST | 0.0501 | | |

| Hippo-3NT | % Control | Avg | Stdev | SEM | Hippo-3NT | % Control | Avg | Stdev | SEM |
|---|---|---|---|---|---|---|---|---|---|
| 216 | 99 | | | | 199 | 84 | | | |
| 217 | 104 | | | | 200 | 88 | | | |
| 220 | 95 | | | | 203 | 103 | | | |
| 223 | 104 | | | | 206 | 112 | | | |
| 224 | 99 | 100 | 4 | 2 | 207 | 113 | 100 | 13 | 6 |
| | | | | | | | | | |
| 218 | 92 | | | | 198 | 90 | | | |
| 219 | 96 | | | | 201 | 86 | | | |
| 221 | 74 | | | | 202 | 87 | | | |
| 222 | 94 | | | | 204 | 82 | | | |
| 225 | 92 | 90 | 9 | 4 | 205 | 65 | 82 | 10 | 4 |
| | TTEST | 0.049 | | | | TTEST | 0.0435 | | |

| Hippo-HNE | % Control | Avg | Stdev | SEM | Hippo-HNE | % Control | Avg | Stdev | SEM |
|---|---|---|---|---|---|---|---|---|---|
| 216 | 93 | | | | 199 | 102 | | | |
| 217 | 101 | | | | 200 | 117 | | | |
| 220 | 112 | | | | 203 | 99 | | | |
| 223 | 97 | | | | | 206 | 83 | | |
| 224 | 96 | 100 | 7 | 3 | 207 | 99 | 100 | 12 | 5 |
| 218 | 105 | | | | 198 | 98 | | | |
| 219 | 99 | | | | 201 | 93 | | | |
| 221 | | 99 | | | | 202 | 91 | | |
| 222 | | 67 | | | | 204 | 81 | | |
| 225 | 25123 | 75 | 89 | 17 | 8 | 205 | 74 | 87 | 10 |
| | | TTEST | 0.212 | | | | TTEST | 0.1018 | |

| Hippo-PC 30nm-30d | % Control | Avg | Stdev | SEM |
|---|---|---|---|---|
| c | 126 | | | |
| c | 113 | | | |
| c | 117 | | | |
| c | 125 | | | |
| c | 80 | | | |
| c | 61 | | | |
| c | 78 | 100 | 26 | 10 |
| | 143 | | | |
| | 128 | | | |
| | 159 | | | |
| | 114 | | | |
| | 147 | | | |
| | 121 | | | |
| | 129 | 134 | 16 | 6 |
| | | 0.012216 | | |

| Hippo-3NT | | 30nm-30d | |
|---|---|---|---|
| **% Control** | **Avg** | **Stdev** | **SEM** |
| 99 | | | |
| 82 | | | |
| 92 | | | |
| 90 | | | |
| 126 | | | |
| 110 | 100 | 16 | 6 |
| 126 | | | |
| 118 | | | |
| 99 | | | |
| 126 | | | |
| 124 | | | |
| 119 | | | |
| 151 | | | |
| 128 | 124 | 14 | 5 |
| | 0.011772 | | 1.702703 |

**Hippo-HNE**

| % Control | Avg | Stdev | SEM |
|---|---|---|---|
| 115 | | | |
| 88 | | | |
| 65 | | | |
| 108 | | | |
| 117 | | | |
| 106 | 100 | 20 | 8 |
| 107 | | | |
| 106 | | | |
| 119 | | | |
| 152 | | | |
| 128 | | | |
| 127 | | | |
| 113 | | | |
| 126 | 122 | 15 | 5 |

0.032935

**H-PC**

| | %Control | Avg | Std | SEM | TTEST |
|---|---|---|---|---|---|
| 1dc | 100 | | | | |
| 1dc | 92 | | | | |
| 1dc | 108 | 100 | 8 | 5 | |
| 1d | 126 | | | | |
| 1d | 129 | | | | |
| 1d | 119 | 125 | 5 | 3 | 0.010266 |
| | | | | | |
| 1wc | 89 | | | | |
| 1wc | 121 | | | | |
| 1wc | 89 | 100 | 19 | 11 | |
| 1w | 149 | | | | |
| 1w | 137 | | | | |
| 1w | 129 | 138 | 10 | 6 | 0.033998 |
| | | | | | |
| 1mc | 85 | | | | |
| 1mc | 93 | | | | |
| 1mc | 122 | 100 | 19 | 11 | |
| 1m | 135 | | | | |
| 1m | 128 | | | | |
| 1m | 142 | 135 | 7 | 4 | 0.041428 |
| | | | | | |
| 3mc | 107 | | | | |
| 3mc | 98 | | | | |
| 3mc | 93 | | | | |
| 3mc | 112 | | | | |
| 3mc | 87 | | | | |
| 3mc | 104 | 100 | 9 | 4 | |
| 3m | 82 | | | | |
| 3m | 100 | | | | |
| 3m | 76 | | | | |
| 3m | 62 | | | | |
| 3m | 81 | | | | |
| 3m | 102 | | | | |
| 3m | 90 | 85 | 14 | 5 | 0.045624 |

| H-3NT | %Control | Avg | Std | SEM | TTEST |
|---|---|---|---|---|---|
| 1dc | 104 | | | | |
| 1dc | 102 | | | | |
| 1dc | 94 | 100 | 5 | 3 | |
| 1d | 111 | | | | |
| 1d | 116 | | | | |
| 1d | 115 | 114 | 3 | 2 | 0.016201 |
| | | | | | |
| 1wc | 105 | | | | |
| 1wc | 96 | | | | |
| 1wc | 98 | 100 | 5 | 3 | |
| 1w | 104 | | | | |
| 1w | 101 | | | | |
| 1w | 92 | 99 | 6 | 4 | 0.836039 |
| | | | | | |
| 1mc | 100 | | | | |
| 1mc | 97 | | | | |
| 1mc | 102 | 100 | 3 | 2 | |
| 1m | 108 | | | | |
| 1m | 110 | | | | |
| 1m | 116 | 111 | 4 | 2 | 0.017827 |
| | | | | | |
| 3mc | 105 | | | | |
| 3mc | 100 | | | | |
| 3mc | 110 | | | | |
| 3mc | 107 | | | | |
| 3mc | 93 | | | | |
| 3mc | 84 | 100 | 10 | 4 | |
| 3m | 97 | | | | |
| 3m | 89 | | | | |
| 3m | 87 | | | | |
| 3m | 85 | | | | |
| 3m | 89 | | | | |
| 3m | 83 | | | | |
| 3m | 88 | 88 | 5 | 2 | 0.015865 |

| H-HNE | %Control | Avg | Std | SEM | TTEST |
|---|---|---|---|---|---|
| 1dc | 94 | | | | |
| 1dc | 101 | | | | |
| 1dc | 105 | 100 | 6 | 3 | |
| 1d | 101 | | | | |
| 1d | 96 | | | | |
| 1d | 111 | 103 | 8 | 5 | 0.68127 |
| | | | | | |
| 1wc | 93 | | | | |
| 1wc | 99 | | | | |
| 1wc | 109 | 100 | 8 | 5 | |
| 1w | 100 | | | | |
| 1w | 103 | | | | |
| 1w | 108 | 104 | 4 | 2 | 0.520642 |
| | | | | | |
| 1mc | 102 | | | | |
| 1mc | 100 | | | | |
| 1mc | 98 | 100 | 2 | 1 | |
| 1m | 108 | | | | |
| 1m | 111 | | | | |
| 1m | 111 | 110 | 2 | 1 | 0.003182 |
| | | | | | |
| 3mc | 89 | | | | |
| 3mc | 104 | | | | |
| 3mc | 102 | | | | |
| 3mc | 102 | | | | |
| 3mc | 106 | | | | |
| 3mc | 97 | 100 | 6 | 3 | |
| 3m | 97 | | | | |
| 3m | 85 | | | | |
| 3m | 95 | | | | |
| 3m | 94 | | | | |
| 3m | 97 | | | | |
| 3m | 100 | | | | |
| 3m | 96 | 95 | 5 | 2 | 0.132053 |

Caspase, IL-1beta, TNF and LC-3AB data

| 1h-20h Caspase- 1-20h | actin | Ratio | Avg | % Control | Avg | Stdev | SEM |
|---|---|---|---|---|---|---|---|
| 1675 | 38992 | 0.042958 | | 96 | | | |
| 2707 | 50631 | 0.053462 | | 120 | | | |
| 2393 | 52814 | 0.045302 | | 101 | | | |
| 1494 | 40299 | 0.037073 | 0.044699 | 83 | 100 | 15 | 8 |
| 3019 | 49885 | 0.060519 | | 135 | | | |
| 2486 | 39947 | 0.062243 | | 139 | | | |
| 2312 | 46658 | 0.049559 | | 111 | | | |
| 2005 | 48707 | 0.041172 | | 92 | 119 | 22 | 11 |
| | | | | | 0.519571 | | |
| 1895 | 35058 | 0.054053 | | 78 | | | |
| 2786 | 38189 | 0.072954 | | 105 | | | |
| 2959 | 39491 | 0.074937 | | 108 | | | |
| 3140 | 41075 | 0.076455 | 0.0696 | 110 | 100 | 15 | 8 |
| 3287 | 38654 | 0.085036 | | 122 | | | |
| 3254 | 34572 | 0.094108 | | 135 | | | |
| 3193 | 38724 | 0.082462 | | 118 | | | |
| 2930 | 41400 | 0.070783 | | 102 | 119 | 14 | 7 |
| | | | | | 0.10613 | | |

| 1d- 7d Caspase- 1-20h | actin | Ratio | Avg | % Control | Avg | Stdev | SEM |
|---|---|---|---|---|---|---|---|
| 26202 | 5817 | 4.504453 | | 107 | | | |
| 30439 | 7178 | 4.240372 | | 101 | | | |
| 25582 | 6603 | 3.874365 | 4.206397 | 92 | 100 | 8 | 4 |
| 25778 | 5999 | 4.296842 | | 102 | | | |
| 29044 | 7643 | 3.800292 | | 90 | | | |
| 30543 | 7573 | 4.033243 | | 96 | 96 | 6 | 3 |
| 22902 | 19435 | 1.178403 | | 113 | | | |
| 20061 | 21331 | 0.940461 | | 90 | | | |
| 25297 | 24915 | 1.015334 | 1.044733 | 97 | 100 | 12 | 7 |
| 21635 | 25768 | 0.83961 | | 80 | | | |
| 25427 | 22446 | 1.132815 | | 108 | | | |
| 18657 | 22461 | 0.83064 | | 80 | 89 | 16 | 10 |
| | | | | | 0.415384 | | |

| | | 30d-90d Caspase- 1-20h | actin | Ratio | Avg | % Control | Avg | Stdev | SEM |
|---|---|---|---|---|---|---|---|---|---|
| 30d C | 209 | 29829 | 9895 | 3.014359 | | 96 | | | |
| 30d C | 225 | 33815 | 9124 | 3.706342 | | 118 | | | |
| 30d C | 227 | 31929 | 9271 | 3.443959 | | 109 | | | |
| 30d C | 228 | 32649 | 11518 | 2.834577 | | 90 | | | |
| 30d C | 231 | 28990 | 10492 | 2.762978 | 3.152443 | 88 | 100 | 13 | 6 |
| | 210 | 30130 | 8218 | 3.666235 | | 116 | | | |
| | 211 | 39160 | 9733 | 4.023479 | | 128 | | | |
| | 212 | 38131 | 10382 | 3.672753 | | 117 | | | |
| | 213 | 34130 | 8441 | 4.04346 | | 128 | | | |
| | 214 | 39285 | 8129 | 4.832478 | | 153 | | | |
| | 230 | 27578 | 10930 | 2.523133 | | | 128 | 15 | 6 |
| | | | | | | | 0.012628 | | |
| 90d C | 246 | 25438 | 20253 | 1.256011 | | 109 | | | |
| 90d C | 248 | 31759 | 28010 | 1.133876 | | 98 | | | |
| 90d C | 251 | 28357 | 26831 | 1.056875 | | 92 | | | |
| 90d C | 254 | 33308 | 24282 | 1.371741 | | 119 | | | |
| 90d C | 256 | 21132 | 22189 | 0.952351 | 1.154171 | 83 | 100 | 14 | 6 |
| | 247 | 31821 | 25291 | 1.258183 | | 109 | | | |
| | 249 | 32004 | 23293 | 1.373964 | | 119 | | | |
| | 250 | 30173 | 21843 | 1.381371 | | 120 | | | |
| | 252 | 28559 | 25430 | 1.123066 | | 97 | | | |
| | 253 | 28835 | 31788 | 0.907103 | | 79 | | | |
| | 255 | 27630 | 22583 | 1.223469 | | 106 | 105 | 15 | 6 |

| IL-1B | actin | Ratio | Avg | % Control | Avg | Stdev | SEM |
|---|---|---|---|---|---|---|---|
| 13890 | 24786 | 0.560399 | | 117 | | | |
| 9565 | 21619 | 0.442426 | | 93 | | | |
| 10640 | 30793 | 0.345533 | | 72 | | | |
| 13851 | 24749 | 0.559655 | 0.477003 | 117 | 100 | 22 | 11 |
| 22147 | 42987 | 0.515212 | | 108 | | | |
| 9535 | 21191 | 0.449961 | | 94 | | | |
| 1324 | 34651 | 0.038215 | | | | | |
| 8278 | 28599 | 0.289452 | | 61 | 88 | 24 | 12 |
| | | | | | 0.446916 | | |
| 11273 | 15363 | 0.733793 | | 103 | | | |
| 13611 | 23292 | 0.584358 | | 82 | | | |
| 12939 | 19770 | 0.654467 | | 92 | | | |
| 15099 | 17247 | 0.875462 | 0.71202 | 123 | 100 | 18 | 9 |
| 14726 | 24415 | 0.603162 | | 85 | | | |
| 13626 | 19484 | 0.699363 | | 98 | | | |
| 9948 | 18939 | 0.52526 | | 74 | | | |
| 14917 | 25926 | 0.575356 | | 81 | 84 | 10 | 5 |
| | | | | | 0.175264 | | |

| IL-1B | actin | Ratio | Avg | % Control | Avg | Stdev | SEM |
|---|---|---|---|---|---|---|---|
| 28591 | 13850 | 2.064267 | | 90 | | | |
| 32641 | 14744 | 2.213825 | | 97 | | | |
| 34061 | 13276 | 2.565592 | 2.281228 | 112 | 100 | 11 | 7 |
| 29969 | 11468 | 2.613142 | | 115 | | | |
| 36302 | 11109 | 3.26767 | | 143 | | | |
| 33245 | 9473 | 3.509525 | | 154 | 137 | 20 | 12 |
| | | | | | 0.05022 | | |
| 22852 | 11262 | 2.02913 | | 87 | | | |
| 23406 | 10003 | 2.339798 | | 100 | | | |
| 28929 | 10874 | 2.660318 | 2.343082 | 114 | 100 | 13 | 8 |

| IL-1B | actin | Ratio | Avg | % Control | Avg | Stdev | SEM |
|---|---|---|---|---|---|---|---|
| 13890 | 24786 | 0.560399 | | 117 | | | |
| 9565 | 21619 | 0.442426 | | 93 | | | |
| 10640 | 30793 | 0.345533 | | 72 | | | |
| 13851 | 24749 | 0.559655 | 0.477003 | 117 | 100 | 22 | 11 |
| 22147 | 42987 | 0.515212 | | 108 | | | |
| 9535 | 21191 | 0.449961 | | 94 | | | |
| 1324 | 34651 | 0.038215 | | | | | |
| 8278 | 28599 | 0.289452 | | 61 | 88 | 24 | 12 |
| | | | | | 0.446916 | | |
| 11273 | 15363 | 0.733793 | | 103 | | | |
| 13611 | 23292 | 0.584358 | | 82 | | | |
| 12939 | 19770 | 0.654467 | | 92 | | | |
| 15099 | 17247 | 0.875462 | 0.71202 | 123 | 100 | 18 | 9 |
| 14726 | 24415 | 0.603162 | | 85 | | | |
| 13626 | 19484 | 0.699363 | | 98 | | | |
| 9948 | 18939 | 0.52526 | | 74 | | | |
| 14917 | 25926 | 0.575356 | | 81 | 84 | 10 | 5 |
| | | | | | 0.175264 | | |

| IL-1B | actin | Ratio | Avg | % Control | Avg | Stdev | SEM |
|---|---|---|---|---|---|---|---|
| 28591 | 13850 | 2.064267 | | 90 | | | |
| 32641 | 14744 | 2.213825 | | 97 | | | |
| 34061 | 13276 | 2.565592 | 2.281228 | 112 | 100 | 11 | 7 |
| 29969 | 11468 | 2.613142 | | 115 | | | |
| 36302 | 11109 | 3.26767 | | 143 | | | |
| 33245 | 9473 | 3.509525 | | 154 | 137 | 20 | 12 |
| | | | | | 0.05022 | | |
| 22852 | 11262 | 2.02913 | | 87 | | | |
| 23406 | 10003 | 2.339798 | | 100 | | | |
| 28929 | 10874 | 2.660318 | 2.343082 | 114 | 100 | 13 | 8 |
| 28955 | 11046 | 2.621283 | | 112 | | | |
| 27860 | 12405 | 2.245818 | | 96 | | | |
| 26749 | 10060 | 2.658828 | | 113 | 107 | 10 | 6 |
| | | | | | 0.502512 | | |

| IL-1B | actin | Ratio | Avg | % Control | Avg | Stdev | SEM |
|---|---|---|---|---|---|---|---|
| 33151 | 10060 | | | | | | |
| 21650 | 9247 | 2.341421 | | 96 | | | |
| 21433 | 9080 | 2.360593 | | 97 | | | |
| 23267 | 9092 | 2.559063 | | 105 | | | |
| 24206 | 9849 | 2.457669 | 2.429686 | 101 | 100 | 4 | 2 |
| 36416 | 9466 | 3.847052 | | 158 | | | |
| 34382 | 9650 | 3.56275 | | 147 | | | |
| 35201 | 10518 | 3.346739 | | 138 | | | |
| 28778 | 9822 | 2.930102 | | 121 | | | |
| 13928 | 8919 | 1.561626 | | | | | |
| 23708 | 8408 | 2.819819 | | 116 | 136 | 18 | 7 |
| | | | | | 0.005729 | | |
| 37548 | 13554 | 2.770204 | | 97 | | | |
| 35950 | 12697 | 2.831521 | | 99 | | | |
| 35861 | 11441 | 3.134454 | | 110 | | | |
| 22892 | 10725 | 2.134462 | | 75 | | | |
| 29994 | 8908 | 3.367071 | 2.847542 | 118 | 100 | 16 | 7 |
| 38924 | 11429 | 3.405639 | | 120 | | | |
| 14328 | 10396 | 1.37826 | | | | | |
| 23843 | 10354 | 2.302882 | | 81 | | | |
| 37385 | 10367 | 3.606143 | | 127 | | | |
| 17967 | 7722 | 2.326693 | | 82 | | | |
| 26095 | 7419 | 3.51754 | | 124 | 106 | 23 | 9 |

| TNF | actin | Ratio | Avg | % Control | Avg | Stdev | SEM |
|---|---|---|---|---|---|---|---|
| 7654 | 26485 | 0.288994 | | 108 | | | |
| 5853 | 24584 | 0.238067 | | 89 | | | |
| 5420 | 21440 | 0.252777 | | 95 | | | |
| 5527 | 19223 | 0.28752 | 0.26684 | 108 | 100 | 10 | 5 |
| 5949 | 30688 | 0.193837 | | 73 | | | |
| 5138 | 27652 | 0.185826 | | 70 | | | |
| 5871 | 26699 | 0.219902 | | 82 | | | |
| 5096 | 28392 | 0.179495 | | 67 | 73 | 7 | 3 |
| | | | | | 0.003524 | | |
| 3789 | 20072 | 0.18875 | | 77 | | | |
| 4497 | 22027 | 0.204158 | | 84 | | | |
| 8425 | 29047 | 0.290043 | | 119 | | | |
| 8803 | 29905 | 0.294379 | 0.244332 | 120 | 100 | 23 | 11 |
| 4955 | 19684 | 0.251714 | | 103 | | | |
| 3225 | 21036 | 0.153296 | | 63 | | | |
| 3475 | 22704 | 0.153035 | | 63 | | | |
| 4945 | 25769 | 0.191913 | | 79 | 77 | 19 | 10 |
| | | | | | 0.168244 | | |

| TNF | actin | Ratio | Avg | % Control | Avg | Stdev | SEM |
|---|---|---|---|---|---|---|---|
| 5848 | 24596 | 0.237751 | | 117 | | | |
| 5202 | 26955 | 0.192982 | | 95 | | | |
| 4772 | 26681 | 0.178844 | 0.203193 | 88 | 100 | 15 | 9 |
| 8748 | 23828 | 0.367144 | | | | | |
| 4435 | 26012 | 0.170482 | | 84 | | | |
| 5836 | 25349 | 0.230226 | | 113 | 99 | 21 | 12 |
| 15516 | 32558 | 0.476556 | | 113 | | | |
| 11381 | 30912 | 0.36817 | | 87 | | | |
| 14530 | 34443 | 0.421851 | 0.422192 | 100 | 100 | 13 | 7 |
| 15394 | 31554 | 0.487871 | | 116 | | | |
| 14024 | 31131 | 0.450473 | | 107 | | | |
| 11744 | 36604 | 0.320834 | | 76 | 99 | 21 | 12 |

| TNF | actin | Ratio | Avg | % Control | Avg | Stdev | SEM |
|---|---|---|---|---|---|---|---|
| 4288 | 26990 | 0.158878 | | 71 | | | |
| 6237 | 19119 | 0.326205 | | 146 | | | |
| 3687 | 19281 | 0.19124 | | 86 | | | |
| 6128 | 20365 | 0.300931 | | 135 | | | |
| 2800 | 20309 | 0.137862 | 0.223023 | 62 | 100 | 38 | 17 |
| 2180 | 24605 | 0.088598 | | 40 | | | |
| 3924 | 23698 | 0.165566 | | 74 | | | |
| 4191 | 22641 | 0.185125 | | 83 | | | |
| 4266 | 21735 | 0.196272 | | 88 | | | |
| 6378 | 19618 | 0.3251 | | | | | |
| 3652 | 17646 | 0.206947 | | 93 | 76 | 21 | 9 |
| | | | | | | | |
| 13973 | 33749 | 0.414026 | | 81 | | | |
| 15636 | 38006 | 0.411409 | | 81 | | | |
| 15454 | 41479 | 0.372577 | | 73 | | | |
| 18424 | 26611 | 0.692328 | | 136 | | | |
| 17222 | 26437 | 0.65144 | 0.508356 | 128 | 100 | 30 | 13 |
| 14268 | 37267 | 0.382866 | | 75 | | | |
| 8272 | 43169 | 0.191626 | | 38 | | | |
| 24431 | 44637 | 0.547324 | | 108 | | | |
| 15284 | 33970 | 0.449915 | | 89 | | | |
| 14763 | 29877 | 0.494126 | | 97 | | | |
| 15660 | 21185 | 0.739184 | | 145 | 92 | 36 | 15 |

| LC-3 | actin | Ratio | Avg | % Control | Avg | Stdev | SEM |
|---|---|---|---|---|---|---|---|
| 117260 | 37652 | 3.114308 | | 120 | | | |
| 98561 | 37922 | 2.599052 | | 100 | | | |
| 100158 | 35767 | 2.800323 | | 107 | | | |
| 76871 | 40317 | 1.906666 | 2.605087 | 73 | 100 | 20 | 10 |
| 110951 | 34521 | 3.214027 | | 123 | | | |
| 104369 | 33605 | 3.105736 | | 119 | | | |
| 78791 | 36179 | 2.177778 | | 84 | | | |
| 72595 | 37930 | 1.913951 | | 73 | 100 | 25 | 13 |
| | | | | | | | |
| 88113 | 39901 | 2.208278 | | 87 | | | |
| 87676 | 38778 | 2.260983 | | 89 | | | |
| 102008 | 37645 | 2.709746 | | 107 | | | |
| 112218 | 37734 | 2.973935 | 2.538235 | 117 | 100 | 14 | 7 |
| 88471 | 40173 | 2.202253 | | 87 | | | |
| 112048 | 36152 | 3.099363 | | 122 | | | |
| 87261 | 39772 | 2.194047 | | 86 | | | |
| 99310 | 37976 | 2.61509 | | 103 | 100 | 17 | 8 |

| LC-3 | actin | Ratio | Avg | % Control | Avg | Stdev | SEM |
|---|---|---|---|---|---|---|---|
| 55534 | 25391 | 2.187138 | | 91 | | | |
| 66982 | 26750 | 2.504016 | | 104 | | | |
| 70844 | 27828 | 2.545786 | 2.412313 | 106 | 100 | 8 | 5 |
| 50457 | 25463 | 1.98161 | | 82 | | | |
| 70318 | 28795 | 2.442034 | | 101 | | | |
| 72514 | 28522 | 2.542423 | | 105 | 96 | 12 | 7 |
| | | | | | | | |
| 89504 | 22613 | 3.958158 | | 98 | | | |
| 85866 | 24804 | 3.461765 | | 86 | | | |
| 130141 | 27980 | 4.651209 | 4.023711 | 116 | 100 | 15 | 9 |
| 102285 | 20496 | 4.990466 | | 124 | | | |
| 132599 | 23949 | 5.536847 | | 138 | | | |
| 125783 | 25925 | 4.851792 | | 121 | 127 | 9 | 5 |
| | | | | | 0.052244 | | |

| LC-3 | actin | Ratio | Avg | % Control | Avg | Stdev | SEM |
|---|---|---|---|---|---|---|---|
| 68398 | 29027 | 2.356367 | | 98 | | | |
| 75630 | 30242 | 2.500823 | | 104 | | | |
| 77250 | 33005 | 2.34058 | | 97 | | | |
| 68316 | 30083 | 2.270928 | | 94 | | | |
| 74331 | 28467 | 2.611116 | 2.415963 | 108 | 100 | 6 | 3 |
| 75226 | 26989 | 2.7873 | | 115 | | | |
| 72948 | 23789 | 3.06646 | | 127 | | | |
| 69009 | 23461 | 2.941448 | | 122 | | | |
| 60497 | 22330 | 2.709219 | | 112 | | | |
| 72226 | 26868 | 2.688168 | | 111 | | | |
| 77475 | 26288 | 2.947164 | | 122 | 118 | 6 | 3 |
| | | | | | 0.000729 | | |
| 142052 | 21667 | 6.556126 | | 115 | | | |
| 132849 | 23789 | 5.584601 | | 98 | | | |
| 116759 | 23207 | 5.031186 | | 88 | | | |
| 94796 | 17667 | 5.365719 | | 94 | | | |
| 92201 | 15511 | 5.944285 | 5.696384 | 104 | 100 | 10 | 5 |
| 133505 | 25013 | 5.337411 | | 94 | | | |
| 129169 | 26110 | 4.947164 | | 87 | | | |
| 112272 | 26140 | 4.295091 | | 75 | | | |
| 95496 | 23364 | 4.087251 | | 72 | | | |
| 95948 | 20566 | 4.665378 | | 82 | | | |
| 93666 | 16817 | 5.569701 | | 98 | 85 | 10 | 4 |
| | | | | | 0.034094 | | |

Ceria nanorod PC, 3NT and HNE at 1 h

| H-PC % Control | Avg | SEM | H-3NT % Control | Avg | SEM | H-HNE % Control | Avg | SEM |
|---|---|---|---|---|---|---|---|---|
| 104 | | | 73 | | | 97 | | |
| 119 | | | 86 | | | 105 | | |
| 96 | | | 120 | | | 96 | | |
| 81 | | | 140 | | | 102 | | |
| 100 | 100 | 6 | 82 | 100 | 13 | 100 | 100 | 2 |
| 50 | | | 115 | | | 98 | | |
| 55 | | | 95 | | | 88 | | |
| 72 | | | 131 | | | 113 | | |
| 95 | | | 75 | | | 82 | | |
| 95 | 73 | 9 | 71 | 97 | 11 | 103 | 97 | 5 |
| | 0.045879 | | | | | | | |

Ceria nanorod PC, 3NT and HNE at 30d

| H-PC % Control | Avg | SEM | H-3NT % Control | Avg | SEM | H-HNE % Control | Avg | SEM |
|---|---|---|---|---|---|---|---|---|
| 108 | | | 78 | | | 103 | | |
| 115 | | | 78 | | | 114 | | |
| 74 | | | 125 | | | 98 | | |
| 74 | | | 119 | | | 79 | | |
| 130 | 100 | 11 | | 100 | 11 | 106 | 100 | 6 |
| 133 | | | 64 | | | 117 | | |
| 116 | | | 105 | | | 105 | | |
| 120 | | | 109 | | | 106 | | |
| 153 | | | 145 | | | 83 | | |
| 159 | 136 | 9 | 177 | 120 | 19 | 99 | 102 | 6 |
| | 0.034014 | | | | | | | |

| 1 h | Codes | H1-catalase | H1-actin | Ratio | Avg | % Control | Avg | Stdev | SEM |
|---|---|---|---|---|---|---|---|---|---|
| C | 300 | 25791 | 104906 | 25 | | 101 | | | |
| C | 302 | 23834 | 94695 | 25 | | 103 | | | |
| C | 304 | 21704 | 88502 | 25 | | 100 | | | |
| C | 306 | 27861 | 111602 | 25 | | 102 | | | |
| C | 308 | 24788 | 107684 | 23 | 24 | 94 | 100 | 3 | 2 |
| | 301 | 18529 | 85905 | 22 | | 88 | | | |
| | 303 | 22402 | 105374 | 21 | | 87 | | | |
| | 305 | 26600 | 86898 | 31 | | 125 | | | |
| | 307 | 23498 | 105424 | 22 | | 91 | | | |
| | 309 | 21175 | 70720 | 30 | | 122 | 103 | 19 | 9 |
| | | | | | | | 0.758464 | | |

| 30 d | Codes | H1-catalase | H1-actin | Ratio | Avg | % Control | Avg | Stdev | SEM |
|---|---|---|---|---|---|---|---|---|---|
| C | 310 | 48843 | 87740 | 56 | | 106 | | | |
| C | 312 | 59617 | 110974 | 54 | | 102 | | | |
| C | 314 | 55210 | 104871 | 53 | | 100 | | | |
| C | 316 | 60859 | 118461 | 51 | | 98 | | | |
| C | 318 | 44771 | 90269 | 50 | 53 | 94 | 100 | 4 | 2 |
| | 311 | 60320 | 105123 | 57 | | 109 | | | |
| | 313 | 54661 | 104248 | 52 | | 100 | | | |
| | 315 | 49007 | 92481 | 53 | | 101 | | | |
| | 317 | 49716 | 94416 | 53 | | 100 | | | |
| | 319 | 51164 | 78146 | 65 | | 124 | 107 | 11 | 5 |
| | | | | | | | 0.220555 | | |

| H1- GPx | H1- actin | Ratio | Avg | % Control | Avg | Stdev | SEM |
|---|---|---|---|---|---|---|---|
| 17960.92 | 84906.1 | 21 | | 75 | | | |
| 25988 | 94694.85 | 27 | | 97 | | | |
| 31226.06 | 88501.5 | 35 | | 125 | | | |
| 34491.29 | 91602 | 38 | | 133 | | | |
| 21399.81 | 107683.7 | 20 | 28 | 70 | 100 | 28 | 13 |
| | | | | | | | |
| 25703.38 | 85904.69 | 30 | | 106 | | | |
| 31565 | 105374.3 | 30 | | 106 | | | |
| 35250.72 | 96898 | 36 | | 129 | | | |
| 17657 | 95423.9 | 19 | | 65 | | | |
| 34971.33 | 90720 | 39 | | 136 | 108 | 28 | 12 |
| | | | | | 0.647705 | | |

| H1- GPx | H1- actin | Ratio | Avg | % Control | Avg | Stdev | SEM |
|---|---|---|---|---|---|---|---|
| 26410 | 87740 | 30 | | 92 | | | |
| 34173 | 110974 | 31 | | 94 | | | |
| 36549 | 104871 | 35 | | 107 | | | |
| 38179 | 118461 | 32 | | 99 | | | |
| 31650 | 90269 | 35 | 33 | 108 | 100 | 7 | 3 |
| | | | | | | | |
| 27632 | 105123 | 26 | | 81 | | | |
| 33728 | 104248 | 32 | | 99 | | | |
| 39190 | 102481 | 38 | | 117 | | | |
| 35343 | 104416 | 34 | | 104 | | | |
| 37192 | 78146 | 48 | | 146 | 109 | 24 | 11 |
| | | | | | 0.43114 | | |

| H2-GR | H2-actin | Ratio | Avg | % Control | Avg | Stdev | SEM |
|---|---|---|---|---|---|---|---|
| 94942.24 | 65455.89 | 145 | | 146 | | | |
| 65358.5 | 71026.85 | 92 | | 93 | | | |
| 62995.75 | 67575.25 | 93 | | 94 | | | |
| 76752.22 | 78393.14 | 98 | | 99 | | | |
| 76415.66 | 111245.6 | 69 | 99 | 69 | 100 | 28 | 13 |
| | | | | | | | |
| 74610.6 | 53758.05 | 139 | | 140 | | | |
| 76930.27 | 59538 | 129 | | 130 | | | |
| 74888.29 | 93177 | 80 | | 81 | | | |
| 75339 | 124171.9 | 61 | | 61 | | | |
| 92995.5 | 91937.76 | 101 | | 102 | 103 | 33 | 15 |
| | | | | | 0.893299 | | |

| H2-GR | H2-actin | Ratio | Avg | % Control | Avg | Stdev | SEM |
|---|---|---|---|---|---|---|---|
| 95660 | 122352 | 78 | | 109 | | | |
| 84515 | 131233 | 64 | | 90 | | | |
| 111991 | 150220 | 75 | | 104 | | | |
| 89449 | 124089 | 72 | | 101 | | | |
| 81165 | 116994 | 69 | 72 | 97 | 100 | 7 | 3 |
| | | | | | | | |
| 121261 | 132661 | 91 | | 127 | | | |
| 105956 | 122771 | 86 | | 120 | | | |
| 70057 | 105593 | 66 | | 93 | | | |
| 75391 | 112765 | 67 | | 93 | | | |
| 80259 | 113755 | 71 | | 98 | 106 | 16 | 7 |
| | | | | | 0.44838 | | |

| H2-MnSOD | H2-actin | Ratio | Avg | % Control | Avg | Stdev | SEM |
|---|---|---|---|---|---|---|---|
| 74571 | 65455.89 | 114 | | 101 | | | |
| 83764 | 71026.85 | 118 | | 105 | | | |
| 87771 | 67575.25 | 130 | | 115 | | | |
| 93895 | 78393.14 | 120 | | 107 | | | |
| 89889 | 111245.6 | 81 | 112 | 72 | 100 | 17 | 7 |
| | | | | | | | |
| 66235 | 53758.05 | 123 | | 110 | | | |
| 83715.5 | 59538 | 141 | | 125 | | | |
| 100662.3 | 93177 | 108 | | 96 | | | |
| 83528 | 124171.9 | 67 | | 60 | | | |
| 90010 | 91937.76 | 98 | | 87 | 96 | 25 | 11 |
| | | | | | 0.743057 | | |

| H2-MnSOD | H2-actin | Ratio | Avg | % Control | Avg | Stdev | SEM |
|---|---|---|---|---|---|---|---|
| 58047 | 122352 | 47 | | 97 | | | |
| 64360 | 131233 | 49 | | 101 | | | |
| 61548 | 130220 | 47 | | 97 | | | |
| 63006 | 124089 | 51 | | 104 | | | |
| 57538 | 116994 | 49 | 49 | 101 | 100 | 3 | 1 |
| | | | | | | | |
| 63843 | 132661 | 48 | | 99 | | | |
| 59203 | 122771 | 48 | | 99 | | | |
| 48856 | 95593 | 51 | | 105 | | | |
| 63124 | 122765 | 51 | | 105 | | | |
| 58429 | 113755 | 51 | | 105 | 103 | 4 | 2 |
| | | | | | 0.228172 | | |

| H3- Hsp-32 | H3-actin | Ratio | Avg | % Control | Avg | Stdev | SEM |
|---|---|---|---|---|---|---|---|
| 34407.75 | 64501 | 53 | | 101 | | | |
| 48206.93 | 73955.29 | 65 | | 123 | | | |
| 30558.02 | 82060.62 | 37 | | 70 | | | |
| 46972.33 | 68506.54 | 69 | | 129 | | | |
| 41121.93 | 100806.4 | 41 | 53 | 77 | 100 | 26 | 12 |
| | | | | | | | |
| 41208.92 | 77315.62 | 53 | | 101 | | | |
| 38618.59 | 87758.08 | 44 | | 83 | | | |
| 41328.41 | 80740.6 | 51 | | 97 | | | |
| 38309.09 | 70582.6 | 54 | | 102 | | | |
| 40822.7 | 76962.11 | 53 | | 100 | 96 | 8 | 4 |
| | | | | | 0.783199 | | |

| H3- Hsp-32 | H3-actin | Ratio | Avg | % Control | Avg | Stdev | SEM |
|---|---|---|---|---|---|---|---|
| 21063 | 108660 | 19 | | 80 | | | |
| 31249 | 100651 | | | | | | |
| 24146 | 88341 | 27 | | 113 | | | |
| 21237 | 89665 | 24 | | 98 | | | |
| 22303 | 83911 | 27 | 24 | 110 | 100 | 15 | 7 |
| | | | | | | | |
| 24661 | 84883 | 29 | | 120 | | | |
| 29342 | 82365 | 36 | | 147 | | | |
| 22284 | 74691 | 30 | | 123 | | | |
| 21520 | 78953 | 27 | | 112 | | | |
| 26065 | 72920 | 36 | | 147 | 130 | 16 | 7 |
| | | | | | 0.024616 | | |

| H4- Hsp-70 | H4-actin | Ratio | Avg | % Control | Avg | Stdev | SEM |
|---|---|---|---|---|---|---|---|
| 22615 | 28573 | 79 | | 73 | | | |
| 17471 | 20315 | 86 | | 79 | | | |
| 18429.35 | 17590.5 | 105 | | 97 | | | |
| 20026 | 16963 | 118 | | 109 | | | |
| 19963 | 13012 | 153 | 108 | 142 | 100 | 27 | 12 |
| | | | | | | | |
| 17148 | 24795 | 69 | | 64 | | | |
| 19246.5 | 20642.09 | 93 | | 86 | | | |
| 22355.24 | 18762.39 | 119 | | 110 | | | |
| 18095.5 | 13790.94 | 131 | | 121 | | | |
| 16390.65 | 11212.6 | 146 | | 135 | 103 | 28 | 13 |
| | | | | | 0.858505 | | |

| H4- Hsp-70 | H4-actin | Ratio | Avg | % Control | Avg | Stdev | SEM |
|---|---|---|---|---|---|---|---|
| 4553 | 67088 | 7 | | 123 | | | |
| 5288 | 69844 | 8 | | 137 | | | |
| 4420 | 71980 | 6 | | 111 | | | |
| 2356 | 67023 | 4 | | 64 | | | |
| 2281 | 63630 | 4 | 6 | 65 | 100 | 34 | 15 |
| | | | | | | | |
| 4975 | 67819 | 7 | | 133 | | | |
| 4230 | 72933 | 6 | | 105 | | | |
| 2629 | 40768 | 6 | | 117 | | | |
| 2955 | 47513 | 6 | | 113 | | | |
| 2607 | 44270 | 6 | | 107 | 115 | 11 | 5 |
| | | | | | 0.378849 | | |

| Hippo-1h Low aspect Hippo | Catalase activity | Avg | %Control | Avg %Cotrol | STDEV | SEM |
|---|---|---|---|---|---|---|
| 310 | 12.25 | | 88 | | | |
| 312 | 12.74 | | 91 | | | |
| 314 | 14.20 | | 102 | | | |
| 316 | 15.01 | | 107 | | | |
| 318 | 15.66 | 13.97 | 112 | 100 | 10 | 5 |
| 311 | 18.96 | | 136 | | | |
| 313 | 14.36 | | 103 | | | |
| 315 | 20.19 | | 144 | | | |
| 317 | 15.66 | | 112 | | | |
| 319 | 16.64 | | 119 | 123 | 17 | 8 |
| | | | | 0.034 | | |
| **Cortex** | | | | | | |
| 310 | 14.36 | | 88 | | | |
| 312 | 17.29 | | 106 | | | |
| 314 | 17.94 | | 110 | | | |
| 316 | 16.15 | | 99 | | | |
| 318 | 15.50 | 16.25 | 95 | 100 | 9 | 4 |
| 311 | 17.61 | | 108 | | | |
| 313 | 20.21 | | 124 | | | |
| 315 | 19.72 | | 121 | | | |
| 317 | 18.59 | | 114 | | | |
| 319 | 18.59 | | 114 | 117 | 6 | 3 |
| | | | | 0.009 | | |
| **Cereb** | | | | | | |
| 310 | 16.64 | | 94 | | | |
| 312 | 16.80 | | 95 | | | |
| 314 | 19.24 | | 109 | | | |
| 316 | 16.80 | | 95 | | | |
| 318 | 18.91 | 17.68 | 107 | 100 | 7 | 3 |
| 311 | 22.49 | | 127 | | | |
| 313 | 22.49 | | 127 | | | |
| 315 | 18.59 | | 105 | | | |
| 317 | 19.24 | | 109 | | | |
| 319 | 23.30 | | 132 | 120 | 12 | 5 |
| | | | | 0.013 | | |

| Hippo-30 days Low aspect Hippo | Catalase activity | Avg | %Control | Avg %Cotrol | STDEV | SEM |
|---|---|---|---|---|---|---|
| 300 | 16.80 | | 104 | | | |
| 302 | 14.20 | | 88 | | | |
| 304 | 16.15 | | 100 | | | |
| 306 | 15.66 | | 97 | | | |
| 308 | 17.82 | 16.13 | 111 | 100 | 8 | 4 |
| 301 | 13.23 | | 82 | | | |
| 303 | 11.60 | | 72 | | | |
| 305 | 13.23 | | 82 | | | |
| 307 | 12.09 | | 75 | | | |
| 309 | 16.80 | | 104 | 83 | 13 | 6 |
| | | | | 0.036 | | |
| **Cortex** | | | | | | |
| 300 | 19.07 | | 100 | | | |
| 302 | 18.42 | | 97 | | | |
| 304 | 21.22 | | 112 | | | |
| 306 | 19.24 | | 101 | | | |
| 308 | 16.96 | 18.98 | 89 | 100 | 8 | 4 |
| 301 | 18.75 | | 99 | | | |
| 303 | 16.31 | | 86 | | | |
| 305 | 18.10 | | 95 | | | |
| 307 | 13.55 | | 71 | | | |
| 309 | 16.47 | | 87 | 88 | 11 | 5 |
| | | | | 0.072 | | |
| **Cereb** | | | | | | |
| 300 | 19.24 | | 99 | | | |
| 302 | 22.00 | | 113 | | | |
| 304 | 20.21 | | 104 | | | |
| 306 | 18.10 | | 93 | | | |
| 308 | 17.77 | 19.46 | 91 | 100 | 9 | 4 |
| 301 | 11.76 | | 60 | | | |
| 303 | 18.10 | | 93 | | | |
| 305 | 18.42 | | 95 | | | |
| 307 | 15.99 | | 82 | | | |
| 309 | 16.80 | | 86 | 83 | 14 | 6 |
| | | | | 0.052 | | |

| 1 h GPx | %Control | Avg | Stdev | SEM |
|---|---|---|---|---|
| **Hippo** | | **%Control** | | |
| C | 89 | | | |
| C | 103 | | | |
| C | 103 | | | |
| C | 89 | | | |
| C | 116 | 100 | 11 | 5 |
| | 116 | | | |
| | 116 | | | |
| | 103 | | | |
| | 129 | | | |
| | 103 | 113 | 11 | 5 |
| | | 0.095 | | |
| **Cortex** | | | | |
| C | 119 | | | |
| C | 92 | | | |
| C | 92 | | | |
| C | 78 | | | |
| C | 119 | 100 | 18 | 8 |
| | 78 | | | |
| | 119 | | | |
| | 119 | | | |
| | 105 | | | |
| | 132 | 111 | 20 | 9 |
| | | 0.403 | | |
| **Cereb** | | | | |
| C | 133 | | | |
| C | 118 | | | |
| C | 103 | | | |
| C | 73 | | | |
| C | 73 | 100 | 27 | 12 |
| | 118 | | | |
| | 103 | | | |
| | 103 | | | |
| | 133 | 114 | 15 | 6 |
| | | 0.374 | | |

**30**

**days**

| Low aspect | GPx activity | Avg | %Control | Avg %Control | Stdev | SEM |
|---|---|---|---|---|---|---|
| **Hippo** | | | | | | |
| C | 57.73 | | 94 | | | |
| C | 49.24 | | 81 | | | |
| C | 66.22 | | 108 | | | |
| C | 66.22 | | 108 | | | |
| C | 66.22 | 61.13 | 108 | 100 | 12 | 6 |
| | 32.26 | | 53 | | | |
| | 57.73 | | 94 | | | |
| | 57.73 | | 94 | | | |
| | 40.75 | | 67 | | | |
| | 49.24 | | 81 | 78 | 18 | 8 |
| | | | | 0.053 | | |
| **Cortex** | | | | | | |
| C | 57.73 | | 87 | | | |
| C | 74.71 | | 113 | | | |
| C | 74.71 | | 113 | | | |
| C | 66.22 | | 100 | | | |
| C | 57.73 | 66.22 | 87 | 100 | 13 | 6 |
| | 40.75 | | 62 | | | |
| | 57.73 | | 87 | | | |
| | 49.24 | | 74 | | | |
| | 57.73 | | 87 | | | |
| | 32.26 | | 49 | 72 | 17 | 7 |
| | | | | 0.017 | | |
| **Cereb** | | | | | | |
| C | 49.24 | | 91 | | | |
| C | 49.24 | | 91 | | | |
| C | 57.73 | | 106 | | | |
| C | 57.73 | | 106 | | | |
| C | 57.73 | 54.33 | 106 | 100 | 9 | 4 |
| | 49.24 | | 91 | | | |
| | 40.75 | | 75 | | | |
| | 49.24 | | 91 | | | |
| | 49.24 | | 91 | | | |
| | 32.26 | | 59 | 81 | 14 | 6 |
| | | | | 0.034 | | |

Anti-HNE-LA dot blot

| | HNE-LA | Avg | % Control | Avg | STDEV | SEM |
|---|---|---|---|---|---|---|
| Control | 18263 | | 80 | | | |
| | 26981 | | 118 | | | |
| | 29291 | | 128 | | | |
| | 25470 | | 111 | | | |
| | 22476 | | 98 | | | |
| | 24033 | | 105 | | | |
| | 21245 | | 93 | | | |
| | 19137 | | 84 | | | |
| | 21695 | | 95 | | | |
| | 20217 | 22881 | 88 | 100 | 15 | 5 |
| | | | | | | |
| AD-IPL | 10621 | | 46 | | | |
| | 18643 | | 81 | | | |
| | 19410 | | 85 | | | |
| | 18847 | | 82 | | | |
| | 18521 | | 81 | | | |
| | 18054 | | 79 | | | |
| | 13733 | | 60 | | | |
| | 21409 | | 94 | | | |
| | 15274 | | 67 | | | |
| | 20215 | | 88 | | | |
| | 14215 | | 62 | | | |
| | 16492 | | 72 | 75 | 14 | 4 |
| | | | | 0.000615 | | |

LADH activity

| Slope | Blank minus | | | | | | |
|---|---|---|---|---|---|---|---|
| -0.0022 | -0.0014 | 0.00304 | | 94 | | | |
| -0.0028 | -0.002 | 0.00434 | | 134 | | | |
| -0.0023 | -0.0015 | 0.00326 | | 101 | | | |
| -0.0024 | -0.0016 | 0.00347 | | 107 | | | |
| -0.0017 | -0.0009 | 0.00195 | | 60 | | | |
| -0.0023 | -0.0015 | 0.00326 | | 101 | | | |
| -0.0024 | -0.0016 | 0.00347 | | 107 | | | |
| -0.0028 | -0.002 | 0.00434 | | 134 | | | |
| -0.0022 | -0.0014 | 0.00304 | | 94 | | | |
| -0.0018 | -0.001 | 0.00217 | 0.00323 | 67 | 100 | 24 | 8 |
| -0.0021 | -0.0013 | 0.00282 | | 87 | | | |
| -0.0013 | -0.0005 | 0.00109 | | 34 | | | |
| -0.0007 | 0.0001 | -0.00022 | | | | | |
| -0.0013 | -0.0005 | 0.00109 | | 34 | | | |
| -0.0007 | 0.0001 | -0.00022 | | | | | |
| -0.0023 | -0.0015 | 0.00326 | | 101 | | | |
| -0.0017 | -0.0009 | 0.00195 | | 60 | | | |
| -0.0016 | -0.0008 | 0.00174 | | 54 | | | |
| -0.0017 | -0.0009 | 0.00195 | | 60 | | | |
| -0.0019 | -0.0011 | 0.00239 | | 74 | | | |
| -0.0017 | -0.0009 | 0.00195 | | 60 | | | |
| -0.0017 | -0.0009 | 0.00195 | 0.00165 | 60 | 62 | 21 | 3 |

LADH levels

| | | | **Dihydrolipoamide dehydrogenase (DHLA) enzyme levels by Western blot** | | | | | | | |
|---|---|---|---|---|---|---|---|---|---|---|
| | | | **DHLA** | **Actin** | | | | | | |
| **Controls** | 1095 | 1 | 40788 | 8319 | 490 | | 112 | | | |
| | 1132 | 2 | 142398 | 30834 | 462 | | 106 | | | |
| | 1142 | 3 | 140928 | 29632 | 476 | | 109 | | | |
| | 1156 | 4 | 135418 | 30786 | 440 | | 101 | | | |
| | 1163 | 6 | 69563 | 17866 | 389 | | 89 | | | |
| | 1170 | 7 | 123386 | 33656 | 367 | 437 | 84 | 100 | 11 | 5 |
| **AD** | 1184 | 8 | 122697 | 49030 | 250 | | 57 | | | |
| | 1036 | 11 | 29476 | 10410 | 283 | | 65 | | | |
| | 1053 | 12 | 82201 | 30908 | 266 | | 61 | | | |
| | 1104 | 14 | 83840 | 29242 | 287 | | 66 | | | |
| | 1180 | 17 | 84308 | 26852 | 314 | | 72 | | | |
| | 1185 | 18 | 95149 | 32031 | 297 | | 68 | | | |
| | 1188 | 19 | 74347 | 22383 | 332 | | 76 | | | |
| | 1196 | 20 | 95777 | 31417 | 305 | | 70 | | | |
| | 1202 | 21 | 100089 | 27064 | 370 | | 85 | | | |
| | 1204 | 22 | 69675 | 21575 | 323 | | 74 | 69 | 8 | 2 |
| | | | | | | | | 1.53E-05 | | |

# REFERENCES


(HEI), H. E. I. (2001) Evaluation of Human Health Risk From Cerium Added to Diesel Fuel, Communication 9.

(OECD), O. f. E. C.-o. a. D. (2010). List of Manufactured Nanomaterials and List of Endpoints for Phase One of the Sponsorship Programme for the Testing of Manufactured Nanomaterials: Revision. . ENV/JM/MONO(2010)46, http://www.oecd.org/officialdocuments/displaydocumentpdf?cote=env/jm/mono(2010)46&doclanguage=en., Environment Directorate, Pesticides and Biotechnology, Organisation for Economic Co-operation and Development. Paris. pp. 16.

Abdelmoez, A., G. Thurner, et al. (2010). "Albumin-based nanoparticles as magnetic resonance contrast agents: II. Physicochemical characterisation of purified and standardised nanoparticles." Histochemistry and Cell Biology 134(2): 171-196.

Ahamed, M., R. Posgai, et al. (2010). "Silver nanoparticles induced heat shock protein 70, oxidative stress and apoptosis in Drosophila melanogaster." Toxicology and Applied Pharmacology 242(3): 263-269.

Akhtar, M. J., M. Ahamed, et al. (2010). "Nanotoxicity of pure silica mediated through oxidant generation rather than glutathione depletion in human lung epithelial cells." Toxicology 276(2): 95-102.

Aksenov, M., M. Aksenova, et al. (2000). "Oxidative Modification of Creatine Kinase BB in Alzheimer's Disease Brain." Journal of Neurochemistry 74(6): 2520-2527.

Aksenov, M. Y., M. V. Aksenova, et al. (1997). "Oxidative Modification of Glutamine Synthetase by Amyloid Beta Peptide." Free Radical Research 27(3): 267-281.

Alvarez, B. and R. Radi (2003). "Peroxynitrite reactivity with amino acids and proteins." Amino Acids 25(3): 295-311.

Amin, K. A., M. S. Hassan, et al. (2011). "The protective effects of cerium oxide nanoparticles against hepatic oxidative damage induced by monocrotaline." International journal of nanomedicine 6: 143-9.

Arck, P. C., A. Gilhar, et al. (2008). "The alchemy of immune privilege explored from a neuroimmunological perspective." Current Opinion in Pharmacology 8(4): 480-489.

Asati, A., S. Santra, et al. (2009). "Oxidase-Like Activity of Polymer-Coated Cerium Oxide Nanoparticles." Angewandte Chemie International Edition 48(13): 2308-2312.

Auffan, M., J. Rose, et al. (2009). "Towards a definition of inorganic nanoparticles from an environmental, health and safety perspective." Nat Nano 4(10): 634-641.

Auffan, M., J. Rose, et al. (2009). "CeO2 nanoparticles induce DNA damage towards human dermal fibroblasts in vitro." Nanotoxicology 3(2): 161-171.

Babu, S., J.-H. Cho, et al. (2010). "Multicolored redox active upconverter cerium oxide nanoparticle for bio-imaging and therapeutics." Chemical Communications 46(37): 6915-6917.

Baca, H. K., C. Ashley, et al. (2006). "Cell-Directed Assembly of Lipid-Silica Nanostructures Providing Extended Cell Viability." Science 313(5785): 337-341.

Bader Lange, M. L. (2010). In vivo oxidative stress in Alzheimer disease brain and a mouse model thereof: Effects of lipid asymmetry and the single methionine

residue of amyloid-β peptide. Department of Chemistry. http://uknowledge.uky.edu/gradschool_diss/117, University of Kentucky. Doctoral Dissertation.
Bagnyukova, T. V., K. B. Storey, et al. (2005). "Adaptive response of antioxidant enzymes to catalase inhibition by aminotriazole in goldfish liver and kidney." Comparative Biochemistry and Physiology 142: 335-341.
Bai, J. X. and A. I. Cederbaum (2001). "Adenovirus-mediated overexpression of catalase in the cytosolic or mitochondrial compartment protects against cytochrome P450 2E1-dependent toxicity in HepG2 cells." Journal of Biological Chemistry 276(6): 4315-4321.
Beal, M. F. (1995). "Aging, energy, and oxidative stress in neurodegenerative diseases." Annals of Neurology 38(3): 357-366.
Bhabra, G., A. Sood, et al. (2009). "Nanoparticles can cause DNA damage across a cellular barrier." Nat Nano 4(12): 876-883.
Bhaskar, S., F. Tian, et al. (2010). "Multifunctional Nanocarriers for diagnostics, drug delivery and targeted treatment across blood-brain barrier: perspectives on tracking and neuroimaging." Particle and Fibre Toxicology 7(3).
Biewenga, G. P., M. A. Dorstijn, et al. (1996). "Reduction of lipoic acid by lipoamide dehydrogenase." Biochemical Pharmacology 51(3): 233-238.
Blakytny, R. and J. J. Harding (1992). "Glycation (non-enzymic glycosylation) inactivates glutathione reductase." Journal of Biochemistry 288: 303-307.
Blaser, S. A., M. Scheringer, et al. (2008). "Estimation of cumulative aquatic exposure and risk due to silver: Contribution of nano-functionalized plastics and textiles." Science of The Total Environment 390(2–3): 396-409.
Bottini, M., S. Bruckner, et al. (2006). "Multi-walled carbon nanotubes induce T lymphocyte apoptosis." Toxicology Letters 160(2): 121-126.
Broillet, M. C. (1999). "S-Nitrosylation of proteins." Cellular and Molecular Life Sciences 55(8): 1036-1042.
Broome, C. S., A. C. Kayani, et al. (2006). "Effect of lifelong overexpression of HSP70 in skeletal muscle on age-related oxidative stress and adaptation after nondamaging contractile activity." The FASEB Journal 20(9): 1549-1551.
Brunner, T. J., P. Wick, et al. (2006). "In Vitro Cytotoxicity of Oxide Nanoparticles: Comparison to Asbestos, Silica, and the Effect of Particle Solubility†." Environmental Science & Technology 40(14): 4374-4381.
Butterfield, D. A. (1997). "beta-Amyloid-associated free radical oxidative stress and neurotoxicity: Implications for Alzheimer's disease." Chemical Research in Toxicology 10(5): 495-506.
Butterfield, D. A. (2006). "Oxidative Stress in Neurodegenerative Disorders." Antioxid Redox Sign 8(11-12): 1971-1973.
Butterfield, D. A., T. Reed, et al. (2007). "Roles of amyloid [beta]-peptide-associated oxidative stress and brain protein modifications in the pathogenesis of Alzheimer's disease and mild cognitive impairment." Free Radical Biology and Medicine 43(5): 658-677.
Butterfield, D. A. and E. R. Stadtman (1997). "Protein oxidation processes in aging brain." Adv Cell Aging Geron 2: 161-191.

Buzea, C., I. Pacheco, et al. (2007). "Nanomaterials and nanoparticles: Sources and toxicity." Biointerphases 2(4): MR17-MR71.
Cabiscol, E., E. Piulats, et al. (2000). "Oxidative Stress Promotes Specific Protein Damage inSaccharomyces cerevisiae." Journal of Biological Chemistry 275(35): 27393-27398.
Calabrese, V., T. E. Bates, et al. (2000). "NO synthase and NO-dependent signal pathways in brain aging and neurodegenerative disorders: The role of oxidant/antioxidant balance." Neurochemical Research 25(9-10): 1315-1341.
Calabrese, V., E. Guagliano, et al. (2007). "Redox Regulation of Cellular Stress Response in Aging and Neurodegenerative Disorders: Role of Vitagenes." Neurochemical Research 32(4): 757-773.
Calabrese, V., G. Scapagnini, et al. (2002). "Regional distribution of heme oxygenase, HSP70, and glutathione in brain: Relevance for endogenous oxidant/antioxidant balance and stress tolerance." Journal of Neuroscience Research 68(1): 65-75.
Calabrese, V., A. M. G. Stella, et al. (2004). "Redox regulation in neurodegeneration and longevity: Role of the heme oxygenase and HSP70 systems in brain stress tolerance." Antioxidants & Redox Signaling 6(5): 895-913.
Calabrese, V., R. Sultana, et al. (2006). "Nitrosative Stress, Cellular Stress Response, and Thiol Homeostasis in Patients with Alzheimer's Disease." Antioxid Redox Sign 8(11-12): 1975-1986.
Calabrese, V., G. Testa, et al. (2000). "HSP70 Induction in the Brain Following Ethanol Administration in the Rat: Regulation by Glutathione Redox State." Biochemical and Biophysical Research Communications 269(2): 397-400.
Calabrese, V. C. M. E. D. A. S. A. M. (2007). "Nitric oxide in the central nervous system: neuroprotection versus neurotoxicity." Nature Reviews Neuroscience 8(10): 766-775.
Cassee, F. R., E. C. van Balen, et al. (2011). "Exposure, Health and Ecological Effects Review of Engineered Nanoscale Cerium and Cerium Oxide Associated with its Use as a Fuel Additive." Critical Reviews in Toxicology 41(3): 213-229.
Celardo, I., M. De Nicola, et al. (2011). "Ce3+ Ions Determine Redox-Dependent Anti-apoptotic Effect of Cerium Oxide Nanoparticles." Acs Nano 5(6): 4537-4549.
Celardo, I., J. Z. Pedersen, et al. (2011). "Pharmacological potential of cerium oxide nanoparticles." Nanoscale 3(4): 1411-1420.
Cerutti, P., R. Ghosh, et al. (1994). "The role of the cellular antioxidant defense in oxidant carcinogenesis." Environmental Health Perspectives 102(10): 123-129.
Chen, J., S. Patil, et al. (2006). "Rare earth nanoparticles prevent retinal degeneration induced by intracellular peroxides." Nat Nano 1(2): 142-150.
Chen, J. P., S. Patil, et al. (2006). "Rare earth nanoparticles prevent retinal degeneration induced by intracellular peroxides." Nature Nanotechnology 1(2): 142-150.
Chen, L., R. Yokel, et al. (2008). "Manufactured Aluminum Oxide Nanoparticles Decrease Expression of Tight Junction Proteins in Brain Vasculature." Journal of Neuroimmune Pharmacology 3(4): 286-295.
Chia, A. J. L., C. E. Goldring, et al. (2010). "Differential effect of covalent protein modification and glutathione depletion on the transcriptional response of Nrf2 and NF-κB." Biochemical Pharmacology 80(3): 410-421.

Cho, W.-S., R. Duffin, et al. (2010). "Metal oxide nanoparticles induce unique inflammatory footprints in the lung: important implications for nanoparticle testing." Environmental Health Perspectives 118(12): 1699-1706.
Choi, J., H. D. Rees, et al. (2005). "Oxidative Modifications and Aggregation of Cu,Zn-Superoxide Dismutase Associated with Alzheimer and Parkinson Diseases." Journal of Biological Chemistry 280(12): 11648-11655.
Choi, J., V. Reipa, et al. (2011). "Physicochemical Characterization and In Vitro Hemolysis Evaluation of Silver Nanoparticles." Toxicological Sciences 123(1): 133-143.
Colon, J., N. Hsieh, et al. (2010). "Cerium oxide nanoparticles protect gastrointestinal epithelium from radiation-induced damage by reduction of reactive oxygen species and upregulation of superoxide dismutase 2." Nanomedicine : nanotechnology, biology, and medicine 6(5): 698-705.
Connor, E. E., J. Mwamuka, et al. (2005). "Gold Nanoparticles Are Taken Up by Human Cells but Do Not Cause Acute Cytotoxicity." Small 1(3): 325-327.
Corma, A., P. Atienzar, et al. (2004). "Hierarchically mesostructured doped CeO2 with potential for solar-cell use." Nat Mater 3(6): 394-397.
D'Angelo, B., S. Santucci, et al. (2009). "Cerium Oxide Nanoparticles Trigger Neuronal Survival in a Human Alzheimer Disease Model By Modulating BDNF Pathway." Current Nanoscience 5(2): 167-176.
Dalle-Donne, I., G. Aldini, et al. (2006). "Protein carbonylation, cellular dysfunction, and disease progression." Journal of Cellular and Molecular Medicine 10(2): 389-406.
Das, M., S. Patil, et al. (2007). "Auto-catalytic ceria nanoparticles offer neuroprotection to adult rat spinal cord neurons." Biomaterials 28(10): 1918-1925.
Davé, R., R. Gupta, et al. (2006). Deagglomeration and Mixing of Nanoparticles. NSF, NIRT NSF Nanoscale Science and Engineering Grantees Conference.
Derfus, A. M., W. C. W. Chan, et al. (2003). "Probing the Cytotoxicity of Semiconductor Quantum Dots." Nano Letters 4(1): 11-18.
Donaldson, K. and V. Stone (2003). "Current hypotheses on the mechanisms of toxicity of ultrafine particles." Ann Ist Super Sanità 39(3): 405-410.
Dutta, D., S. K. Sundaram, et al. (2007). "Adsorbed Proteins Influence the Biological Activity and Molecular Targeting of Nanomaterials." Toxicological Sciences 100(1): 303-315.
Eom, H.-J. and J. Choi (2009). "Oxidative stress of CeO2 nanoparticles via p38-Nrf-2 signaling pathway in human bronchial epithelial cell, Beas-2B." Toxicology Letters 187(2): 77-83.
Esposito, V. and E. Traversa (2008). "Design of Electroceramics for Solid Oxides Fuel Cell Applications: Playing with Ceria." Journal of the American Ceramic Society 91(4): 1037-1051.
Esterbauer, H., R. J. Schaur, et al. (1991). "Chemistry and biochemistry of 4-hydroxynonenal, malonaldehyde and related aldehydes." Free radical biology & medicine 11(1): 81-128.
Estevez, A. Y., S. Pritchard, et al. (2011). "Neuroprotective mechanisms of cerium oxide nanoparticles in a mouse hippocampal brain slice model of ischemia." Free Radical Biology and Medicine 51(6): 1155-1163.

Evans, P. and B. Halliwell (1999). "Free Radicals and Hearing: Cause, Consequence, and Criteria." Ann NY Acad Sci 884(OTOTOXICITY: Basic Science and Clinical Applications): 19-40.
Feng, X., D. C. Sayle, et al. (2006). "Converting Ceria Polyhedral Nanoparticles into Single-Crystal Nanospheres." Science 312(5779): 1504-1508.
Fernhoff, N. B., E. R. Derbyshire, et al. (2009). "A nitric oxide/cysteine interaction mediates the activation of soluble guanylate cyclase." Proceedings of the National Academy of Sciences 106(51): 21602-21607.
Forman, H. J. and D. A. Dickinson (2003). "Oxidative signaling and glutathione synthesis." BioFactors 17(1-4): 1-12.
Fubini, B. (1997). "Surface reactivity in the pathogenic response to particulates." Environ Health Perspectives 105(5): 1013-1020.
Fubini, B., M. Ghiazza, et al. (2010). "Physico-chemical features of engineered nanoparticles relevant to their toxicity." Nanotoxicology 4(4): 347-363.
Fubini, B. and A. Hubbard (2003). "Reactive oxygen species (ROS) and reactive nitrogen species (RNS) generation by silica in inflammation and fibrosis." Free Radical Biology and Medicine 34(12): 1507-1516.
Gao, K. and X. Jiang (2006). "Influence of particle size on transport of methotrexate across blood brain barrier by polysorbate 80-coated polybutylcyanoacrylate nanoparticles." International Journal of Pharmaceutics 310(1–2): 213-219.
Garrison, W. M. (1987). "Reaction mechanisms in the radiolysis of peptides, polypeptides, and proteins." Chemical Reviews 87(2): 381-398.
Garrison, W. M., M. E. Jayko, et al. (1962). "Radiation-induced oxidation of protein in aqueous solution." Radiation Research 16: 483-502.
Ghersi-Egea, J. F., P. D. Gorevic, et al. (1996). "Fate of Cerebrospinal Fluid-Borne Amyloid β-Peptide: Rapid Clearance into Blood and Appreciable Accumulation by Cerebral Arteries." Journal of Neurochemistry 67(2): 880-883.
Gilliss, S. R., J. Bentley, et al. (2005). "Electron energy-loss spectroscopic study of the surface of ceria abrasives." Applied Surface Science 241(1–2): 61-67.
Goodman, C. M., C. D. McCusker, et al. (2004). "Toxicity of Gold Nanoparticles Functionalized with Cationic and Anionic Side Chains." Bioconjugate Chemistry 15(4): 897-900.
Gottlieb, R. A. and R. S. Carreira (2010). "Autophagy in health and disease. 5. Mitophagy as a way of life." American Journal of Physiology - Cell Physiology 299(2): C203-C210.
Greenacre, S. A. B. and H. Ischiropoulos (2001). "Tyrosine nitration: Localisation, quantification, consequences for protein function and signal transduction." Free Radical Research 34(6): 541-581.
Guo, Y.-Y., J. Zhang, et al. (2011). "Cytotoxic and genotoxic effects of multi-wall carbon nanotubes on human umbilical vein endothelial cells in vitro." Mutation Research/Genetic Toxicology and Environmental Mutagenesis 721(2): 184-191.
Hafiz, M. A. and D. A. Butterfield (2007). "Involvement of PI3K/PKG/ERK1/2 signaling pathways in cortical neurons to trigger protection by cotreatment of acetyl-L-carnitine and α-lipoic acid against HNE-mediated oxidative stress and neurotoxicity: Implications for Alzheimer's disease." Free Radical Biology and Medicine 42(3): 371-384.

Halliwell, B. (1992). "REACTIVE OXYGEN SPECIES AND THE CENTRAL-NERVOUS-SYSTEM." Journal of Neurochemistry 59(5): 1609-1623.
Halliwell, B. (2006). "Oxidative stress and neurodegeneration: where are we now?" Journal of Neurochemistry 97(6): 1634-1658.
Halliwell, B. (2007). "Biochemistry of oxidative stress." Biochemical Society Transactions 35: 1147-1150.
Halliwell, B. and J. M. C. Gutteridge (2007). Free Radicals in Biology and Medicine, Clarendon Press Oxford.
Halliwell, B. and M. Whiteman (2004). "Measuring reactive species and oxidative damage in vivo and in cell culture: how should you do it and what do the results mean?" British Journal of Pharmacology 142(2): 231-255.
Halliwell, B., K. Zhao, et al. (1999). "Nitric oxide and peroxynitrite. The ugly, the uglier, and the not so good: A personal view of recent controversies." Free Radical Research 31: 651-659.
Hamilton, R. F., N. Wu, et al. (2009). "Particle length-dependent titanium dioxide nanomaterials toxicity and bioactivity." Particle and Fibre Toxicology 6(35).
Han W-Q, Wu L, et al. (2006). Characterization of CeO2-x nanotubes by HRTEM, EELS and XANES. 231st ACS National Meeting, Atlanta, GA, USA.
Hao, L., Z. Wang, et al. (2009). "Effect of sub-acute exposure to TiO2 nanoparticles on oxidative stress and histopathological changes in Juvenile Carp (Cyprinus carpio)." Journal of Environmental Sciences 21(10): 1459-1466.
Hardas, S. S., D. A. Butterfield, et al. (2010). "Brain distribution and toxicological evaluation of a systemically delivered engineered nanoscale ceria." Toxicological Sciences.
Hariharan, N., P. Zhai, et al. (2011). "Oxidative Stress Stimulates Autophagic Flux During Ischemia or Reperfusion." ANTIOXIDANTS & REDOX SIGNALING 14(11): 2179-2190.
Hartl, F. U. and M. Hayer-Hartl (2002). "Molecular Chaperones in the Cytosol: from Nascent Chain to Folded Protein." Science 295(5561): 1852-1858.
Hayes, J. D. and L. I. McLellan (1999). "Glutathione and glutathione-dependent enzymes represent a co-ordinately regulated defence against oxidative stress." Free Radical Research 31(4): 273-300.
Hazelton, G. A. and C. A. Lang (1980). "Glutathione Contents of Tissues in the Aging Mouse." Journal of Biochemistry 188(1): 25-30.
He, X., H. Zhang, et al. (2010). "Lung deposition and extrapulmonary translocation of nano-ceria after intratracheal instillation " Nanotechnology 21(28).
Heckert, E. G., A. S. Karakoti, et al. (2008). "The role of cerium redox state in the SOD mimetic activity of nanoceria." Biomaterials 29(18): 2705-2709.
Helland, A., P. Wick, et al. (2007). "Reviewing the Environmental and Human Health Knowledge Base of Carbon Nanotubes." Environ Health Perspect 115(8).
Hirst, S. M., A. Karakoti, et al. (2011). "Bio-distribution and in vivo antioxidant effects of cerium oxide nanoparticles in mice." Environmental Toxicology: n/a-n/a.
Hirst, S. M., A. S. Karakoti, et al. (2009). "Anti-inflammatory Properties of Cerium Oxide Nanoparticles." Small 5(24): 2848-2856.
Hissin, P. J. and R. Hilf (1976). "A fluorometric method for determination of oxidized and reduced glutathione in tissues." Analytical Biochemistry 74(1): 214-226.

Hiura, T. S., M. P. Kaszubowski, et al. (1999). "Chemicals in Diesel Exhaust Particles Generate Reactive Oxygen Radicals and Induce Apoptosis in Macrophages." The Journal of Immunology 163(10): 5582-5591.
Humphries, K. M. and L. I. Szweda (1998). "Selective Inactivation of α-Ketoglutarate Dehydrogenase and Pyruvate Dehydrogenase: Reaction of Lipoic Acid with 4-Hydroxy-2-nonenal†." Biochemistry 37(45): 15835-15841.
Hunter, A. and J. G. Lindsay (1986). "Immunological and biosynthetic studies on the mammalian 2-oxoglutarate dehydrogenase multienzyme complex." European Journal of Biochemistry 155(1): 103-109.
Hussain, S. M., K. L. Hess, et al. (2005). "In vitro toxicity of nanoparticles in BRL 3A rat liver cells." Toxicology in Vitro 19(7): 975-983.
Iijima, S. (1991). "Helical microtubules of graphitic carbon." Nature 354(6348): 56-58.
Inc., I. L. S. (2006). Chemical information profile for ceric oxide [CAS No. 1306-38-3]. Supporting Nomination for Toxicological Evaluation by the National Toxicology Program., In: National Toxicology Program, NIEHS, Research Triangle Park, NC, USA.
Izu, N., W. Shin, et al. (2003). "The effects of the particle size and crystallite size on the response time for resistive oxygen gas sensor using cerium oxide thick film." Sensors and Actuators B: Chemical 94(2): 222-227.
Jana, C. K., N. Das, et al. (2002). "Specificity of Age-Related Carbonylation of Plasma Proteins in the Mouse and Rat." Archives of Biochemistry and Biophysics 397(2): 433-439.
Jiang, J., G. Oberdörster, et al. (2008). "Does nanoparticle activity depend upon size and crystal phase?" Nanotoxicology 2(1): 33-42.
Joshi, G., S. Hardas, et al. (2007). "Glutathione elevation by γ-glutamyl cysteine ethyl ester as a potential therapeutic strategy for preventing oxidative stress in brain mediated by in vivo administration of adriamycin: Implication for chemobrain." Journal of Neuroscience Research 85(3): 497-503.
Kagan, V. E., A. Shvedova, et al. (1992). "Dihydrolipoic acid—a universal antioxidant both in the membrane and in the aqueous phase: Reduction of peroxyl, ascorbyl and chromanoxyl radicals." Biochemical Pharmacology 44(8): 1637-1649.
Kamata, H. and H. Hirata (1999). "Redox Regulation of Cellular Signalling." Cellular Signalling 11(1): 1-14.
Kang, S. J., B. M. Kim, et al. (2009). "Titanium dioxide nanoparticles induce apoptosis through the JNK/p38-caspase-8-Bid pathway in phytohemagglutinin-stimulated human lymphocytes." Biochemical and Biophysical Research Communications 386(4): 682-687.
Karakoti, A., S. Singh, et al. (2009). "Redox-active radical scavenging nanomaterials." Chemical Society Reviews 39(11): 4422-4432.
Karakoti, A. S., N. A. Monteiro-Riviere, et al. (2008). "Nanoceria as antioxidant: Synthesis and biomedical applications." Jom 60(3): 33-37.
Karakoti, A. S., S. Singh, et al. (2009). "PEGylated Nanoceria as Radical Scavenger with Tunable Redox Chemistry." Journal of the American Chemical Society 131(40): 14144-14145.

Keenan, C. R., R. Goth-Goldstein, et al. (2009). "Oxidative Stress Induced by Zero-Valent Iron Nanoparticles and Fe(II) in Human Bronchial Epithelial Cells." Environmental Science & Technology 43(12): 4555-4560.
Kehrer, J. P. (2000). "The Haber–Weiss reaction and mechanisms of toxicity." Toxicology 149(1): 43-50.
Khan, A. M., M. Tania, et al. (2010). "Antioxidant enzymes and cancer." Chinese Journal of Cancer Research 22(2): 87-92.
Kim, J. S., K. S. Song, et al. (2010). "Determination of Cytotoxicity Attributed to Multiwall Carbon Nanotubes (MWCNT) in Normal Human Embryonic Lung Cell (WI-38) Line." Journal of Toxicology and Environmental Health, Part A 73(21-22): 1521-1529.
Kim, S., J. E. Choi, et al. (2009). "Oxidative stress-dependent toxicity of silver nanoparticles in human hepatoma cells." Toxicology in Vitro 23(6): 1076-1084.
Kirchner, C., T. Liedl, et al. (2004). "Cytotoxicity of Colloidal CdSe and CdSe/ZnS Nanoparticles." Nano Letters 5(2): 331-338.
Klaine, S. J., P. J. J. Alvarez, et al. (2008). "Nanomaterials in the environment: Behavior, fate, bioavailability, and effects." Environmental Toxicology and Chemistry 27(9): 1825-1851.
Korotchkina, L. G., H.-S. Yang, et al. (2001). "Protection by thiols of the mitochondrial complexes from 4-hydroxy-2-nonenal." Free Radical Biology and Medicine 30(9): 992-999.
Korsvik, C., S. Patil, et al. (2007). "Superoxide dismutase mimetic properties exhibited by vacancy engineered ceria nanoparticles." Chemical Communications(10): 1056-1058.
Kostarelos, K. (2008). "The long and short of carbon nanotube toxicity." Nat Biotech 26(7): 774-776.
Koziara, J. M., P. R. Lockman, et al. (2006). "The Blood-Brain Barrier and Brain Drug Delivery." Journal of Nanoscience and Nanotechnology 6(9-10): 2712-2735.
Lam, C.-W., J. T. James, et al. (2004). "Pulmonary Toxicity of Single-Wall Carbon Nanotubes in Mice 7 and 90 Days After Intratracheal Instillation." Toxicological Sciences 77(1): 126-134.
Lauderback, C. M., J. M. Hackett, et al. (2001). "The glial transporter, GLT-1, is oxidatively modified by 4-hydroxy-2-nonenal in the Alzheimer's disease brain: Role of Ab(1-42)." Journal of Neurochemistry 78: 413-416.
Lee, H.-R., J.-M. Cho, et al. (2008). "Adaptive response to GSH depletion and resistance to L-buthionine-(S,R)-sulfoximine: involvement of Nrf2 activation." Molecular and Cellular Biochemistry 318(1): 23-31.
Lewinski, N., V. Colvin, et al. (2008). "Cytotoxicity of Nanoparticles." Small 4(1): 26-49.
Li, N., J. Alam, et al. (2004). "Nrf2 Is a Key Transcription Factor That Regulates Antioxidant Defense in Macrophages and Epithelial Cells: Protecting against the Proinflammatory and Oxidizing Effects of Diesel Exhaust Chemicals." The Journal of Immunology 173(5): 3467-3481.
Li, N., M. Hao, et al. (2003). "Particulate air pollutants and asthma: A paradigm for the role of oxidative stress in PM-induced adverse health effects." Clinical Immunology 109(3): 250-265.

Li, N., T. Xia, et al. (2008). "The role of oxidative stress in ambient particulate matter-induced lung diseases and its implications in the toxicity of engineered nanoparticles." Free Radical Biology and Medicine 44(9): 1689-1699.
Liang, G., Y. Pu, et al. (2009). "Influence of Different Sizes of Titanium Dioxide Nanoparticles on Hepatic and Renal Functions in Rats with Correlation to Oxidative Stress." Journal of Toxicology and Environmental Health, Part A 72(11-12): 740-745.
Limón-Pacheco, J. H., N. A. Hernández, et al. (2007). "Glutathione depletion activates mitogen-activated protein kinase (MAPK) pathways that display organ-specific responses and brain protection in mice." Free Radical Biology and Medicine 43(9): 1335-1347.
Lin, W., Y.-w. Huang, et al. (2006). "Toxicity of Cerium Oxide Nanoparticles in Human Lung Cancer Cells." International Journal of Toxicology 25(6): 451-457.
Lin, W. S., Y. W. Huang, et al. (2006). "Toxicity of cerium oxide nanoparticles in human lung cancer cells." International Journal of Toxicology 25(6): 451-457.
Lindsay, J. G. (1989). "Targeting of 2-Oxo Acid Dehydrogenase Complexes to the Mitochondriona." Annals of the New York Academy of Sciences 573(1): 254-266.
Linse, S., C. Cabaleiro-Lago, et al. (2007). "Nucleation of protein fibrillation by nanoparticles." Proceedings of the National Academy of Sciences 104(21): 8691-8696.
Lioy, P. J., N. C. G. Freeman, et al. (2002). "Dust: a metric for use in residential and building exposure assessment and source characterization." Environ Health Perspectives 110(10): 969-983.
Lippmann, M. (1990). "Effects of fiber characteristics on lung deposition, retention, and disease." Environ Health Perspect 88.
Luoma, S. N. (2008). Silver nanotechnologies and the environment : old problems or new challenges ? W. W. I. C. f. S. P. o. E. Nanotechnologies. http://www.nanotechproject.org/, Woodrow Wilson International Center for Scholars Project on Emerging Nanotechnologies: 72.
Luther, W. (2004). Industrial application of nanomaterials - chances and risks. Technology analysis. Düsseldorf, VDI-Technologiezentrum GmbH: 119.
Ma, L., J. Liu, et al. (2010). "Oxidative stress in the brain of mice caused by translocated nanoparticulate TiO2 delivered to the abdominal cavity." Biomaterials 31(1): 99-105.
Magrez, A., L. Horváth, et al. (2009). "Cellular Toxicity of TiO2-Based Nanofilaments." Acs Nano 3(8): 2274-2280.
Mai, H.-X., L.-D. Sun, et al. (2005). "Shape-Selective Synthesis and Oxygen Storage Behavior of Ceria Nanopolyhedra, Nanorods, and Nanocubes." The Journal of Physical Chemistry B 109(51): 24380-24385.
Mandoli, C., F. Pagliari, et al. (2010). "Stem Cell Aligned Growth Induced by CeO2 Nanoparticles in PLGA Scaffolds with Improved Bioactivity for Regenerative Medicine." Advanced Functional Materials 20(10): 1617-1624.
Marambio, P., B. Toro, et al. (2010). "Glucose deprivation causes oxidative stress and stimulates aggresome formation and autophagy in cultured cardiac myocytes." Biochimica et Biophysica Acta 18(2): 509-518.

Margonis, K., I. G. Fatouros, et al. (2007). "Oxidative stress biomarkers responses to physical overtraining: Implications for diagnosis." Free Radical Biology and Medicine 43(6): 901-910.
Markesbery, W. R. (1997). "Oxidative Stress Hypothesis in Alzheimer's Disease." Free Radical Biology and Medicine 23(1): 134-147.
Markesbery, W. R. and M. A. Lovell (1998). "Four-Hydroxynonenal, a Product of Lipid Peroxidation, is Increased in the Brain in Alzheimer's Disease." Neurobiology of Aging 19(1): 33-36.
Mastrogiacomo, F., J. G. Lindsay, et al. (1996). "Brain protein and α-ketoglutarate dehydrogenase complex activity in alzheimer-s disease." Annals of Neurology 39(5): 592-598.
Mayer, M. and B. Bukau (2005). "Hsp70 chaperones: Cellular functions and molecular mechanism." Cellular and Molecular Life Sciences 62(6): 670-684.
Maynard, A. D., P. A. Baron, et al. (2004). "Exposure to Carbon Nanotube Material: Aerosol Release During the Handling of Unrefined Single-Walled Carbon Nanotube Material." Journal of Toxicology and Environmental Health, Part A 67(1): 87-107.
Meister, A. and M. E. Anderson (1983). "Glutathione." Annual Review of Biochemistry 52(1): 711-760.
Meng, H., T. Xia, et al. (2009). "A Predictive Toxicological Paradigm for the Safety Assessment of Nanomaterials." Acs Nano 3(7): 1620-1627.
Miyamoto, Y., Y. Young Ho Koh, et al. (2003). "Oxidative Stress Caused by Inactivation of Glutathione Peroxidase and Adaptive Responses." Biological Chemistry 384(4): 567-574.
Molin, S., M. Gazda, et al. (2008). "Electrical properties of porous nanocrystalline undoped ceria oxygen sensor." Elektronika 49: 253-254.
Monteiro-Riviere, N. A., R. J. Nemanich, et al. (2005). "Multi-walled carbon nanotube interactions with human epidermal keratinocytes." Toxicology Letters 155(3): 377-384.
Moreira, P. I., P. L. R. Harris, et al. (2007). "Lipoic Acid and N-acetyl Cysteine Decrease Mitochondrial-Related Oxidative Stress in Alzheimer Disease Patient Fibroblasts." Journal of Alzheimer's Disease 12(2): 195-206.
Muller, F. L., M. S. Lustgarten, et al. (2007). "Trends in oxidative aging theories." Free Radical Biology and Medicine 43(4): 477-503.
Muller, J., F. Huaux, et al. (2005). "Respiratory toxicity of multi-wall carbon nanotubes." Toxicology and Applied Pharmacology 207(3): 221-231.
Murakami, K., T. Kondo, et al. (1998). "Mitochondrial Susceptibility to Oxidative Stress Exacerbates Cerebral Infarction That Follows Permanent Focal Cerebral Ischemia in Mutant Mice with Manganese Superoxide Dismutase Deficiency." The Journal of Neuroscience 18(1): 205-213.
Murray, E. P., T. Tsai, et al. (1999). "A direct-methane fuel cell with a ceria-based anode." Nature 400(6745): 649-651.
Nakagawa, Y., T. Suzuki, et al. (2011). "Cytotoxic effects of hydroxylated fullerenes on isolated rat hepatocytes via mitochondrial dysfunction." Archives of Toxicology: 1-12.

Nazem, A. and G. A. Mansoor (2011). "Nanotechnology for Alzheimer's disease detection and treatment." Insciences J. 1(4): 169-193.
Nel, A., T. Xia, et al. (2006). "Toxic potential of materials at the nanolevel." Science 311(5761): 622-627.
Nel, A. E., L. Madler, et al. (2009). "Understanding biophysicochemical interactions at the nano-bio interface." Nat Mater 8(7): 543-557.
Nemmar, A., M. F. Hoylaerts, et al. (2002). "Ultrafine Particles Affect Experimental Thrombosis in an In Vivo Hamster Model." American Journal of Respiratory and Critical Care Medicine 166(7): 998-1004.
Nesic, O., G.-Y. Xu, et al. (2004). "IL-1 Receptor Antagonist Prevents Apoptosis and Caspase-3 Activation after Spinal Cord Injury " Journal of Neurotrauma 18(9): 947-956.
Niederkorn, J. Y. (2006). "See no evil, hear no evil, do no evil: the lessons of immune priviledge." Nature Immunology 7(4): 354-359.
NIEHS (2006). "Integrated Laboratory Systems. Chemical Information Profiole for Ceric Oxide [CAS No. 1306-38-3] Supporting Nomination for Toxicological Evaluation by the National Toxicology Program. ." National Toxicological Program, Research Triangle Park, NC. (Available at:http://ntp.niehs.nih.gov /files/Ceric_oxide2.pdf. Accessed May 24, 2010.).
Niu, J., A. Azfer, et al. (2007). "Cardioprotective effects of cerium oxide nanoparticles in a transgenic murine model of cardiomyopathy." Cardiovascular Research 73(3): 549-559.
Niu, J., K. Wang, et al. (2011). "Cerium Oxide Nanoparticles Inhibits Oxidative Stress and Nuclear Factor-κB Activation in H9c2 Cardiomyocytes Exposed to Cigarette Smoke Extract." Journal of Pharmacology and Experimental Therapeutics 338(1): 53-61.
NSET "Nanoscale Science, Engineering and Technology (NSET) Subcommittee of the U.S. National Science and Technology Council (NSTC): Nanotechnology definition, National Science Foundation. [http://www.nsf.gov/crssprgm/nano/reports/omb_nifty50.jsp]."
O'Brien, N. and E. Cummins (2008). "Recent Developments in Nanotechnology and Risk Assessment Strategies for Addressing Public and Environmental Health Concerns." Human and Ecological Risk Assessment: An International Journal 14(3): 568-592.
Oberdorster, G., A. Elder, et al. (2009). "Nanoparticles and the Brain: Cause for Concern?" Journal of Nanoscience and Nanotechnology 9(8): 4996-5007.
Oberdörster, G., J. Ferin, et al. (1994). "Correlation between Particle Size, In Vivo Particle Persistence, and Lung Injury." Environmental Health Perspectives 102(ArticleType: research-article / Issue Title: Supplement 5: Biopersistence of Respirable Synthetic Fibers and Minerals / Full publication date: Oct., 1994 / Copyright © 1994 The National Institute of Environmental Health Sciences (NIEHS)): 173-179.
Oberdörster, G., E. Oberdörster, et al. (2005). "Nanotoxicology: An Emerging Discipline Evolving from Studies of Ultrafine Particles." Environ Health Perspect 113(7).
Oberdörster, G. (1988). "Lung Clearance of Inhaled Insoluble and Soluble Particles." Journal of Aerosol Medicine 1(4): 289-330.

Opii, W. O., V. N. Nukala, et al. (2007). "Proteomic Identification of Oxidized Mitochondrial Proteins following Experimental Traumatic Brain Injury." Journal of Neurotrauma 24(5): 772-789.
Owens Iii, D. E. and N. A. Peppas (2006). "Opsonization, biodistribution, and pharmacokinetics of polymeric nanoparticles." International Journal of Pharmaceutics 307(1): 93-102.
Panessa-Warren, B. J., J. B. Warren, et al. (2006). "Biological Cellular Response to Carbon Nanoparticle Toxicity." J. Physics: Condens. Mater. 18: S2185– S2201.
Park, B., P. Martin, et al. (2007). "Initial in vitro screening approach to investigate the potential health and environmental hazards of Envirox$^{TM}$—A nanoparticulate cerium oxide diesel fuel additive." Part. Fibre Toxicol. 4(12).
Park, E.-J., J. Yi, et al. (2008). "Oxidative stress and apoptosis induced by titanium dioxide nanoparticles in cultured BEAS-2B cells." Toxicology Letters 180(3): 222-229.
Park, E. J., J. Choi, et al. (2008). "Oxidative stress induced by cerium oxide nanoparticles in cultured BEAS-2B cells." Toxicology 245(1-2): 90-100.
Patrick, L. (2002). "Mercury toxicity and antioxidants: Part 1: role of glutathione and alpha-lipoic acid in the treatment of mercury toxicity." Alternative medicine review : a journal of clinical therapeutic 7(6): 456-71.
Pauluhn, J. (2010). "Subchronic 13-Week Inhalation Exposure of Rats to Multiwalled Carbon Nanotubes: Toxic Effects Are Determined by Density of Agglomerate Structures, Not Fibrillar Structures." Toxicological Sciences 113(1): 226-242.
Pigeolet, E., P. Corbisier, et al. (1990). "GLUTATHIONE-PEROXIDASE, SUPEROXIDE-DISMUTASE, AND CATALASE INACTIVATION BY PEROXIDES AND OXYGEN DERIVED FREE-RADICALS." Mechanisms of Ageing and Development 51(3): 283-297.
Pirmohamed, T., J. M. Dowding, et al. (2010). "Nanoceria exhibit redox state-dependent catalase mimetic activity." Chemical Communications 46(16): 2736-2738.
Poon, H. F., V. Calabrese, et al. (2004). "Free radicals: Key to brain aging and heme oxygenase as a cellular response to oxidative stress." Journals of Gerontology Series a-Biological Sciences and Medical Sciences 59(5): 478-493.
Qi, L., A. Sehgal, et al. (2008). "Redispersible Hybrid Nanopowders: Cerium Oxide Nanoparticle Complexes with Phosphonated-PEG Oligomers." Acs Nano 2(5): 879-888.
Radi, R., J. F. Turrens, et al. (1991). "DETECTION OF CATALASE IN RAT-HEART MITOCHONDRIA." Journal of Biological Chemistry 266(32): 22028-22034.
Radu, M., M. C. Munteanu, et al. (2010). "Depletion of intracellular glutathione and increased lipid peroxidation mediate cytotoxicity of hematite nanoparticles in MRC-5 cells." Acta Biochemica Polonica 57(3): 355-360.
Rahman, I., S. K. Biswas, et al. (2005). "Glutathione, Stress Responses, and Redox Signaling in Lung Inflammation " Antioxidants & Redox Signaling 7(1-2): 42-59.
Rahman, M. F., J. Wang, et al. (2009). "Expression of genes related to oxidative stress in the mouse brain after exposure to silver-25 nanoparticles." Toxicology Letters 187(1): 15-21.
Reed, T., M. Perluigi, et al. (2008). "Redox proteomic identification of 4-Hydroxy-2-nonenal-modified brain proteins in amnestic mild cognitive impairment: Insight

into the role of lipid peroxidation in the progression and pathogenesis of Alzheimer's disease." Neurobiology of Disease 30(1): 107-120.
Reese, T. S. and M. J. Karnovsky (1967). "FINE STRUCTURAL LOCALIZATION OF A BLOOD-BRAIN BARRIER TO EXOGENOUS PEROXIDASE." The Journal of Cell Biology 34(1): 207-217.
Risom, L., P. Møller, et al. (2005). "Oxidative stress-induced DNA damage by particulate air pollution." Mutation Research/Fundamental and Molecular Mechanisms of Mutagenesis 592(1–2): 119-137.
Rodea-Palomares, I., K. Boltes, et al. (2011). "Physicochemical characterization and ecotoxicological assessment of CeO2 nanoparticles using two aquatic microorganisms." Toxicol. Sci. 119: 135-145.
Roduner, E. (2006). "Size matters: why nanomaterials are different." Chemical Society Reviews 35(7).
Roh, J. Y., Y. K. Park, et al. "Ecotoxicological investigation of CeO(2) and TiO(2) nanoparticles on the soil nematode Caenorhabditis elegans using gene expression, growth, fertility, and survival as endpoints. ." Environ. Toxicol. Pharmacol. 29: 167-172.
Rushton, E. K., J. Jiang, et al. (2010). "Concept of Assessing Nanoparticle Hazards Considering Nanoparticle Dosemetric and Chemical/Biological Response Metrics." Journal of Toxicology and Environmental Health, Part A 73(5-6): 445-461.
Rzigalinski, B. A., K. Meehan, et al. (2006). "Radical nanomedicine." Nanomedicine (Lond) 1(4): 399-412.
Sayes, C. M., J. D. Fortner, et al. (2004). "The Differential Cytotoxicity of Water-Soluble Fullerenes." Nano Letters 4(10): 1881-1887.
Schäf, O., H. Ghobarkar, et al. (2004). Hydrothermal Synthesis of Nanomaterials
Nanostructured Materials. P. Knauth and J. Schoonman, Springer US. 8: 23-41.
Schaur, R. J. (2003). "Basic aspects of the biochemical reactivity of 4-hydroxynonenal." Molecular Aspects of Medicine 24(4–5): 149-159.
Schubert, D., R. Dargusch, et al. (2006). "Cerium and yttrium oxide nanoparticles are neuroprotective." Biochemical and Biophysical Research Communications 342(1): 86-91.
Schuessler, H. and K. Schilling (1984). "Oxygen Effect in the Radiolysis of Proteins." International Journal of Radiation Biology 45(3): 267-281.
Shakibaei, M., T. John, et al. (2007). "Resveratrol Inhibits IL-1β–Induced Stimulation of Caspase-3 and Cleavage of PARP in Human Articular Chondrocytes in Vitro." Annals of the New York Academy of Sciences 1095(1): 554-563.
Sharma, H. S. and A. Sharma (2007). Nanoparticles aggravate heat stress induced cognitive deficits, blood–brain barrier disruption, edema formation and brain pathology. Progress in Brain Research. S. Hari Shanker, Elsevier. Volume 162: 245-273.
Shibata, M., S. Yamada, et al. (2000). "Clearance of Alzheimer's amyloid-β1-40 peptide from brain by LDL receptor–related protein-1 at the blood-brain barrier." The Journal of Clinical Investigation 106(12): 1489-1499.

Shigenaga, M. K., T. M. Hagen, et al. (1994). "Oxidative damage and mitochondrial decay in aging." Proceedings of the National Academy of Sciences 91(23): 10771-10778.
Shoults-Wilson, W. A., B. C. Reinsch, et al. (2011). "Effect of silver nanoparticle surface coating on bioaccumulation and reproductive toxicity in earthworms (Eisenia fetida)." Nanotoxicology 5(3): 432-444.
Shoults-Wilson, W. A., B. C. Reinsch, et al. (2011). Role of Particle Size and Soil Type in Toxicity of Silver Nanoparticles to Earthworms. Madison, WI, ETATS-UNIS, Soil Science Society of America.
Shoults-Wilsona, W. A., B. C. Reinschb, et al. (2010). "Role of Particle Size and Soil Type in Toxicity of Silver Nanoparticles to Earthworms." Soil Science Society of America Journal 75(2): 365-377.
Shrivastava, K., D. Shukla, et al. (2008). "Neuroprotective effect of cobalt chloride on hypobaric hypoxia-induced oxidative stress." Neurochemistry International 52(3): 368-375.
Shvedova, A., V. Castranova, et al. (2003). "Exposure to Carbon Nanotube Material: Assessment of Nanotube Cytotoxicity using Human Keratinocyte Cells." Journal of Toxicology and Environmental Health, Part A 66(20): 1909-1926.
Shvedova, A. A., E. R. Kisin, et al. (2005). "Unusual inflammatory and fibrogenic pulmonary responses to single-walled carbon nanotubes in mice." American Journal of Physiology - Lung Cellular and Molecular Physiology 289(5): L698-L708.
Si, R., Y.-W. Zhang, et al. (2005). "Rare-Earth Oxide Nanopolyhedra, Nanoplates, and Nanodisks." Angewandte Chemie International Edition 44(21): 3256-3260.
Siems, W. and T. Grune (2003). "Intracellular metabolism of 4-hydroxynonenal." Molecular Aspects of Medicine 24(4–5): 167-175.
Simko, M. (2007). "Cell Type Specific Redox Status is Responsible for Diverse Electromagnetic Field Effects." Current Medicinal Chemistry 14(10): 1141-1152.
Simkó, M., A. Gazsó, et al. (2011). Nanoparticles, free radicals and oxidative stress. The NanoTrust Dossiers. A.-V. Institute of Technology Assessment (ITA); Strohgasse 45/5. The NanoTrust Dossiers: epub.oeaw.ac.at/ita/nanotrust-dossiers/dossier012en.pdf, Austrian Academy of Sciences. 012en.
Simko, M. and M.-O. Mattsson (2010). "Risks from accidental exposures to engineered nanoparticles and neurological health effects: A critical review." Particle and Fibre Toxicology 7(1): 42.
Singh, N., C. A. Cohen, et al. (2007). "Treatment of Neurodegenerative Disorders with Radical Nanomedicine." Annals of the New York Academy of Sciences 1122(1): 219-230.
Smith, P. K., R. I. Krohn, et al. (1985). "Measurement of protein using bicinchoninic acid." Analytical Biochemistry 150(1): 76-85.
Soenen, S. J., P. Rivera-Gil, et al. (2011). "Cellular toxicity of inorganic nanoparticles: Common aspects and guidelines for improved nanotoxicity evaluation." Nano Today 6(5): 446-465.
Speciale, A., S. Anwar, et al. (2011). "Cellular adaptive response to glutathione depletion modulates endothelial dysfunction triggered by TNF-α." Toxicology Letters 207(3): 291-297.

Spiteller, G. (2001). "Lipid peroxidation in aging and age-dependent diseases." Experimental Gerontology 36(9): 1425-1457.
Srinivas, A., P. J. Rao, et al. (2011). "Acute inhalation toxicity of cerium oxide nanoparticles in rats." Toxicology Letters 205(2): 105-115.
Stadtman, E. R. (1990). "Metal ion-catalyzed oxidation of proteins: Biochemical mechanism and biological consequences." Free Radical Biology and Medicine 9(4): 315-325.
Stadtman, E. R. (2006). "Protein oxidation and aging." Free Radical Research 40(12): 1250-1258.
Stadtman, E. R. and R. L. Levine (2003). "Free radical-mediated oxidation of free amino acids and amino acid residues in proteins." Amino Acids 25(3): 207-218.
Stern, S. T. and S. E. McNeil (2008). "Nanotechnology Safety Concerns Revisited." Toxicological Sciences 101(1): 4-21.
Stone, V. and K. Donaldson (2006). "Nanotoxicology Signs of Stress." Nature Nanotechnology 1.
Subramaniam, R., F. Roediger, et al. (1997). "The Lipid Peroxidation Product, 4-Hydroxy-2-trans-Nonenal, Alters the Conformation of Cortical Synaptosomal Membrane Proteins." Journal of Neurochemistry 69(3): 1161-1169.
Swallow, A. J. (1960). Effect of ionizing radiation on proteins, RCO groups, peptide bond cleavage, inactivation, -SH oxidation. Radiation chemistry of organic compounds, New York: Pergamon Press.
Talalay, P., A. T. Dinkova-Kostova, et al. (2003). "Importance of phase 2 gene regulation in protection against electrophile and reactive oxygen toxicity and carcinogenesis." Advances in Enzyme Regulation 43(1): 121-134.
Tangpong, J., M. P. Cole, et al. (2006). "Adriamycin-induced, TNF-α-mediated central nervous system toxicity." Neurobiology of Disease 23(1): 127-139.
Tanzi, R. E., R. D. Moir, et al. (2004). "Clearance of Alzheimer's Aβ Peptide: The Many Roads to Perdition." Neuron 43(5): 605-608.
Tarnuzzer, R. W., J. Colon, et al. (2005). "Vacancy engineered ceria nanostructures for protection from radiation-induced cellular damage." Nano Letters 5(12): 2573-2577.
Thill, A., O. Zeyons, et al. (2006). "Cytotoxicity of CeO2 nanoparticles for Escherichia coli. Physico-chemical insight of the cytotoxicity mechanism." Environmental Science & Technology 40(19): 6151-6156.
Thomas, K. and P. Sayre (2005). "Research strategies for safety evaluation of nanomaterials, Part I: evaluating the human health implications of exposure to nanoscale materials." Toxicological sciences 87(2): 316-321.
Thomassen, L. C. J., A. Aerts, et al. (2009). "Synthesis and Characterization of Stable Monodisperse Silica Nanoparticle Sols for in Vitro Cytotoxicity Testing." Langmuir 26(1): 328-335.
Trovarelli, A. (1996). "Catalytic Properties of Ceria and CeO2-Containing Materials." Catalysis Reviews 38(4): 439-520.
Unfried, K., C. Albrecht, et al. (2007). "Cellular responses to nanoparticles: Target structures and mechanisms." Nanotoxicology 1(1): 52-71.

Unrine, J., P. Bertsch, et al. (2008). Bioavailability, Trophic Transfer, and Toxicity of Manufactured Metal and Metal Oxide Nanoparticles in Terrestrial Environments. Nanoscience and Nanotechnology, John Wiley & Sons, Inc.: 345-366.

Usenko, C. Y., S. L. Harper, et al. (2008). "Fullerene C60 exposure elicits an oxidative stress response in embryonic zebrafish." Toxicology and Applied Pharmacology 229(1): 44-55.

VanHoecke, K., J. T. K. Quik, et al. (2009). "Fate and effects of CeO2 nanoparticles in aquatic ecotoxicity tests. ." Environ. Sci. Technol. 43: 4537–4546.

Vertegel, A. A., R. W. Siegel, et al. (2004). "Silica Nanoparticle Size Influences the Structure and Enzymatic Activity of Adsorbed Lysozyme." Langmuir 20(16): 6800-6807.

Vincent, A., S. Babu, et al. (2009). "Protonated Nanoparticle Surface Governing Ligand Tethering and Cellular Targeting." Acs Nano 3(5): 1203-1211.

Waeg, G., G. Dimsity, et al. (1996). "Monoclonal antibodies for detection of 4-hydroxynonenal modified proteins." Free Radical Research 25(2): 149-59.

Walters, J., C. Pop, et al. (2009). "A constitutively active and uninhibitable caspase-3 zymogen efficiently induces apoptosis." Biochemical Journal 424(3): 335-345.

Wang, D., F. Li, et al. (2011). "Potential relationship among three antioxidant enzymes in eliminating hydrogen peroxide in penaeid shrimp." Cell Stress and Chaperones: 1-11.

Wang, J., M. F. Rahman, et al. (2009). "Expression changes of dopaminergic system-related genes in PC12 cells induced by manganese, silver, or copper nanoparticles." NeuroToxicology 30(6): 926-933.

Wang, J., P. Sun, et al. (2011). "Cytotoxicity of single-walled carbon nanotubes on PC12 cells." Toxicology in Vitro 25(1): 242-250.

Wang, Z., L. Liu, et al. (2006). "Increased Expression of Heat Shock Protein 72 Protects Renal Proximal Tubular Cells from Gentamicin-induced Injury." J Korean Med Sci 21(5): 904-910.

Warheit, D. B., B. R. Laurence, et al. (2004). "Comparative Pulmonary Toxicity Assessment of Single-wall Carbon Nanotubes in Rats." Toxicological Sciences 77(1): 117-125.

WHO/EURO, T. C. f. M. a. E. A. and MMMF: (1985). Reference methods for measuring airborne man-made mineral fibres (MMMF), WHO/EURO MMMF Reference Scheme, Monitoring concentration using a phase contrast optical microscope, Determining size using a scanning electron microscope. . World Health Organization. Regional Office for Europe, Copenhagen;. 64.

Wittmaack, K. (2006). "In Search of the Most Relevant Parameter for Quantifying Lung Inflammatory Response to Nanoparticle Exposure: Particle Number, Surface Area, or What?" Environ Health Perspect 115(2).

Wolfgang, L. (2004). Industrial application of nanomaterials - chances and risks. Technology analysis. Düsseldorf, VDI-Technologiezentrum GmbH: 119.

Wu, W.-h., X. Sun, et al. (2008). "TiO2 nanoparticles promote β-amyloid fibrillation in vitro." Biochemical and Biophysical Research Communications 373(2): 315-318.

Xia, T., M. Kovochich, et al. (2006). "Comparison of the Abilities of Ambient and Manufactured Nanoparticles To Induce Cellular Toxicity According to an Oxidative Stress Paradigm." Nano Letters 6(8): 1794-1807.

Xia, T., M. Kovochich, et al. (2008). "Comparison of the Mechanism of Toxicity of Zinc Oxide and Cerium Oxide Nanoparticles Based on Dissolution and Oxidative Stress Properties." Acs Nano 2(10): 2121-2134.
Xia, T., M. Kovochich, et al. (2007). "Cationic Polystyrene Nanosphere Toxicity Depends on Cell-Specific Endocytic and Mitochondrial Injury Pathways." Acs Nano 2(1): 85-96.
Xia, T., N. Li, et al. (2009). "Potential Health Impact of Nanoparticles." Annual Review of Public Health 30(1): 137-150.
Xiao, G. G., M. Wang, et al. (2003). "Use of Proteomics to Demonstrate a Hierarchical Oxidative Stress Response to Diesel Exhaust Particle Chemicals in a Macrophage Cell Line." Journal of Biological Chemistry 278(50): 50781-50790.
Xiong, D., T. Fang, et al. (2011). "Effects of nano-scale TiO2, ZnO and their bulk counterparts on zebrafish: Acute toxicity, oxidative stress and oxidative damage." Science of The Total Environment 409(8): 1444-1452.
Yang, S. and L. Gao (2006). "Controlled Synthesis and Self-Assembly of CeO2 Nanocubes." Journal of the American Chemical Society 128(29): 9330-9331.
Yin, H., H. P. Too, et al. (2005). "The effects of particle size and surface coating on the cytotoxicity of nickel ferrite." Biomaterials 26(29): 5818-5826.
Yokel, R. A., T. C. Au, et al. (2012). "Distribution, Elimination, and Biopersistence to 90 Days of a Systemically Introduced 30 nm Ceria-Engineered Nanomaterial in Rats." Toxicological Sciences 127(1): 256-268.
Yokel, R. A., R. L. Florence, et al. (2009). "Biodistribution and oxidative stress effects of a systemically-introduced commercial ceria engineered nanomaterial." Nanotoxicology 3(3): 234-248.
Yokel, R. A. and R. C. MacPhail (2011). "Engineered nanomaterials: exposures, hazards, and risk prevention." Journal of Occupational Medicine and Toxicology 6(7).
Younce, C. W. and P. E. Kolattukudy (2010). "MCP-1 causes cardiomyoblast death via autophagy resulting from ER stress caused by oxidative stress generated by inducing a novel zinc-finger protein, MCPIP." Biochemical Journal 426(1): 43-53.
Younce, C. W., K. Wang, et al. (2010). "Hyperglycaemia-induced cardiomyocyte death is mediated via MCP-1 production and induction of a novel zinc-finger protein MCPIP." Cardiovascular Research 87(4): 665-674.
Young, J. C., J. M. Barral, et al. (2003). "More than folding: localized functions of cytosolic chaperones." Trends in Biochemical Sciences 28(10): 541-547.
Yu, T., J. Joo, et al. (2005). "Large-Scale Nonhydrolytic Sol–Gel Synthesis of Uniform-Sized Ceria Nanocrystals with Spherical, Wire, and Tadpole Shapes." Angewandte Chemie 117(45): 7577-7580.
Yuan, Q., H.-H. Duan, et al. (2009). "Controlled synthesis and assembly of ceria-based nanomaterials." Colloid Interface Sci. 335: 151-167.
Zeyons, O., A. Thill, et al. (2009). "Direct and indirect CeO2 nanoparticles toxicity for Escherichia coli and Synechocystis." Nanotoxicology 3: 284-295.
Zhang, F., P. Wang, et al. (2004). "Cerium oxidation state in ceria nanoparticles studied with X-ray photoelectron spectroscopy and absorption near edge spectroscopy." Surface Science 563(1-3): 74-82.

Zhang, H., X. He, et al. (2010). "Nano-CeO2 exhibits adverse effects at environmental relevant concentrations. ." Environ. Sci. Technol. 45 3725–3730.
Zhang, Y., W. Chen, et al. (2007). "In Vitro and In Vivo Toxicity of CdTe Nanoparticles." Journal of Nanoscience and Nanotechnology 7(2): 497-503.
Zhou, X., L. L. Wong, et al. (2011). "Nanoceria Inhibit the Development and Promote the Regression of Pathologic Retinal Neovascularization in the Vldlr Knockout Mouse." PLoS ONE 6(2): e16733.
Zitta, K., B. Brandt, et al. (2010). "Interleukin-1β regulates cell proliferation and activity of extracellular matrix remodelling enzymes in cultured primary pig heart cells." Biochemical and Biophysical Research Communications 399(4): 542-547.
Zlokovic, B. V. (2005). "Neurovascular mechanisms of Alzheimer's neurodegeneration." Trends in Neurosciences 28(4): 202-208.

# VITA

Sarita S. Hardas was born in Maharashtra, India on June 19, 1980. Sarita obtained her bachelor's degree in chemistry from Fergusson College Pune, India. After completion of bachelor's degree Sarita joined University of Pune, Department of Chemistry, where she obtained here Master's degree in Inorganic chemistry. Immediately after completion of Master's degree Sarita was offered a job as Research assistance in Unilever Research India, Bangalore through on-campus interview. Sarita worked in Unilever for 3-years on instrumental and analytical analysis related projects. While working in Unilever, Sarita applied to universities in USA for higher education in chemistry. To pursue PhD in biological chemistry, Sarita came to University of Kentucky, Lexington. Sarita completed her PhD research in the newly immerging field of neuro-nanotoxicity under the aegis of Dr. D. Allan Butterfield.

SCIENTIFIC PUBLICATIONS

Olga V. Tsyusko, ‡**Sarita S. Hardas,** W. Aaron Shoults-Wilson, Catherine Starnes, Greg Joice, D. Allan Butterfield, Jason M. Unrine, "Short-term molecular-level effects of silver nanoparticle exposure on the earthworm, Eisenia fetida.", manuscript in preparation. ‡C-first author

**Sarita S. Hardas,** Rukhsana Sultana, Govind Warrier, Mo Dan, Jason M. Unrine, Uschi M. Graham, Peng Wu, Eric A. Grulke, Michael T. Tseng, Robert A. Yokel, and D. Allan Butterfield "Modulation of Oxidative Stress Effects and Their Mechanisms in time-dependant manner in Rat Brain After Systemic Administration of 30 Nm Ceria Engineered Nanomaterial.", manuscript in preparation.

**Sarita S. Hardas**, Rukhsana Sultana, Govind Warrier, Mo Dan, Rebecca L. Florence, Peng Wu, Eric A. Grulke, Michael T. Tseng, Jason M. Unrine, Uschi M. Graham, Robert A. Yokel, D. Allan Butterfield, "Rat brain pro-oxidant effects of peripherally administered 5 nm ceria 30 days after exposure.", Neurotox., submitted (2012).

Tseng MT, Lu X, Duan X, Sarita S. Hardas, Sultana R, Wu P, Unrine JM, Graham U, Butterfield DA, Grulke EA, Yokel RA. "Alteration of hepatic structure and oxidative stress induced by intravenous nanoceria.", Toxicol Appl Pharmacol.,(2012), ahead of print.

Robert A. Yokel, Tu C. Au, Robert MacPhail, **Sarita S. Hardas**, D. Allan Butterfield, Rukhsana Sultana, Michael Goodman, Michael T. Tseng, Mo Dan, Hamed Haghnazar, Jason M. Unrine, Uschi M. Graham, Peng Wu and Eric A. Grulke, "Distribution, elimination and biopersistence to 90 days of a systemically-introduced 30 nm ceria engineered nanomaterial in rats.", Tox. Sci., 127(1), 256-268, (2012).

Paritosh P. Wattamwar, **Sarita S. Hardas**, D. Allan Butterfield, Kimberly W. Anderson, and Thomas D. Dzuibla, "Tuning of the prooxidant and antioxidant of the trolox through the controlled release from biodegradable poly (trolox ester) polymers", J Biomed Mater Res A.,99(2):184-91,(2011).

**Sarita S. Hardas,** Butterfield, D.A., Sultana, R.L., Tseng, M.T., Dan, M., Florence, R., Unrine, J.M., Graham, U.M., Wu, P., Grulke, E.A., **Yokel, R.A.,** "Brain distribution and toxicological evaluation of a systemically delivered engineered nanoscale ceria.", Tox. Sci.,116(2), 562-576, (2010).

D. Allan Butterfield, **Sarita Hardas**, and Miranda L. Bader Lange, "Oxidatively Modified Glyceraldehyde-3-Phosphate Dehydrogenase (GAPDH) and Alzheimer Disease: Many Pathways to Neurodegeneration", J Alzheimer's Dis., 20 (2), 369- 393 (2010).

Alagirisamy N, Sarita S. Hardas, Jayaraman S, "Novel colorimetric sensor for oral malodour.", Anal Chim Acta., 19;661(1):97-102 (2010).

Yokel, Robert A., Florence, Rebecca L., Unrine, Jason M., Tseng, Michael T., Graham, Uschi M., Wu, Peng, Grulke, Eric A., Sultana, Rukhsana, **Sarita S. Hardas,** and Butterfield, D. Allan "Biodistribution and oxidative stress effects of a systemically-introduced commercial ceria engineered nanomaterial", Nanotoxicology, 3(3),234 -248 (2009).

Gururaj Joshi, **Sarita Hardas**, Rukhsana Sultana, Daret K. St. Clair , Mary Vore , D. Allan Butterfield , "Glutathione elevation by γ-glutamyl cysteine ethyl ester as a potential therapeutic strategy for preventing oxidative stress in brain mediated by in vivo administration of adriamycin: Implication for chemobrain," J. Neurosci Res., 85, 497-503 (2006).